Molekulare Mechanismen der Wirkung von Spannungssensor–Toxinen aus Skorpionen und marinen Kegelschnecken auf spannungsgesteuerte Natriumkanäle

Dissertation
zur Erlangung des akademischen Grades doctor rerum naturalium (Dr. rer. nat.)

vorgelegt dem Rat der Biologisch-Pharmazeutischen Fakultät der Friedrich-Schiller-Universität Jena

von Diplom-Biochemiker Enrico Leipold

geboren am 23.06.1977 in Sonneberg

1. Gutachter: Prof. Dr. Stefan H. Heinemann
   Friedrich Schiller-Universität, Jena
2. Gutachter: Prof. Dr. Ingo Dahse
   Friedrich Schiller-Universität, Jena
3. Gutachter: Prof. Dr. Dietrich Mebs
   Johann Wolfgang Goethe-Universität, Frankfurt am Main

Inhaltsverzeichnis

1. Einleitung

1.1 Spannungsgesteuerte Natriumkanäle

Spannungsgesteuerte Natriumkanäle (Na_V-Kanäle) sind entscheidend an der Entstehung und der gerichteten Weiterleitung von Aktionspotentialen in erregbaren Zellen beteiligt. Damit sind sie von zentraler Bedeutung für die elektrische Signalgebung in Menschen und Tieren (Catterall, 1992). Neun humane Na_V-Kanäle wurden bereits kloniert und funktionell charakterisiert (Abb. 1). Die Kanal-kodierenden Gene liegen auf verschiedenen Chromosomen und sind wahrscheinlich durch Genduplikation entstanden (Plummer und Meisler, 1999; Goldin, 2002) (Abb.1).

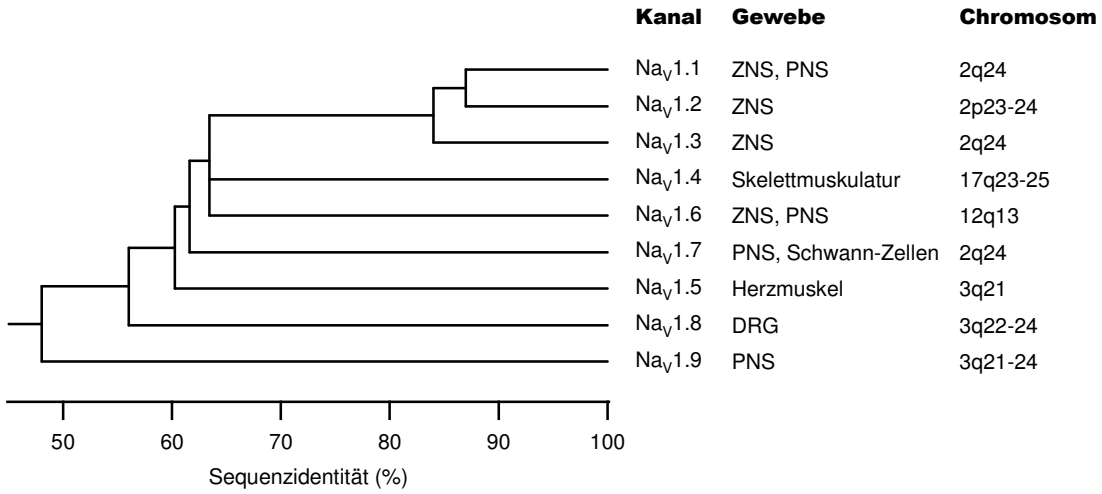

Abb. 1: Bereits klonierte und funktionell charakterisierte humane Na_V-Kanäle. Die vollständigen Aminosäuresequenzen der humanen Subtypen $Na_V1.1$-1.9 wurden verglichen und die prozentuale Identität der Sequenzen dargestellt. ZNS: Zentralnervensystem, PNS: peripheres Nervensystem, DRG: dorsal root ganglion.

Elektrophysiologische Experimente am Tintenfischaxon lieferten die Grundlagen zum qualitativen und quantitativen Verständnis der Vorgänge bei der Entstehung von Aktionspotentialen (Hodgkin und Huxley, 1952). Beim Ruhepotential (ca. -80 mV) sind die spannungsabhängigen Ionenkanäle erregbarer Zellen geschlossen. Aufgrund ihres schnellen Schaltverhaltens öffnen Na_V-Kanäle sehr schnell (<1 ms) bei einer Depolarisation der Zellmembran und bewirken durch den Einstrom von Na^+-Ionen in die Zelle eine weitere Depolarisation der Membran, welche weitere Na_V-Kanäle aktiviert (öffnet). Diese positive Rückkopplung ist für den *Alles-oder-Nichts*-Mechanismus des Aktionspotentials verantwortlich. Kurze Zeit (1-2 ms) nach ihrer Aktivierung inaktivieren (schließen) Na_V-Kanäle spontan. Dieser Vorgang sichert die gerichtete Ausbreitung von Aktionspotentialen. Die Zurückführung

der Na_V-Kanäle in ihre deaktivierte Konformation ist die Voraussetzung für ihre erneute Aktivierung und wird durch die Aktivität spannungsabhängiger Kaliumkanäle (K_V-Kanäle) gesichert. K_V-Kanäle aktivieren bei Depolarisation der Zellmembran mit einer zeitlichen Verzögerung und lassen intrazelluläre K^+-Ionen aus der Zelle heraustreten. Da K_V-Kanäle gewöhnlich nicht schnell inaktivieren, bewirken sie deshalb die Rückkehr zum Ruhepotential (Repolarisation) und damit die Deaktivierung der zuvor aktivierten Na_V-Kanäle.

1.2 Struktur der Na_V-Kanäle

Der kombinierte Einsatz elektrophysiologischer und molekularbiologischer Techniken führte zu einem allgemein akzeptierten Modell der Na_V-Kanalstruktur. Nach heutiger Kenntnis besteht der Na_V-Kanalkomplex aus einer α-Untereinheit und einer oder mehreren gewebsspezifischen β-Untereinheiten, wobei die α-Untereinheit alleine bereits einen funktionstüchtigen Kanal formt (Noda et al., 1986a, 1986b; Goldin et al., 1986). Aus Hydropathieuntersuchungen der Proteinsequenz des Na_V-Kanals konnte die wahrscheinliche Membrantopologie der porenformenden α-Untereinheit abgeleitet werden (Noda et al., 1984). Diesem Modell entsprechend besteht die α-Untereinheit aus einem einzigen Proteinstrang mit einer Länge von ca. 2000 Aminosäuren und durchspannt die Zellmembran 24-mal. Jeweils sechs Transmembransegmente (S1-S6) gruppieren sich dabei zu einer der vier homologen Kanaldomänen (D1-D4, Abb. 2).

Übereinstimmend mit dieser Strukturvorhersage zeigten Sato et al. (1998) mit Hilfe der Elektronenmikroskopie, dass sich die vier homologen Domänen um eine zentrale Pore anordnen. Als porenbildende Strukturen gelten die extrazellulären Schleifen, welche die Transmembransegmente S5 und S6 der einzelnen Domänen miteinander verbinden. Auf diese Weise liefert jede der vier Domänen einen Bestandteil der Pore. Aminosäureseitenketten in den vier Porenschleifen formen zudem einen ringförmigen Selektivitätsfilter (Heinemann et al., 1992). Strukturen, die eine Änderung des Membranpotentials detektieren können und somit dem Schalten der Na_V-Kanäle Spannungsabhängigkeit verleihen, sind die jeweils vierten Transmembransegmente (S4) der vier homologen Domänen. Schon die ersten Untersuchungen an S4 in D1 bestätigten die Funktion dieser Segmente als Spannungssensoren (Stühmer et al., 1989). Da die Spannungssensoren mehrere positiv geladene Aminosäureseitenketten tragen, nimmt man an, dass sie auf eine depolarisationsinduzierte Änderung des elektrischen Feldes in der Membran mit einer Bewegung durch dieses Feld reagieren. Diese spannungsabhängige Konformationsänderung der S4-Segmente führt zur Aktivierung der Na_V-Kanäle und damit zur Öffnung der Pore (Yang und Horn, 1995; Yang et al., 1996). Das eigentliche Aktivierungstor, welches als maßgebliche Struktur zum Öffnen der Pore mit den Spannungssensoren zusammenwirkt, wird zwar auf der

intrazellulären Seite der Kanäle vermutet, seine genaue Lokalisation ist jedoch noch nicht gelungen (Armstrong und Hille, 1998).

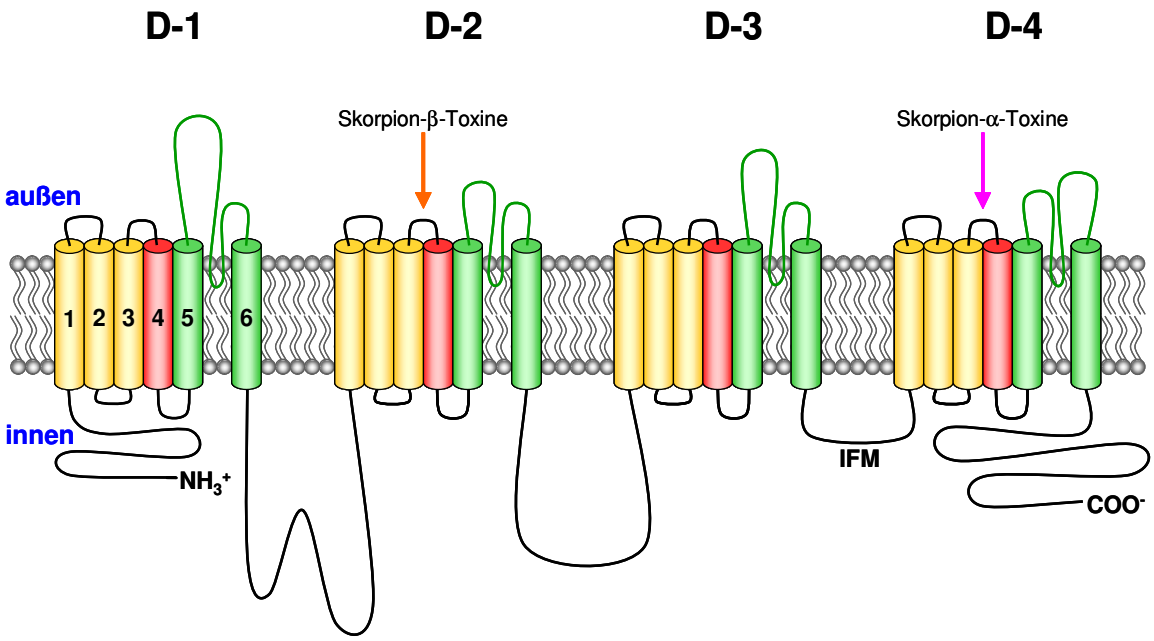

Abb. 2: Membrantopologie der α-Untereinheit eines Na_V-Kanals. Die vier homologen Domänen (D1-4) werden von je sechs Transmembransegmenten (S1-S6) geformt. Die Spannungssensoren sind rot und die porenbildenden Kanalbereiche grün dargestellt. Die Interaktionsstellen der Skorpion-α- und -β-Toxine an den Spannungssensoren in D2 und D4 sind mit Pfeilen gekennzeichnet.

Die spontan einsetzende Aktivierung der Kanäle vermittelt ein hydrophobes Isoleucin-Phenylalanin-Methionin-Motiv (IFM-Motiv) im Linker, welcher D3 mit D4 verbindet (Vassilev et al., 1989; West et al., 1992). Ein Verschluss der intrazellulären Seite der Pore durch die IFM-Triade scheint dabei den Mechanismus der schnellen Kanalinaktivierung darzustellen (Eaholtz et al., 1994). Die Interaktionsstellen für den IFM-Inaktivierungslinker befinden sich am intrazellulären Ende von S6 in D4 (McPhee et al., 1995), im Linker S4-S5 in D3 (Smith und Goldin, 1997) sowie im Linker S4-S5 in D4 (Lerche et al., 1997; Filatov et al., 1998; McPhee et al., 1998; Tang et al., 1998). Neben dem IFM-Linker wurden jedoch auch C-terminale Strukturen der Kanäle mit dem Inaktivierungsvorgang in Verbindung gebracht (Cormier et al., 2002).

Eine weitere, jedoch weniger gut verstandene Form der Kanalinaktivierung ist durch eine besonders langsam verlaufende Rückkehr zur aktivierbaren Kanalkonformation charakterisiert. Ein Mitwirken der Porenschleifen der vier homologen Domänen der α-Untereinheit und der assoziierten β-Untereinheiten an diesem als langsame Inaktivierung bezeichneten Vorgang konnte bereits nachgewiesen werden (z.B. Vilin et al., 1999).

1.3 Na_V-Kanal-spezifische Neurotoxine aus Skorpionen und marinen Kegelschnecken

Viele Tiere setzen Gift ein, um ihre Beute schnell zu töten und um Fressfeinde abzuwehren. Eine sehr effiziente Strategie ist dabei die Störung der Erregungsleitung der Opfer mit Hilfe spezifischer Neurotoxine. Aufgrund der tragenden Rolle der Na_V-Kanäle bei der Verarbeitung elektrischer Reize ist es deshalb nicht verwunderlich, dass einige giftige Tiere auch äußerst potente Na_V-Kanal-spezifische Toxine entwickelt haben. Diese Toxine werden, entsprechend ihrer Fähigkeit zur gegenseitigen Kompetition, unterschiedlichen Bindestellen am Kanal, sog. *receptor sites* (RS), zugeordnet (z.B. Janiszewski, 1990; Catterall et al., 1992; Cestèle und Catterall, 2000). Basierend auf ihrer chemischen Natur werden diese Neurotoxine in zwei Gruppen gegliedert - in Peptidtoxine und niedermolekulare Substanzen. Neben giftigen Tieren produzieren aber auch einige giftige Pflanzen Na_V-Kanal-spezifische Toxine. Tabelle 1 gibt einen Überblick über bekannte Na_V-Kanal-aktive Toxine giftiger Tiere und Pflanzen sowie deren Wirkung auf die Kanäle.

RS	Toxine	Effekte
1	Tetrodotoxin (TTX) Saxitoxin (STX) μ-Conotoxine	Blockade der Kanalpore
2	Batrachotoxin (BTX) Veratridin Aconitin Grayanotoxin	Persistente Kanalaktivierung
3	Skorpion-α-Toxine einige Seeanemonen- und Spinnentoxine	Unterdrückung der schnellen Inaktivierung
4	Skorpion-β-Toxine	Senkung der Aktivierungsschwelle
5	Brevetoxin Ciguatoxin	Senkung der Aktivierungsschwelle, Unterdrückung der schnellen Inaktivierung
6	*δ-Conotoxine	Unterdrückung der schnellen Inaktivierung
n.d.	*stimulierende Skorpiontoxine	Fördern die Erregungsleitung
n.d.	*dämpfende Skorpiontoxine	Dämpfen die Erregungsleitung
n.d	*μO-Conotoxine	Kanalblockade
n.d.	**Goniopora*-Korallentoxin	Unterdrückung der schnellen Inaktivierung

Tab. 1: Übersicht über bekannte Na_V-Kanal-spezifische Neurotoxine aus giftigen Tieren und Pflanzen. Bisher wurden sechs Toxinbindestellen (RS) definiert (RS1-6) und fünf davon (RS1-5) molekular näher charakterisiert (z.B. Janiszewski, 1990; Catterall et al., 1992; Cestèle und Catterall, 2000). Für die mit * gekennzeichneten Toxinklassen ist weder ihre RS auf molekularer Ebene noch der zugrunde liegende Wirkmechanismus bekannt (n.d.: nicht definiert).

Wie aus dieser Übersicht zu entnehmen ist, können die einzelnen Toxinklassen völlig verschiedene Effekte induzieren. Beispielsweise bindet das niedermolekulare Nervengift TTX aus Kugelfischen an RS1 in der Kanalpore (Terlau et al., 1991) und blockiert auf diese Weise sehr effizient den Fluss von Na^+-Ionen in die Zelle. Die ebenfalls niedermolekularen RS2-Toxine, wie z.B. das Alkaloidsteroid BTX aus dem Sekret von Fröschen der Gattung *Phyllobates*, induzieren hingegen einen persistierenden Na^+-Einstrom in die Zelle, der zur Übererregung führt (Trainer et al., 1996). Eine besondere Stellung unter den Na_V-Kanaltoxinen nehmen jedoch einige Peptide aus Skorpionen und marinen Kegelschnecken ein, da sie trotz homologer Raumstrukturen unterschiedliche, ja sogar völlig gegensätzliche Effekte in den Kanälen hervorrufen.

Das Gift von Skorpionen enthält zwei Klassen von Na_V-Kanal-spezifischen Peptidtoxinen: α- und β-Toxine. Sie zählen mit einer Länge von 58-76 Aminosäuren zu den langkettigen Skorpiontoxinen (z.B. Rodríguez de la Vega und Possani, 2005; Zuo und Ji, 2004). Die Aminosäuresequenzen beider Klassen unterscheiden sich zwar stark, doch ihre räumliche Struktur ist hoch konserviert: Vier Disulfidbrücken stabilisieren eine kurze α-Helix und ein meist dreisträngiges β-Faltblatt (Possani et al., 1999; Abb. 3A). Während α-Toxine an RS3 binden und die schnelle Inaktivierung von Na_V-Kanälen hemmen, binden β-Toxine an RS4 und senken die Aktivierungsschwelle der Kanäle.

Die α-Toxine interagieren sowohl mit den Porenschleifen in D1 und D4 als auch mit dem Linker S3-S4 der vierten Kanalaldomäne (Tejedor und Catterall, 1988; Thomson und Catterall, 1989; Rogers et al., 1996). Der Linker D4S3-S4 stellt dabei jedoch den funktionell wichtigsten Bestandteil von RS3 dar (Rogers et al., 1996) (Abb. 2). Der Verschluss der Kanalpore durch das IFM-Motiv ist an die Auswärtsbewegung (Aktivierung) des D4-Spannungssensors gekoppelt. Es wird vermutet, dass α-Toxine die depolarisationsinduzierte Auswärtsbewegung dieses Spannungssensors durch eine Interaktion mit dem Linker D4S3-S4 blockieren und auf diese Weise die Inaktivierung der Kanäle verlangsamen (Rogers et al., 1996; Sheets et al., 1999). Ähnlich wie α-Toxine wirken auch β-Toxine über die Interaktion mit einem Spannungssensor der Kanäle, jedoch nicht in D4, sondern in D2 (Abb. 2). Man nimmt an, dass β-Toxine spezifisch die aktivierte (auswärtsbewegte) Konformation des D2-Spannungssensors stabilisieren und somit die Aktivierungsschwelle des gesamten Kanals herabsetzen. Auf diese Weise öffnen Na_V-Kanäle in Gegenwart von β-Toxinen bereits bei Membranspannungen, bei denen sie normalerweise noch geschlossen sind (Cestèle et al., 1998). Dieser als *voltage sensor trapping* bezeichnete Mechanismus impliziert zudem eine *use-dependence* (Aktivitätsabhängigkeit) der β-Toxine, d.h. β-Toxine wirken umso stärker, je häufiger die Kanäle aktiviert werden. Dennoch sind β-Toxine in

der Lage, neben der Senkung der Aktivierungsschwelle gleichzeitig einen Teil der Na_V-Kanäle zu blockieren (z.B. Yatani et al., 1988; Gordon et al., 2003; Borges et al., 2004). Die molekulare Basis dieser dualen Wirkung ist jedoch unbekannt. Weitere Interaktionsstellen der β-Toxine befinden sich wahrscheinlich in der Porenschleife von Domäne-3 und dem extrazellulären Linker, welcher die Transmembransegmente S1 und S2 der zweiten Kanaldomäne miteinander verbindet (Gordon et al., 1992; Cestèle et al., 1998). Aufgrund ihrer Interaktion mit Spannungssensoren der Na_V-Kanäle zählen sowohl α- als auch β-Toxine zur Gruppe der Spannungssensor-Toxine. Abbildung 3 stellt die unterschiedlichen Effekte des α-Toxins Lqh3 aus *Leiurus quinquestriatus hebraeus* und des β-Toxins Tz1 aus *Tityus zulianus* exemplarisch am Skelettmuskelkanal $Na_V1.4$ gegenüber.

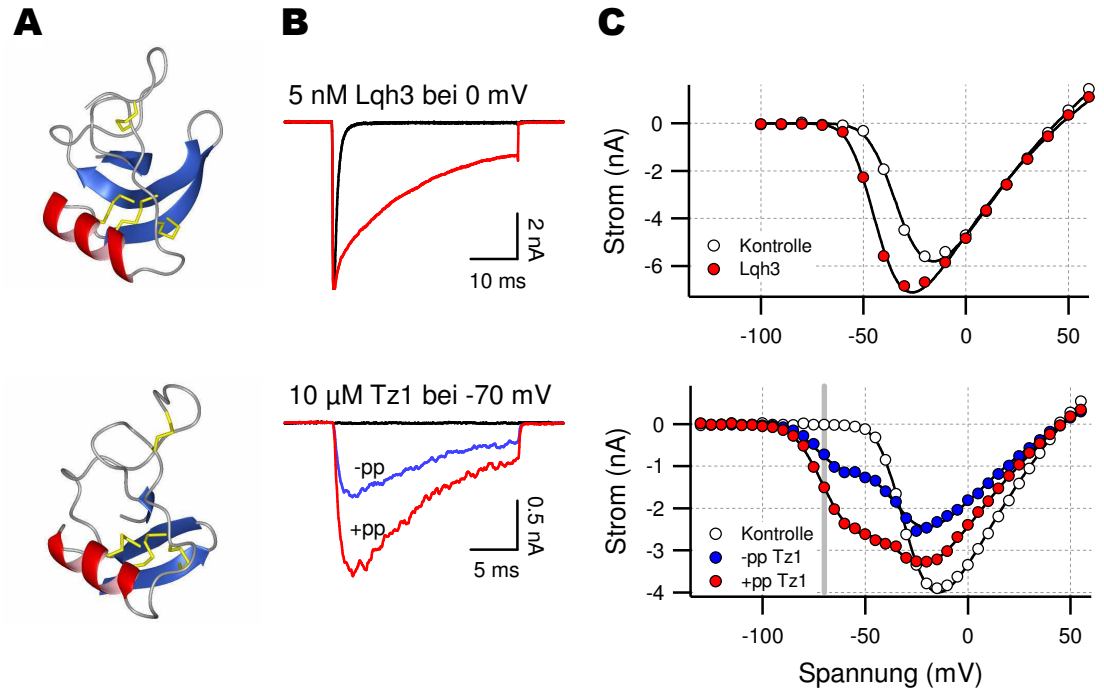

Abb. 3: Daten zur Illustration der Wirkung von Skorpion-α- und -β-Toxinen auf $Na_V1.4$-Kanäle der Ratte *Rattus norvegicus*. **(A)** Raumstrukturen des α-Toxins Lqh3 (oben: 1BMR, Krimm et al., 1999) und des β-Toxins Ts1 (unten: 1NPI, Pinheiro et al., 2003). Ts1 und Tz1 besitzen eine zu 63% identische Aminosäuresequenz. **(B)** Die obere Figur zeigt Stromantworten von $Na_V1.4$-Kanälen bei einer Membranspannung von 0 mV vor (schwarz) sowie nach (rot) Applikation von Lqh3. Die untere Figur zeigt Stromantworten von $Na_V1.4$-Kanälen bei einer Membranspannung von -70 mV in Abwesenheit (schwarz) und Gegenwart von Tz1 vor (blau, -pp) sowie nach (rot, +pp) Applikation eines Spannungspulses (pp) auf -10 mV. Der Spannungspuls auf -10 mV dient dabei der Kanalaktivierung vor dem zweiten Testpuls (rot, +pp) und macht die *use-dependence* von Tz1 sichtbar (Borges et al., 2004). **(C)** Strom-Spannungs-Charakteristiken von $Na_V1.4$-Kanälen in Abwesenheit und Gegenwart von 5 nM Lqh3 (oben) und 10 µM Tz1 (unten). Der graue Balken in der unteren Figur markiert -70 mV, ein Potential bei dem Na_V-Kanäle normalerweise geschlossen sind.

Die Peptide im Gift mariner Kegelschnecken gliedern sich in Disulfid-freie und Disulfid-reiche Conotoxine. Entsprechend der Anordnung der Cysteinreste in ihrer Primärstruktur werden diese Toxine in Strukturfamilien eingeteilt. Die ca. 25-35 Reste langen Conotoxine der O-Familie enthalten drei Disulfidbrücken und sind durch die Cysteinabfolge C-C-CC-C-C in ihrer Aminosäuresequenz charakterisiert (Terlau und Olivera, 2004). Neben den Na_V-Kanal-spezifischen δ- und μO-Conotoxinen gehören auch die κ- und ω-Conotoxine, welche mit spannungsabhängigen Kalium- bzw. Kalziumkanälen interagieren, zur O-Familie. Helix- und Faltblattstrukturen sind jedoch in den Raumstrukturen dieser Toxinfamilie weniger stark ausgeprägt als in den Strukturen der langkettigen Skorpiontoxine.

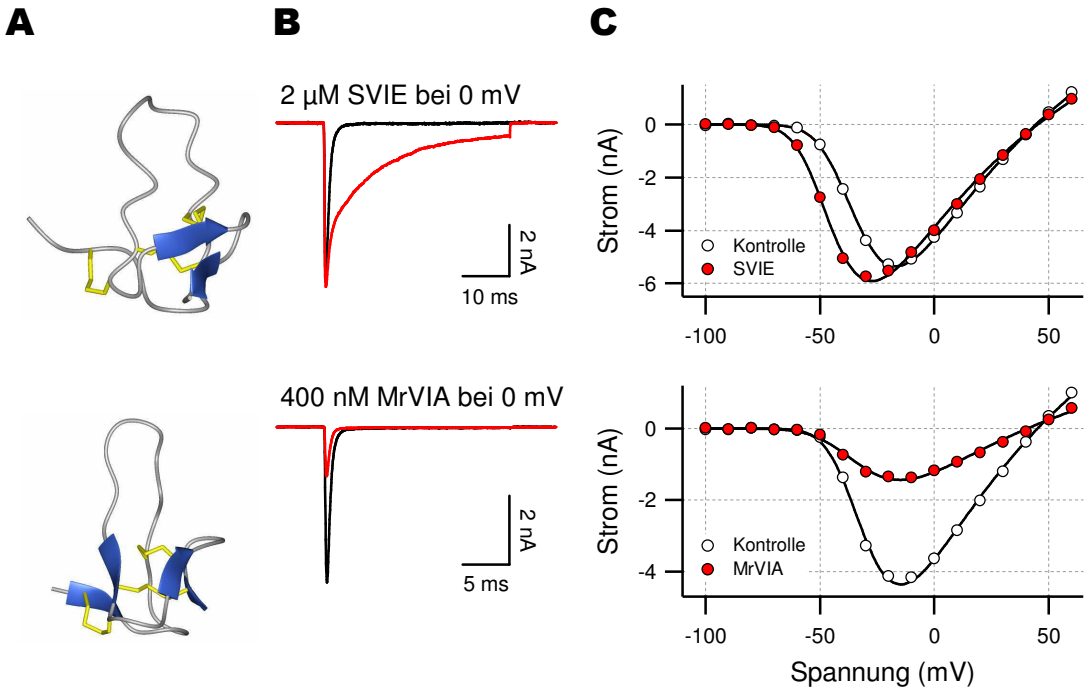

Abb. 4: Daten zur Illustration der Wirkung von δ- und μO-Conotoxinen auf $Na_V1.4$-Kanäle der Ratte *Rattus norvegicus*. **(A)** Raumstrukturen des δ-Toxins EVIA (oben: 1G1P, Volpon et al., 2000; 32% Sequenzidendität zu SVIE) und des μO-Toxins MrVIB (unten: 1RMK, Daly et al., 2004; 90% Sequenzidendität zu MrVIA). **(B)** Stromantworten von $Na_V1.4$-Kanälen bei einer Membranspannung von 0 mV vor (schwarz) und nach (rot) Applikation von SVIE (oben) sowie MrVIA (unten). **(C)** Strom-Spannungs-Charakteristiken von $Na_V1.4$-Kanälen in Abwesenheit und Gegenwart von 2 μM SVIE (oben) und 400 nM MrVIA (unten).

Weitere Besonderheiten der Conotoxine sind ihre ausgeprägte Hydrophobizität sowie das Auftreten posttranslational modifizierter Aminosäuren (z.B. 4-Hydroxyprolin und γ-Carboxyglutamat) in ihrer Proteinsequenz (Craig et al., 1999). Während δ-Conotoxine, ähnlich wie Skorpion-α-Toxine, die schnelle Inaktivierung von Na_V-Kanälen verlangsamen, blockieren μO-Conotoxine Na_V-Kanäle.

Für δ-Conotoxine wurde zwar RS6 als Bindestelle an Na_V-Kanälen definiert (Fainzilber et al., 1994), doch weder die Lokalisation von RS6 noch die Aufklärung des Wirkmechanismus der δ-Conotoxine ist bisher gelungen (Cestèle und Catterall, 2000; Tab.1). Die Erforschung ihrer Interaktion mit Na_V-Kanälen wird weiterhin durch die Tatsache erschwert, dass die meisten bekannten δ-Conotoxine, wie z.B. TxVIA und GmVIA, spezifisch für Na_V-Kanäle aus Mollusken sind (Hillyard et al., 1989; Hasson et al., 1993; Sohn et al., 1994) und demzufolge nicht an den gut zugänglichen Säugerkanälen untersucht werden können. Ähnlich ist die Situation bei μO-Conotoxinen. MrVIA und MrVIB, beide aus *Conus marmoreus*, sind die einzigen bekannten Vertreter der Klasse der μO-Conotoxine. Sie blockieren Na_V-Kanäle, werden jedoch nicht durch den potenten und gut untersuchten Porenblocker STX von ihrer Bindestelle verdrängt (Terlau et al., 1996). Dieses Resultat belegt, dass die Blockade von Na_V-Kanälen durch μO-Conotoxine nicht auf einen Verschluss der Kanalpore durch diese Toxine zurückgeführt werden kann. Auch für μO-Conotoxine sind die Interaktionsstellen an Na_V-Kanälen sowie der zugrunde liegende Wirkmechanismus unbekannt. Die Effekte von δ-Conotoxin SVIE aus *Conus striatus* und μO-Conotoxin MrVIA auf $Na_V1.4$-Kanäle sind in Abb. 4 dargestellt.

Die in Abb. 3 und 4 gezeigten Daten belegen eine komplexe Verwandtschaft der Skorpion-α- und -β-Toxine mit den δ- und μO-Conotoxinen. Obwohl sich Skorpion-α- und δ-Conotoxine bezüglich ihrer Herkunft und ihrer Raumstrukturen ganz erheblich unterscheiden, sind sie funktionell verwandt, denn die Vertreter beider Toxinklassen hemmen die schnelle Inaktivierung von Na_V-Kanälen (Vergleich Abb. 3 und Abb. 4). Andererseits bilden α- mit β-Toxinen und δ- mit μO-Toxinen je eine strukturverwandte Gruppe. Dennoch unterscheiden sich die Wirkungen der Toxine innerhalb einer Strukturgruppe stark. Es stellt sich somit die Frage, wie einerseits strukturell unterschiedliche Toxine eine identische Wirkung auf Na_V-Kanäle erzielen und wie andererseits Toxine mit homologen Strukturen verschiedene Wirkungen auf die Kanäle ausüben können. Da diese Toxine die Kanalfunktionen offensichtlich in sehr komplizierter Weise modulieren, trägt die Erforschung ihrer molekularen Wirkmechanismen auch zu einem umfassenderen Verständnis der Funktionsweise von Na_V-Kanälen bei.

Eine weitere Eigenschaft dieser Neurotoxine ist ihre Fähigkeit, oftmals nur bestimmte Na_V-Kanalsubtypen einer Spezies, z.B. nur neuronale Kanäle, in ihrer Funktion zu beeinflussen. Aufgrund dieser Subtypspezifität stellen diese Toxine interessante Leitstrukturen zur Entwicklung subtypspezifischer und somit nebenwirkungsarmer Therapeutika dar. Beispielsweise wären Substanzen, welche die neuronalen Kanäle $Na_V1.7$, 1.8 bzw. 1.9 spezifisch blockieren, erfolgversprechende Analgetika (Waxman et al., 1999). Die Na_V-Kanal-hemmenden μO-Conotoxine haben diesbezüglich ein

entsprechendes Potential (Daly et al., 2004). Viele Na_V-Kanal-spezifische Toxine unterscheiden jedoch nicht nur zwischen den verschieden Kanalsubtypen einer Spezies, sondern auch zwischen den Kanälen verschiedener Phyla. Beispielsweise besitzen Na_V-Kanal-spezifische Skorpiontoxine oftmals eine unterschiedliche Spezifität für Insekten- und Säugerkanäle. Der Einsatz insektenspezifischer Na_V-Kanaltoxine aus Skorpionen als alternative Insektizide wird deshalb bereits erprobt (Moeda et al., 1991; Stewart et al., 1991; Zlotkin et al., 2000; Regev et al., 2003).

Trotz des enormen Potentials der Na_V-Kanal-spezifischen Toxine aus Skorpionen und marinen Kegelschnecken ist die molekulare Basis ihrer Subtypspezifität nur wenig erforscht. Ein genaues Verständnis dieser Subtypspezifität auf molekularer Ebene ist jedoch die Voraussetzung, um die komplexen Wirkmechanismen dieser Toxine zu entschlüsseln. In der vorliegenden Dissertation habe ich deshalb die Wirkung ausgewählter Vertreter der Skorpion-α- und β-Toxine sowie der δ- und μO-Conotoxine auf verschiedene, heterolog-exprimierte, Na_V-Kanalsubtypen aus Säugern systematisch untersucht. Die folgenden Arbeiten enthalten die Resultate meiner Untersuchungen zur Subtypspezifität der Skorpion-α-Toxine Lqh2, Lqh3, LqhαIT, des Skorpion-β-Toxins Tz1 sowie der μO-Conotoxine MrVIA und MrVIB:

Leipold E., Lu S., Gordon D., Hansel A. and Heinemann S.H. (2004). Combinatorial interaction of scorpion toxins Lqh-2, Lqh-3 and LqhαIT with sodium channel receptor sites-3 Molecular Pharmacology *65*: 685-691.

Borges A., Alfonzo M.J., Garcia C.C., Winand N.J., Leipold E., and Heinemann S.H. (2004). Isolation, molecular cloning and functional characterization of a novel β-toxin from the Venezuelan scorpion, *Tityus zulianus.* Toxicon *43*: 671-684.

Leipold E., Hansel A., Borges A. and Heinemann S.H. (2006a). Subtype specificity of scorpion β-toxin Tz1 interaction with voltage-gated sodium channels is determined by the pore loop of domain-3. *zur Publikation angenommen bei* Molecular Pharmacology.

Zorn S., Leipold E., Hansel A., Bulaj G., Olivera B.M., Terlau H. and Heinemann S.H. (2006). The μO-conotoxin MrVIA inhibits voltage-gated sodium channels by associating with domain-3. FEBS Letters *580*: 1360-1364.

In diesen Arbeiten konnten die Kanalepitope identifiziert werden, welche den Na_V-Kanälen aus Säugern die Sensitivität für die unterschiedlichen Neurotoxine verleihen. Damit wurden auch die Voraussetzungen zur Aufklärung der molekularen Wirkmechanismen dieser Toxine geschaffen. Basierend auf diesen Untersuchungen ist es mir in den folgenden Arbeiten gelungen, die bisher unbekannten Wirkmechanismen der δ- und μO-Conotoxine aufzudecken und den allgemein akzeptierten Wirkmechanismus der Skorpion-β-Toxine um wichtige Aspekte zu erweitern:

Leipold E., Hansel A., Olivera B.M., Terlau H. and Heinemann S.H. (2005). Molecular interaction of δ-conotoxins with voltage-gated sodium channels. FEBS Letters *579*: 3881-3884.

Leipold E., Borges A. and Heinemann S.H. (2006b). Quantitative description of the interaction between scorpion β-toxin Tz1 and voltage-gated sodium channels. *in Vorbereitung für* Journal of General Physiology.

Leipold E., Zorn S., Hansel A., Terlau H., Olivera B.M. and Heinemann S.H. (2006c). The μO conotoxin MrVIA inhibits voltage-gated sodium channels by immobilizing the voltage sensor in domain-2. *in Vorbereitung für* The Journal of Neuroscience.

2. Übersicht zu den Manuskripten

Leipold E., Lu S., Gordon D., Hansel A. and Heinemann S.H. (2004). Combinatorial interaction of scorpion toxins Lqh-2, Lqh-3 and LqhαIT with sodium channel receptor sites-3. Molecular Pharmacology *65*: 685-691.

Inhalt:

In dieser Studie wurden verschiedene Na_V-Kanalwildtypen sowie -mutanten in HEK293-Zellen exprimiert und hinsichtlich ihrer Sensitivität gegenüber Lqh2, Lqh3 und LqhαIT (aus *Leiurus quinquestriatus hebreaus*) funktionell untersucht. Die unterschiedliche Sensitivität einiger Kanalsubtypen für diese Toxine konnten wir auf zwei nicht konservierte Aminosäuren im Linker S3-S4 der homologen Domäne-4 der Kanäle zurückführen. Diese beiden Positionen determinieren die unterschiedliche Sensitivität der untersuchten Natriumkanäle für Lqh2, Lqh3 und LqhαIT in kombinatorischer Weise.

Eigenanteil:

	Tätigkeit	Eigenanteil
Zellkultur	Pflege und Transfektion von HEK293-Zellen	70%
Molekularbiologie	Herstellung von Kanalmutanten	0%
Elektrophysiologie	Messung transient sowie stabil transfizierter HEK293-Zellen mittels der Patch-Clamp-Technik	70%
Präsentation	Analyse und Auswertung der Daten Anfertigung des Manuskripts	15% 10%

Leipold E., Hansel A., Olivera B.M., Terlau H. and Heinemann S.H. (2005). Molecular interaction of δ-conotoxins with voltage-gated sodium channels. FEBS Letters *579*: 3881-3884.

Inhalt:

In dieser Arbeit untersuchten wir nach welchem molekularen Mechanismus das δ-Conotoxin SVIE aus der marinen Kegelschnecke *Conus striatus* die schnelle Inaktivierung von Na_V-Kanälen beeinflusst. Während SVIE mit dem α-Toxin Lqh2 um die Bindung an Natriumkanäle konkurriert, wirkt es in Kombination mit dem α-Toxin Lqh3 in synergistischer Weise. Am Beispiel von SVIE zeigten wir erstmals, dass δ-Conotoxine, ähnlich wie Skorpion-α-Toxine, mit dem Spannungssensor der vierten Kanaldomäne wechselwirken.

Eigenanteil:

	Tätigkeit	Eigenanteil
Zellkultur	Pflege und Transfektion von HEK293-Zellen	100%
Molekularbiologie	Herstellung von Kanalmutanten	10%
Elektrophysiologie	Messung transient transfizierter HEK293-Zellen mittels der Patch-Clamp-Technik	100%
Präsentation	Analyse und Auswertung der Daten Anfertigung des Manuskripts	90% 10%

Borges A., Alfonzo M.J., Garcia C.C., Winand N.J., Leipold E., and Heinemann S.H. (2004). Isolation, molecular cloning and functional characterization of a novel β-toxin from the Venezuelan scorpion, *Tityus zulianus*. Toxicon *43*: 671-684.

Inhalt:

Diese Arbeit beschreibt die Isolation, die Klonierung sowie die funktionelle Charakterisierung von Tz1, der Hauptkomponente des Venoms vom venezuelanischen Skorpion *Tityus zulianus*. Wir identifizierten Tz1 als typisches Skorpion-β-Toxin und charakterisierten seine Wirkung auf die muskulären Kanäle $Na_V1.4$ und $Na_V1.5$.

Eigenanteil:

	Tätigkeit	Eigenanteil
Zellkultur	Pflege und Transfektion von HEK293-Zellen	100%
Elektrophysiologie	Messung transient sowie stabil transfizierter HEK293-Zellen mittels der Patch-Clamp-Technik	100%
Präsentation	Analyse und Auswertung der Daten	10%
	Anfertigung des Manuskripts	10%

Leipold E., Hansel A., Borges A. and Heinemann S.H. (2006a). Subtype specificity of scorpion β-toxin Tz1 interaction with voltage-gated sodium channels is determined by the pore loop of domain-3. *zur Publikation angenommen bei* Molecular Pharmacology.

Tag der Annahme: 25.04.2006

Inhalt:

Das Skorpion β-Toxin Tz1 verringert subtypspezifisch die Aktivierungsschwelle von Natriumkanälen. Wir zeigten, dass die spezifische Struktur der Porenschleife der homologen Kanaldomäne-3 die unterschiedliche Sensitivität neuronaler ($Na_V1.2$, $Na_V1.6$, $Na_V1.7$) sowie muskulärer Kanäle ($Na_V1.4$) gegenüber Tz1 determiniert. Die Rezeptorstelle für β-Toxine besteht demnach aus mindestens zwei funktionell wichtigen Teilen, einem spezifitätsvermittelnden Epitop in der Porenschleife von Domäne-3 und einem Wirkepitop im Spannungssensor von Domäne-2 der Kanäle.

Eigenanteil:

	Tätigkeit	Eigenanteil
Zellkultur	Pflege und Transfektion von HEK293-Zellen	100%
Molekularbiologie	Herstellung von Kanalchimären und -mutanten	100%
Elektrophysiologie	Messung transient transfizierter HEK293-Zellen mittels der Patch-Clamp-Technik	100%
Präsentation	Analyse und Auswertung der Daten Anfertigung des Manuskripts	100% 30%

***Zorn S., *Leipold E., Hansel A., Bulaj G., Olivera B.M., Terlau H. and Heinemann S.H. (2006). The µO-conotoxin MrVIA inhibits voltage-gated sodium channels by associating with domain-3. FEBS Letters *580*: 1360-1364.**

*diese Autoren leisteten gleiche Beiträge

Inhalt:

Die µO-Conotoxine MrVIA und MrVIB blockieren Natriumkanäle subtypspezifisch mit Hilfe eines noch unverstandenen Mechanismus. Am Beispiel von MrVIA zeigten wir erstmals, dass µO-Conotoxine mit der Porenschleife der homologen Domäne-3 der Na_V-Kanäle interagieren und dass die Struktur dieser Schleife die Kanal-spezifische Sensitivität für MrVIA vermittelt.

Eigenanteil:

	Tätigkeit	Eigenanteil
Zellkultur	Pflege und Transfektion von HEK293-Zellen	0%
Molekularbiologie	Herstellung von Kanalchimären und -mutanten	100%
Elektrophysiologie	Messung transient sowie stabil transfizierter HEK293-Zellen mittels der Patch-Clamp-Technik	0%
Präsentation	Analyse und Auswertung der Daten, Anfertigung des Manuskripts	0%

Leipold E., Borges A. and Heinemann S.H. (2006b). Quantitative description of the interaction between scorpion β-toxin Tz1 and voltage-gated sodium channels. *in Vorbereitung für* Journal of General Physiology.

Inhalt:

Neben der Verringerung der Aktivierungsschwelle von Natriumkanälen zeigen Skorpion-β-Toxine einen weiteren, jedoch kaum untersuchten Effekt: Sie blockieren Natriumkanäle in Abhängigkeit vom Membranpotential. In dieser Studie untersuchten wir die gegensätzlichen Effekte „Reduzierung der Aktivierungsschwelle“ und „Kanalblock“ des β-Toxins Tz1 quantitativ. Die erhaltenen Ergebnisse sprechen für ein Modell, in dem Tz1 den Spannungssensor der Domäne-2 in Abhängigkeit der Membranspannung in seiner aktivierten Konformation („Reduzierung der Aktivierungsschwelle“) oder seiner deaktivierten Konformation („Kanalblock“) stabilisiert.

Eigenanteil:

	Tätigkeit	Eigenanteil
Zellkultur	Pflege und Transfektion von HEK293-Zellen	100%
Molekularbiologie	Herstellung von Kanalmutanten	100%
Elektrophysiologie	Messung transient sowie stabil transfizierter HEK293-Zellen mittels der Patch-Clamp-Technik	100%
Präsentation	Analyse und Auswertung der Daten Anfertigung des Manuskripts	80% in Vorbereitung

Leipold E., Zorn S., Hansel A., Terlau H., Olivera B.M. and Heinemann S.H. (2006c). The µO conotoxin MrVIA inhibits voltage-gated sodium channels by immobilizing the voltage sensor in domain-2. ***in Vorbereitung für*** **The Journal of Neuroscience.**

Inhalt:

In dieser Arbeit klärten wir den bis dahin unbekannten molekularen Wirkmechanismus der µO-Conotoxine am Beispiel von MrVIA auf. Während die Sensitivität der Kanäle für dieses Toxin von deren Porenschleife in Domäne-3 vermittelt wird, blockt MrVIA die Kanäle, indem es spezifisch die Aktivierung des Spannungssensors der Kanaldomäne-2 und somit die Aktivierung des gesamten Kanals unterbindet. Entsprechend unseren Ergebnissen benötigen µO-Conotoxine, ähnlich wie Skorpion-β-Toxine, zwei Epitope an Na_V-Kanälen, um ihre Wirkung zu entfalten, ein Bindeepitop in der Porenschleife von Domäne-3 sowie ein Wirkepitop am Spannungssensor in Domäne-2 der Kanäle.

Eigenanteil:

	Tätigkeit	Eigenanteil
Zellkultur	Pflege und Transfektion von HEK293-Zellen	30%
Molekularbiologie	Herstellung von Kanalmutanten	100%
Elektrophysiologie	Messung transient sowie stabil transfizierter HEK293-Zellen mittels der Patch-Clamp-Technik	30%
Präsentation	Analyse und Auswertung der Daten Anfertigung des Manuskripts	in Vorbereitung

0026-895X/04/6503-685–691$20.00
MOLECULAR PHARMACOLOGY
Copyright © 2004 The American Society for Pharmacology and Experimental Therapeutics
Mol Pharmacol 65:685–691, 2004

Vol. 65, No. 3
2969/1132905
Printed in U.S.A.

Combinatorial Interaction of Scorpion Toxins Lqh-2, Lqh-3, and LqhαIT with Sodium Channel Receptor Sites-3

Enrico Leipold, Songqing Lu, Dalia Gordon, Alfred Hansel, and Stefan H. Heinemann

Research Unit "Molecular and Cellular Biophysics", Medical Faculty of the Friedrich Schiller University Jena, Jena, Germany (E.L., S.L., A.H., S.H.H.); and Department of Plant Sciences, Tel Aviv University, Tel Aviv, Israel (D.G.)

Received September 15, 2003; accepted December 3, 2003

This article is available online at http://molpharm.aspetjournals.org

ABSTRACT

Scorpion α-toxins LqhαIT, Lqh-2, and Lqh-3 are representatives of three groups of α-toxins that differ in their preference for insects and mammals. These α-insect, antimammalian, and α-like toxins bind to voltage-gated sodium channels and slow down channel inactivation. Sodium channel mutagenesis studies using various α-toxins have shown that they interact with receptor site 3, which is composed mainly of a short stretch of amino-acid residues between S3 and S4 of domain 4. Variation in this region results in marked differences between various subtypes of sodium channels with respect to their sensitivity to the three Lqh toxins. We incorporated the S3-S4 linker of domain 4 from $hNa_V1.2$/$hNa_V1.1$, $hNa_V1.3$, $hNa_V1.6$, and $hNa_V1.7$ channels as well as individual point mutations into the $rNa_V1.4$ skeletal muscle sodium channel. Our data show that the affinity of Lqh-3 and LqhαIT to sodium channels is markedly determined by an aspartate residue (Asp1428 in $rNa_V1.4$); when mutated to glutamate, as is present in $Na_V1.1$–1.3 channels, Lqh-3–channel interactions are abolished. The interaction of Lqh-2 and LqhαIT, however, is strongly reduced when a lysine residue (Lys1432 in $rNa_V1.4$) is replaced by threonine (as in $hNa_V1.7$), whereas this substitution is without effect for Lqh-3. The influence of Lys1432 on Lqh-2 and LqhαIT strongly depends on the context of the Asp/Glu site at position 1428, giving rise to a wide variety of toxicological phenotypes by means of a combinatorial mixing and matching of only a few residues in receptor site 3.

Voltage-gated sodium (Na_V) channels consist of a large (~260 kDa) pore-forming α-subunit, composed of four homologous domains (D1–D4), each with six transmembrane segments (S1–S6) and a hairpin-like pore region between S5 and S6. Because of their structural conservation in vertebrates and invertebrates and their pivotal role in cellular excitability, Na_V channels are targeted by a large variety of chemically distinct toxins, many of which do not differentiate among channel subtypes (Catterall, 1992; Gordon, 1997). However, some scorpion neurotoxins show specificity for insect or mammalian Na_V channels, and others are able to differentiate between Na_V subtypes in mammalian neurons (Gordon et al., 2002). This selectivity is attributed to differences of active sites on the toxins and to variations in receptor binding sites on distinct Na_V channels that, when identified, may be used for design of selective drugs.

Scorpion toxins affecting Na_V channels are 61- to 76-residue polypeptides that comprise two major classes, α- and β-toxins, according to their mode of action and binding properties to distinct sites (receptor sites-3 and -4, respectively) on Na_V channels (Martin-Eauclaire and Couraud, 1995; Gordon et al., 1998). α-Toxins inhibit Na_V channel inactivation in various excitable preparations, but they show vast differences in preference for insect and mammalian Na_V channels. Accordingly, they are divided into classic α-toxins, which are highly active in mammalian brain [e.g., Lqh-2 (*Leiurus quinquestriatus hebraeus*)]; α-toxins, which are very active in insects (e.g., LqhαIT); and α-like toxins, which are active in both the mammalian and insect central nervous system (CNS) (e.g., Lqh-3) (Gordon et al., 1996, 2002; Sautiere et al., 1998; Gilles et al., 1999, 2000a; Krimm et al., 1999).

Despite differences in toxicity and binding properties, all scorpion α-toxins bind to receptor site 3, the structural features of which are still elusive, but known to involve the extracellular loops S5–S6 of D1 and D4 (Tejedor and Catterall, 1988; Thomson and Catterall, 1989) and S3–S4 of D4 of rat $Na_V1.2$ (Catterall, 1992, 2000; Rogers et al., 1996). Mutagenesis within the external linker S3–S4 in domain 4 of rat brain $Na_V1.2$ identified a negatively charged residue, Glu1613, as a major determinant that affects the binding of a classic scorpion α-toxin (Rogers et al., 1996).

Mammalian Na_V channels are encoded by a gene family.

This work was supported by grants from the Deutsche Forschungsgemeinschaft (HE 2993/5, to S.H.H.) and in part by research grant IS-3259–01 from BARD, The United States-Israel Binational Agricultural Research and Development Fund (to D.G.).

ABBREVIATIONS: Na_V channels, voltage-gated sodium channels; CNS, central nervous system; Lqh, *Leiurus quinquestriatus hebraeus*; HEK, human embryonic kidney.

Some members are broadly expressed in the CNS ($Na_v1.1$–1.3, $Na_v1.6$), whereas the expression of others is restricted to specific tissues, such as the peripheral nervous system ($Na_v1.7$), sensory neurons ($Na_v1.8$ and $Na_v1.9$), skeletal muscle ($Na_v1.4$), and cardiac muscle ($Na_v1.5$). In most instances, neuronal Na_V channels (except $Na_v1.8$ and $Na_v1.9$) mediate tetrodotoxin-sensitive Na^+ currents and have similar electrophysiological properties. Interestingly, most neurons were found to express various Na_V channel subtypes in their cell bodies or at distinct membrane regions; such expression is plastically regulated under developmental and pathological conditions (Goldin, 1999; Catterall, 2000). The identification of these channel subtypes and elucidation of their role is technically limited and requires specific probes. Scorpion α-toxins provide a unique tool for such identification because their affinity for different channel subtypes is very diverse. For example, LqhαIT is ~2000-fold less active in mouse brain than Lqh-2 and competes only at micromolar concentrations for binding to rat brain synaptosomes. The α-like toxin, Lqh-3, is highly toxic in the mouse brain but is a very weak competitor for Lqh-2 binding to rat brain synaptosomes (Gordon et al., 1996, 2002; Gilles et al., 1999, 2000a). Moreover, Lqh-3 and LqhαIT barely affect the Na^+ current mediated by the heterologously expressed $rNa_v1.2$ in contrast to the strong inhibition of inactivation induced by Lqh-2 (Gilles et al., 1999, 2000a, 2001). Conversely, under patch-clamp conditions, Lqh-3 strongly inhibits the Na_V channel inactivation in rat CA1 pyramidal neurons in hippocampal slices, whereas Lqh-2 has no effect (Gilles et al., 1999). Thus, α-like toxins do not target the majority of Na_V channel subtypes in brain synaptosomes (e.g., $rNa_v1.2$/1.2a and most likely $rNa_v1.1$) but are active on another as-yet unidentified brain Na_V channel that is insensitive to Lqh-2. In contrast, the three α-toxins, Lqh-2, Lqh-3, and LqhαIT, similarly affect muscular Na_V channels expressed in mammalian cells (Chen et al., 1999; Gilles et al., 2000a; Chen and Heinemann, 2001). Both Lqh-2 and Lqh-3 inhibit tetrodotoxin-sensitive Na_V channel inactivation in dorsal root ganglia neurons but their effect differs prominently, suggesting that the target channels are not identical (Gilles et al., 2000a). This is corroborated by the higher affinity of Lqh-3 for the peripheral nerve channel, $hNa_v1.7$, compared with that of Lqh-2 (Chen et al., 2002). Evidently, the target Na_V channel subtype for α-like toxins in the mammalian brain and in the peripheral nervous system still needs to be elucidated.

In this study, we analyzed those Na_V channel features in the external linker S3–S4 in domain 4, which enable the selective recognition of each of the three different α-toxins. We employed two complementary approaches; the first was to construct channel chimeras, in which the S3–S4-linker of $rNa_V1.4$ (about equally sensitive to all toxins) is replaced by the amino acid variable stretch present in each of the other neuronal Na_V channel subtypes. In the second approach, site-directed mutations were introduced in the background of the wild-type and the chimeras to elucidate the role of individual residues for each toxin effect. Our results demonstrate that a single charge-conserving substitution in this linker absolutely confers channel sensitivity to Lqh-3. Other residues confer sensitivity for LqhαIT and Lqh-2 in a background-dependent manner.

Materials and Methods

Site-Directed Mutagenesis. The channel constructs used in this study were expressed from the mammalian expression vector pcDNA3. Mutations were introduced in the background of the $rNa_V1.4$ channel (Trimmer et al., 1989) in the linker between the membrane-spanning segments S3 and S4 in the fourth homologous domain of rNav1.4 using PCR-based site-directed mutagenesis. The mutants are summarized in Fig. 1. The sequences of all mutants were verified by sequence analysis. Plasmid DNA was isolated from *E. coli* using the Midi- or Maxi-plasmid purification kit (QIAGEN, Hilden, Germany).

Cell Culture and Transfection. HEK 293 cells (CAMR, Porton Down, Salisbury, UK) were maintained in 45% Dulbecco's modified Eagle's medium and 45% Ham's F12, supplemented with 10% fetal calf serum in a 5% CO_2 incubator at 37°C. HEK 293 cells were trypsinized, diluted with culture medium, and grown in 35-mm dishes. When HEK 293 cells were grown to 30 to 50% confluence, transient transfection was performed using the Superfect transfection kit (QIAGEN). HEK 293 cells were transfected with a 5:1 ratio of the Na_v channel expression plasmids and a vector encoding the CD8 antigen (Jurman et al., 1994). The cells were used for electrophysiological recordings 2 to 3 days after transfection. Dynabeads (Deutsche Dynal GmbH, Hamburg, Germany) were used for visual identification of individual transfected cells, and many bead-decorated cells expressed Na_v channels.

Electrophysiological Measurements. Whole-cell voltage-clamp experiments were performed as described previously (Chen et al., 1999). Briefly, patch pipettes with resistances of 0.9 to 2.0 MΩ were used. The series resistance was compensated for by more than 80% to minimize voltage errors. An EPC9 patch-clamp amplifier was operated by Pulse+PulseFit and PatchMaster software (both from HEKA Elektronik, Lambrecht, Germany). Leak and capacitive currents were corrected with a p/n method. Currents were low-pass filtered at 5 kHz and sampled at a rate of 25 kHz. All experiments were performed at constant temperature, 19 to 21°C. Data analysis was performed using PulseFit, PatchMaster (HEKA) and IgorPro (WaveMetrics, Lake Oswego, OR).

The patch pipettes contained 35 mM NaCl, 105 mM CsF, 10 mM EGTA, and 10 mM HEPES, pH adjusted to 7.4 with CsOH. The bath solution contained 150 mM NaCl, 2 mM KCl, 1.5 mM $CaCl_2$, 1 mM $MgCl_2$, and 10 mM HEPES, pH adjusted to 7.4 with NaOH. The

Channel type, mutant name	Residue number	S3(D4)											
		G	L	A	L	S	D	L	I	Q	K	Y	F
$Na_V1.4$, µI, SkM1	1423												
$hNa_V1.2$, Brain I+II	1608		M	F		A	E			E			
$hNa_V1.3$, hBrain III, rPN1	1554		M	F		A	E	M		E			
$hNa_V1.6$, Scn8a, NaCh6	1598		M	F		A		I		E			
$hNa_V1.7$, hPN1	1581		M	F		A				E	T		
$Na_V1.4$_DtoE							E						
$Na_V1.2$_EtoD			M	F		A				E			
$Na_V1.7$_DtoE			M	F		A	E			E	T		
$Na_V1.4$_QtoE										E			
$Na_V1.4$_KtoT											T		
$Na_V1.4$_LA-StoMF-A			M	F		A							

Fig. 1. Receptor site 3 in S3/4(D4) for various Na_V channel subtypes and mutants used in this study. Alignment of the major component of toxin receptor site 3 (i.e., the linker between S3 and S4 in domain 4). The part of the sequence belonging to S3(D4) is highlighted by vertical lines. The first five sequences show the residues found in $Na_V1.4$ [here considered wild type (wt)], $Na_V1.2$/$Na_V1.1$, human $Na_V1.3$ (or rat $Na_V1.7$), $Na_V1.6$, and human $Na_V1.7$. The sequences of the indicated neuronal Na_V channels were inserted into $rNa_V1.4$. In addition, individual residues or groups of residues were exchanged, giving rise to the mutants listed in the last six rows. Negatively charged residues are highlighted in dark gray, positive residues in light gray.

application of toxin was performed with an application pipette as described previously (Chen et al., 1999).

Activation. From a holding potential of −120 mV, test depolarizations in the range from −80 to +60 mV in steps of 10 mV were applied at an interval of 5 s. The peak currents were fit with a Hodgkin-Huxley activation formalism involving $m = 3$ activation gates and a single-channel characteristics according to Goldman-Hodgkin-Katz.

$$I_{peak}(V) = \frac{I_{max}}{(1 + e^{-(V - V_m)/K_m})^3}$$

$$I_{max} = \Gamma V \frac{1 - e^{-(V - E_{rev})/25\ mV}}{1 - e^{-V/25\ mV}} \quad (1)$$

V_m is the voltage of half-maximal gate activation, k_m is the corresponding slope factor, Γ is the maximal conductance of all channels, and E_{rev} is the reversal potential.

Voltage Dependence of Fast Inactivation. From a holding potential of −120 mV, cells were conditioned for 500 ms at voltages ranging from −120 to −25 mV in steps of 5 mV. Subsequently, peak current was determined at −20 mV. The repetition interval was 10 s. The peak current plotted versus the conditioning voltage was described with a Boltzmann function.

$$I(V) = \frac{I_{min}}{(1 + e^{-(V - V_h)/k_h})} \quad (2)$$

with the half-maximal inactivation voltage V_h and the corresponding slope factor k_h that indicates the voltage dependence of steady-state fast inactivation.

Toxin Dependence of Fast Inactivation. Currents were recorded in the absence and the presence of several toxin concentrations. The degree of fast inactivation was assayed at 0 mV by measuring the peak current as well as the mean current level between 4.5 and 5 ms after the start of the depolarization. This ratio $I_{5\ ms}/I_{peak}$ gives an estimate of the probability for the channels not to be inactivated after 5 ms; a value of zero represents complete inactivation within 4.5 ms and a value of 1 represents no inactivation. The dose dependence for toxin-induced removal of fast inactivation was measured by plotting $I_{5\ ms}/I_{peak}$ as a function of toxin concentrations. The concentration dependence was described with the Hill equation.

$$\frac{I_{5\ ms}}{I_{peak}}(0\ mV) = a_0 + \frac{a_1}{1 + \left(\frac{EC_{50}}{[toxin]}\right)^{n_H}} \quad (3)$$

where n_H is the Hill coefficient, [toxin] is the toxin concentration, and a_0 is the offset. The amplitude, a_1 plus a_0, provides the maximal value of $I_{5\ ms}/I_{peak}$ at 0 mV indicating the expected maximal effect of the toxin on fast inactivation. EC_{50} provides a measure for the concentration of half-maximal inhibition of fast inactivation. For data fits, the a_0 values always were held to the values obtained under control conditions. To reduce variability, h was set to 1 in all cases. Because even high toxin concentrations did not result in a full α-toxin effect for some mutants, $a_0 + a_1$ was set to a constant value (0.75) for all dose-response fits. Data points were weighted according to the standard error of the mean; error estimates for EC_{50} values were obtained from these fits with the IgorPro program.

All data were presented as mean ± S.E.M. (n = number of independent experiments). Significance of differences between two groups of data were tested with a two-sided Student's t test.

Results

Receptor site 3 of voltage-gated sodium channels is largely determined by the extracellularly accessible loop between segments 3 and 4 of domain 4. Interestingly, although most parts of the core domains of Na_V channels are rather conserved, there is considerable variability in this region among mammalian sodium channels (Fig. 1). In addition, various α-toxin groups have different effects on the same Na_V channel; e.g., whereas Lqh-2 is very active on $Na_V1.2$ channels, Lqh-3 is almost inactive (Chen et al., 2002). To gain insight into the molecular mechanisms underlying the mutual toxin-channel specificity, we applied a mutagenesis approach. Based on the rat $Na_V1.4$ channel, which is similarly sensitive to the three groups of α-toxins, we replaced the S3–S4 linker in domain 4 by its counterparts present in various Na_V channel subtypes and examined the effects of the three different α-toxins on each channel mutant. Starting from $Na_v1.4$ wild-type channels, we first introduced receptor sites from the human neuronal channels $Na_V1.1$/$Na_V1.2$ (in the putative receptor site 3, these channels are identical), $Na_V1.3$, $Na_V1.6$, and $Na_V1.7$. Note that the sequences of receptor site 3 of human $Na_V1.3$ and rat $Na_V1.7$ are identical (Fig. 1). In addition, we generated channel mutants in which, based on the background receptor site 3, sequences of $Na_V1.2$-, $Na_V1.4$-, and $hNa_V1.7$-specific residues or groups of residues were replaced by others. In particular, we applied this approach to specifically test the influence of residues Asp1428, Gln1431, and Lys1432 (residue numbers of $rNa_V1.4$).

Functional Parameters of Mutated Na_V Channels. All these mutants were expressed in HEK 293 cells giving rise to functional Na_V channels. The mutations had no impact on the current densities obtained. The function of the mutated Na_V channels was assayed by measuring and analyzing current-voltage relationships and steady-state inactivation. Sample data for channel activation are shown in Fig. 2A. The half-maximal activation voltage V_m and the slope factors k_m for all mutants are plotted in Fig. 2C; variations for V_m were within ±4 mV and for k_m within ±1 mV. Thus, no big changes in activation parameters were detected, implying that alterations of receptor site 3 have only a marginal impact on the channel-activating movement of the S4 segment in domain 4.

Steady-state inactivation after 500-ms conditioning was described by a single Boltzmann function. The resulting half-maximal inactivation voltages V_h and the slope factors k_h are also shown in Fig. 2C. Again, for most mutants the variation of V_h was within ±4 mV and the variation for k_h within ±1 mV. However, the resulting V_h for mutant $Na_v1.3$ was shifted by about −20 mV with respect to the wild type (−73.9 ± 0.7 mV, $n = 43$ for $Na_V1.4$; −93.4 ± 0.8, $n = 37$ for mutant $hNa_V1.3$, $P \ll 0.001$). This shift can be attributed to the residue exchange L1429M, because this is the only difference between mutants $hNa_V1.3$ and $Na_V1.2$ ($V_h = -76.0 \pm 0.7$, $n = 48$, $P \ll 0.001$). The slope factors were not affected. The shift in V_h did not result from a contribution of slow inactivation, because similar experiments using conditioning pulses of 50 ms also resulted in such a shift, whereas protocols assaying slow inactivation (with 5-s conditioning) did not show shifts (data not shown). Besides this effect of mutant $hNa_V1.3$, all other mutants show inactivation parameters indistinguishable from that of wild type. Therefore, altered gating properties did not contaminate the subsequent assessment of toxin effects—this is an important prerequisite, because the effects of scorpion α-toxins are state- and voltage-dependent. In addition, it is noteworthy that even substantial nonconservative mutagenesis of receptor site 3

does not affect channel inactivation, even though toxin binding to that site has a strong effect on inactivation.

Receptor Site 3 Chimeras. In a first screening, all mutants were tested with regard to the effect of 20 nM Lqh-3, LqhαIT, and Lqh-2. In Fig. 3 sample traces at −20 mV are shown for those mutants harboring receptor sites-3 of other neuronal channel types. First, it is evident that mutagenesis does not influence kinetics of fast inactivation; this is also true for all other mutants not shown in Fig. 2. Upon application of 20 nM of Lqh-3, LqhαIT, and Lqh-2, inactivation is strongly impaired in wild-type $Na_V1.4$ channels, almost reaching saturation (Fig. 2, top row). Mutagenesis of receptor site 3 has a differential impact on the three toxins' effects. Whereas mutants $Na_V1.2$ and $hNa_V1.3$ are basically insensitive to Lqh-3 and only weakly sensitive to LqhαIT, there is only a small effect on the activity of Lqh-2. Mutation $Na_V1.6$ only weakly influences the effect of all toxins. Unexpectedly, for mutant $hNa_V1.7$ the strongest effect is obtained for the activity of LqhαIT, followed by Lqh-2 and Lqh-3. Thus, variation in the structure of receptor site 3 among neuronal Na_V channels modulates the action of the three α-toxins in a complex manner, as suggested by the native channels $Na_V1.2$/$Na_V1.7$ and Lqh-3/Lqh-2 (Chen et al., 2002).

On the one hand, this raises the possibility of using these toxins for the identification of specific Na_V channel subtypes present in various neurons. On the other hand, the variability obtained by the exchange of only a few residues in a constant background (of $Na_V1.4$) provides an ideal basis for a more detailed characterization of the molecular determinants responsible for the mutual toxin–channel recognition sites. Therefore, we constructed conservative mutants in which only single residues (or groups) were exchanged on the basis of $Na_V1.4$ or of one of the site 3 swap mutants (see Fig. 1).

Single-Site Mutants. For all mutants, the toxin effects were assayed quantitatively by applying different toxin concentrations to compile dose-response relationships. In Fig. 4, such dose-response data are shown for a selection of mutants together with the superimposed fit results. The maximal effect obtained with application of active α-toxins depends mainly on the linker between domains 3 and 4 as well as the regions forming the receptor for the inactivation domain. Therefore, we assume that mutation of the extracellularly accessible receptor site 3 does not alter the theoretically obtainable toxin effect (i.e., the residual speed of inactivation upon toxin saturation). Hence, we constrained the dose-response fits to a maximal $a_0 + a_1$ value (see eq. 3) of 0.75. The Hill coefficients were set to unity, such that the data could be described by the EC_{50} values as the only free parameter. The resulting EC_{50} values of all mutants investigated are listed in Table 1.

All data are listed in Table 1, but the results are not easily extracted. Therefore, we show in Fig. 5 on a logarithmic scale the relative impact of specific mutations on the effects of all three toxins. The data are grouped according to the site of interest. Most remarkable is mutation D1428E. For Lqh-3, it seems to be a necessary criterion to have an aspartate at position 1428 in receptor site 3. Mutagenesis to glutamate (only a CH_2-group difference from aspartate) results in a reduction of >1000-fold in Lqh-3 effect. In contrast, this mutation has no impact at all for Lqh-2. In the background of receptor site 3 of $hNa_V1.7$ (i.e., in the presence of Thr1432), the exchange D1428E even increases the effect of Lqh-2. For LqhαIT, the situation is somewhat intermediate: whereas D1428E has a very strong impact in the background of $Na_V1.4$ wild-type and mutant $Na_V1.2$ (i.e., in the presence of Lys1432), it does not change the activity of LqhαIT in the

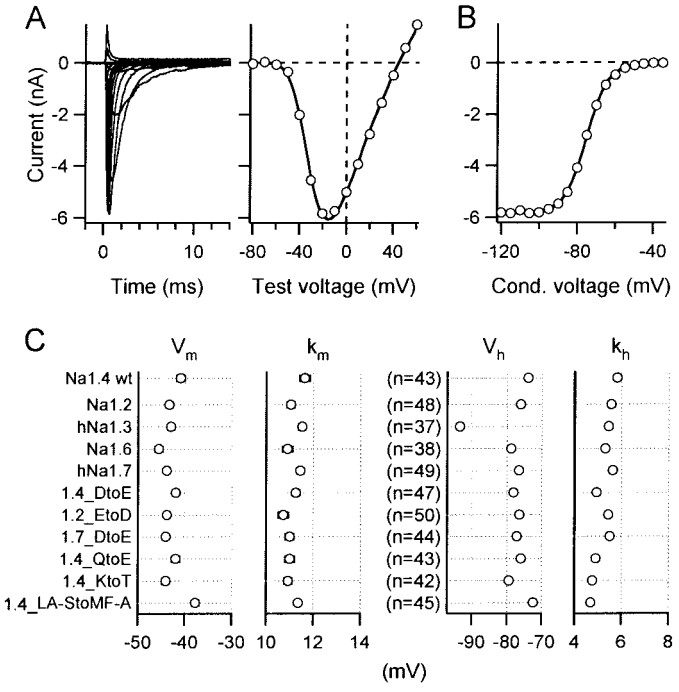

Fig. 2. A, sample current-voltage relationship of $rNa_V1.4$ channels expressed in HEK 293 cells. From a holding potential of −120 mV, step-depolarizations ranging from −80 to +60 mV in steps of 10 mV were applied; the resulting current traces are shown superimposed, low-pass filtered at 5 kHz (left). The peak currents were plotted as a function of the test potential to yield current-voltage relationships (right). These were fit with eq. 1, yielding the half-maximal activation voltage per V_m and the slope factor k_m. B, sample steady-state inactivation curve, fit with a first-order Boltzmann function (eq. 2), yielding the half-maximal inactivation voltage V_h and the slope factor k_h. C, steady-state activation and inactivation parameters for all mutants.

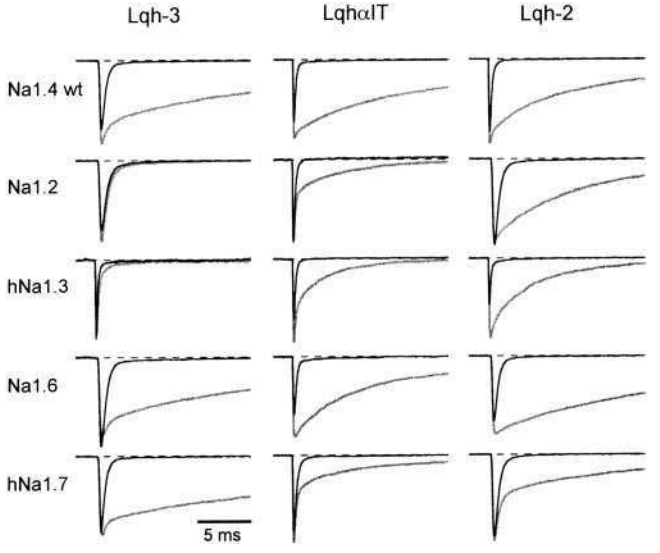

Fig. 3. Sample current traces of mutants with receptor sites-3 resembling the indicated neuronal channel types at −20 mV before (black) and after application of 20 nM of the indicated toxin (gray).

background of hNa$_V$1.7 (i.e., in the presence of Thr1432). Thus, LqhαIT behaves like Lqh-3 with Lys1432 and like Lqh-2 with Thr1432. Notably, the affinity of LqhαIT strongly depends on both residues Asp1428 and Lys1432 in Na$_V$1.4, whereas that of Lqh-3 depends mainly on Asp1428. In other words, Lqh-3 action seems to be independent from the residue at position 1432, whereas the other two toxins depend strongly on the nature of this residue.

This rather indirect inference is directly shown in the next group of data, captioned "K1432T". As expected, the Lqh-3 effect does not strongly depend on whether there is a lysine or a threonine at position 1432. However, the effects of LqhαIT (and, to a lesser extent, Lqh-2) are reduced when Lys1432 is mutated to Thr. However, this is true only in the background of a receptor site 3 harboring Asp1428. In summary, the channel sensitivity to Lqh-3 is determined mainly by the Asp/Glu exchange at position 1428 in receptor site 3. LqhαIT recognizes D1428E only in the presence of Lys1432 and Lqh-2 only in the presence of Thr1432. Both LqhαIT and Lqh-2 recognize K1432T only in the background of Asp1428.

The conservative changes at positions Leu1429 (to Ile or Met) and LA-S1424MF-A have only small impacts on the effects of Lqh toxins. Q1431E, however, leaves the effects of Lqh-3 and LqhαIT unchanged, whereas it decreases the effect of Lqh-2. This differential modulation is seen only in the background of the Na$_V$1.4 channel; when receptor site 3 is more neuronal-like (i.e., with MF-A1424 in place of LA-S), mutation Q1431E has only a marginal impact on all three toxins. Thus, also in this case, individual parts of receptor site 3 are of very differential importance for the association of the three Lqh toxins—and this in a context-dependent manner.

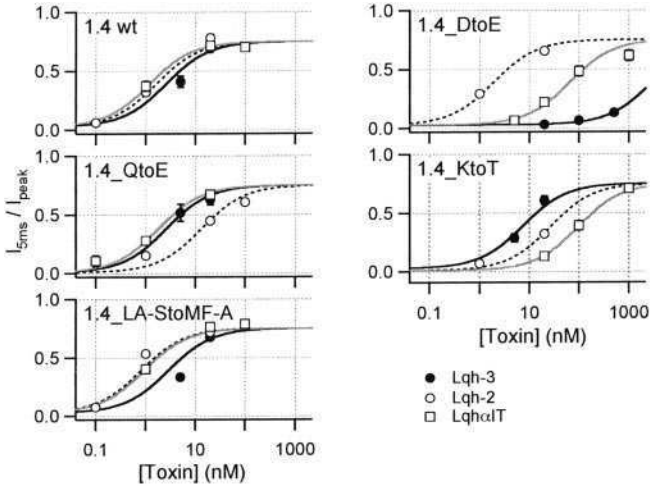

Fig. 4. Selection of dose-response relationships for Lqh-3 (black), LqhαIT (gray), and Lqh-2 (dashed). For data fits according to eq. 3, the maximal value was fixed to 0.75 and the Hill coefficient to 1.0.

TABLE 1
EC$_{50}$ values derived from dose-response curves shown in Fig. 4

Mutant	Lqh-3	LqhαIT	Lqh-2
		nM	
rNa$_V$1.4, wt	1.83 ± 0.25	1.19 ± 0.24	1.64 ± 0.16
Na$_V$1.2 (Na$_V$1.1)	1840 ± 173	20.6 ± 0.9	0.969 ± 0.071
hNa$_V$1.3 (rNa$_V$1.7)	3890 ± 1110	190 ± 11	2.35 ± 0.29
Na$_V$1.6	9.48 ± 0.82	0.247 ± 0.041	0.778 ± 0.058
hNa$_V$1.7	6.22 ± 0.64	50.8 ± 5.2	7.00 ± 1.15
Na$_V$1.4_DtoE	2980 ± 282	65.7 ± 6.1	1.92 ± 0.23
Na$_V$1.2_EtoD	5.52 ± 0.56	0.338 ± 0.028	0.53 ± 0.08
Na$_V$1.7_DtoE	2290 ± 220	42.1 ± 4.0	1.56 ± 0.15
Na$_V$1.4_QtoE	2.59 ± 0.89	1.80 ± 0.25	13.2 ± 1.1
Na$_V$1.4_KtoT	7.46 ± 1.21	96.1 ± 7.9	26.2 ± 2.7
Na$_V$1.4_LA-StoMF-A	2.88 ± 0.22	0.934 ± 0.169	0.804 ± 0.054

Discussion

Functional Impacts of Receptor Site 3 Mutagenesis. In this study, we assayed various Na$_V$1.4 channel types that were mutated in the S3–S4 linker of domain 4. None of these mutants showed strong alterations in the voltage dependence of activation. This is consistent with a minor role of domain 4 for channel activation (Chahine et al., 1994; Chen et al., 1996). In addition, most mutants did not alter the inactivation properties either. This is surprising because binding of α-toxins to that site has a strong impact on channel inactivation. An exception is mutation L1429M, which leads to a clear shift in steady-state inactivation to more hyperpolarizing potentials, indicating a stabilized inactivated state. This can be explained molecularly by a coupling of voltage-sensor movement in domain 4 and fast inactivation (Catterall, 2002). However, at present, we cannot determine whether the particular site 1429 is necessary for transmitting effects on channel inactivation or the nature of the introduced residue (here methionine) is important. It is interesting to note,

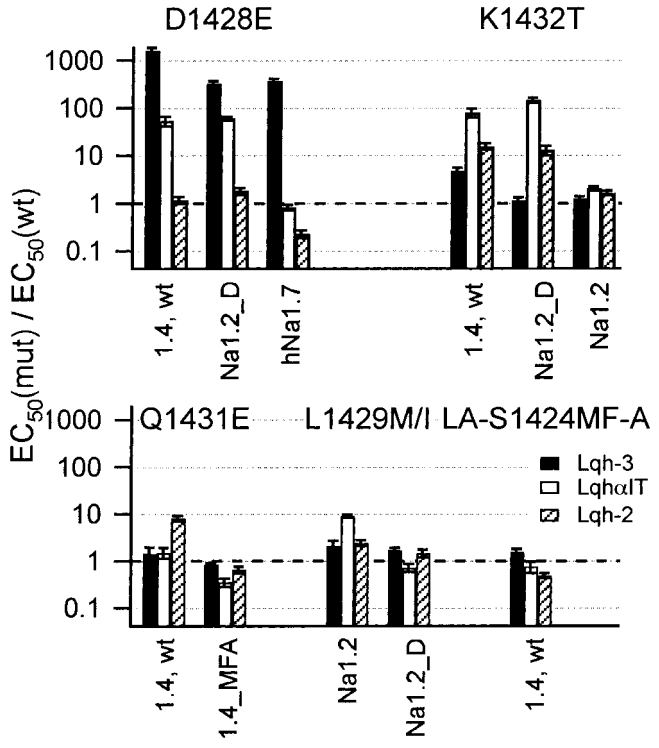

Fig. 5. Relative change in apparent EC$_{50}$ values introduced by the indicated mutations. The data are grouped according to the site of mutagenesis (e.g., Arg1428). The small labeling of the histogram bars indicates the background used for mutagenesis (e.g., "Na1.2" under "K1432T" means that Thr1432 was introduced in the background of rNa$_V$1.4 mutant "Na$_V$1.2"; i.e., "Na$_V$1.7_DtoE") (see Table 1). The shading of the histogram bars indicates the toxins: Lqh-3 (black), LqhαIT (white), Lqh-2 (hatched). For this sequence of toxins, the ratio values for the most relevant mutations are as follows: D1428E: Na$_V$1.4, wt: 1633, 55.0, 1.18; Na1.2_EtoD: 333, 60.9, 1.82; hNa1.7: 368, 0.828, 0.223; K1432T: Na$_V$1.4, wt: 4.88, 80.5, 16.0; Na1.2_EtoD: 1.13, 150, 13.1; Na1.2: 1.24, 2.04, 1.61.

however, that $hNa_V1.3$ and $rNa_V1.7$ channels are unique in harboring a methionine residue at that position.

The different effects of mutations in the S3–S4 linker in domain 4 of Na_V channels on the affinity of each of the three Lqh α-toxins suggest that they bind to receptor site 3 in different fashions. Although all the distinct α-toxins interact with residues in this short linker, they may bind to partially overlapping sites, which may depend on the functional surface of each toxin. Moreover, because the impact on the affinity of Lqh-2, the most potent anti-mammalian α-toxin, by two mutations, Lys to Thr and Gln to Glu, was relatively small (Fig. 5 and Table 1), it is conceivable that other parts of the channel may be involved in formation of receptor site 3 and in the high affinity of Lqh-2 to most mammalian Na_V channels. This assumption is supported by the low affinity of Lqh-2 to insect Na_V channels, which are practically identical to the mammalian $Na_V1.6$ in the S3–S4 region in domain 4, to which Lqh-2 reveals high affinity (Table 1).

Use of Lqh Toxins for Identifying Na_V Channels. The combinatorial use of Lqh toxins provides a tool for identifying neuronal Na_V channel types. Although in some cases there is still some uncertainty about whether the site 3 swap confers the full toxin-binding properties of the respective wild types, the discriminative power of the three Lqh toxins, particularly when used in combination, will be very helpful in targeting specific Na_V channels, either for research purposes or for pharmacological applications. Fluorescent labeling of these toxins as performed for other, less specific α- and β-toxins (Massensini et al., 2002) may provide further insight into Na_V channel distributions in nervous tissues.

Limitations in Drawing Toxicological Conclusions for Humans Based on Animal Experiments. Receptor site 3 mainly determines the mode by which Na_V channels interact with scorpion α-toxins. However, toxicological studies using laboratory animals may yield results that are not easily transferred to the human system. Herein, we show that receptor site 3 of $hNa_V1.3$ channels is identical to the site of rat $Na_V1.7$ channels. The site of rat $Na_V1.3$ channels is identical to those of $Na_V1.1$ and $Na_V1.2$ channels. Thus, with respect to Lqh-3 rat and human $Na_V1.7$ channels are expected to behave in a completely different manner (factor of about 1000); therefore, rat $Na_V1.7$ channels are not suitable as models for their human orthologs.

Combinatorial Determination of Toxin-Channel Specificity. The strong diversity of functional effects exerted by the three Lqh toxins studied must be reflected in their molecular structure. Particularly intriguing is the molecular basis that allows for a very sensitive discrimination of glutamate versus aspartate in the receptor site, as shown for Lqh-3.

Thus far, the bioactive surfaces of two α-toxins were investigated systematically: LqhαIT (α-insect toxin; Tugarinov et al., 1997; Zilberberg et al., 1997) and BmK-M1 (α-like toxin; Wang et al., 2003). Mutagenesis of LqhαIT revealed that Tyr21 (Gilles et al., 2000b) and Arg64 (Tugarinov et al., 1997; Zilberberg et al., 1997) might be important for the interaction with Na_V channels. Other residues that might be part of the bioactive surface are Tyr10, Phe17, Lys8, Arg18, and Arg62 (Zilberberg et al., 1997). Site-directed mutagenesis of BmK-M1 showed that Lys62 and His64 together with Lys8 form a unique tertiary arrangement that may directly interact with receptor site 3 on the Na_V channel surface (Wang et al., 2003). These findings are consistent with a second mutagenesis approach on BmK-M1 in which aromatic residues (Tyr5, Tyr35, Trp38, Tyr42, Trp47) affected toxin properties, most likely by structural stabilization (Sun et al., 2003). The functional importance of residues that are located in a turn near the N terminus (8–10) was shown in a chimeric approach between LqhαIT and BotXIV, an α-like toxin (Bouhaouala-Zahar et al., 2002). All together, it is generally accepted that the so-called five-residue turn (residues 8–12 in the Lqh toxins used here) together with the C-terminal end of the toxins forms the channel interaction site.

At least two of the three Lqh toxins used in this study differentiate effectively between Asp1428 and Glu1428 in the background of $Na_V1.4$ channels. Together with the finding that a positive surface potential of α-toxins may correlate with their binding affinity to Na_V channels (Zilberberg et al., 1997; Krimm et al., 1999), one can speculate that positively charged residues on the toxin surface should be in physical contact with negatively charged residues in receptor site 3. The lack of positive charges in the five-residue turn in Lqh-2 and Lqh-3 highlights the C-termini with the Lys/Arg and His/Arg moieties as excellent candidates for harboring the critical interaction site. More mutagenesis studies combined with double cycle analysis are needed to clarify this point.

Because the Lys/Thr sites at position 1432 in receptor site 3 determines how strongly the Lqh toxins (in particular Lqh-2 and LqhαIT) depend on the Asp/Glu residues at position 1428, it will be important to elucidate the direct interaction partner on the bioactive surface of the toxins. Only then can the combinatorial and nonadditive contribution of these residues on toxin binding be understood on a molecular level. However, comparison of the Lqh-2, Lqh-3, and LqhαIT sequences does not readily suggest a candidate for a direct interaction partner for the Lys/Thr site of receptor site 3. Therefore, rather than examining single toxin mutants, a chimeric approach using Lqh-2 and Lqh-3 might be the strategy of choice for solving this problem.

In summary, the individual residues in receptor site 3 do not add linearly to the binding strength of Lqh toxins; rather, they give rise to a combinatorial mixing and matching of toxins and channel subtypes. As a result, simply recombining a few amino acid residues in receptor site 3 of voltage-gated sodium channels generates a very wide variety of toxicological phenotypes.

Acknowledgments

We thank A. Roßner and S. Arend for technical assistance and Dr. P. Sautière for his generous gift of scorpion α-toxins.

References

Bouhaouala-Zahar B, Benkhalifa R, Srairi N, Zenouaki I, Ligny-Lemaire C, Drevet P, Sampieri F, Pelhate M, El Ayeb M, et al. (2002) A chimeric scorpion α-toxin displays de novo electrophysiological properties similar to those of α-like toxins. *Eur J Biochem* **269:**2831–2841.

Catterall WA (1992) Cellular and molecular biology of voltage-gated sodium channels. *Physiol Rev* **72**(4 Suppl)**:**S15–S48.

Catterall WA (2000) From ionic currents to molecular mechanisms: the structure and function of voltage-gated sodium channels. *Neuron* **26:**13–25.

Catterall WA (2002) Molecular mechanisms of gating and drug block of sodium channels. *Novartis Found Symp* **241:**206–218; discussion 218–232.

Chahine M, George AL Jr, Zhou M, Ji S, Sun W, Barchi RL, and Horn R (1994) Sodium channel mutants in paramyotonia congenita uncouple inactivation from activation. *Neuron* **12:**281–294.

Chen H, Gordon D, and Heinemann SH (1999) Modulation of cloned skeletal muscle Na channels by the scorpion toxins Lqh II, Lqh III and LqhαIT. *Pflueg Arch Eur J Physiol* **439:**423–432.

Chen H and Heinemann SH (2001) Interaction of scorpion α-toxins with cardiac

sodium channels: binding properties and enhancement of slow inactivation. *J Gen Physiol* **117:**505–518.

Chen H, Lu SQ, Leipold E, Gordon D, Hansel A, and Heinemann SH (2002) Differential sensitivity of recombinant sodium channels from the central and peripheral nervous system to the scorpion toxins Lqh-2 and Lqh-3. *Eur J Neurosci* **16:**767–770.

Chen LQ, Santarelli V, Horn R, and Kallen RG (1996) A unique role for the S4 segment of domain 4 in the inactivation of sodium channels. *J Gen Physiol* **108:**549–556.

Gilles N, Blanchet B, Shichor I, Zaninetti M, Lotan I, Bertrand D, and Gordon D (1999) A scorpion α-like toxin active on insects and mammals reveals an unexpected specificity and distribution of sodium channel subtypes in rat brain neurons. *J Neurosci* **19:**8730–8739.

Gilles N, Chen HJ, Wilson H, LeGall F, Montoya G, Molgo J, Schönherr R, Nicholson G, Heinemann SH, and Gordon D (2000a) Scorpion α- and α-like toxins differentially interact with sodium channels in mammalian CNS and periphery. *Eur J Neurosci* **12:**2823–2832.

Gilles N, Krimm I, Bouet F, Froy O, Gurevitz M, Lancelin JM, and Gordon D (2000b) Structural implications on the interaction of scorpion α-like toxins with the sodium channel receptor site inferred from toxin iodination and pH-dependent binding. *J Neurochem* **75:**1735–1745.

Gilles N, Leipold E, Chen HJ, Heinemann SH, and Gordon D (2001) Effect of depolarization on binding kinetics of scorpion α-toxin highlights conformational changes of rat brain sodium channels. *Biochemistry* **40:**14576–14584.

Goldin AL (1999) Diversity of mammalian voltage-gated sodium channels. *Ann NY Acad Sci* **868:**38–50.

Gordon D, Gilles N, Bertrand D, Molgò J, Nicholson GM, Sauviat MP, Benoit E, Shichor I, Lotan I, Gurevitz M, et al. (2002) Scorpion toxins differentiating among neuronal sodium channel subtypes: nature's guide for design of selective drugs, in *Perspectives in Molecular Toxinology* (Ménez A ed) pp 215–238, Wiley and Sons, Chichister, England.

Gordon D (1997) Sodium channels as targets for neurotoxins: mode of action and interaction of neurotoxins with receptor sites on Na channels, in *Toxins And Signal Transduction* (Gutman Y and Lazarovici P eds) pp 119–149, Cellular and Molecular Mechanisms of Toxin Action, Vol. 1, Harwood Academic Press, Amsterdam.

Gordon D, Martin-Eauclaire MF, Cestele S, Kopeyan C, Carlier E, Khalifa RB, Pelhate M, and Rochat H (1996) Scorpion toxins affecting sodium current inactivation bind to distinct homologous receptor sites on rat brain and insect sodium channels. *J Biol Chem* **271:**8034–8045.

Gordon D, Savarin P, Gurevitz M, and Zinn-Justin S (1998) Functional anatomy of scorpion toxins affecting sodium channels. *J Toxicol Toxin Rev* **17:**131–159.

Jurman ME, Boland LM, Liu Y, and Yellen G (1994) Visual identification of individual transfected cells for electrophysiology using antibody-coated beads. *Biotechniques* **17:**876–881.

Krimm I, Gilles N, Sautiere P, Stankiewicz M, Pelhate M, Gordon D, and Lancelin JM (1999) NMR structures and activity of a novel alpha-like toxin from the scorpion *Leiurus quinquestriatus hebraeus*. *J Mol Biol* **285:**1749–1763.

Martin-Eauclaire MF and Couraud F (1995) Scorpion neurotoxins: effects and mechanisms, in *Handbook of Neurotoxicology* (Chang LW and Dyer RS eds) pp 688–722, Marcel Dekker, New York.

Massensini AR, Suckling J, Brammer MJ, Moraes-Santos T, Gomez MV, and Romano-Silva MA (2002) Tracking sodium channels in live cells: confocal imaging using fluorescently labeled toxins. *J Neurosci Methods* **166:**189–196.

Rogers JC, Qu Y, Tanada TN, Scheuer T, and Catterall WA (1996) Molecular determinants of high affinity binding of α-scorpion toxin and sea anemone toxin in the S3–S4 extracellular loop in domain IV of the Na^+ channel α subunit. *J Biol Chem* **271:**15950–15962.

Sautiere P, Cestele S, Kopeyan C, Martinage A, Drobecq H, Doljansky Y, and Gordon D (1998) New toxins acting on Na channels from the scorpion *Leiurus quinquestriatus hebraeus* suggest a clue to mammalian vs insect selectivity. *Toxicon* **36:**1141–1154.

Sun YM, Bosmans F, Zhu RH, Goudet C, Xiong YM, Tytgat J, and Wang DC (2003) Importance of the conserved aromatic residues in the scorpion α-like toxin BmK M1: the hydrophobic surface revisited. *J Biol Chem* **278:**24125–24131.

Tejedor FJ and Catterall WA (1988) Site of covalent attachment of α-toxin derivatives in domain I of the sodium channel α subunit. *Proc Natl Acad Sci USA* **85:**8742–8746.

Thomson WJ and Catterall WA (1989) Localization of the receptor site for α-scorpion toxins by antibody mapping: implications for sodium channel topology. *Proc Natl Acad Sci USA* **86:**10161–10165.

Trimmer JS, Cooperman SS, Tomiko SA, Zhou JY, Crean SM, Boyle MB, Kallen RG, Sheng ZH, Barchi RL, Sigworth FJ, et al. (1989) Primary structure and functional expression of a mammalian skeletal muscle sodium channel. *Neuron* **3:**33–49.

Tugarinov V, Kustanovich I, Zilberberg N, Gurevitz M, and Anglister J (1997) Solution structure of a highly insecticidal recombinant scorpion α-toxin and a mutant with increased activity. *Biochemistry* **36:**2414–2424.

Wang CG, Gilles N, Hamon A, Le Gall F, Stankiwicz M, Pelhate M, Xiong YM, Wang DC, and Chi CW (2003) Exploration of the functional site of a scorpion alpha-like toxin by site directed mutagenesis. *Biochem* **42:**4699–4707.

Zilberberg N, Froy O, Loret E, Cestéle S, Arad D, Gordon D, and Gurevitz M (1997) Identification of structural elements of a scorpion α-neurotoxin important for receptor site recognition. *J Biol Chem* **272:**14810–14816.

Address correspondence to: Prof. Dr. Stefan H. Heinemann, Molecular and Cellular Biophysics, Friedrich Schiller University Jena, Drackendorfer Str. 1, D-07747 Jena, Germany. E-mail: stefan.h.heinemann@uni-jena.de

Molecular interaction of δ-conotoxins with voltage-gated sodium channels

Enrico Leipold[a], Alfred Hansel[a], Baldomero M. Olivera[b], Heinrich Terlau[c], Stefan H. Heinemann[a,*]

[a] *Institute of Molecular Cell Biology, Research Unit Molecular and Cellular Biophysics, Friedrich Schiller University Jena, Drackendorfer Strasse 1, D-07747 Jena, Germany*
[b] *Department of Biology, University of Utah, Salt Lake City, Utah 84112, USA*
[c] *Max Planck Institute for Experimental Medicine, Research Unit Molecular and Cellular Neuropharmacology, Hermann-Rein-Strasse 3, D-37075 Göttingen, Germany*

Received 10 May 2005; accepted 31 May 2005

Available online 16 June 2005

Edited by Maurice Montal

Abstract Various neurotoxic peptides modulate voltage-gated sodium (Na_V) channels and thereby affect cellular excitability. δ-Conotoxins from predatory cone snails slow down inactivation of Na_V channels, but their interaction site and mechanism of channel modulation are unknown. Here, we show that δ-conotoxin SVIE from *Conus striatus* interacts with a conserved hydrophobic triad (YFV) in the domain-4 voltage sensor of Na_V channels. This site overlaps with that of the scorpion α-toxin Lqh-2, but not with the α-like toxin Lqh-3 site. δ-SVIE functionally competes with Lqh-2, but exhibits strong cooperativity with Lqh-3, presumably by synergistically trapping the voltage sensor in its "on" position.

Keywords: Conotoxin; Inactivation; Receptor site; Scorpion toxin; Sodium channel; Neurotoxin

1. Introduction

Na_V channel proteins are responsible for the rapid electrical signaling of neurons and muscle cells. They consist of four homologous domains and respond to changes in the transmembrane electric field by a translocation of their voltage sensor elements formed by the segments S3/S4 in each domain. The investigation of Na_V channels and the discrimination of different isoforms was largely facilitated by various neurotoxins that affect channel function in specific ways. In addition, neurotoxins have attracted attention with respect to their use as drugs, e.g., for pain treatment. Studies of the physical interaction between Na_V channels and neurotoxins have revealed various binding sites for neurotoxins on the channel proteins (termed receptor site-1 through site-9 [1,2]), where only sites 1–5 are molecularly defined. Several classes of neurotoxins of completely different structure affect Na_V channel inactivation. However, it is not known whether they exert their effects according to a common mechanism and if there is a functional coupling between them. Long-chain scorpion α-toxins, for example, consisting of 60–70 amino acids, target receptor site-3 mainly located in the S3/S4 linker of domain-4 and inhibit rapid channel inactivation. Cone-snail δ-conotoxins [3], peptides consisting of about 30 amino acid residues, exert a similar effect on Na_V channels. However, previous competition experiments measuring the binding of radioactively labeled toxins to membrane preparations containing Na_V channels have suggested that their molecular receptor site ("site-6") is distinct from that of scorpion α-toxins [4–6].

Many δ-conotoxins, such as δ-GmVIA and δ-TxVIA [7–10]], are specific for mollusks; δ-EVIA is poorly active on mammals, but exhibits some subtype specificity [11]. In this report, we show that the δ-conotoxin SVIE from *Conus striatus* affects mammalian Na_V channels. In addition, we identify the interaction motif of δ-SVIE with the voltage sensor of domain-4 in Na_V channels and show that this motif is not shared with the α-like toxin Lqh-3 while it is shared with the α-toxin Lqh-2. The interaction pattern with the voltage sensor determines whether neurotoxins functionally compete (δ-SVIE and Lqh-2) or even exhibit a strong functional synergism (δ-SVIE and Lqh-3).

2. Materials and methods

2.1. Channel constructs and mutagenesis

The Na_V channel type used was rat skeletal muscle sodium channel I, $rNa_V1.4$ (M26643) [12]. For single site-directed exchanges of amino acids 1431–1440 against cysteines, an *Nhe*I restriction site was introduced between basepairs 4268 and 4273 of the $rNa_V1.4$-encoding ORF [12], using the QuikChange mutagenesis kit (Stratagene, LaJolla, CA, USA). PCR primers containing this *Nhe*I site and the respective mutation were used in PCRs together with a primer binding on the opposite strand at the end of the ORF, including a second *Nhe*I site following the stop codon. The obtained PCR fragments were ligated into the pGemT vector (Promega, Madison, USA) and then sequenced prior to transferring the *Nhe*I-digested fragments into the $rNa_V1.4$-*Nhe*I-pcDNA3 expression plasmid. Correct insertion was verified by sequencing.

2.2. Cell culture and transfection

HEK 293 cells (CAMR, Porton Down, Salisbury, UK) were maintained in 45% Dulbecco's Modified Eagle's Medium (DMEM) and 45% F12, supplemented with 10% fetal calf serum in a 5% CO_2 incubator at 37 °C. They were transiently transfected with a 5:1 ratio of the Na_V channel expression plasmids and a vector encoding the CD8 antigen using the Superfect transfection kit (Quiagen, Hilden, Germany). Dynabeads (Deutsche Dynal GmbH, Hamburg, Germany) were used for visual identification of individual transfected cells.

*Corresponding author. Fax: +49 3641 9 32 56 82.
E-mail address: stefan.h.heinemann@uni-jena.de (S.H. Heinemann).

0014-5793/$30.00
doi:10.1016/j.febslet.2005.05.077

2.3. Electrophysiological measurements and analysis

Whole-cell voltage clamp experiments and toxin application were performed as described previously [13]. Data were acquired with an EPC-10 patch clamp amplifier operated by PatchMaster software (HEKA Elektronik, Lambrecht, Germany). Data analysis was performed using FitMaster (HEKA) and IgorPro (WaveMetrics, Lake Oswego, OR, USA). The patch pipettes contained (mM): 35 NaCl, 105 CsF, 10 EGTA, 10 HEPES (pH 7.4 with CsOH). The bath solution contained (mM): 150 NaCl, 2 KCl, 1.5 $CaCl_2$, 1 $MgCl_2$, 10 HEPES (pH 7.4 with NaOH). The degree of fast inactivation was assayed at 0 mV by measuring the peak current as well as the mean current level between 4.5 and 5 ms after the start of the depolarization. The ratio $I_{5\,ms}/I_{peak}$ gives an estimate of the probability for the channels not to be inactivated after 5 ms [13]. The dose dependence for toxin-induced removal of fast inactivation was measured by plotting $I_{5\,ms}/I_{peak}$ as a function of toxin concentrations. The concentration dependence was described with the Hill equation, $I_{5\,ms}/I_{peak} = a_0 + a_1/(1 + (EC_{50}/[\text{toxin}])^h)$, where h is the Hill coefficient, [toxin] the toxin concentration, a_0 the offset. The amplitude, a_1 plus a_0, provides the maximal value of $I_{5\,ms}/I_{peak}$ indicating the expected maximal effect of the toxin on fast inactivation. EC_{50} provides a measure for the concentration of half-maximal inhibition of fast inactivation. All data are expressed as arithmetic means ± S.E.M. (n = number of independent experiments).

2.4. Toxin purification and synthesis

δ-SVIE (Q9XZK5) was synthesized as previously described [14]. The scorpion α-toxins Lqh-2 (P59355) and Lqh-3 (P56678) [15] from *Leiurus quinquestriatus hebraeus* were generous gifts of D. Gordon (University Tel Aviv, Israel).

3. Results and discussion

3.1. Effect of δ-SVIE on channel inactivation

The δ-conotoxin SVIE investigated here, proved to be highly potent in modifying the gating of rat skeletal muscle $Na_V1.4$ channels expressed in mammalian cells (Fig. 1A). The major effect of δ-SVIE is to impair rapid channel inactivation. The concentration dependence for slowing channel inactivation at 0 mV yielded an apparent K_D value of the toxin effect of 500 ± 130 nM (n = 5; Fig. 1B) and a Hill coefficient close to unity (0.93 ± 0.18) suggesting a simple one-to-one reaction between toxin and channel molecule.

The effect of δ-SVIE on $Na_V1.4$ channel inactivation is similar to that of scorpion α-toxins, which bind to receptor site-3 [13,16–19]. This prompted us to perform an analysis of the functional impact of δ-SVIE on $Na_V1.4$ channel mutants that were previously shown to exhibit quite different properties regarding their interaction with the scorpion α-toxins Lqh-2 and Lqh-3 [15]. Rat $Na_V1.2$, a representative of Na_V channels from the central nervous system is insensitive to Lqh-3, and human $Na_V1.7$ from peripheral nerves, is less sensitive to Lqh-2 than $Na_V1.4$, when expressed in HEK 293 cells [13]. This difference in toxin-channel interaction could be attributed to single charged residues in the S3/S4 linker of domain-4 (Fig. 1C). Mutation D1428E of $Na_V1.4$ reduces the activity of Lqh-3 by about a factor of 1000; Q1431E and K1432T had strong impacts for the action of Lqh-2 ([19], Fig. 1E). However, as illustrated in Fig. 1D and E, these mutations did not result in a reduction of the ability of 2 μM δ-SVIE to remove inactivation of the channels.

3.2. Identification of the δ-SVIE interaction site at the Na_V voltage sensor element

Alterations of non-conserved residues in the putative interaction site for scorpion α-toxins only had moderate impacts

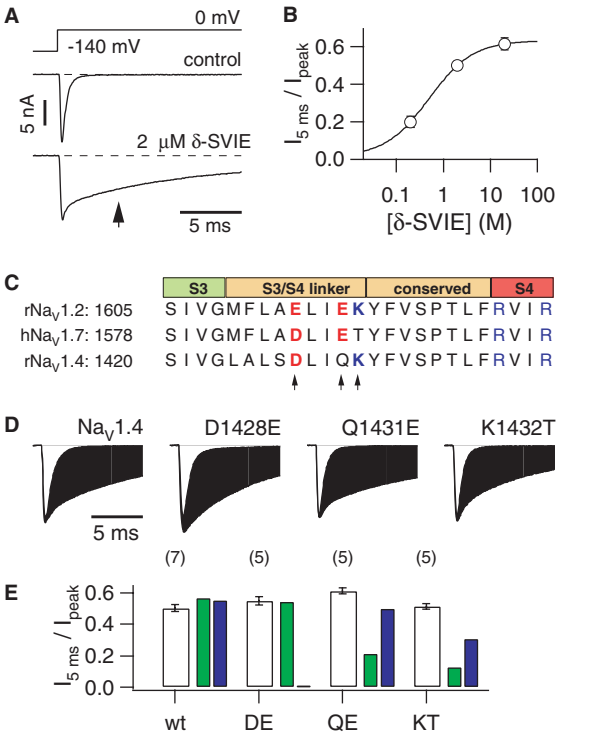

Fig. 1. Effect of δ-SVIE on wild-type $Na_V1.4$ channels and receptor site-3 mutants. (A) Current responses to depolarizations to 0 mV for $Na_V1.4$ channels under control conditions (center) and after application of 2 μM δ-SVIE (bottom). The arrow marks 5 ms, the time where inactivation of the channels was assayed. (B) Dose–response curve for the effect of δ-SVIE to remove inactivation at 0 mV (n = 5). (C) Alignment of the S3/S4 linker of domain-4 of the indicated mammalian Na_V channel types. Residues that were shown to take part in forming receptor site-3 are highlighted (arrows). The residues following to the right, i.e., towards the voltage sensor S4 are rather conserved. (D) Normalized current records at −20 mV of the wild-type channel $Na_V1.4$ as well as the indicated single-point mutants in the background of $Na_V1.4$. The control currents are superimposed to the records taken after application of 2 μM δ-SVIE. The difference between the two traces is shown as filled surface to indicate the increase in current integral upon toxin application. (E) Analysis of the mean inactivation at 0 mV, here expressed as $I_{5\,ms}/I_{peak}$, after application of 2 μM δ-SVIE. The filled bars indicate the corresponding values for the effect of 5 nM Lqh-2 (green) and 5 nM Lqh-3 (blue) (from [18,19]).

on the effect of the δ-conotoxin. Therefore, a cysteine-scanning mutagenesis of the conserved part of the S3/S4 linker of domain-4 was carried out, starting from Q1431C and ending at F1440C, the residue before the first arginine of the voltage sensor (Fig. 1C). All mutants were functionally expressed in HEK 293 cells and the effects of 2 μM δ-SVIE, 5 nM Lqh-2, and 5 nM Lqh-3, concentrations producing about the same effect on the inactivation of wild-type $Na_V1.4$ channels, were tested (Fig. 2A). The potency of δ-SVIE was slightly reduced by K1432C while the toxin was basically inactive on mutants Y1433C and F1434C. Surprisingly, it exhibited stronger effects on mutant V1435C. Thus, the ability of δ-SVIE to functionally modify $Na_V1.4$ channels is mainly determined by the hydrophobic triad Y1433–F1434–V1435 supporting the hypothesis of a hydrophobic interaction of δ-conotoxins with Na_V channels [10,20].

Interestingly, cysteine substitutions in the hydrophobic triad also modulate the effects of the α-toxin Lqh-2, while they leave the effects of the α-like toxin Lqh-3 unchanged (Fig. 2B).

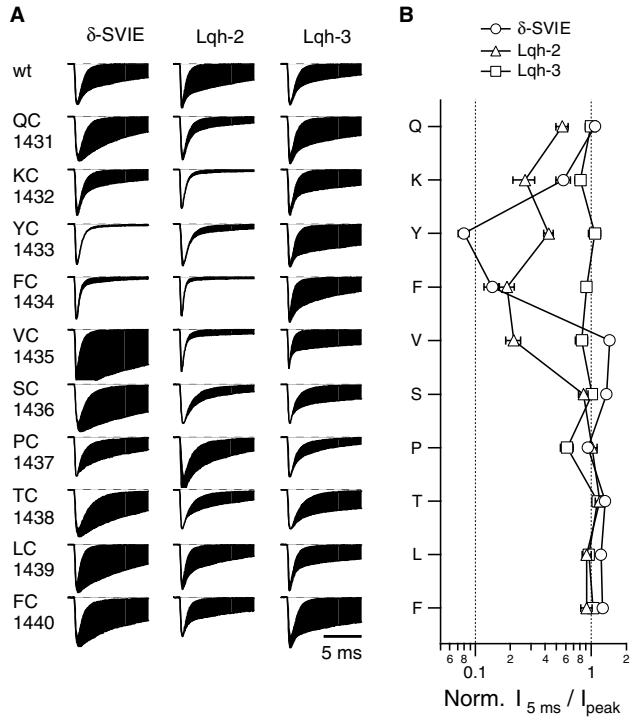

Fig. 2. Cysteine scan of the S3/S4 linker. (A) Cysteine-substituted $Na_V1.4$ channels were expressed in HEK 293 cells and current responses to −20 mV before and after application of 2 μM δ-SVIE, 5 nM Lqh-2, or 5 nM Lqh-3 were recorded. The shaded areas illustrate the increase in current integral upon toxin application. (B) The effect of the toxins on the inactivation time course at 0 mV was normalized to the values obtained for the wild-type ($Na_V1.4$) and is plotted as a function of the position of the mutated residue on a logarithmic scale. While mutagenesis of the channel sequence had virtually no impact on the effect of Lqh-3 (squares), both δ-SVIE (circles) and Lqh-2 (triangles) are strongly affected when cysteines are introduced between residues K1432 and V1435.

Together, these results are compatible with Lqh-2 and δ-SVIE sharing common interaction epitopes on Na_V channels. Considering that the S3/S4 linker in domain-4 of Na_V channels is longer than the S3/S4 linkers in the other domains, it is conceivable that it harbors both, parts of receptor site-3 and site-6, where site-3 is located more towards S3 and site-6 towards S4.

It can be concluded that a broad variety of neurotoxins affecting inactivation of Na_V channels (e.g. [16,21–24]) all function according to a common mechanism. One part of the toxin presumably binds to the surface of the channel protein. This channel section forms the major part of a "receptor site", i.e., receptor site-3 for α-toxins and receptor site-6 for δ-conotoxins. With a second moiety the toxins attack the voltage sensor of domain-4, which is tightly coupled to the process of inactivation.

3.3. Competition and synergism between δ-conotoxin SVIE and scorpion α-toxins

Scorpion α-toxins interact with the channel in a state-dependent manner. When the membranes are subjected to depolarizations strong enough to drive all channels into an open state, the toxin effect is diminished, i.e., the toxin appears to dissociate from its binding site. Such an experiment with the δ-conotoxin δ-SVIE is shown in Fig. 3A, where a 170-ms depolarization to +80 mV removes part of the toxin effect in the following test depolarization. Varying the time of depolarization yields a single-exponential dissociation (Fig. 3B, open circles). Hence, also δ-SVIE appears to bind to Na_V channels depending on the channel's conformational state.

The apparent overlap of residues in the channel protein important for the interaction with δ-SVIE and Lqh-2 should result in functional competition of these toxins for the overlapping site; this may not be the case for δ-SVIE and Lqh-3. To address whether there are functionally competitive interactions between toxins, we measured toxin dissociation when membranes were depolarized to +80 mV for 2 μM δ-SVIE and for 200 nM of the α-toxins, separately and in combination. Dissociation proceeds with a single-exponential time course (Fig. 3B–D) when only one type of toxin is present; the individual toxins had the following dissociation time constants: δ-SVIE, 247 ± 12 ms; Lqh-2, 29 ± 2 ms; Lqh-3, 488 ± 19 ms ($n = 4$ each). Coapplication of δ-SVIE and Lqh-2 resulted in a biphasic disappearance of the toxin effect with roughly the same time constants, consistent with the toxins competing for the same binding domain (Fig. 3B). The same holds true for Lqh-2 and Lqh-3 (Fig. 3C).

In the presence of δ-SVIE and Lqh-3, however, the dissociation rate under depolarization was very much slowed down. Although the more slowly dissociating α-toxin Lqh-3 exhibits

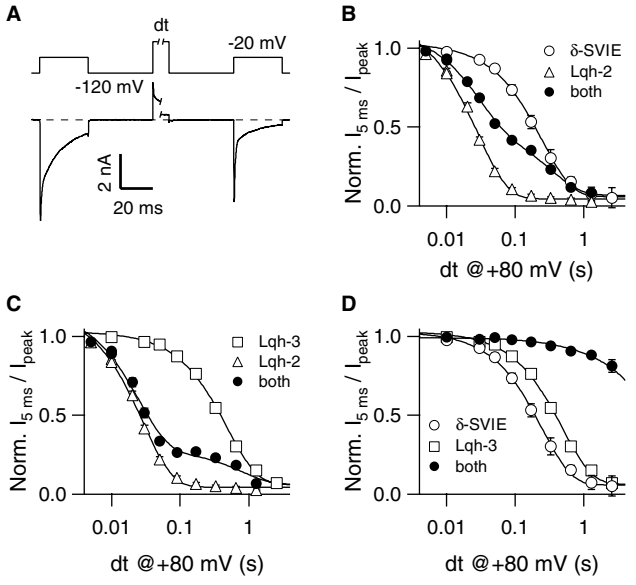

Fig. 3. Competition and synergy between δ-conotoxin SVIE and scorpion α-toxins. (A) Current trace in the presence of 2 μM δ-SVIE for the indicated pulse protocol. The center pulse to +80 mV was given for variable durations, here shown for 170 ms. (B) Time course of depolarization-induced loss of toxin effect for 200 nM Lqh-2, 2 μM δ-SVIE, and both toxins together. The apparent dissociation of the individual toxins was described by single-exponentials yielding time constants of 247 ms (δ-SVIE) and 29 ms (Lqh-2). The combination of both was described by a double-exponential with $\tau_1 = 29$ ms (56%) and $\tau_2 = 340$ ms (44%). (C) Similar experiments as in (B) but with Lqh-3 and Lqh-2, yielding 490 ms for Lqh-3. The combination of both toxins obeyed a double-exponential time course: $\tau_1 = 25$ ms (78%) and $\tau_2 = 810$ ms (22%). (D) Dissociation experiments with Lqh-3 and δ-SVIE. In combination with δ-SVIE the toxin effect could not even be eliminated by very long depolarizations. Only about 3% of the channels showed a dissociation constant of 490 ms. For the remaining 97% a time constant of at least 15 s was estimated. Such long depolarizations cannot be tested experimentally because of slow channel inactivation taking place ($n = 5$).

a dissociation time constant of about 500 ms, a pulse of 2.5 s to +80 mV only removed about 10% of the toxin effect when 2 μM δ-SVIE was coapplied. Therefore, the two toxins clearly do not directly compete for the same binding site at the voltage sensor (Fig. 3D). Instead, they apparently stabilize each other at their target sites such that these toxins affect the gating of Na_V channels in a highly synergistic manner.

When applied together, Lqh-3 and δ-SVIE dissociated at a strikingly slower rate from the channel protein during depolarization than would have been predicted from the off-times of each of the individual toxins. Translocation of the domain-4 S3/S4 voltage sensor element is presumably required before the faster dissociation kinetics can occur. If the voltage sensor with both toxins bound were unable to undergo this conformational change upon depolarization, in effect, Lqh-3 and δ-SVIE immobilized the domain-4 S3/S4 element in a conformation different from that of the fully translocated voltage sensor.

With respect to the interaction motif between the S3/S4 linker and neurotoxins various possibilities are utilized in nature yielding competition or synergism between neurotoxins. δ-SVIE and Lqh-3, which are unrelated in structure and origin, co-operate in immobilizing the channel's voltage sensor. The results, thus, identify the molecular mechanism of δ-conotoxin action on Na_V channels and present an unprecedented synergism of neurotoxins with therapeutic potential.

Acknowledgments: We thank D. Gordon (University of Tel Aviv) for providing Lqh-2 and Lqh-3, J.S. Trimmer (SUNY, Stony Brook) for $Na_V1.4$, and S. Arend and A. Rossner for technical assistance. This work was supported by the Deutsche Forschungsgemeinschaft (HE 2993/5 to S.H.H.) and the BioFuture Prize of the German Ministry of Education and Research (#0311859 to H.T.).

References

[1] Zlotkin, E. (1999) The insect voltage-gated sodium channel as target of insecticides. Annu. Rev. Entomol. 44, 429–455.
[2] Cestele, S. and Catterall, W.A. (2000) Molecular mechanisms of neurotoxin action on voltage-gated sodium channels. Biochimie 82, 883–892.
[3] Terlau, H. and Olivera, B.M. (2004) *Conus* venoms: a rich source of novel ion channel-targeted peptides. Physiol. Rev. 84, 41–68.
[4] Fainzilber, M., Kofman, O., Zlotkin, E. and Gordon, D. (1994) A new neurotoxin receptor site on sodium channels is identified by a conotoxin that affects sodium channel inactivation in molluscs and acts as an antagonist in rat brain. J. Biol. Chem. 269, 2574–2580.
[5] Fainzilber, M., Lodder, J.C., Kits, K.S., Kofman, O., Vinnitsky, I., Van Rietschoten, J., Zlotkin, E. and Gordon, D. (1995) A new conotoxin affecting sodium current inactivation interacts with the δ-conotoxin receptor site. J. Biol. Chem. 270, 1123–1129.
[6] Shichor, I., Fainzilber, M., Pelhate, M., Malecot, C.O., Zlotkin, E. and Gordon, D. (1996) Interactions of δ-conotoxins with alkaloid neurotoxins reveal differences between the silent and effective binding sites on voltage-sensitive sodium channels. J. Neurochem. 67, 2451–2460.
[7] Hillyard, D.R., Olivera, B.M., Woodward, S., Corpuz, G.P., Gray, W.R., Ramilo, C.A. and Cruz, L.J. (1989) A molluscivorous Conus toxin: conserved frameworks in conotoxins. Biochemistry 28, 358–361.
[8] Hasson, A., Fainzilber, M., Gordon, D., Zlotkin, E. and Spira, M.E. (1993) Alteration of sodium currents by new peptide toxins from the venom of a molluscivorous Conus snail. Eur. J. Neurosci. 5, 56–64.
[9] Shon, K.J., Hasson, A., Spira, M.E., Cruz, L.J., Gray, W.R. and Olivera, B.M. (1994) δ-Conotoxin GmVIA, a novel peptide from the venom of Conus gloriamaris. Biochemistry 33, 11420–11425.
[10] Kohno, T., Sasaki, T., Kobayashi, K., Fainzilber, M. and Sato, K. (2002) Three-dimensional solution structure of the sodium channel agonist/antagonist δ-conotoxin TxVIA. J. Biol. Chem. 277, 36387–36391.
[11] Barbier, J., Lamthanh, H., Le Gall, F., Favreau, P., Benoit, E., Chen, H., Gilles, N., Ilan, N., Heinemann, S.H., Gordon, D., Menez, A. and Molgo, J. (2004) A δ-conotoxin from *Conus ermineus* venom inhibits inactivation in vertebrate neuronal Na^+ channels but not in skeletal and cardiac muscles. J. Biol. Chem. 279, 4680–4685.
[12] Trimmer, J.S., Cooperman, S.S., Tomiko, S.A., Zhou, J.Y., Crean, S.M., Boyle, M.B., Kallen, R.G., Sheng, Z.H., Barchi, R.L. and Sigworth, F.J., et al. (1989) Primary structure and functional expression of a mammalian skeletal muscle sodium channel. Neuron 3, 33–49.
[13] Chen, H., Gordon, D. and Heinemann, S.H. (2000) Modulation of cloned skeletal muscle sodium channels by the scorpion toxins Lqh II, Lqh III, and LqhαIT. Pflügers Arch. 439, 423–432.
[14] Bulaj, G., DeLaCruz, R., Azimi-Zonooz, A., West, P., Watkins, M., Yoshikami, D. and Olivera, B.M. (2001) δ-Conotoxin structure/function through a cladistic analysis. Biochemistry 40, 13201–13208.
[15] Sautiere, P., Cestele, S., Kopeyan, C., Martinage, A., Drobecq, H., Doljansky, Y. and Gordon, D. (1998) New toxins acting on sodium channels from the scorpion *Leiurus quinquestriatus hebraeus* suggest a clue to mammalian vs. insect selectivity. Toxicon 36, 1141–1154.
[16] Rogers, J.C., Qu, Y., Tanada, T.N., Scheuer, T. and Catterall, W.A. (1996) Molecular determinants of high affinity binding of α-scorpion toxin and sea anemone toxin in the S3–S4 extracellular loop in domain IV of the Na^+ channel alpha subunit. J. Biol. Chem. 271, 15950–15962.
[17] Gilles, N., Leipold, E,, Chen, H., Heinemann, S.H. and Gordon, D. (2001) Effect of depolarization on binding kinetics of scorpion α-toxin highlights conformational changes of rat brain sodium channels. Biochemistry 40, 14576–14584.
[18] Chen, H., Lu, S., Leipold, E., Gordon, D., Hansel, A. and Heinemann, S.H. (2002) Differential sensitivity of sodium channels from the central and peripheral nervous system to the scorpion toxins Lqh-2 and Lqh-3. Eur. J. Neurosci. 16, 767–770.
[19] Leipold, E., Lu, S., Gordon, D., Hansel, A. and Heinemann, S.H. (2004) Combinatorial interaction of scorpion toxins Lqh-2, Lqh-3, and LqhαIT with sodium channel receptor sites-3. Mol. Pharmacol. 65, 685–691.
[20] Volpon, L., Lamthanh, H., Barbier, J., Gilles, N., Molgo, J., Menez, A. and Lancelin, J.M. (2004) NMR solution structures of δ-conotoxin EVIA from *Conus ermineus* that selectively acts on vertebrate neuronal Na^+ channels. J. Biol. Chem. 279, 21356–21366.
[21] Little, M.J., Zappia, C., Gilles, N., Connor, M., Tyler, M.I., Martin-Eauclaire, M.F., Gordon, D. and Nicholson, G.M. (1998) δ-Atracotoxins from Australian funnel-web spiders compete with scorpion α-toxin binding but differentially modulate alkaloid toxin activation of voltage-gated sodium channels. J. Biol. Chem. 273, 27076–27083.
[22] Benzinger, G.R., Kyle, J.W., Blumenthal, K.M. and Hanck, D.A. (1998) A specific interaction between the cardiac sodium channel and site-3 toxin anthopleurin B. J. Biol. Chem. 273, 80–84.
[23] Kinoshita, E., Maejima, H., Yamaoka, K., Konno, K., Kawai, N., Shimizu, E,, Yokote, S., Nakayama, H. and Seyama, I. (2001) Novel wasp toxin discriminates between neuronal and cardiac sodium channels. Mol. Pharmacol. 59, 1457–1463.
[24] de Lima, M.E., Stankiewicz, M., Hamon, A., de Figueiredo, S.G., Cordeiro, M.N., Diniz, C.R., Martin-Eauclaire, M. and Pelhate, M. (2002) The toxin Tx4(6-1) from the spider *Phoneutria nigriventer* slows down Na^+ current inactivation in insect CNS via binding to receptor site 3. J. Insect. Physiol. 48, 53–61.

ELSEVIER

Toxicon 43 (2004) 671–684

TOXICON

www.elsevier.com/locate/toxicon

Isolation, molecular cloning and functional characterization of a novel β-toxin from the Venezuelan scorpion, *Tityus zulianus*

Adolfo Borges[a,*], Marcelo J. Alfonzo[a], Carmen C. García[a], Nena J. Winand[b], Enrico Leipold[c], Stefan H. Heinemann[c]

[a]*Sección de Biomembranas, Instituto de Medicina Experimental, Facultad de Medicina, Universidad Central de Venezuela, Box 50587, Sabana Grande, Caracas 1051, Venezuela*

[b]*Department of Molecular Medicine, College of Veterinary Medicine, Cornell University, Ithaca, NY, USA*

[c]*Research Unit Molecular and Cellular Biophysics, Medical Faculty of the Friedrich Schiller University Jena, Drackendorfer St 1, D-07747 Jena, Germany*

Received 23 December 2003; revised 26 February 2004; accepted 27 February 2004

Abstract

Sting in children by *Tityus zulianus* scorpions (western Venezuela) often produces cardiorespiratory arrest and death by pulmonary oedema. To assess its toxicity, lethality in mice of *T. zulianus* soluble venom was determined. Toxin composition was studied by fractionating the crude venom through reversed-phase HPLC. The most abundant peptide, Tz1, was purified further and its N-terminal sequence, amino acid composition and molecular mass (by electron-spray ionization mass spectrometry) determined. In the presence of Tz1, activation of recombinant rat skeletal muscle sodium channels ($Na_V1.4$) was shifted about 35 mV in the hyperpolarizing direction in a prepulse-dependent manner. This typical β-toxin effect had an apparent EC_{50} of 3.5 μM. A cDNA sequence encoding Tz1 was isolated from *T. zulianus* venom gland RNA using a combination of 5′- and 3′-RACE PCR. Analysis of the encoded sequence indicated that Tz1 is the processed product of a precursor containing: (i) a 20-residue long leader peptide; (ii) the amino acid sequence of the mature toxin (64 residues); and (iii) an extra Gly-Lys tail at the C-terminus, probably removed post-translationally. A comparison of Tz1 with *Tityus serrulatus* β-toxin Ts1 revealed that some of the non-conservative replacements in Tz1 lie in regions potentially involved in receptor recognition.

Keywords: *Tityus*; *Tityus zulianus*; Beta-scorpion toxin; Sodium channel activation; Receptor site-4

1. Introduction

Tityus is the largest and most lethal Neotropical scorpion genus including over 140 species (Fet and Lowe, 2000). Lethality of *Tityus* scorpion venoms is related to the content of long-chain (60–76 amino acid-long) toxins active on voltage-gated sodium (Na_V) channels in excitable cells, affecting either its activation (β-type) or inactivation (α-type toxin) mechanism (Barhanin et al., 1982; Becerril et al., 1997; Kalapothakis and Chávez-Olortegui, 1997). Most *Tityus* toxinological information is derived from research on the Brazilian species, *Tityus serrulatus*, which produces both α- (Ts3) and β-type (Ts1, Ts2) toxins. Particularly Ts1, the most abundant *T. serrulatus* venom component, has been extensively characterized by physiological (Vijverberg et al., 1984; Yatani et al., 1988), immunological (De Lima et al., 1993; Chávez-Olortegui et al., 2002), molecular (Becerril et al., 1993; Martin-Eauclaire et al., 1992), and structural

Abbreviations: ESI/MS, electrospray ionization mass spectrometry; Na_V, voltage-gated sodium channel; K_V, voltage-gated potassium channel; TFA, trifluoroacetic acid; RACE, random amplification of cDNA ends.

* Corresponding author. Tel.: +212-605-3629; fax: +212-605-3499.

E-mail address: aborges22000@yahoo.com (A. Borges).

0041-0101/$ - see front matter © 2004 Elsevier Ltd. All rights reserved.
doi:10.1016/j.toxicon.2004.02.022

(Polikarpov et al., 1999; Pinheiro et al., 2003) means. Toxic proteins have also been isolated from the Brazilian scorpions *Tityus bahiensis* (Becerril et al., 1996; Pimenta et al., 2001), *Tityus stigmurus* (Becerril et al., 1996), and *Tityus cambridgei* (Batista et al., 2002). However, toxin structure and mechanism of action from other *Tityus* spp. elsewhere in South America remain poorly known in spite that many are responsible for acute envenomation cases (Lourenço and Cuéllar, 1995). In Venezuela, where up to 40 *Tityus* species have been described (De Sousa et al., 2000; González-Sponga, 2001), differences in clinical symptoms have been noted depending upon geographical origin. Sting by *Tityus zulianus* (northern Mérida and Táchira States, western Venezuela) often produces respiratory arrest and death by pulmonary oedema in envenomed children (Borges, 1996; Borges et al., 2002; Mazzei de Dávila et al., 2002) whereas envenomation by *Tityus discrepans* (range north-central Venezuela) mainly causes pancreatic and gastrointestinal complications (Mota et al., 1994; Rossomando et al., 1997). *T. discrepans* venom is known to contain Na_V channel-active toxins (D'Suze et al., 1996; Tsushima et al., 1999) but only scarce information is available on *T. zulianus* venom lethality and toxin composition.

Given that differential venom toxicity may be related to species-specific toxin repertoires, we have studied the venom produced by *T. zulianus* to compare its composition and active components to other Venezuelan and South American *Tityus* toxins. First, we investigated the lethality of *T. zulianus* crude venom in mice. We then isolated a 7.4 kDa peptide, named Tz1, the most abundant component in *T. zulianus* venom. An electrophysiological approach on recombinant $Na_V1.4$, $Na_V1.5$ and $K_V1.5$ channels revealed the membership of Tz1 to the β-type scorpion toxin family. Whereas the novel β-type toxin Tz1 specifically interferes with the activation process of skeletal muscle Na_V channels ($Na_V1.4$) it was not effective on cardiac $Na_V1.5$ or on voltage-dependent K^+ ($K_V1.5$) channels.

2. Materials and methods

2.1. Venom extraction

Adult *T. zulianus* scorpions were collected at night around the villages of El Bordo, Mesa Bolívar, and Santa Cruz de Mora, western Mérida State, Venezuela, using the ultraviolet detection method (Stachel et al., 1999). Venom was milked by manual stimulation of the telson (Shulov and Zlotkin, 1969), and lyophilized at −50 °C and 30 mBar. Similarly, venom was obtained from adult *T. discrepans* scorpions collected near San Antonio de los Altos, Miranda Sate, central Venezuela, to compare its venom production to that of *T. zulianus*. Data are shown as mean ± standard error of the mean. Statistical analysis was performed using paired Student's *t* test to determine statistical significance. Protein concentration in solubilized venom samples was determined according to Lowry et al. (1951).

2.2. Tz1 isolation by reversed-phase high-pressure liquid chromatography (HPLC)

T. zulianus crude venom was solubilized in water and centrifuged at 10,000*g* for 5 min. Venom aliquots (300 μg protein) were fractionated through a C_{18} Vydac (218TP54) reverse phase column using a linear gradient from 25 to 35% acetonitrile containing 0.1% TFA over 55 min. The eluate was collected manually, pooled into fractions according to their retention times (F1–F6), and dried in a Speed-Vac drier (Savant). Fractions derived from several chromatographic runs were pooled for bioassays. Toxic peptide 4.1 was re-chromatographed in the C_{18} column with a linear gradient of 30–45% acetonitrile containing 0.1% TFA over 55 min.

2.3. Lethality tests

Toxicity of crude venom or chromatographic fraction pools was tested using albino mice strain CD1 (20.0 ± 1.0 g, National Institute of Hygiene, Caracas). For chromatographic pools, aliquots containing 50 μg of protein were injected intraperitoneally. Mice were observed for 24 h after inoculation for symptoms of intoxication such as spastic paralysis of rear limbs, increased salivation, apnea, diarrhea, respiratory failure and death. A fraction pool was considered: (1) non-toxic, if behavior of injected mice after 24 h resembled that of control animals, injected with 0.9% (v/v) sodium chloride; (2) toxic, if one or more of the symptoms listed above were elicited, and (3) lethal, if it was able to cause death of the challenged animals. *T. zulianus* crude venom lethality was assessed *via* intravenous inoculation as described by Borges et al. (1990); LD_{50} values were calculated according to Litchfield and Wilcoxon (1949).

2.4. Amino acid composition

Amino acids were analyzed using a Waters PicoTag® Amino Acid Analysis System according to the procedure of Bidlingmeyer et al. (1984). Cysteine residues were determined as cysteic acid after oxidation with performic acid according to the method of Hirs (1967).

2.5. N-terminal sequencing

Tz1 N-terminal sequence was determined in a gas-phase microsequencer (Porton Instruments, model 2090), using on-line phenylthiohydantoin analysis (Biotechnology Service Centre, Department of Clinical Biochemistry, University of Toronto).

2.6. Electrospray mass spectrometry (ESI/MS)

Tz1 molecular weight was estimated by mass spectrometry in a Perkin–Elmer Sciex (Thornhill, Canada) API III triple quadrupole mass spectrometer fitted with an Ion Spray source. The average spectrum from the samples injected was computed, and deconvolution of the series of multiply charged ions found in the spectrum into a true molecular mass spectrum was achieved with the Hypermass computer program (version 3.3, PE Sciex, Ont., Canada). Calculation of protein molecular weights was achieved with the MacBiospec computer program (version 1.0.1, PE Sciex, Ont., Canada), based on the MacProMass computer program (Lee and Vemuri, 1990). Molecular masses are reported as $[M + H^+]$.

2.7. RNA extraction

Total RNA was extracted from venom glands dissected from adult *T. zulianus* scorpions 24 h after venom extraction, a procedure shown to stimulate scorpion toxin gene transcription (Alami et al., 2001). Glands were snap-frozen in liquid nitrogen, and RNA extracted using the standard guanidinium isothiocyanate method (Chomczynski and Sacchi, 1987). Integrity of RNA was confirmed by agarose gel electrophoresis in the presence of formaldehyde (Sambrook et al., 1989).

2.8. Reverse transcriptase-mediated polymerase chain reaction (RT-PCR) for Tz1 mRNA

One microgram of total venom gland RNA was suspended in 20 μl of reverse transcriptase (RT) buffer (GIBCO BRL), 1 mM each of dATP, dCTP, dGTP, and dTTP, 20 U of ribonuclease inhibitor, 2.5 μM of a modified oligo(dT) primer (5′-GGCCACGCGTCGACTAGTAC-TTTTTTTTTTTTTTT-3′), and 200 U of SuperScriptII RT (GIBCO BRL), and incubated at 42 °C for 50 min. The reaction was stopped by heat inactivation at 70 °C for 5 min, chilled on ice and then incubated with 2 U of ribonuclease for 20 min at 37 °C. Appropiate amounts of cDNA products were amplified by PCR using Advantage 2 polymerase mix (Clontech Labs., Palo Alto, CA). Forward primer (2.5 μM) was a degenerate oligonucleotide designed to anneal to the sequence encoding the Tz1 N-terminus (KDGYLVGNDG) [5′-*GGATCC*AAA**(A/G)GA(C/T)GGITA(C/T)(C/T)TIG-TIGGIAA(C/T)GG**-3′; nucleotide sequence in bold encodes Tz1 N-terminal sequence; italicized nucleotides correspond to a *Bam*HI site; deoxyinosine (I) was included to reduce degeneracy (Kilpatrick et al., 1996)]. Reverse primer (0.5 μM) was 5′-GGCCACGCGTCGACTAGTAC-3′, which anneals to the 3′ end of the oligo(dT) (modified)-primed cDNA. The temperature profile of amplification consisted of one cycle at 94 °C (3 min), 35 cycles consisting of three steps at 94 °C (30 s), 40 °C (10 min), and 60 °C (2 min), respectively, and one last cycle at 72 °C (7 min).

2.9. Cloning and characterization of PCR products

PCR fragments were ligated to the vector pCR2.1-TOPO (Invitrogen). Sequences were determined using M13 universal forward and reverse primers (5′-GTAAAAC-GACGGCCAG-3′ and 5′-CAGGAAACA-GCTATGAC-3′, respectively) in an ABI377 DNA sequencer.

2.10. 5′RACE

5′-Rapid amplification of cDNA ends (5′-RACE) was carried out using a 5′-RACE Kit (GIBCO BRL), using *T. zulianus* Tz1-specific antisense primers (primer 1, 5′-TTTGCCTCTTCCGCATCTATTTGTAGC-3′; primer 2, 5′-CACCCAATTTGGCAT-ACTGTAGC-3′ and primer 3, 5′-GCATTCGTTAGCGCAATAGGTCCC-3′); cDNA was synthesized using SuperScript II RT (GIBCO BRL) as described previously, and primer 1 as gene-specific primer. The synthesized cDNA was tailed with poly(dC) upon incubation with terminal transferase and amplified by PCR with a poly[d(GI)]-anchor primer and primer 2. A further amplification using the anchor primer and primer 3 was performed to confirm identity of the 5′-RACE product. Fig. 3B summarizes the PCR strategy and primer sets utilized for amplification of the full-length Tz1 cDNA.

2.11. Cell culture

HEK 293 cells (CAMR, Porton Down, Salisbury, UK) were maintained in Dulbecco's Minimal Eagle's Medium (DMEM), supplemented with 10% fetal calf serum and F12 in a 5% CO_2 incubator. Cells were trypsinized, diluted with culture medium and grown in 35 mm dishes. Electrophysiological experiments were performed 1–3 days after plating. In this study we used HEK 293 cells stably expressing rat $Na_V1.4$ [μI or Skm1 (Chen et al., 2000)] and human $Na_V1.5$ [hH1 or Skm2 (Chen and Heinemann, 2001)] channels. Human $K_V1.5$ channels (Kamb et al., 1989) were transfected transiently using the Superfect transfection kit (Qiagen, Hilden, Germany).

2.12. Electrophysiological measurements

Whole-cell voltage clamp experiments were performed as described previously (Chen et al., 2000). Briefly, patch pipettes with resistances of 0.9–2.0 MΩ were used. The series resistance was compensated for by more than 80% in order to minimize voltage errors. A patch clamp amplifier EPC9 was operated by PatchMaster software (both HEKA Elektronik, Lambrecht, Germany). Holding potential was −120 mV. Leak and capacitive currents were corrected with a *p/n* method with a leak holding voltage of −140 mV, a leak pulse scaling factor of −0.1 and $n = 10$ leak pulses. Due to the toxin-induced left-shift in activation, this procedure was necessary in order to avoid the recording of ionic current during the leak pulses. Currents were low-pass

filtered at 5 kHz and sampled at a rate of 25 kHz. All experiments were performed at constant temperature 19–21 °C. Data analysis was performed using IgorPro (WaveMetrics, Lake Oswego, OR, USA). All data were presented as mean ± standard error of the mean (n = number of independent experiments). The patch pipettes contained (in mM): 35, NaCl; 105, CsF; 10, EGTA; 10, Hepes (pH 7.4 with CsOH). The bath solution contained (in mM): 150, NaCl; 2, KCl, 1.5, $CaCl_2$; 1, $MgCl_2$; 10, Hepes (pH 7.4 with NaOH). The application of toxin was performed with an application pipette as described previously (Chen et al., 2000).

2.13. Current–voltage relationships

From a holding potential of −120 mV cells were depolarized with a three-step protocol (see Fig. 4A). The first and the last depolarization of 20 ms duration ranged from −130 to +55 mV in steps of 5 mV. The central pulse to −10 mV for 50 ms was used as a prepulse to prime the channels. The segments of 50 ms at −140 mV ensured recovery from inactivation. The peak currents during the first and third depolarization were plotted as a function of voltage, yielding two current–voltage relationships, one without and one with prepulse. Repetition interval was 5 s. The current-voltage relationships of the control records were fit according to a Hodgkin–Huxley formalism with $m = 3$ activation gates and a single-channel conductance according to the Goldman–Hodgkin–Katz equation. Data after toxin application were described with an additional component with $m = 1$ and the weighting factor P_{tox} indicating the fraction of channels with strongly shifted activation threshold.

$$I_{peak}(V) = I_{max}\left[\frac{1-P_{tox}}{(1+e^{-(V-V_m)/k_m})^3} + \frac{P_{tox}}{1+e^{-(V-V_{tox})/k_{tox}}}\right]$$

$$I_{max} = \Gamma V \frac{1-e^{-(V-E_{rev})/25\ mV}}{1-e^{-V/25\ mV}} \quad (1)$$

V_m is the voltage of half-maximal gate activation and k_m the corresponding slope factor. V_{tox} is the voltage of half-maximal activation of toxin-modified channels and k_{tox} the corresponding slope factor. Γ is the maximal conductance of all channels. 25 mV reflects the thermal energy of one electron charge at room temperature (kT/e).

2.14. Voltage dependence of fast inactivation

From a holding potential of −120 mV cells were conditioned for 500 ms at voltages ranging from −140 to −35 mV in steps of 5 mV. Subsequently, peak current was determined at −20 mV. The repetition interval was 10 s. The peak current plotted versus the conditioning voltage was described with a double Boltzmann function:

$$I(V) = I_{min}\left[\frac{1-P_{tox}}{(1+e^{-(V-V_h)/k_h})} + \frac{P_{tox}}{(1+e^{-(V-V_{htox})/k_{htox}})}\right] \quad (2)$$

with the half-maximal inactivation voltage V_h and the corresponding slope factor k_h indicating the voltage dependence for channels in the absence of toxin. V_{htox} and k_{htox} denote the corresponding values for toxin modified channels, and P_{tox} is the probability of toxin modification.

2.15. Dose-response curves

P_{tox} obtained from the current-voltage relationships (Eq. (1)) was plotted as a function of the toxin concentration. The concentration dependence was described with the Hill equation:

$$P_{tox} = \frac{P_{max}}{1+\left(\frac{EC_{50}}{[toxin]}\right)^h} \quad (3)$$

where h is the Hill coefficient, [toxin] is the toxin concentration, and P_{max} corresponds to the maximally obtained P_{tox} value. EC_{50} provides a measure for the concentration of half-maximal β-toxin effect. Errors for EC_{50} and P_{max} were obtained from these fits with the IgorPro Program.

3. Results

3.1. Crude venom yield and lethality

Venom yield by manual stimulation (in mg of venom dry weight per specimen) was significantly higher ($p > 0.01$) in *T. zulianus* (1.66 ± 0.20, $n = 23$) than in *T. discrepans* (0.54 ± 0.10 mg, $n = 23$). The medium-lethal dose in mice (*via* i.v.) of *T. zulianus* soluble venom was 1.54 ± 0.02 mg/kg ($n = 4$). Mice inoculated with lethal doses of *T. zulianus* venom exhibited neurotoxic signs typical of scorpion envenomation, e.g. spastic paralysis of rear limbs, increased salivation, apnea, tachycardia, and increased perspiration; however, the pronounced diarrhea observed in mice inoculated with *T. discrepans* venom was absent from *T. zulianus* envenomed mice.

3.2. Tz1 isolation and chemical characterization

The soluble venom of *T. zulianus* was fractionated by HPLC into at least 30 components (Fig. 1). Since we are interested in *T. zulianus* peptides toxic to vertebrates, HPLC peaks were pooled into fractions F1–F6 for toxicity assay by intraperitoneal injection in mice. Although fractions F3 and F5 were toxic, fraction F4 showed the most severe effects, being lethal at the dose (50 μg) inoculated. Main peptides Tz4.1 and Tz4.2 from fraction F4 (Fig. 1) were collected separately and subjected to further purification. Molecular weights obtained by ESI/MS for peptides Tz4.1 and Tz4.2 were 7367.16 ± 0.57 ($n = 4$) and 7295.42 ± 0.50 ($n = 3$), respectively, indicating that they belong to the long-chain class of scorpion neurotoxins that

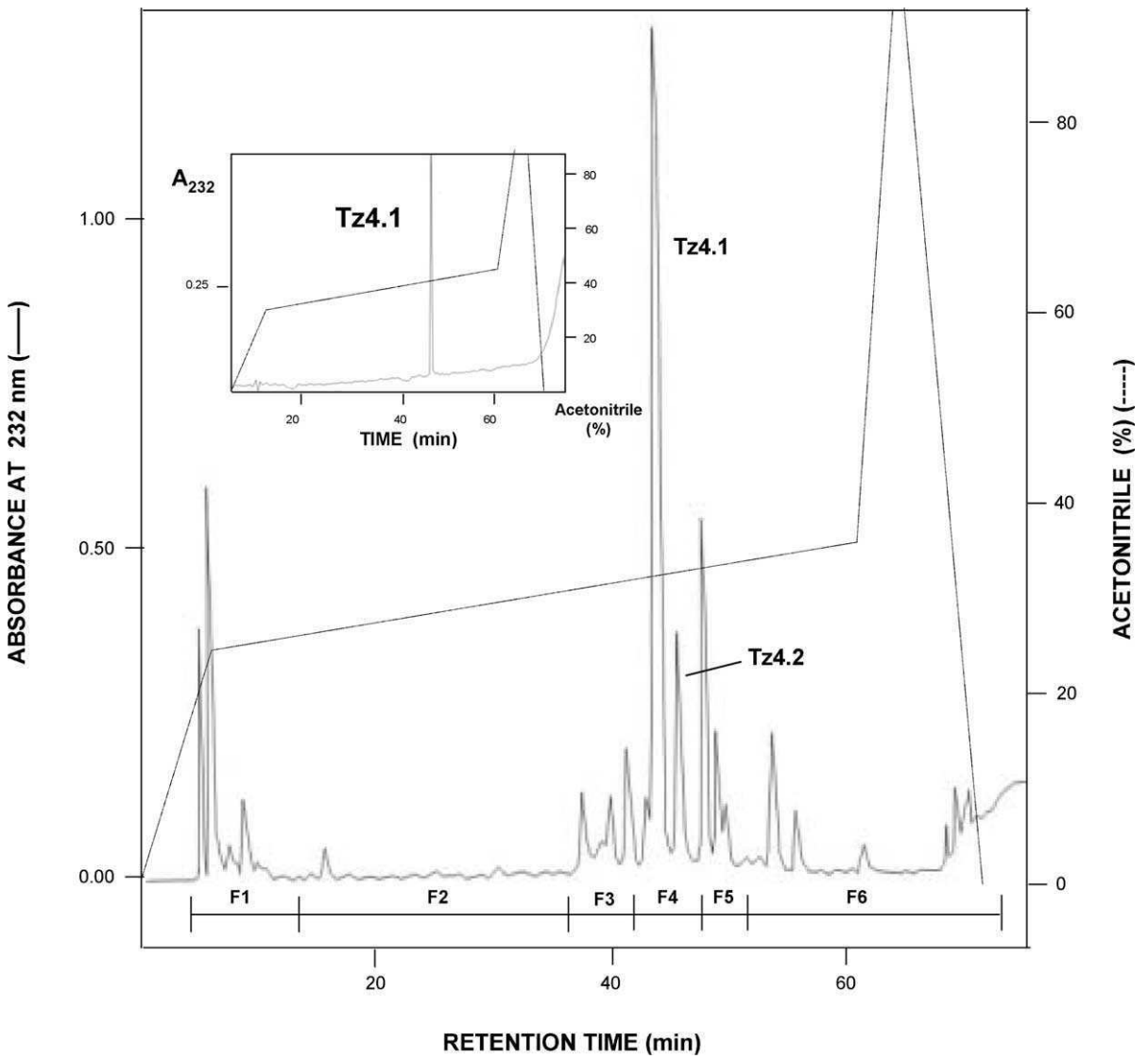

Fig. 1. High-performance liquid chromatography separation of *Tityus zulianus* venom. Aliquots (300 μg each) of soluble venom were loaded repeatedly onto a C_{18} reverse phase HPLC column, equilibrated with 0.1% TFA, given essentially the same profile. Column was eluted with a linear gradient of acetonitrile containing 0.1%TFA (25–35% run for 55 min, then 35–100% run for 5 min) at a flow rate of 0.5 ml/min and the absorbance recorded at 232 nm. Fractions F1–F6 used for bioassays are indicated by horizontal bars. The arrows indicate peaks containing peptides present in fraction F4. Inset shows final purification of peptide Tz4.1, later identified as toxin Tz1, using a linear 30–45% acetonitrile gradient (in 0.1% TFA).

target voltage-gated sodium channels (Possani et al., 1999). Profile of final purification of Tz4.1 is shown in the inset of Fig. 1. Given its abundancy, we proceeded with the chemical and physiological characterization of peptide Tz4.1.

Fig. 2 shows the ESI/MS spectrum for the purified Tz4.1. Deconvolution of the multiply charged ions found in the spectrum into a true molecular mass spectrum rendered a single peak of 7367.16 Da (not shown). Amino acid analysis was also carried out on Tz4.1, producing a molar composition as shown in Table 1. The first 10 N-terminal amino acid residues for Tz4.1 were KDGYLVGNDG, as determined by Edman degradation of pure Tz4.1. Taken together, the N-terminal sequencing and amino acid analyses and mass spectral studies suggest that Tz4.1 is a pure component with no detectable protein impurities. Following the nomenclature suggested by Becerril et al. (1997), Tz4.1 is named Tz1, as the first toxin characterized from *T. zulianus*.

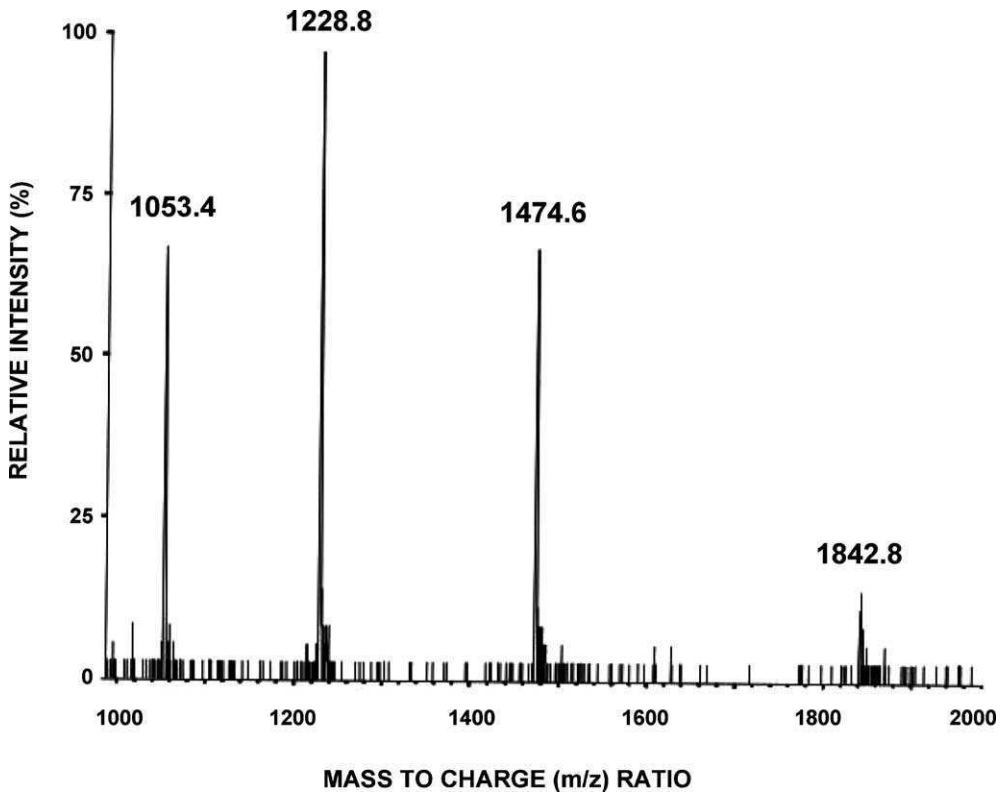

Fig. 2. Electrospray ionization mass spectrum of the purified toxin Tz1. The peaks from left to right are the +7, +6, +5, and +4 ionization states. Deconvolution of the multiply charged ions found in the spectrum into a true molecular mass spectrum rendered a single peak (not shown) of 7367.16 ± 0.57 Da ($n = 4$). The observed molecular weight was within 0.01% of the calculated weight (7367.33) for the protein containing four intrachain disulfide bonds, assuming a C-terminal processing where the dipeptide Gly-Lys is removed post-translationally.

3.3. Tz1 molecular characterization

To determine the full primary structure of Tz1, a molecular approach was undertaken, using a combination of 3′- and 5′-RACE amplifications starting from total venom gland RNA. After 3′-RACE amplification and cloning, all *Escherichia coli* DH5α transformants analyzed for plasmid sequencing harbored an identical 299 bp-long insert, coding for a 66 amino acid-long polypeptide containing eight cysteine residues with a sequence highly homologous to other known scorpion toxins. A 5′-RACE amplification was then carried out to confirm the 5′-end sequence of this cDNA and also to deduce the primary structure of the leader peptide region known to precede the toxin-coding region in the precursor. Fig. 3A (lane 1) shows the product of amplification derived from the terminal transferase-driven reaction using total *T. zulianus* venom gland cDNA as template. Lane 2 shows confirmation of the identity of this product *via* nested PCR. Both of these products were sequenced and confirmed to code for overlapping sequences. Fig. 3B shows the full nucleotide sequence for the cDNA encoding toxin Tz1 combining the sequences obtained by the 3′- and 5′-RACE protocols. The open reading frame for the Tz1 pro-toxin is 258 bp-long, including a 60 bp-long region coding for the signal peptide, and ending with a TAG stop codon. This latter, 20 amino acid-long leader region, is predominantly hydrophobic and is assumed to be released by the means of a signal peptidase acting at a small neutral residue (possibly Cys(-1) in Tz1) upon toxin maturation (Becerril et al., 1997). Sequencing of the Tz1 precursor also reveals the presence of a putative polyadenylation signal, located 59 bp from the termination codon, the site for endonucleolytic cleavage before synthesis of the poly(A) tail (Wahle and Ruegsegger, 1999).

3.4. Tz1 functional characterization

To test for the functional effects of isolated Tz1, we performed electrophysiological whole-cell patch clamp experiments with HEK 293 cells stably expressing rat skeletal muscle $Na_V1.4$ channels. As it is known that scorpion β-toxins induce a left-shift in the voltage dependence of channel activation in a use-dependent manner (e.g. Tsushima et al., 1999; Cestèle et al., 1998), we employed a three-pulse stimulation protocol as indicated in Fig. 4A: From −140 mV channels were activated with

Table 1
Tz1 amino acid composition determined by chemical analysis (AA) and cDNA sequencing. Molar composition calculated by amino acid analysis is expressed as mol of residue per mol of Tz1 based on Tz1 mol. weight determined by ESI/MS (7367.16). Composition based on DNA sequence is derived from Fig. 3. N.D., not determined

Amino acid	AA	cDNA
Asp + Asn	7.6	7
Glu + Gln	1.4	1
Ser	3.0	3
Gly	6.7	7
His	0.0	0
Arg	4.9	5
Thr	3.9	4
Ala	4.0	4
Pro	2.4	2
Tyr	6.6	7
Val	2.9	3
Met	1.8	2
Ile	0.1	0
Leu	0.9	1
Phe	1.2	1
Lys	5.0	5
Trp	N.D.	3
Cys-HSO_3[a]	7.3	8

[a] Cysteic acid, determined after protein oxidation with performic acid.

brief depolarizations between −130 and +55 mV in a first pulse, P_1. Subsequently, channels were conditioned by a 50 ms depolarization to −10 mV. During that period toxin binding should be facilitated. After a recovery from fast inactivation, channel activation was assayed in pulse P_2. Superpositions of representative current records from one cell are shown below. Under control conditions channels start to activate around −40 mV and undergo rapid inactivation. Upon application of 1 μM Tz1 activation already occurs at lower voltages (see highlighted trace at −60 mV). This toxin-induced activation is prepulse dependent as the current amplitude in P_2 is larger than in P_1. In panel B of Fig. 4 some current traces in P2 are superimposed for the indicated voltages. It is clearly seen that in the presence of 1 mM Tz1 even at −80 mV channels open. In addition, traces at 0 mV clearly show that the speed of inactivation is not altered, i.e. no effect typical for scorpion α-toxins is observed.

Using a three-pulse protocol with P1 and P2 to −60 mV the time course of the onset and recovery of the toxin effect was assayed (data not shown). Upon application of 1 μM Tz1, the toxin effect developed with an exponential time course with a time constant of 14.1 ± 3.3 s ($n = 8$). Upon washout of the toxin, the effect disappeared completely within 30 s.

Current–voltage (I–V) relationships were analyzed quantitatively by describing them according to a simple Hodgkin–Huxley formalism (Eq. (1)). In the absence of toxin, I–Vs were described with three independent activation gates yielding a half-maximal activation voltage per gate, V_m, of about −40 mV. Upon application of toxin mainly two things happened: (1) Even at low concentrations of Tz1 (10 nM), V_m shifted slightly to the negative direction. (2) A much more left-shifted component appeared at higher concentrations (>100 nM). The maximal left shift of that component was estimated by Eq. (1) with a second activation Boltzmann component with $m = 1$ for high-concentration data. The fit results yielded an apparent $V_{m,tox}$ of −75 mV, giving rise to substantial activation of channels even at −100 mV. In the example shown in Fig. 4C the strongly shifted component was 11% of all channels in 1 μM and 48% in 10 μM Tz1. It is also seen that the fraction of channels with strongly shifted I–V characteristics is smaller in the absence of a prepulse (gray symbols).

The thereby estimated probabilities of toxin-channel interaction (P_{tox}) were plotted in Fig. 5A as a function of Tz1 concentration. Assuming a Hill coefficient of 1, a data fit with a Hill equation (Eq. (3)) yielded an apparent EC_{50} of 3.5 ± 0.7 μM and a maximal toxin occupancy of 63 ± 6%. Without prepulse (gray symbols) the results were $EC_{50} = 11.1 \pm 3.1$ μM, and $P_{tox,max} = 68 \pm 10\%$ (fit not shown), clearly indicating that toxin binding is strongly facilitated by the prepulse to −10 mV.

The rather small shift observed for the V_m parameters are further shown in Fig. 5B as a function of Tz1 concentration. This shift is similarly observed for with and without prepulse at 10 nM Tz1 (between −5 and −10 mV) and seems to saturate at about 1 μM Tz1 between −10 and −15 mV. At present we cannot conclude whether this effect is non-specific due, e.g. to a surface activity of Tz1, or if it reflects an additional specific high-affinity binding of Tz1 on a receptor site on $Na_V1.4$ channels distinct from toxin binding site-4.

An effect often observed when applying α- or β-toxins to Na_V channels is an increase or decrease of the peak current. To assay a potential effect of Tz1 on the single-channel amplitude and/or the open-probability we analyzed the maximal conductance, Γ, obtained in I–V recordings (see Eq. (1)). As shown in Fig. 5C, Γ slightly decreases in 1 μM Tz1 to 90 ± 8% ($n = 7$) and in 10 μM Tz1 to 67 ± 7% ($n = 5$) of the control. Note that the conductance was reduced although the maximal peak inward current in I–V recordings was increased upon toxin application (Fig. 4C).

Channel inactivation was assayed by 500 ms conditioning pulses to varying voltages and a subsequent test for channel availability at −20 mV. As shown in Fig. 6A, steady-state inactivation was also left-shifted. In the presence of 1 μM Tz1, the half-maximal inactivation voltage, V_h, being around −70 mV under control conditions, was shifted by −13.0 ± 2.2 mV ($n = 7$), but also a small, more left-shifted component became apparent. This was much clearer at

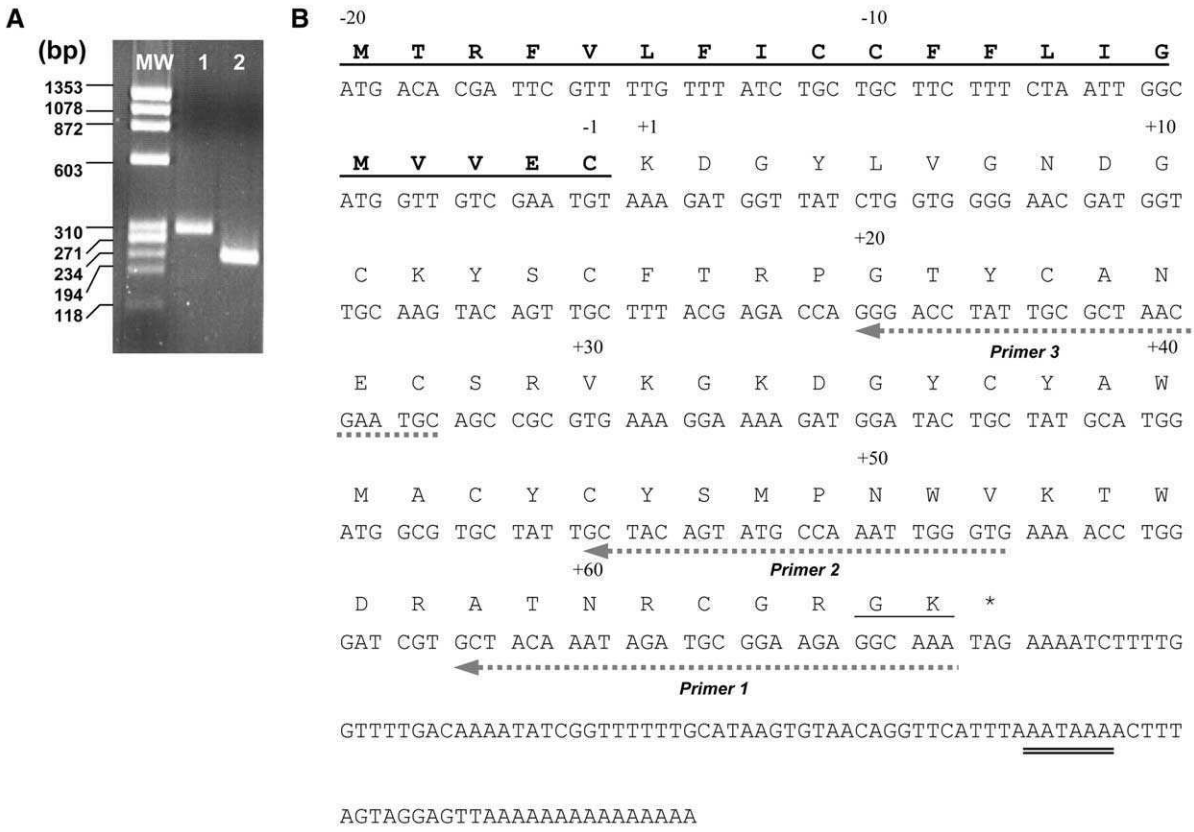

Fig. 3. Molecular characterization of Tz1. (A) Agarose gel electrophoresis showing (lane 1) the fragment obtained after amplification of the terminal transferase-driven reaction product starting from total venom gland *Tityus zulianus* cDNA. Lane 2 shows product after amplification via nested PCR from 5′-RACE fragment shown in lane 1 (see Section 2 for details). (B) Nucleotide sequence of the cDNA encoding the Tz1 precursor. The predicted protein sequence is shown above the nucleotide sequence and is numbered starting from the toxin N-terminal residue (+1); underlined amino acid residues are putatively processed post-translationally; the signal peptide is in bold face; the stop codon is indicated by an asterisk; a potential polyadenylation site (AAUAAA) is doubly underlined. Primers used in the 5′-RACE experiments are shown.

10 μM Tz1 (Fig. 6A, right). Here, a second component with $V_{h,tox}$ of −113.5 ± 4.4 mV ($n = 5$) with a relative amplitude of 53 ± 3% appeared. Thus, Tz1 shows typical effects of a β-toxin, namely a strong use-dependent left-shift in activation and a shift in steady-state inactivation without marked effects on the time course of inactivation. In Fig. 6B the shift in V_h is shown as a function of Tz1 concentration. Like for V_m (Fig. 5B), V_h only shifts by about −10 to −15 mV in a saturating manner.

Tz1 was also tested on human cardiac muscle sodium channels ($Na_V1.5$). As shown for other β-toxins (e.g. Ts1 (Marcotte et al., 1996); CssII (Cestèle et al., 1998); Lqhβ1 (Gordon et al., 2002)), Tz1 also showed only a weak effect on these channels. At 1 μM Tz1 activation as shifted by −8.3 ± 0.7 mV and inactivation by −9.7 ± 1.0 mV ($n = 5$). Tz1 (10 μM) shifted by −3.1 ± 1.0 mV and inactivation by −5.7 ± 1.4 mV ($n = 3$). Thus, it can be assumed that the molecular determinants of toxin receptor site-4, namely the extracellular S3/S4 loop of domain-2 are also important for Tz1.

Similarly to $Na_V1.4$, a reduction in the maximal conductance was observed for $Na_V1.5$ channels when 10 μM Tz1 was applied: to 90 ± 2% ($n = 5$) for 1 μM and to 69 ± 9% ($n = 3$) for 10 μM Tz1. This finding is consistent with previous reports (Cestèle et al., 1998; Marcotte et al., 1996) in which it was shown that the β-toxin effect on activation threshold, but not on conductance, is determined by the S3/S4 loop of domain 2. It should be noted at this point that an apparent reduction of the total conductance, and hence a reduction of peak current, is easily obtained by β-toxins owing to their potential of shifting the steady-state inactivation voltage dependence. Thus, we have paid particular attention to this point by applying very negative holding potentials (−140 mV) prior to the collection of $I–V$ data.

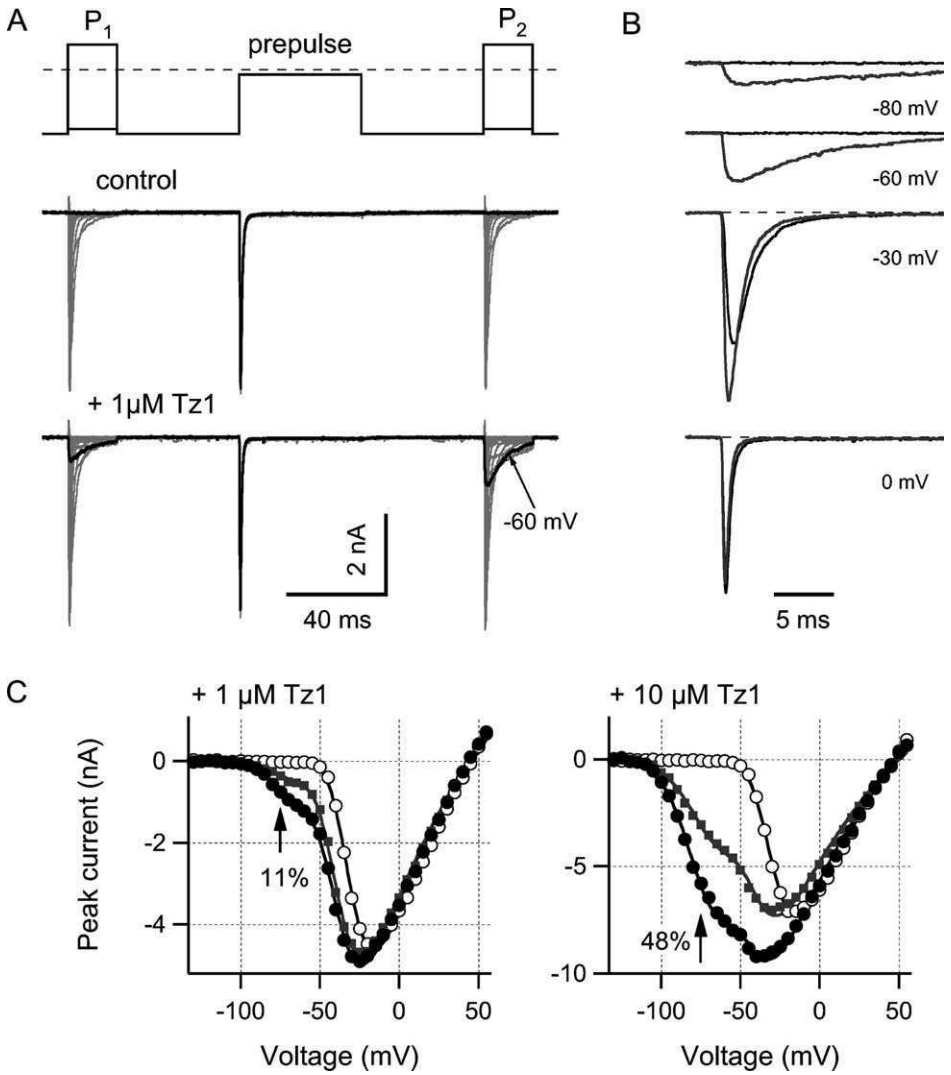

Fig. 4. Effect of Tz1 on Na^+ currents mediated by $Na_V1.4$ channels in HEK 293 cells. (A) *top*, Pulse protocol used to elicit Na^+ currents at potentials ranging from − 130 to +55 mV in steps of 5 mV. P_1 denotes the first depolarization pulse; P_2 is a second depolarization pulse applied after a 50 ms conditioning prepulse to − 10 mV. *Bottom*, The current traces are shown for 10-mV intervals, the traces with P_1 and P_2 at -60 mV are highlighted in black. Application of 1 μM Tz1 results in strong activation of current at − 60 mV in a prepulse-dependent manner. (B) Superposition of individual current traces during the P_2 pulse for the indicated voltages. (C) Current–voltage relationships for $Na_V1.4$ channels before (open circles) and after application of the indicated concentration of Tz1 with (filled circles) and without prepulse (gray squares). The continuous curves indicate fit results according to Eq. (1). The estimated percentage of channels undergoing a strong hyperpolarizing activation shift is indicated.

A potential activity of Tz1 as a potassium channel blocker was assayed by expressing and analyzing human $K_V1.5$ channels in HEK 293 cells. Tz1 at a concentration of up to 1 μM had no effect on $K_V1.5$ ($n = 4$, data not shown).

4. Discussion

The evidence presented in this work demonstrates the lethality of *T. zulianus* venom for vertebrates, supporting its original classification, based on clinical reports, as a species of medical importance in Venezuela (Borges, 1996). The venom LD_{50} is comparable to that reported for the Brazilian scorpions *T. serrulatus*, *T. bahiensis*, and *T. costatus*, considered as highly toxic (Nishikawa et al., 1994). Significantly, *T. zulianus* venom is 1.6-fold more toxic than the central Venezuelan species, *T. discrepans* (2.51 mg/kg; Borges et al., 1990), evaluated under similar conditions. Taken together with *T. zulianus* higher venom production, this observation may explain, at least in part, the differences in clinical outcome in humans stung by these two Venezuelan species (Borges et al., 2002). Although

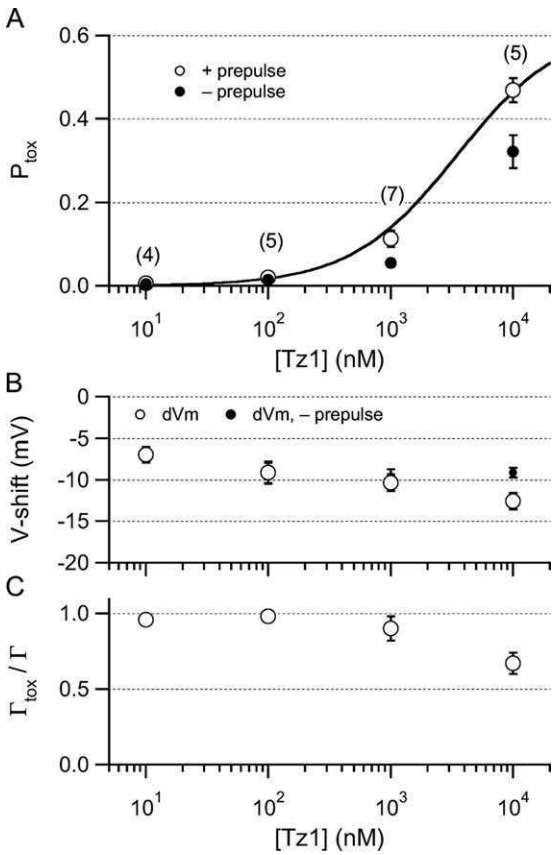

Fig. 5. Dose dependence of Tz1 effects on $Na_V1.4$ channels. (A) The estimated probability of toxin binding as a function of Tz1 concentration with (open circles) and without prepulse (filled circles). The continuous curve is a Hill function (Eq. (3)) yielding an apparent EC_{50} value of 3.5 ± 0.7 μM and a maximal effect of $63 \pm 6\%$. The Hill coefficient was set to 1. The numbers in parentheses indicate the number of independent cells measured. (B) Dose dependence of the voltage shifts observed in the current–voltage relationships (dV_m with and without prepulse). Note that these shifts in voltage dependence do not reflect the shift of the early-activating fraction of channels. (C) Fraction of maximal Na^+ conductance of the cells after toxin application obtained from current–voltage relationships as shown in Fig. 4C.

some epitopes might be shared between *T. zulianus* and *T. discrepans* toxins, as indicated by immunoblotting (Borges et al., 1999), structural and/or functional differences should exist to explain the partial in vivo neutralization of *T. zulianus* venom by the anti-*T. discrepans* serum (A.B., unpublished results).

The investigation of *T. zulianus* toxin repertoire is also initiated in this report with the characterization, using molecular and electrophysiological approaches, of the first isolated long-chain *T. zulianus* toxic protein, Tz1. Upon search of the Swiss Prot and NCBI data banks, Tz1 predicted amino acid sequence was found most similar to those corresponding to *Tityus* and *Centruroides* neurotoxins previously characterized as β-type toxins, as shown in Fig. 7A. The most closely related protein, with an identity of 64%, is toxin Ts1, from the Brazilian scorpion *T. serrulatus*, whose crystal structure has been elucidated recently (Polikarpov et al., 1999; Pinheiro et al., 2003). A similar scaffold to that found in Ts1 (and also in the structure of the Mexican β-toxin Cn2 (Pintar et al., 1999)) must occur in Tz1 given the strict conservation of the disulfide-bridge forming cysteine residues (Fig. 7A). Most of the residues belonging to the three beta sheets and the alpha helix found in the Ts1 structure are conserved in Tz1 (Fig. 7B) with the exception of Ala24-Asn25 (in the helical region), which are highly variable residues among toxins from *Tityus* spp. (Fig. 7A (Pimenta et al., 2001)). Residues Lys12, Trp39 and Trp54 (Trp40 and Trp55 in Tz1 numbering), known by chemical modification of Ts1 to be critical for binding to Na_V channels (Hassani et al., 1999), are also found in the *T. zulianus* toxin. The presence in Tz1 of residues Lys1 and Lys12, conserved in all β-toxins (Fig. 7A) but absent from α-toxins (Gordon et al., 1998), was a strong indication that Tz1 is a β-type scorpion neurotoxin.

Like shown for other β-toxins (Cestèle et al., 1998; Gordon et al., 2002), Tz1 shifts the activation threshold of sodium channels in the hyperpolarizing direction very efficiently for $Na_V1.4$ but not for $Na_V1.5$. In addition, this effect became much stronger when the channels were primed with a prepulse. This use-dependent modulation of the Na_V channel activation is typical for scorpion β-toxins. As shown by Cestèle et al. (1998) for the interaction of CssII with $Na_V1.2a$ channels, a prepulse, presumably exposing the S3/S4 loop of domain-2 to the extracellular side, enhances β-toxin association and thereby causes a trapping of the voltage sensor in its activated position. Hence, the ability of Tz1 to affect channel activation most likely depends on the state of the voltage sensor in domain-2. Cestèle et al. (1998) have identified Gly845 (in $Na_V1.2a$ channels) as an important determinant for channel recognition by CssII: when mutated to Asn, as present in $Na_V1.5$ channels, the β-toxin effect on activation is abolished. Since this critical Gly residue is conserved in mammalian tetrodotoxin-sensitive Na_V channels (Gly658 in $Na_V1.4$), it is very likely that this residue is also involved in the action of Tz1 on $Na_V1.4$.

Analysis of the cDNA-based predicted Tz1 amino acid sequence leads us to suggest that a post-translational modification at the C-terminus may occur upon toxin maturation, with the removal of the diad Gly65-Lys66 by a carboxyl-end peptidase (Possani et al., 1999), leaving Arg64 as the C-terminal most residue. It is not known at present whether Arg64 is amidated in Tz1, although the current rules of carboxyl-end processing for long-chain scorpion toxins predict that the amino group of Gly65 would be used to amidate this residue (Possani et al., 1999). The calculated molecular weight of such putatively processed Tz1 is 7367.33 (assuming that the toxin contains four intrachain disulfide bonds), which coincides with

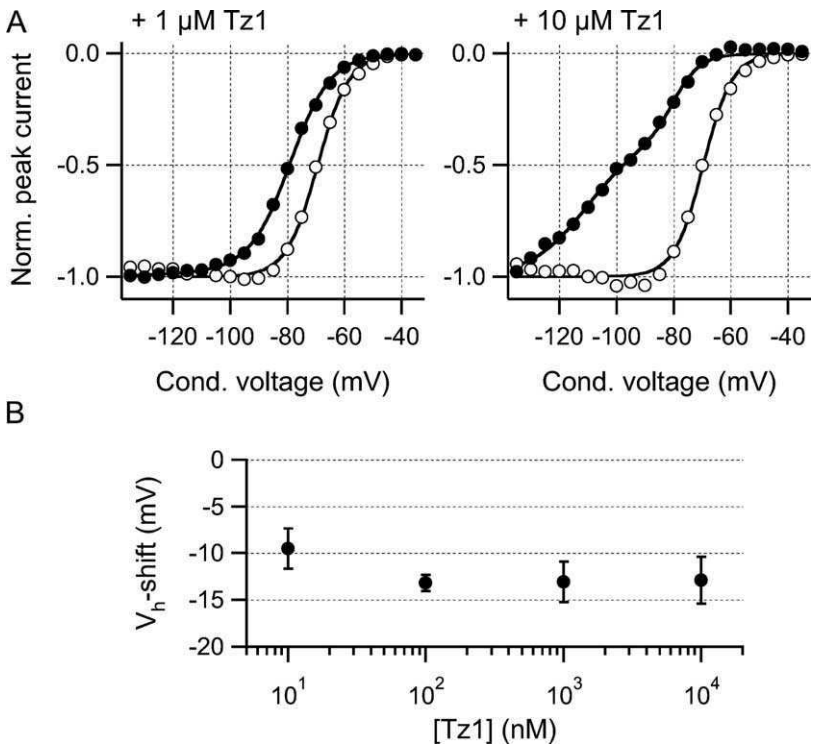

Fig. 6. Steady-state inactivation. (A) Normalized peak current at −20 mV after 500 ms conditioning at the indicated voltages under control conditions (open circles) and after toxin application (filled circles). The continuous curves are fits according to Eq. (2). (B) Dose-response plot for the shift in the mid-potential of half-inactivation (V_h). Note that this shift does not reflect the strong toxin-induced shift expressed by the second Boltzmann component.

the ESI-MS measured molecular weight of the purified protein (7367.16 Da). It should also be noted that amino acid composition of such predicted processed Tz1 fully agrees with the chemical composition obtained for the purified Tz1 (Table 1).

Although Tz1 primary structure suggests this protein to be related structurally and functionally to *T. serrulatus* Ts1, some differences should be noted. For instance, conformation of the polypeptide chain in the region connecting beta-sheets β2 and β3 probably differs between Tz1 and Ts1. An additional residue, Tyr38, is found at the C-terminus of Tz1 β2 which is in register with the equivalent Tyr41/42 in *Centruroides* toxins but lacking in Ts1 and other *Tityus* β-toxins (Fig. 7A). In *C. noxius* Cn2, Tyr42 has been found to contribute to the hydrophobic patch putatively involved in receptor binding (Pintar et al., 1999). In addition, Pro40 is found in the *cis* conformation in Ts1, contributing to the tight bend of loop 3 (Polikarpov et al., 1999; Pinheiro et al., 2003). This residue, also conserved in other Brazilian β-toxins, is replaced by Met41 in Tz1, in register with the conserved Phe43/44 residue of *Centruroides* toxins (Fig. 7A). Such differences could affect in Tz1 the environment of the residue Trp40, critical for β-toxin activity (Hassani et al., 1999). Other non-conservative replacements in loops 1 and 2 (e.g. Gly7 and Lys33) may introduce positional charge differences in Tz1 with respect to Ts1 (Fig. 7B). Our molecular, spectral and amino acid composition data also suggest that Tz1 bears a C-terminal extension (Gly63-Arg64) absent in Ts1. It is known that the C-terminal region and the loops connecting the secondary structure elements encompass bioactive surfaces involved in receptor recognition by scorpion toxins (Gurevitz et al., 2001; Gordon and Gurevitz, 2003). Taken together, the above differences could contribute to a differential selectivity of Tz1 for sodium channel subtypes in comparison with other *Tityus* β-toxins.

In conclusion, *T. zulianus* is classified as a highly toxic scorpion species from western Venezuela. The most abundant component of all HPLC-resolved *T. zulianus* venom peptides, Tz1, is a new *Tityus* β-toxin whose predicted aminoacid sequence reveals structural similarities as well as differences with previously characterized *T. serrulatus* β-toxins, implying functional consequences. Cloning of the gene encoding *T. zulianus* Tz1 paves the way for production of the recombinant protein and the design of site-directed mutants to probe structure–function relationships in toxins from the genus *Tityus* and in β-scorpion toxins in general.

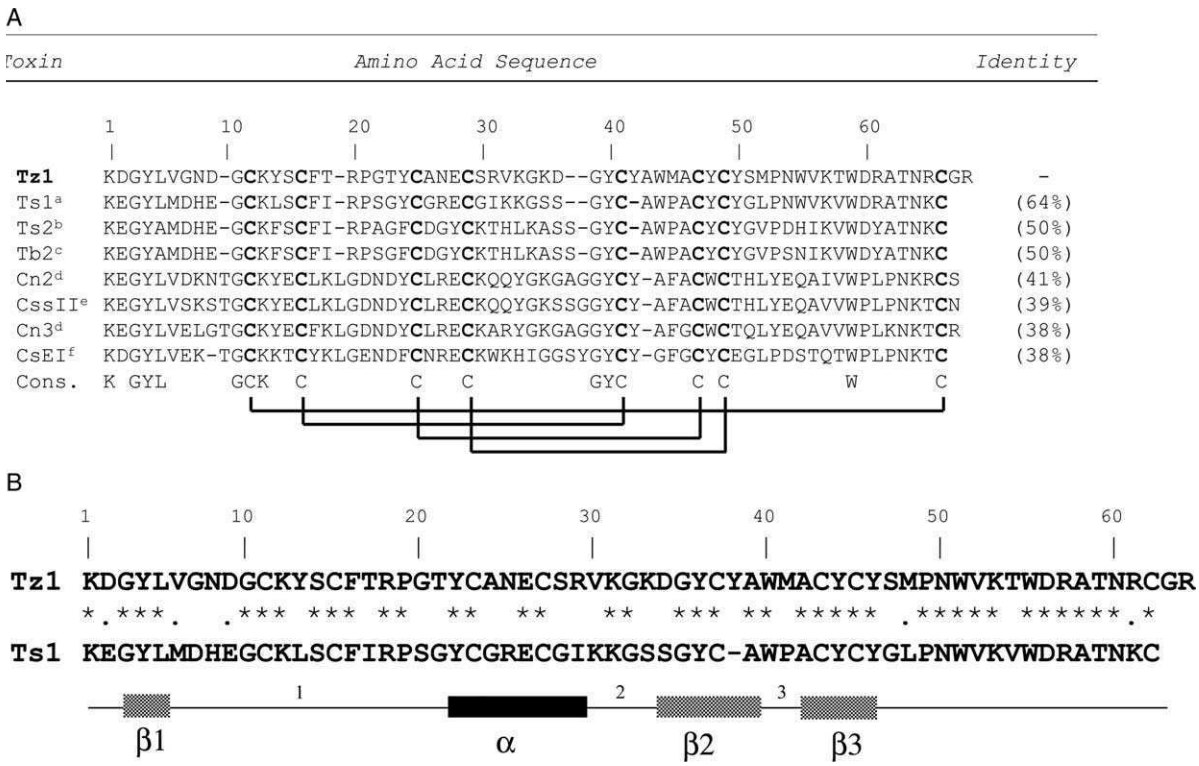

Fig. 7. (A) Primary structure comparison of North- and South American β-type scorpion toxins. Cn, *Centruroides noxius*; CsE, *Centruroides sculpturatus*; Css, *Centruroides suffusus suffusus*; Ts, *Tityus serrulatus*; Tz, *Tityus zulianus*. Arabic numbers after scorpion species denote toxin number. Gaps were introduced to maximize alignment of cysteine residues. 'cons.', identical residues found in all sequences. The typical disulfide-bonding pattern of long-chain peptide toxins is indicated. References: (a) Bechis et al. (1984) and Possani et al. (1985); (b) Mansuelle et al. (1992); (c) Pimenta et al. (2001); (d) Zamudio et al. (1992); (e) Martin et al. (1987); (f) Babin et al. (1975). (B) Sequence alignment of Tz1 with the *T. serrulatus* β-toxin Ts1. Residues strictly conserved are marked with asterisks, conservative exchanges with dots. Structural motifs (α, alpha helix; β, beta-sheet) found in the solved Ts1 structure according to Polikarpov et al. (1999) are shown below the sequence. The loops connecting these secondary structure elements are numbered.

Acknowledgements

The authors convey their thanks to Professor Manuel González-Sponga for his help in the identification of scorpions. We also acknowledge the help of the people of El Bordo, Mesa Bolívar, and Santa Cruz de Mora (Mérida) during *T. zulianus* collections. This work was supported by grants S1-2001000674 from Fonacit (Venezuela), and CDCH-UCV 09.33.4371.2003, and 09.33.4857.2001 (to A.B) and the Deutsche Forschungsgemeinschaft (grant HE 2993/5 to S.H.H.).

References

Alami, M., Ouafik, L., Céard, B., Legros, C., Bougis, P.E., Martin-Eauclaire, M.F., 2001. Characterization of the gene encoding the α-toxin AmmV from the scorpion *Androctonus mauretanicus mauretanicus*. Toxicon 39, 1579–1585.

Babin, D.R., Watt, D.D., Goos, S.M., Mlejnek, R.V., 1975. Amino acid sequence of neurotoxin I from *Centruroides sculpturatus* Ewing. Arch. Biochem. Biophys 166, 125–134.

Barhanin, J., Giglio, J.R., Leopold, P., Schmid, A., Sampaio, S.V., Lazdunski, M., 1982. *Tityus serrulatus* venom contains two classes of toxins. *Tityus gamma* toxin is a new tool with a very high affinity for studying the Na channel. J. Biol. Chem. 257, 12553–12558.

Batista, C.V.F., Zamudio, F., Lucas, S., Fox, J.W., Frau, A., Prestipino, G., Posanni, L.D., 2002. Scorpion toxins from *Tityus cambridgei* that affect Na(+)-channels. Toxicon 40, 557–562.

Becerril, B., Corona, M., Mejia, M.C., Martin, B.M., Lucas, S., Bolivar, F., Posanni, L.D., 1993. The genomic region encoding toxin gamma from the scorpion *Tityus serrulatus* contains an intron. FEBS Lett. 335, 6–8.

Becerril, B., Corona, M., Coronas, F., Zamudio, F., Calderón-Aranda, E., Fletcher, P.L., Martin, B.M., Posanni, L.D., 1996. Toxic peptides and genes encoding toxin gamma of the Brazilian scorpions *Tityus bahiensis* and *Tityus stigmurus*. Biochem. J. 313, 753–760.

Becerril, B., Marangoni, S., Possani, L.D., 1997. Toxins and genes isolated from scorpions of the genus *Tityus*. Toxicon 35, 821–835.

Bechis, G., Sampieri, F., Yuan, P.M., Brando, T., Martin, M.-F., Diniz, C.R., Rochat, H., 1984. Amino acid sequence of Toxin

VII, a new β-toxin from the venom of the scorpion *Tityus serrulatus*. Biochem. Biophys. Res. Commun. 139, 296–302.

Bidlingmeyer, B.A., Cohen, S.A., Tarvin, T.L., 1984. Rapid analysis of amino acids using pre-column derivatization. J. Chromatogr. 336, 93–104.

Borges, A., Arantes, E.C., Giglio, J.R., 1990. Isolation and characterization of toxic proteins from the venom of the Venezuelan scorpion, *Tityus discrepans* (Karsch). Toxicon 28, 1011–1027.

Borges, A., 1996. Scorpionism in Venezuela. Acta Biol. Venez. 16, 65–76.

Borges, A., Tsushima, R.G., Backx, P.H., 1999. Antibodies against *Tityus discrepans* venom do not abolish the effect of *Tityus serrulatus* venom on the rat sodium and potassium channels. Toxicon 37, 661–687.

Borges, A., Arandia, J., Colmenares de Arias, Z., Vargas, A.M., Alfonzo, M.J., 2002. Epidemiological and toxicological characterization of the envenomation by *Tityus zulianus* (Scorpiones, Buthidae). Rev. Fac. Medicina (Caracas) 25, 60–63.

Cestèle, S., Qu, V., Rogers, J.C., Rochat, H., Scheuer, T., Catterall, W.A., 1998. Voltage sensor-trapping enhanced activation of sodium channels by beta-scorpion toxin bound to the S3-S4 loop in domain II. Neuron 21, 919–931.

Chavez-Olortegui, C., Molina, F., Granier, C., 2002. Molecular basis for the cross-reactivity of antibodies elicited by a natural anatoxin with alpha- and beta-toxins from the venom of *Tityus serrulatus* scorpion. Mol. Immunol. 38, 867–876.

Chen, H., Gordon, D., Heinemann, S.H., 2000. Modulation of cloned skeletal muscle sodium channels by the scorpion toxins Lqh II, Lqh III, and Lqh alphaIT. Pflügers Arch. 439, 423–432.

Chen, H., Heinemann, S.H., 2001. Interaction of scorpion alpha-toxins with cardiac sodium channels: binding properties and enhancement of slow inactivation. J. Gen. Physiol. 117, 505–518.

Chomczynski, P., Sacchi, N., 1987. Single-step method of RNA isolation by acid guanidinium thiocyanate–phenol–chloroform extraction. Anal. Biochem. 162, 156–159.

De Lima, M.E., Martin-Eauclaire, M.F., Chavez-Olortegui, C., Diniz, C.R., Granier, C., 1993. *Tityus serrulatus* venom toxin display a complex pattern of antigenic reactivity. Toxicon 31, 223–227.

De Sousa, L., Parrilla-Alvarez, P., Quiroga, M., 2000. An epidemiological review of scorpion stings in Venezuela: the Northeastern region. J. Venom. Anim. Toxins 6, 127–165.

D'Suze, G., Corona, F., Possani, L.D., Sevcik, C., 1996. High performance liquid chromatography purification and amino acid sequence of toxins from the muscarinic fraction of *Tityus discrepans* scorpion venom. Toxicon 34, 591–598.

Fet, V., Lowe, G., 2000. Genus Tityus C.L. Koch, 1836. In: Fet, V., Sissom, W.D., Lowe, G., Braunwalder, M.E. (Eds.), Catalog of the Scorpions of the World, New York Entomological Society, New York, pp. 228–265.

González-Sponga, M.A., 2001. Arácnidos de Venezuela: cuatro especies nuevas del género *Tityus* (Scorpionida: Buthidae). Acta Biol. Venez. 21, 69–83.

Gordon, D., Savarin, P., Gurevitz, M., Zinn-Justin, S., 1998. Functional anatomy of scorpion toxins affecting sodium channels. J. Toxicol. Toxin Rev. 17, 131–159.

Gordon, D., Gilles, N., Bertrand, D., Molgò, J., Nicholson, G.M., Sauviat, M., Benoit, E., Shichor, I., Lotan, I., Gurevitz, M., Kallen, R.G., Heinemann, S.H., 2002. Scorpion toxins differentiating among neuronal sodium channel subtypes: nature's guide for design of selective drugs. In: Menez, A., (Ed.), Perspectives in Molecular Toxinology, Wiley, Chichester, pp. 215–238.

Gordon, D., Gurevitz, M., 2003. The selectivity of scorpion alpha-toxins for sodium channel subtypes is determined by subtle variations at the interacting surface. Toxicon 41, 125–128.

Gurevitz, M., Gordon, D., Ben-Natan, S., Turkov, M., Froy, O., 2001. Diversification of neurotoxins by C-tail wiggling: a scorpion recipe for survival. FASEB J. 15, 1201–1205.

Hassani, O., Mansuelle, P., Cestéle, S., Bourdeaux, M., Rochat, H., Sampieri, F., 1999. Role of lysine and tryptophan residues in the biological activity of toxin VII (γ) from the scorpion *Tityus serrulatus*. Eur. J. Biochem. 260, 76–86.

Hirs, C.H.W., 1967. Performic acid oxidation. Meth. Enzymol. 11, 197–199.

Kamb, A., Weir, M., Rudy, B., Varmus, H., Kenyon, C., 1989. Identification of genes from pattern formation, tyrosine kinase, and potassium channel families by DNA amplification. Proc. Natl Acad. Sci. USA 86, 4372–4376.

Kalapothakis, E., Chavez-Olortegui, C., 1997. Venom variability among several *Tityus serrulatus* specimens. Toxicon 35, 1523–1529.

Kilpatrick, D.R., Nottay, B., Yang, C.F., Yang, S.J., Mulders, M.N., Holloway, B.P., Pallansch, M.A., Kew, O.M., 1996. Group--specific identification of polioviruses by PCR using primers containing mixed-base or deoxyinosine residue at positions of codon degeneracy. J. Clin. Microbiol. 34, 2990–2996.

Lee, T.D., Vemuri, S., 1990. MacProMass: a computer program to correlate mass spectral data to peptide and protein structures. Biomed. Environ. Mass Spectrom. 19, 639–645.

Litchfield, J.T., Wilcoxon, F., 1949. A simplified method for evaluating dose-effect experiments. J. Pharmacol. Exp. Ther. 96, 99–113.

Lourenco, W.R., Cuéllar, O., 1995. Scorpions, scorpionism, life history strategies and parthenogenesis. J. Venom. Anim. Toxins 1, 51–62.

Lowry, O.N., Rosebrough, N.H., Farr, A.L., Randall, R.J., 1951. Protein measurement with the Folin phenol reagent. J. Biol. Chem. 193, 257–265.

Mansuelle, P., Martin-Eauclaire, M.F., Chavez-Olortegui, C., De Lima, M.E., Rochat, H., Granier, C., 1992. The β-type toxin Ts II from the scorpion *Tityus serrulatus*: amino acid sequence determination and assessment of biological and antigenic properties. Nat. Toxins 1, 119–125.

Marcotte, P., Chen, L.Q., Kallen, R.G., Chahine, M., 1996. Effects of *Tityus serrulatus* scorpion toxin gamma on voltage-gated sodium channels. Circ. Res. 80, 363–369.

Martin, M.F., García y Pérez, L.G., El Ayeb, M., Kopeyan, C., Bechis, C., Jover, E., Rochat, H., 1987. Purification and chemical and biological characterizations of seven toxins from the Mexican scorpion, *Centruroides suffusus suffusus*. J. Biol. Chem. 262, 4452–4459.

Martin-Eauclaire, M.F., Ceard, B., Ribeiro, A.M., Diniz, C.R., Rochat, H., Bougis, P.E., 1992. Molecular cloning and nucleotide sequence analysis of the cDNA encoding the main β-neurotoxin from the venom of the South American scorpion *Tityus serrulatus*. FEBS Lett. 302, 220–222.

Mazzei de Dávila, C.A., Dávila, D., Donis, J., Arata de Bellabarba, G., Villarreal, V., Barboza, J.S., 2002. Sympathetic nervous system activation, antivenin administration and cardiovascular manifestations of scorpion envenomation. Toxicon 40, 1339–1346.

Mota, J.V., Ghersy, M.T., Bastardo, M., Rodríguez, J., Duque, L., Freytez, L.A., 1994. Emponzoñamiento escorpiónico: clínica y laboratorio usando antivenina. Bol. Hosp. Niños (Caracas) 30, 35–40.

Nishikawa, A.K., Caricati, C.P., Lima, M.L.S.R., Kipnis, T.L., Eickstedt, V.R.D., Da Silva, M.H., Higashi, H.G., Da Silva, W., 1994. Antigenic cross-reactivity among the venoms from several species of Brazilian scorpions. Toxicon 32, 989–998.

Pimenta, A.M., Martin-Eauclaire, M.F., Rochat, H., Figueiredo, S.G., Kalapothakis, E., Afonso, L.C., De Lima, M.E., 2001. Purification, amino-acid sequence and partial characterization of two toxins with anti-insect activity from the venom of the South American scorpion *Tityus bahiensis* (Buthidae). Toxicon 39, 1009–1019.

Pinheiro, C.B., Marangoni, S., Toyama, M.H., Polikarpov, I., 2003. Structural analysis of *Tityus serrulatus* Ts1 neurotoxin at atomic resolution: insights into interactions with Na^+ channels. Acta Crystallogr. D59, 405–415.

Pintar, A., Possani, L.D., Delepierre, M., 1999. Solution structure of toxin 2 from *Centruroides noxius* Hoffmann, a β-scorpion neurotoxin acting on sodium channels. J. Mol. Biol. 287, 359–367.

Polikarpov, I., Sanches Matilde, M., Marangoni, S., Toyama, M.H., Teplyakov, A., 1999. Crystal structure of neurotoxin Ts1 from *Tityus serrulatus* provides insights into the specificity and toxicity of scorpion toxins. J. Mol. Biol. 290, 175–184.

Possani, L.D., Martin, B.M., Svendsen, I., Rode, G.S., Erickson, B.W., 1985. Scorpion toxins from *Centruroides noxius* and *Tityus serrulatus*. Primary structures and sequence comparison by metric analysis. Biochem. J. 227, 739–750.

Possani, L.D., Becerril, B., Delepierre, M., Tytgat, J., 1999. Scorpion toxins specific for Na^+-channels. Eur. J. Biochem. 264, 287–300.

Rossomando, A., Rosillo, M., Chacón, E., Barra, V., Moreno, E., Albán, A.E., 1997. Pancreatitis aguda por emponzoñamiento escorpiónico. Estudio retrospectivo. GEN 51, 258–262.

Sambrook, J., Fritsch, E.F., Maniatis, T., 1989. Molecular Cloning: a Laboratory Manual, Cold Spring Harbor Laboratory Press, Cold Spring Harbor.

Shulov, A., Zlotkin, E., 1969. A simple device for collecting scorpion venom. Toxicon 2, 169–170.

Stachel, S.J., Stockwell, S.A., van Vranken, D.L., 1999. The fluorescence of scorpions and caractogenesis. Chem. Biol. 6, 531–539.

Tsushima, R.G., Borges, A., Backx, P.H., 1999. Inactivated state dependence of sodium channel modulation by β-scorpion toxin. Pflügers Arch. 437, 661–668.

Vijverberg, H.P.M., Pauron, D., Lazdunski, M., 1984. The effect of *Tityus serrulatus* scorpion toxin γ on Na channels. Pflügers Arch. 401, 297–303.

Wahle, E., Ruegsegger, U., 1999. 3-′ end processing of pre-mRNA in eukaryotes. FEMS Microbiol. Rev. 23, 277–295.

Yatani, A., Kirsch, G.E., Possani, L.D., Brown, A.M., 1988. Effect of New World scorpion toxins on single-channel and whole-cell cardiac sodium currents. Am. J. Physiol. 254, H443–H455.

Zamudio, F., Saavedra, R., Martin, B.M., Gurrola-Briones, G., Hérion, P., Posanni, L.D., 1992. Amino acid sequence and immunological characterization with monoclonal antibodies of two toxins from the venom of the scorpion *Centruroides noxius* Hoffmann. Eur. J. Biochem. 204, 281–292.

Molecular Pharmacology Fast Forward. Published on April 25, 2006 as doi:10.1124/mol.106.024034

Subtype specificity of scorpion β-toxin Tz1 interaction with voltage-gated sodium channels is determined by the pore loop of domain-3

Enrico Leipold, Alfred Hansel, Adolfo Borges, and Stefan H. Heinemann

Institute of Molecular Cell Biology, Research Unit "Molecular and Cellular Biophysics", Medical Faculty of the Friedrich Schiller University Jena, Jena, Germany (E.L., A.H., S.H.H.); and Sección de Biomembranas, Instituto de Medicina Experimental, Facultad de Medicina, Universidad Central de Venezuela, Caracas, Venezuela (A.B.)

Running title: Subtype specificity of scorpion β-toxins

‡ **Correspondence:**

Prof. Dr. Stefan H. Heinemann

Institute of Molecular Cell Biology

Molecular and Cellular Biophysics

Friedrich Schiller University Jena

Drackendorfer Str. 1

D-07747 Jena, Germany

Tel: ++49-3641-9 32 56 80

Fax: ++49-3641-9 32 56 82

e-Mail: Stefan.H.Heinemann@uni-jena.de

Text pages: 20

Figures: 5

Tables: 1

References: 25

Abstract: 229 words

Introduction: 563 words

Discussion: 1339 words

Abbreviations:

Na_V channel, voltage-gated sodium channel.

Abstract

Voltage-gated sodium (Na_V) channels are modulated by a variety of specific neurotoxins. Scorpion β-toxins affect the voltage-dependence of channel gating: In their presence Na_V channels activate at sub-threshold membrane voltages. Previous mutagenesis studies have revealed that the β-toxin Css4 interacts with the extracellular linker between segments 3 and 4 in domain-2 of Na_V channels with the effect to trap this voltage sensor in an open position (Cestèle et al., 1998, Neuron 21:919-931). The voltage sensor of domain-2 was thus identified to constitute a major part of neurotoxin receptor site-4. Here we studied the effects of the β-toxin Tz1 from the Venezuelan scorpion *Tityus zulianus* on various mammalian Na_V channel types expressed in HEK 293 cells. While skeletal muscle channels ($Na_V1.4$) were strongly affected by Tz1, the neuronal channels $Na_V1.6$ and $Na_V1.2$ were less sensitive, the cardiac $Na_V1.5$ and the peripheral nerve channel $Na_V1.7$ basically insensitive. Analysis of channel chimeras in which whole domains of $Na_V1.2$ were inserted into a $Na_V1.4$ background revealed that the $Na_V1.2$ phenotype was not conferred to $Na_V1.4$ by domain-2 but by domain-3. The interaction epitope could be narrowed down to residues E1251, K1252 and H1257 located in the C-terminal pore loop in domain-3. The receptor site for β-toxin interaction with Na_V channels is thus spanning domains 2 and 3 where the pore loop in domain-3 specifies the pharmacological properties of individual neuronal Na_V channel types.

Introduction

Voltage-gated sodium channels (Na_V channels) consist of a large (~260 kDa) pore-forming α-subunit, composed of four homologous domains each with six transmembrane segments (S1-S6) and a hairpin-like pore region between S5 and S6, split in an N-terminal (SS1) and a C-terminal part (SS2). Na_V channels play a pivotal role in cellular excitability and are targeted by a large variety of chemically distinct toxins (Janiszewski, 1990; Catterall, 1992; Gordon et al., 1998). Understanding the molecular mechanisms underlying the toxin action is not only important for toxicological research; various toxic substances serve as lead structures for novel therapeutics such as analgesics.

Scorpion venoms are a rich source of neurotoxins. Scorpion toxins affecting Na_V channels typically are 60-76 residues long polypeptides comprising α- and β-toxins. They are classified according to their mode of action and binding properties to distinct sites (receptor sites-3 and -4, respectively) on Na_V channels (Martin-Eauclaire and Couraud, 1995; Gordon et al., 1998; Possani et al., 1999; Zuo and Ji, 2004). While α-toxins inhibit rapid Na_V channel inactivation, β-toxins show a rather complex effect. They shift the voltage dependence of channel activation to cause sub-threshold channel opening. Interestingly, this shift is enhanced when channels are preactivated by a depolarizing pulse. This led to the current picture of β-toxins being voltage-sensor toxins: They specifically interact with the voltage sensor in domain-2 of Na_V channels to “trap” the sensor in an open position and, hence, to facilitate channel opening (Cestèle et al., 1998, 2001; Mantegazza and Cestèle, 2005).

These results have been obtained by elegant studies of Cestèle et al. (1998) who compared the effect of β-toxin Css4 (*Centruroides suffusus suffusus*) on rat brain sodium channels ($Na_V1.2$) with that on cardiac muscle sodium channels $Na_V1.5$. While $Na_V1.2$ was strongly affected by Css4, the toxin was without effect on the voltage dependence of $Na_V1.5$ activation. A mutagenesis approach revealed that a single residue (G845) located in the domain-2 S3-S4 linker of $Na_V1.2$ is critical for the toxin effect. When mutated to asparagine

as present in $Na_V1.5$ channels, the channel mutant was rendered insensitive to Css4. Interestingly, the identified glycine is conserved in most members of the mammalian Na_V channel gene family. It is found in central and peripheral nervous system channels ($Na_V1.1$-1.3, $Na_V1.6$, $Na_V1.7$) as well as in the skeletal muscle channels ($Na_V1.4$), anticipating that there may not be much subtype specificity for β-toxins in addition to the insensitivity of cardiac $Na_V1.5$. However, no systematic investigation of the effects of a single scorpion β-toxin on various types of mammalian Na_V channels under comparable conditions has been performed to date.

Therefore, we studied how Tz1, the major β-toxin from the Venezuelan scorpion *Tityus zulianus*, affects various mammalian Na_V channel types expressed in HEK 293 cells. As shown previously, Tz1 clearly shifts the voltage dependence of $Na_V1.4$ channel activation, but, similarly to Css4, has no effect on the activation of $Na_V1.5$ channels (Borges et al., 2004). Although the critical glycine residue is conserved in the neuronal channels $Na_V1.2$, $Na_V1.6$, and $Na_V1.7$ and in skeletal muscle channels ($Na_V1.4$), we find very diverse effects of Tz1 on these channel types. With channel chimera constructs we show that the subtype specificity is not determined by the voltage sensor of domain-2 but by the pore loop of domain-3. As a result, scorpion β-toxin receptor site-4 in Na_V channels consists of at least two major parts, one in domain-2 and one in domain-3.

Materials and Methods

Site-directed mutagenesis. The wild-type sodium channel constructs used in this study were the rat isoforms of $Na_V1.2$ (P04775; Noda et al., 1986) and $Na_V1.4$ (P15390; Trimmer et al., 1989), the human isoforms of $Na_V1.5$ (Q14524; Gellens et al., 1992) and $Na_V1.7$ (NP002968; Klugbauer et al., 1995), and the mouse isoform of $Na_V1.6$ (Q9WTU3; Kohrman et al., 1996). The construction of chimeras between $Na_V1.2$ and $Na_V1.4$ (2444, 4244, 4424, 4442, 44p(1.2)4, 22p(1.4)2) was described previously (Zorn et al., 2006). We used a similar approach to construct $Na_V1.4$ channels with the C-terminal part of the domain-3 pore loop from $Na_V1.5$, $Na_V1.6$ or $Na_V1.7$ (44p(1.5)4, 44p(1.6)4 or 44p(1.7)4), respectively. In $Na_V1.4$ we replaced nucleotides 3724-3864 by the homologous residues of $Na_V1.5$, $Na_V1.6$ or $Na_V1.7$. The amino acid substitutions in the resulting pore loop chimeras are as follows: 44p(1.2)4: E1251N, K1252V, E1254L, H1257K, V1260D; 44p(1.5)4: E1251G, K1252Y, H1257Q, Y1258W, V1260Y, L1266I; 44p(1.6)4: E1251K, K1252P, E1253D, H1257D, V1260D, L1262I, L1266I; 44p(1.7)4: R1250V, E1251N, K1252V, E1253D, E1254K, H1257K, V1260Y, N1261S, L1266I, I1270V (all $Na_V1.4$ numbering); 22p(1.4)2: N1436E, V1437K, L1439E, K1442H, D1445V ($Na_V1.2$ numbering). Single amino-acid substitutions Q657E, G658N, E1251N, K1252V, E1254L, H1257K and V1260D were introduced into $Na_V1.4$ using PCR-based site-directed mutagenesis. Primers were obtained from MWG (Ebersberg, Germany). All clones were verified by DNA sequencing. Plasmid DNA was isolated from *E. coli* using the Midi- or Maxi-plasmid purification kit (Qiagen, Hilden, Germany).

Cell culture and transfection. HEK 293 cells (CAMR, Porton Down, Salisbury, UK) were maintained in 45% Dulbecco's Minimal Eagles Medium (DMEM) and 45% F12, supplemented with 10% fetal calf serum in a 5% CO_2 incubator at 37°C. Cells were trypsinized, diluted with culture medium and grown in 35-mm dishes. When cells were grown to 30-50% confluence, transient transfection was performed using the Superfect transfection kit (Qiagen). HEK 293 cells were transfected with a 5:1 ratio of the Na_V channel expression plasmids and a vector encoding the CD8 antigen (Jurman et al., 1994). The cells were used

for electrophysiological recordings 2-3 days after transfection. Individual transfected cells were visualized with Dynabeads (Deutsche Dynal GmbH, Hamburg, Germany) binding to CD8.

Electrophysiological measurements. Whole-cell voltage clamp experiments were performed as described previously (Chen et al., 1999). Briefly, patch pipettes with resistances of 0.9-1.8 MΩ were used. The series resistance was compensated for by more than 80% in order to minimize voltage errors. A patch-clamp amplifier EPC10 was operated by PatchMaster software (both HEKA Elektronik, Lambrecht, Germany). Leak and capacitive currents were corrected with a p/n method. Currents were low-pass filtered at 5 kHz and sampled at a rate of 25 kHz. All experiments were performed at constant temperature, 19-21°C. Digitally filtered data (3 kHz) were analyzed using FitMaster (HEKA Elektronik) and IgorPro (WaveMetrics, Lake Oswego, OR, USA).

The patch pipettes contained (mM): 35 NaCl; 105 CsF; 10 EGTA; 10 Hepes (pH 7.4 with CsOH). The bath solution contained (mM): 150 NaCl; 2 KCl, 1.5 $CaCl_2$; 1 $MgCl_2$; 10 Hepes (pH 7.4 with NaOH). The application of toxin was performed with an application pipette as described previously (Chen et al., 1999).

To measure the use-dependence of Tz1 action, a double-pulse protocol was used (Borges et al. 2004). From a holding potential of –120 mV a set of test depolarizations in the range from –130 to +55 mV in steps of 5 mV was applied followed by a constant prepulse to –10 mV for 50 ms prior to a second set of test pulses with identical parameters as the first set. To ensure recovery from fast inactivation, the cells were held at –120 mV for 50 ms before and after the prepulse. The repetition interval was 5 s. Open probabilities (P_o) were calculated from current-voltage relationships:

$$I(V) = P_o(V)\,\Gamma_{\max}\,V\,\frac{1-e^{-(V-E_{rev})/25mV}}{1-e^{-V/25mV}} \qquad \text{(eq. 1)}$$

Γ_{max} is the maximal conductance of all channels and E_{rev} the measured reversal potential. V is the test pulse voltage and I the peak test pulse current. For a quantitative data description the open probabilities were plotted against the test pulse voltages and fit with a double Boltzmann formalism:

$$P_o(V) = \frac{1 - P_{tox}}{\left(1 + e^{-(V - V_m)/k_m}\right)^3} + \frac{P_{tox}}{\left(1 + e^{-(V - V_m - \Delta V)/k_m}\right)^2}$$

(eq. 2)

V_m is the half-maximal gate activation and k_m the corresponding slope factor. P_{tox} represents the probability of channels to be toxin-modified and ΔV is the voltage by which the activation of toxin-modified channels is shifted. In control experiments, i.e. in the absence of toxin, P_{tox} was set to 0. Using this formalism means to describe activation of control channels according to a Hodgkin & Huxley theory, i.e. using three independent activation gates. Toxin-modified channels are assumed to activate with two independent gates as one is trapped in an activated position. For a phenomenological description of channel opening the voltages for P_o = 0.5 ($V_{0.5}$) were back-calculated from eq. (2) and are provided in the figures and tables.

The voltage dependence of fast inactivation was assayed by conditioning cells for 500 ms at voltages ranging from –140 to –25 mV in steps of 5 mV and a repetition interval of 30 s. Subsequently, peak current was determined at –20 mV. The peak current plotted versus the conditioning voltage was described with a Boltzmann function. The holding potential was –120 mV in all cases.

All data were presented as mean ± standard error of the mean (n = number of independent experiments).

Toxin purification**. *Tityus zulianus* scorpions were collected near Santa Cruz de Mora, Mérida State, western Venezuela, and venom extracted by manual stimulation.** Tz1 was

purified from the crude venom using reverse phase HPLC essentially as described by Borges et al. (2004).

Results

Effect of Tz1 on wild-type Na_V channels. In a previous study we identified Tz1, the main component in the venom of the Venezuelan scorpion *Tityus zulianus,* as a typical β-toxin that shifts the half-maximal activation voltage of $Na_V1.4$ channels in the negative direction with an apparent K_D of about 3.5 µM (Borges et al., 2004). Tz1, however, did not shift the activation voltage of $Na_V1.5$ channels. Here we extended this study to neuronal sodium channels in order to elucidate the subtype specificity of Tz1.

$Na_V1.4$, $Na_V1.5$ and the neuronal isoforms $Na_V1.2$, $Na_V1.6$, and $Na_V1.7$ were expressed in HEK 293 cells and the voltage-dependent channel activation was investigated in the absence and presence of 2 and 10 µM Tz1 using the whole-cell voltage-clamp technique. Since a β-toxin-induced shift in the voltage dependence of activation can often be potentiated by depolarizations preceding the test pulse, we applied a first series of test voltages followed by a constant prepulse to preactivate the channels prior to a second test pulse series. In Figure 1A current traces obtained at –70 mV, i.e. a voltage at which channels are normally closed, are shown. This approach provides a measure of the Tz1 effect to lower the activation threshold of the channels with and without such a prepulse in one experiment.

Figure 1B shows representative normalized conductance-voltage relationships of single cells expressing $Na_V1.4$, $Na_V1.6$, $Na_V1.2$, $Na_V1.7$, and $Na_V1.5$ channels, respectively, under control conditions and after application of 10 µM Tz1 in the absence and presence of a prepulse. The vertical line marks –70 mV, a potential where channels are closed under control conditions. P_{tox}, the probability of the channels to display a lowered activation threshold is given in Table 1 and was derived from double Boltzmann fits of the normalized conductance-voltage relationships (eq. 2). In Figure 1C P_{tox} is shown for the wild-type channels with and without preactivation. Based on this analysis $Na_V1.4$ is the most sensitive target for Tz1 with a P_{tox} value of about 67% followed by $Na_V1.6$ (23%) and $Na_V1.2$ (7%) for

10 µM Tz1. The shift of half-maximal channel activation, indicated by ΔV, was about –50 mV for the neuronal isoforms $Na_V1.2$, $Na_V1.6$, and $Na_V1.7$. $Na_V1.4$ displayed a slightly less pronounced activation shift of about –42 mV. Only a very small fraction of $Na_V1.5$ and $Na_V1.7$ channels was shifted by 10 µM Tz1 in the presence of a prepulse, the magnitude of ΔV, however, was similar to that of the other channels. Tz1 therefore shifts activation of all channel isoforms by about the same magnitude, but it exhibits pronounced subtype specificity regarding the percentage of channels affected. It has a strong preference for the skeletal muscle channel $Na_V1.4$ and differentiates well between neuronal sodium channels in the order $Na_V1.6 >> Na_V1.2 > Na_V1.7$.

Analysis of the voltage sensor in domain-2. Cestèle et al. (1998) found that β-toxin Css4 strongly affects the activation of $Na_V1.2$ channels but does not modify the activation threshold of $Na_V1.5$ channels. This difference could be attributed to a single site in the S3-S4 linker of domain-2: After mutating G845 in $Na_V1.2$ to asparagine (N), as present in $Na_V1.5$, the channel became insensitive to Css4.

Similar to these results, Tz1 is unable to shift the activation threshold of $Na_V1.5$ suggesting that the identified glycine residue could also be important for the action of Tz1. A direct comparison of the amino acid sequences of the domain-2 S3-S4 linkers from $Na_V1.2$, $Na_V1.4$, $Na_V1.5$, $Na_V1.6$, and $Na_V1.7$ reveals that G845 (numbering of $Na_V1.2$) is conserved among the channels except for $Na_V1.5$ (Fig. 2A). Furthermore, compared to all channels investigated, $Na_V1.5$ displays the least conserved domain-2 S3-S4 linker. Given that Tz1 discriminates between $Na_V1.4$, $Na_V1.6$, $Na_V1.2$, and $Na_V1.7$, the identified glycine cannot be the sole molecular determinant for the subtype specificity of Tz1 shown in Figure 1.

Nevertheless, we first tested for the impact of the conserved glycine on the action of Tz1 by constructing and assaying mutant G658N in the background of $Na_V1.4$. As shown in Figure 2B, the conductance-voltage relationship of $Na_V1.4$-G658N channels was not shifted by Tz1. Thus, similarly to what Cestèle and coworkers (1998) found for Css4, the conserved glycine

in the domain-2 S3-S4 linker of Na_V channels is also crucial for the effect of Tz1 and is therefore of general importance.

However, as indicated by the alignment in Figure 2A, this position in the domain-2 S3-S4 linker cannot account for the differences found for the neuronal channels. To test whether or not this linker is important in this respect at all, we analyzed mutant $Na_V1.4$-E657Q as it represents an $Na_V1.4$ channel with the domain-2 S3-S4 linker of $Na_V1.2$. This mutant is as sensitive to Tz1 as the wild-type $Na_V1.4$ (Fig. 2B), i.e. it does *not* reflect properties of $Na_V1.2$. From this experiment we can safely conclude that the domain-2 S3-S4 linker is *not* the determinant for the subtype specificity of Tz1 with respect to neuronal Na_V channels.

Domain chimeras. Since there may be determinants outside the domain-2 S3-S4 linker responsible for the pronounced Tz1 subtype specificity, we applied a more rigorous approach by formation of domain chimeras between $Na_V1.4$ and $Na_V1.2$ channels, i.e. we inserted individual domains of $Na_V1.2$ into an $Na_V1.4$ background. The resulting four chimeric channels (domain-1: 2444; domain-2: 4244; domain-3: 4424; domain-4: 4442, see Fig. 3A) were expressed in HEK 293 cells and assayed for their response to 10 µM Tz1. Whereas 2444 and 4442 exhibited a phenotype very similar to $Na_V1.4$ channels, 4244 appeared more sensitive to Tz1 (Fig. 3, Table 1). Surprisingly, chimera 4424, a construct in which domain-3 was from $Na_V1.2$, showed a toxin sensitivity comparable to $Na_V1.2$ channels. As indicated in Table 1, all four domain chimeras displayed voltage-dependent gating parameters similar to that of wild-type $Na_V1.4$ channels. An altered gating behavior can therefore be excluded as the reason for their different sensitivities to Tz1. Thus, domain-3 seems to play a major role in determining the differential effects of Tz1 on neuronal Na_V channels.

Pore loop of domain-3. In order to further narrow down a putative interaction site, we analyzed a multiple sequence alignment of domain-3 from various Na_V channels and highlighted their pore domain as a region of high variability. In addition, previous binding studies of Cestèle et al. (1998) identified the C-terminal pore loop (SS2) of domain-3 as a

potential interaction site for the β-toxin Css4. An alignment (Fig. 4A) shows that $Na_V1.4$ and $Na_V1.2$ only differ in five residues in this region. When the SS2 loop of domain-3 from $Na_V1.2$ was introduced into $Na_V1.4$, the resulting channel, 44p(1.2)4, became less sensitive to Tz1 (Fig. 4B, C, Table 1), comparable to $Na_V1.2$ wild-type channels. In order to rule out nonspecific allosteric effects, we also constructed the reverse chimera 22p(1.4)2, i.e. a construct in which the domain-3 SS2 loop of $Na_V1.4$ was inserted into $Na_V1.2$. This chimera was readily sensitive to Tz1, comparable to wild-type $Na_V1.4$ channels. In addition, we generated $Na_V1.4$ channel mutants with the domain-3 SS2 loops of $Na_V1.5$, $Na_V1.6$, and $Na_V1.7$. As shown in Fig. 4 and Table 1, introduction of the SS2 loop from $Na_V1.5$ resulted in channels with high sensitivity towards Tz1 (44p(1.5)4). Introduction of the SS2 loops from $Na_V1.6$ and $Na_V1.7$ conferred the Tz1 sensitivity of the respective wild types (44p(1.6)4 and 44p(1.7)4, respectively). Thus, the SS2 loop of domain-3 critically determines how β-toxin Tz1 interacts with voltage-gated sodium channels. The specific structures of the domain-3 SS2 loops from neuronal channels strongly diminish the action of Tz1, while the SS2 loop of $Na_V1.5$ supports a Tz1 effect.

Single-site mutations in domain-3. Since the domain-3 SS2 loop completely conferred Tz1 sensitivity between the $Na_V1.2$ and $Na_V1.4$ wild-type channels, we analyzed the potential structural determinants in more detail. As shown in Figure 4A, only five residues are different between $Na_V1.2$ and $Na_V1.4$. Therefore, mutations yielding the residues of $Na_V1.2$ were introduced into $Na_V1.4$. The analysis of these mutants, presented in Figure 5 and Table 1, indicates that at least three amino-acid positions are crucial for Tz1-induced modulation of the channel. The strongest effect of 10 µM Tz1 was measured in mutant H1257K reducing P_{tox} to 17% followed by E1251N with a P_{tox} of 20% indicating their importance for the Tz1 subtype specificity. Interestingly, K1252V increased P_{tox} of $Na_V1.4$ from 67% to about 96% making this mutant more sensitive to Tz1. Mutants E1254L and V1260D exhibited toxin sensitivity slightly smaller than wild-type $Na_V1.4$ channels. Judging from the toxin effect at 2

and 10 μM, the sensitivity has the following order: K1252V > wild type > E1254L, V1260D > E1251N, H1257K.

Like the replacement of whole channel domains, single-site substitutions in the domain-3 SS2 region had no noticeable influence on the gating properties of $Na_V1.4$ channels (Table 1). Therefore, the differential influence of the SS2 mutations on the Tz1 effect cannot be accounted for alterations of channel gating. Instead, the results demonstrate that the SS2 region of domain-3 determines the subtype specificity of Na_V channels for the β-toxin Tz1.

Discussion

Subtype specificity of Tz1. Na_V channel-specific neurotoxins are intensively investigated gating modulators. According to their functional properties β-toxins can be clustered into (1) insect-selective toxins with an excitatory or depressant function, (2) classical mammalian-specific toxins, (3) toxins which are active on mammals and insects, and (4) toxins which compete with excitatory insect β-toxins as well as with classical α- and β-toxins for binding to the channels (Possani et al., 1999). Since recent research mostly concentrated on their specificity for different phyla (e.g. Shichor et al., 2002; Cohen et al., 2004; Bosmans et al., 2005), only little information is available about the specificity of β-toxins for different channel isoforms.

Using an electrophysiological approach we assayed for the first time the use-dependent potency of a scorpion β-toxin to alter the activation of the Na_V channel isoforms 1.2, 1.4, 1.5, 1.6, and 1.7. This functional approach revealed Tz1 as most active on the skeletal muscle channels $Na_V1.4$. The gating of about 67% of the $Na_V1.4$ channels expressed in transfected HEK 293 cells were modified by application of 10 µM Tz1, i.e. this fraction showed a half-maximal activation which was Tz1-shifted by more than –40 mV (Table 1). Qualitatively, the other channel types tested displayed a very similar shift in activation threshold. However, the percentage of channels affected by Tz1 was markedly reduced for $Na_V1.2$ and $Na_V1.6$ channels. The cardiac and peripheral nerve isoforms ($Na_V1.5$ and $Na_V1.7$, respectively) were basically insensitive to 10 µM Tz1. Thus, Tz1 strongly distinguishes between neuronal and muscular Na_V channels in a graded manner, giving rise to potential applications of β-toxins as research tools or even as pharmacologically relevant drugs.

Potential value of β-toxins. Since Na_V channel-specific scorpion toxins selectively modify either inactivation (α-toxins) or activation (β-toxins), they are proven tools for functional studies. Based on their Na_V channel-specific nature, Massensini et al. (2002) used fluorescently labeled members of both groups as probes for tracking Na_V channels in living

cells. Applications like these are important for studying complex neuronal networks. Assuming that the functional subtype specificity of Tz1 reflects subtype-specific binding to channels, this toxin could be used to track $Na_V1.4$ specifically. It should be feasible to develop specific probes on a toxin basis in order to uncover the Na_V channel composition in living material. Besides the potential as molecular probes for research, scorpion toxins are discussed to replace conventional insecticides because of resistances developed in some insect species against classically used agents like phyrethroids (Bosmans et al., 2005). The value of Tz1 for such purposes remains to be evaluated by analyzing its effect on insect sodium channels.

The strong specificity of some β-toxins also makes them ideal tools for studying Na_V channel defects. For example, a loss of $Na_V1.4$ function is the basis for hypokalaemic periodic paralysis of type 2 (hypoPP2; Sternberg et al., 2001), a skeletal muscle disorder. The pronounced $Na_V1.4$ specificity of Tz1 could be used to specifically "activate" hypoPP2 channels while promising to exhibit only limited neuronal and cardiac side effects when administered to experimental animals.

Identification of domain-3 as major interaction site. Gordon et al. (1992) showed that antibodies directed against the SS2 pore regions of domains 1, 3 and 4 of insect Na_V channels displaced radiolabeled $LqhIT_2$, an insect β-toxin from *Leiurus quinquestriatus hebraeus*, as well as AahIT, a β-toxin from *Androctonus australis hector*. In a further study Cestèle et al. (1998) constructed various chimeras between the differentially Css4-sensitive $Na_V1.2$ and $Na_V1.5$ channels in order to identify the sites that are important for binding this β-toxin. Although a glycine residue in the domain-2 S3-S4 linker of $Na_V1.2$ was identified as a major difference to $Na_V1.5$, the pore loops of domains 1 and 3 as well as the S1-S2 linker in domain-3 were found to have some impact on binding Css4.

Our strategy of analyzing the β-toxin – channel interaction was to start with the functional characterization of Tz1 on five different Na_V channel isoforms ($Na_V1.2$, $Na_V1.4$-1.7). This

approach revealed Tz1 as highly selective towards $Na_V1.4$ and able to distinguish with high potency between $Na_V1.2$, $Na_V1.6$, and $Na_V1.7$ channels. Using a step-by-step mutagenesis approach together with a functional assay, we identified the domain-3 SS2 pore region as the major molecular determinant for the β-toxin sensitivity of these channels: The domain-3 SS2 loops of the neuronal channels confer the Tz1 phenotypes to the respective wild-types to $Na_V1.4$ channels. This functional assignment does not hold for $Na_V1.5$: Although $Na_V1.5$ channels are insensitive towards Tz1, domain-3 SS2 from $Na_V1.5$ strongly enhances the Tz1 effect when inserted into a $Na_V1.4$ background. On the other hand, a $Na_V1.5$-like phenotype can be produced in $Na_V1.4$ channels by changing G658 to N as present in $Na_V1.5$ (Fig. 2), suggesting that a $Na_V1.5$-like domain-2 S3-S4 linker dominates a $Na_V1.5$-like domain-3 SS2 pore loop. These results indicate an exceptional role of $Na_V1.5$ with regard to scorpion β-toxins suggesting that the domain-3 SS2 loop of the $Na_V1.5$ channel is perfectly able to interact with Tz1, but the induction of a functional effect on channel gating is impaired by the specific structure of the domain-2 S3-S4 linker.

The observation that $Na_V1.2$ and $Na_V1.4$ only differ in five amino acid residues in the region pointed out as being important for the discrimination between the two channels by Tz1 prompted us to construct and assay single-site mutations for each of these residues. While the differences at positions 1260 and 1254 had a minor impact on toxin efficacy, an exchange of the histidine at position 1257 in $Na_V1.4$ to the lysine present in $Na_V1.2$ as well as the exchange of the negatively charged glutamate at position 1251 for asparagine present in $Na_V1.2$ both strongly impaired the toxin effect. Thus, the negative charge at position 1251 seems to support interaction with the toxin, possibly with a positively charged amino acid on the toxin as the counterpart. In the case of position 1257, the positive charge present in $Na_V1.2$ seems to impair interaction with the toxin as well. Intriguingly, a valine at the lysine-1252 position seems to support toxin interaction, since this mutant is even more sensitive for Tz1 than the most sensitive wild-type $Na_V1.4$ channel. In this case either the positive charge

or the bulkiness of the side chain may be decisive, since the neutral valine is also much smaller than lysine.

With these results on the impact of individual residues on the effect of Tz1 one may speculate about the expected sensitivity of other Na_V channels. The rat isoforms of $Na_V1.1$ and $Na_V1.3$ share a conserved domain-2 S3/S4 linker with $Na_V1.2$, differ, however, in the SS2 loop of domain-3. Since in $Na_V1.1$ the critical residues assayed in Fig. 5 are the same as in $Na_V1.2$, one can expect that $Na_V1.1$ is insensitive towards Tz1. The situation for $Na_V1.3$ is more complex: The SS2 loop in domain-3 differs in four residues from the sequence of $Na_V1.2$, among them are those residues that proved important for the Tz1 effect in our experiments. Since all residues mutated showed an impact on the Tz1 effect, the Tz1 sensitivity of $Na_V1.3$ cannot be predicted in a straightforward manner – it can be different to both, $Na_V1.2$ and $Na_V1.4$.

In conclusion, the scorpion β-toxin Tz1 is a valuable molecular tool as it discriminates well between various types of voltage-gated sodium channel isoforms, being most specific for channels from skeletal muscle. The subtype specificity for various neuronal channel types is not brought about, as initially assumed, by the classical receptor site-4, i.e., the domain-2 S3-S4 linker, but by the C-terminal pore loop (SS2) of domain-3. Therefore, receptor site-4 is composed of at least two major components, an interaction site determining the channel specificity in domain-3 and a site where the toxin interacts with the voltage sensor in domain-2. Based on recently obtained structural data of a voltage-gated potassium channel (Long et al., 2005), one can predict that the domain-2 S3-S4 linker and the domain-3 SS2 loop are very close in three-dimensional space such that a scorpion β-toxin with a diameter of about 3 nm could make contact to both functional modules of the sodium channel simultaneously.

Acknowledgments. We thank S. Arend for technical assistance.

References

Borges A, Alfonzo MJ, Garcia CC, Winand NJ, Leipold E, and Heinemann SH (2004) Isolation, molecular cloning and functional characterization of a novel β-toxin from the Venezuelan scorpion, *Tityus zulianus*. *Toxicon* **43:**671–684.

Bosmans F, Martin-Eauclaire MF, and Tytgat J (2005) The depressant scorpion neurotoxin LqqIT2 selectively modulates the insect voltage-gated sodium channel. *Toxicon* **45:**501–507.

Catterall WA (1992) Cellular and molecular biology of voltage-gated sodium channels. *Physiol Rev* **72:**15–48.

Cestèle S, Qu Y, Rogers JC, Rochat H, Scheuer T, and Catterall WA (1998) Voltage sensor-trapping: Enhanced activation of sodium channels by β-scorpion toxin bound to the S3-S4 loop in domain II. *Neuron* **21:**919–931.

Cestèle S, Scheuer T, Mantegazza M, Rochat H, and Catterall WA (2001) Neutralization of gating charges in domain II of the sodium channel α subunit enhances voltage-sensor trapping by a β-scorpion toxin. *J Gen Physiol* **118:**291–301.

Chen H, Gordon D, and Heinemann SH (1999) Modulation of cloned skeletal muscle sodium channels by the scorpion toxins Lqh II, Lqh III, and LqhαIT. *Pflügers Arch* **439:**423–432.

Cohen L, Karbat I, Gilles N, Froy O, Corzo G, Angelovici R, Gordon D, and Gurevitz M (2004) Dissection of the functional surface of an anti-insect excitatory toxin illuminates a putative "hot spot" common to all scorpion β-toxins affecting Na^+ channels. *J Biol Chem* **279:**8206–8211.

Gellens ME, George Jr AL, Chen LQ, Chahine M, Horn R, Barchi RL, and Kallen RG (1992) Primary structure and functional expression of the human cardiac tetrodotoxin-insensitive voltage-dependent sodium channel. *Proc Natl Acad Sci USA* **89:**554–558.

Gordon D, Moskowitz H, Eitan M, Warner C, Catterall WA, and Zlotkin E (1992) Localization of receptor sites for insect-selective toxins on sodium channels by site-directed antibodies. *Biochemistry* **31:**7622–7628.

Gordon D, Savarin P, Gurevitz M, and Zinn-Justin S (1998) Functional anatomy of scorpion toxins affecting sodium channels. *J Toxicol - Toxin Rev* **17:**131–159.

Janiszewski L (1990) The action of toxins on voltage-gated sodium channels. *Pol J Pharmacol Pharm* **42:**581–588.

Jurman ME, Boland LM, Liu Y, and Yellen G (1994) Visual identification of individual transfected cells for electrophysiology using antibody-coated beads. *Biotechniques* **17:**876–881.

Klugbauer N, Lacinova L, Flockerzi V, and Hofmann F (1995) Structure and functional expression of a new member of the tetrodotoxin-sensitive voltage-activated sodium channel family from human neuroendokrine cells. *EMBO J* **14:**1084–1090.

Kohrman DC, Smith MR, Goldin AL, Harris J, and Meisler MH (1996) A missense mutation in the sodium channel Scn8a is responsible for cerebellar ataxia in the mouse mutant jolting. *J Neurosci* **16:**5993–5999.

Long SB, Campbell EB, and MacKinnon R (2005) Crystal structure of a mammalian voltage-dependent Shaker family K^+ channel. *Science* **309**:897–903.

Mantegazza M and Cestèle S (2005) β-scorpion toxin effects suggest electrostatic interactions in domain II of voltage-dependent sodium channels. *J Physiol* **568:**13–30.

Martin-Eauclaire MF and Couraud F (1995) Scorpion neurotoxins: Effects and Mechanisms. In *Handbook of Neurotoxicology* (LW Chang & RS Dyer eds) pp 683–716, Marcel Dekker, NY.

Massensini AR, Suckling J, Brammer MJ, Moraes-Santos T, Gomez MV, and Romano-Silva MA (2002) Tracking sodium channels in live cells: confocal imaging using fluorescently labeled toxins. *J Neurosci Methods* **116:**189–196.

Noda M, Ikeda T, Suzuki H, Takeshima H, Takahashi T, Kuno M, and Numa S (1986) Expression of functional sodium channels from cloned cDNA. *Nature* **322:**826–828.

Possani LD, Becerril B, Delepierre M, and Tytgat J (1999) Scorpion toxins specific for Na^+-channels. *Eur J Biochem* **264:**287–300.

Shichor I, Zlotkin E, Ilan N, Chikashvili D, Stühmer W, Gordon D, and Lotan I (2002) Domain 2 of *Drosophila* para voltage-gated sodium channel confers insect properties to a rat brain channel. *J Neuroscience* **22:**4364–4371.

Sternberg D, Maisonobe T, Jurkat-Rott K, Nicole S, Launay E, Chauveau D, Tabti N, Lehmann-Horn F, and Hainque B (2001) Hypokalaemic periodic paralysis type 2 caused by mutations at codon 672 in the muscle sodium channel gene SCN4A. *Brain* **124:**1091–1099.

Trimmer JS, Cooperman SS, Tomiko SA, Zhou JY, Crean SM, Boyle MB, Kallen RG, Sheng ZH, Barchi RL, Sigworth FJ, Goodman RH, Agnew WS, and Mandelet G (1989) Primary structure and functional expression of a mammalian skeletal muscle sodium channel. *Neuron* **3:**33–49.

Zorn S, Leipold E, Hansel A, Bulaj G, Olivera BM, Terlau H, and Heinemann SH (2006) The μO-conotoxin MrVIA inhibits voltage-gated sodium channels by associating with domain-3. *FEBS Letters* **580:**1360–1364.

Zuo XP and Ji YH (2004) Molecular mechanism of scorpion neurotoxins acting on sodium channels. *Molecular Neurobiology* **30:**265–278.

Footnotes

This work was supported by grants from the Deutsche Forschungsgemeinschaft (HE 2993/5, to S.H.H.) and S1-2001000674 (Fonacit-Venezuela) and PI-2004000385 (Fonacit-CNPq, Venezuela-Brazil) (to A.B.).

Legends for Figures

Fig. 1. Effect of Tz1 on wild-type Na_V channels expressed in HEK 293 cells.

(**A**) Current responses of $Na_V1.4$, $Na_V1.6$, $Na_V1.2$, $Na_V1.7$, and $Na_V1.5$ channels to a test voltage of –70 mV, where channels are closed under control conditions (gray traces). Dashed traces represent currents in the presence of 10 µM Tz1 without a prepulse (–pp) and black traces with a prepulse (+pp). (**B**) Normalized conductance–voltage plots for the indicated channel types. Open circles: control conditions; open triangles: 10 µM Tz1 without preactivation; filled circles: 10 µM Tz1 with preactivation. (**C**) P_{tox} values for the indicated channels as horizontal histograms with (++pp) or without (–pp) a prepulse. The white bars indicate the P_{tox} values for 10 µM Tz1 (*n* see Table 1), the black bars for 2 µM Tz1 (*n* = 4 each).

Fig. 2. Analysis of the voltage sensor in domain-2.

(**A**) Alignment of the major part of receptor site-4, i.e. the S3-S4 linker of domain-2. (**B**) Normalized conductance–voltage plots for $Na_V1.4$ mutants G658N and E657Q and 10 µM Tz1 with a use of symbols as in Fig. 1. (**C**) P_{tox} values with a use of symbols as in Fig. 1. The triagles mark the P_{tox} values for wild-type $Na_V1.2$, the diamonds those for wild-type $Na_V1.4$ channels.

Fig. 3. Effect of 10 µM Tz1 on domain chimeras between $Na_V1.4$ and $Na_V1.2$.

(**A**) Cartoons illustrating the composition of the channel chimeras ($Na_V1.4$: white; $Na_V1.2$: black). (**B**) Normalized conductance–voltage plots for chimeras 2444, 4244, 4424, and 4442. (**C**) P_{tox} values. Symbols in B and C were used as in Figs 1 and 2.

Fig. 4. Pore loop chimeras.

(**A**) Alignment of the SS2 loop in domain-3 for $Na_V1.4$, $Na_V1.2$, $Na_V1.6$, $Na_V1.7$, and $Na_V1.5$. (**B**) Normalized conductance–voltage plots for 44p(1.2)4, 22p(1.4)2, 44p(1.6)4, 44p(1.7)4, and 44p(1.5)4 before (open circles) and after application of 10 µM Tz1, with (filled circles) and without (open triangles) prepulse. (**C**) P_{tox} values. The dashed lines mark the P_{tox} values for the background channels (either $Na_V1.2$ or $Na_V1.4$), the solid lines those for the wild types that donated the domain-3 pore loop. Symbols in B and C were used as in Figs 1 and 2.

Fig. 5. Analysis of the domain-3 SS2 loop.

(**A**) Normalized conductance–voltage plots for mutants E1251N, K1252V, E1254L, H1257K, and V1260D in the background of $Na_V1.4$ before (open circles) and after application of 10 µM Tz1, with (filled circles) and without prepulse (open triangles). (**B**) P_{tox} values for 2 µM (black) and 10 µM Tz1 (white bars). The triagles mark the P_{tox} values for wild-type $Na_V1.2$, the diamonds those for wild-type $Na_V1.4$ channels. Symbols in A and B were used as in Figs 1 and 2.

Tables

Table 1. Parameters characterizing wild-type channels, channel chimeras, and single-site mutants

Channel	Activation			P_{tox}		*n*
	$V_{0.5}$ (mV)	ΔV (mV)	k_m (mV)	–pp (%)	+pp (%)	
$Na_V1.4$	-34.74 ± 2.51	-42.32 ± 0.94	8.65 ± 0.48	41.2 ± 2.9	66.8 ± 3.6	9
$Na_V1.6$	-35.15 ± 1.08	-49.29 ± 1.81	10.33 ± 0.51	8.4 ± 0.8	22.7 ± 2.5	7
$Na_V1.2$	-27.11 ± 3.23	-49.56 ± 0.75	10.38 ± 0.26	2.9 ± 0.9	7.1 ± 1.2	5
$Na_V1.7$	-34.72 ± 0.68	-49.52 ± 0.88	9.70 ± 0.84	0.5 ± 0.3	1.0 ± 0.3	4
$Na_V1.5$	-48.82 ± 2.93	-46.10 ± 0.43	11.14 ± 0.54	0.0 *	1.1 ± 0.4	4
2444	-35.56 ± 1.31	-41.31 ± 0.79	8.82 ± 0.22	38.6 ± 3.4	70.0 ± 3.8	4
4244	-32.56 ± 1.95	-39.67 ± 0.79	8.80 ± 0.17	70.8 ± 4.5	90.5 ± 2.4	5
4424	-32.49 ± 2.41	-39.25 ± 1.45	7.62 ± 0.76	7.6 ± 1.3	10.9 ± 1.7	5
4442	-38.77 ± 2.76	-42.17 ± 0.51	8.78 ± 0.45	35.4 ± 3.2	59.4 ± 4.4	6
44p(1.2)4	-36.25 ± 1.85	-41.54 ± 1.97	7.71 ± 0.35	4.5 ± 0.5	7.9 ± 0.9	5
44p(1.5)4	-40.27 ± 2.92	-40.62 ± 0.81	7.74 ± 0.28	76.6 ± 2.6	96.9 ± 1.7	4
44p(1.6)4	-38.05 ± 2.71	-44.44 ± 1.17	8.18 ± 0.21	22.6 ± 1.9	37.5 ± 3.2	6
44p(1.7)4	-31.45 ± 1.79	-45.21 ± 0.42	9.47 ± 0.68	0.3 ± 0.3	1.5 ± 0.5	5
22p(1.4)2	-31.86 ± 1.62	-39.47 ± 0.48	10.59 ± 0.43	55.0 ± 3.1	87.5 ± 0.6	4
Q657E	-39.71 ± 1.46	-38.54 ± 1.07	7.78 ± 0.45	41.5 ± 5.7	58.3 ± 7.1	6
G658N	-39.60 ± 2.38	-46.68 ± 3.27	10.93 ± 1.51	2.6 ± 1.2	3.7 ± 1.5	5
E1251N	-37.52 ± 3.31	-41.81 ± 0.89	7.83 ± 0.67	8.8 ± 1.0	20.2 ± 2.7	5
K1252V	-34.82 ± 1.44	-39.28 ± 0.49	8.14 ± 0.32	68.0 ± 2.3	95.3 ± 0.7	4
E1254L	-34.99 ± 1.27	-41.04 ± 0.57	8.47 ± 0.24	50.0 ± 2.3	57.2 ± 2.9	5

H1257K	-34.85 ± 2.63	-39.84 ± 0.83	7.77 ± 0.57	6.8 ± 1.0	16.7 ± 2.1	5
V1260D	-31.54 ± 2.76	-39.13 ± 1.31	8.58 ± 0.88	40.1 ± 3.0	61.7 ± 4.2	5

Current-voltage relationships of the indicated channel isoforms and mutants before and after application of 10 µM Tz1 were analyzed according to eqn 1 and 2 to yield the voltage where 50% of the channels are opened under control conditions ($V_{0.5}$) and the corresponding slope factor for a single gate (k_m). Application of Tz1 shifted channel activation by ΔV. The P_{tox} values indicate the percentage of channels being Tz1-modified in the absence (–pp) and presence (+pp) of a conditioning prepulse. *n* is the number of independent experiments. * no measurable effect.

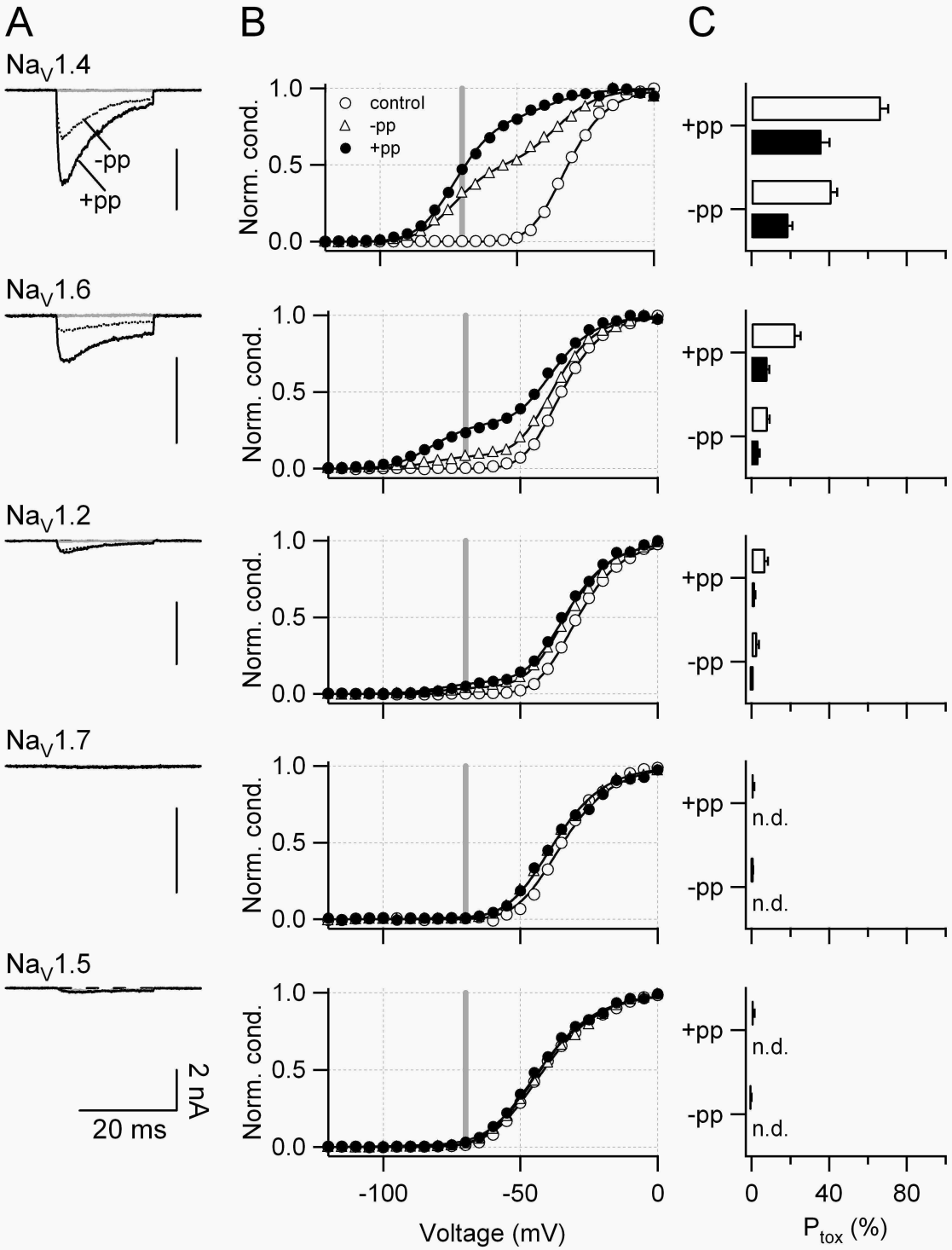
A
B
C
$Na_V1.4$
$Na_V1.6$
$Na_V1.2$
$Na_V1.7$
$Na_V1.5$
-pp
+pp
2 nA
20 ms
control
-pp
+pp
Norm. cond.
1.0
0.5
0.0
-100
-50
0
Voltage (mV)
+pp
-pp
n.d.
0
40
80
P_{tox} (%)

Figure 1

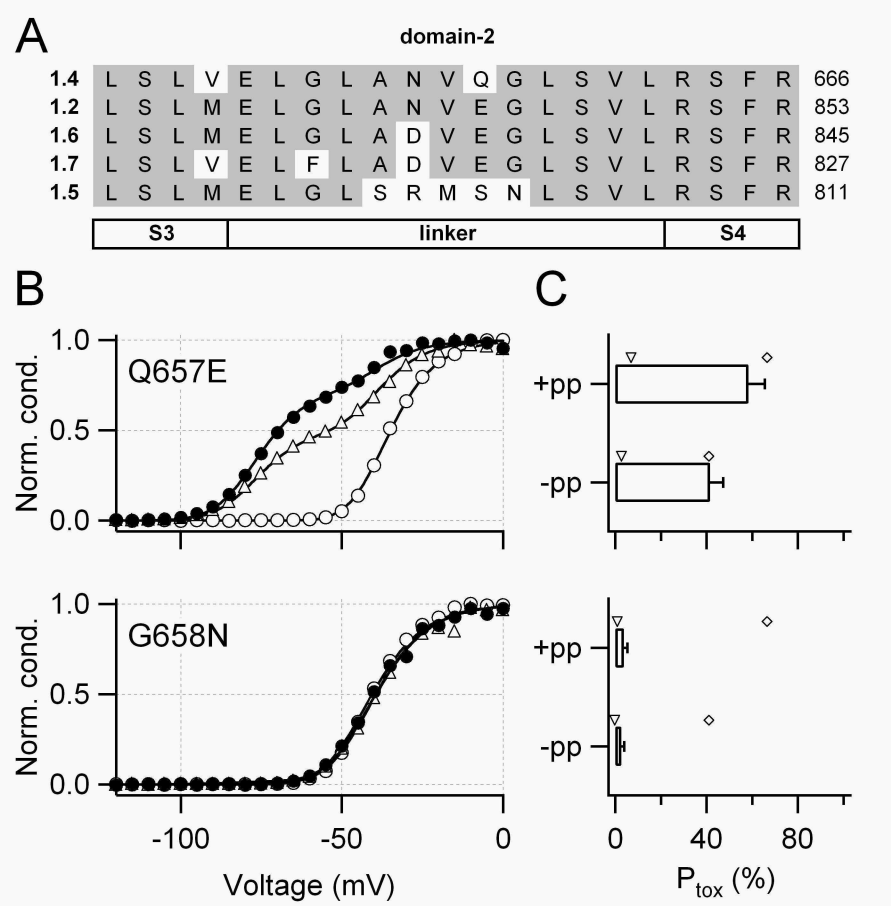
A
domain-2
1.4 L S L V E L G L A N V Q G L S V L R S F R 666
1.2 L S L M E L G L A N V E G L S V L R S F R 853
1.6 L S L M E L G L A D V E G L S V L R S F R 845
1.7 L S L V E L F L A D V E G L S V L R S F R 827
1.5 L S L M E L G L S R M S N L S V L R S F R 811
S3
linker
S4
B
Q657E
Norm. cond.
1.0
0.5
0.0
G658N
Norm. cond.
1.0
0.5
0.0
-100
-50
0
Voltage (mV)
C
+pp
-pp
+pp
-pp
0
40
80
P tox (%)

Figure 2

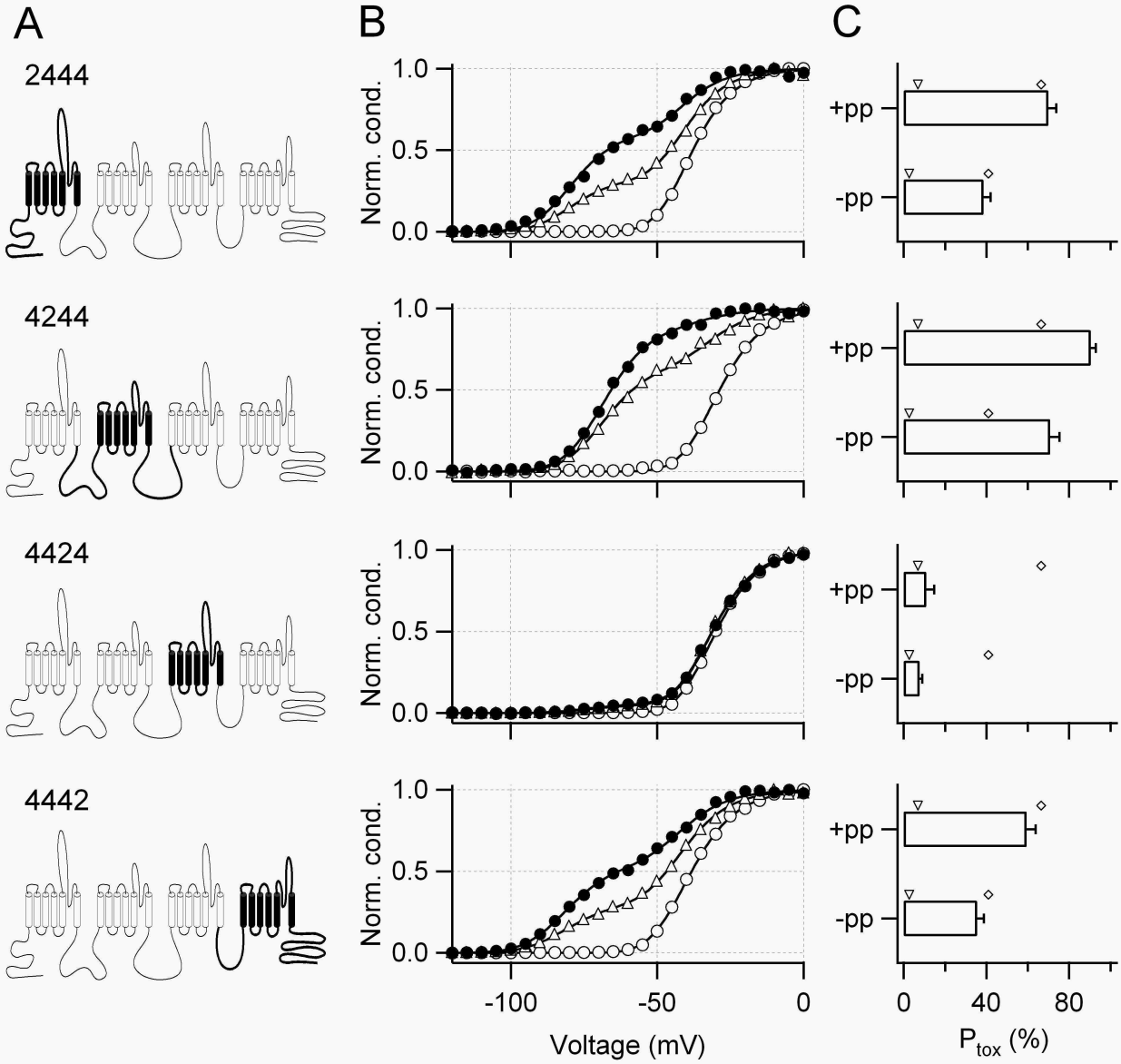
A
2444
4244
4424
4442
B
Norm. cond.
1.0
0.5
0.0
-100
-50
0
Voltage (mV)
C
+pp
-pp
0
40
80
P_tox (%)

Figure 3

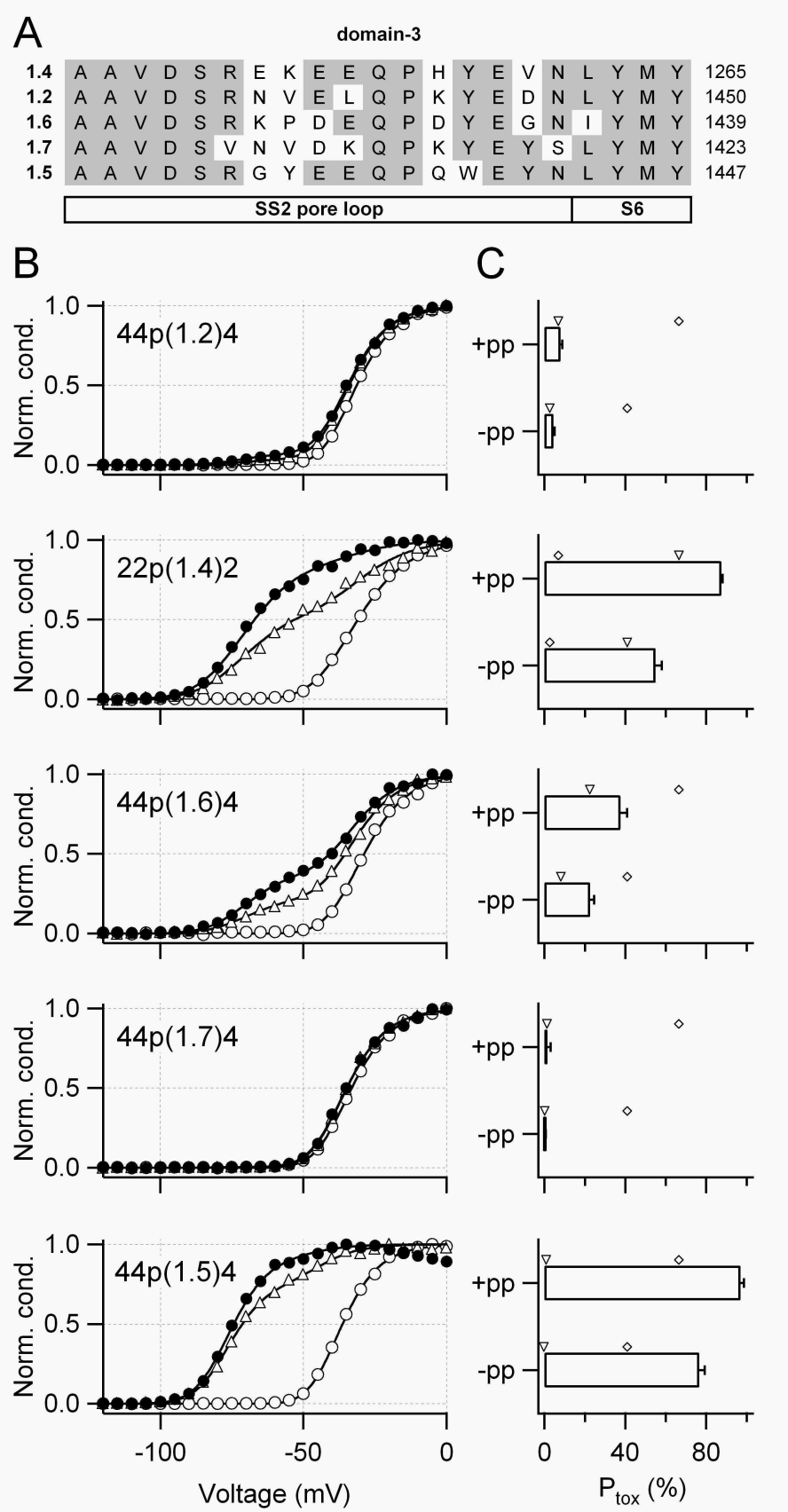
A
domain-3
1.4 A A V D S R E K E E Q P H Y E V N L Y M Y 1265
1.2 A A V D S R N V E L Q P K Y E D N L Y M Y 1450
1.6 A A V D S R K P D E Q P D Y E G N I Y M Y 1439
1.7 A A V D S V N V D K Q P K Y E Y S L Y M Y 1423
1.5 A A V D S R G Y E E Q P Q W E Y N L Y M Y 1447
SS2 pore loop
S6
B
C
44p(1.2)4
22p(1.4)2
44p(1.6)4
44p(1.7)4
44p(1.5)4
Norm. cond.
1.0
0.5
0.0
+pp
-pp
-100
-50
0
Voltage (mV)
0
40
80
P_tox (%)

Figure 4

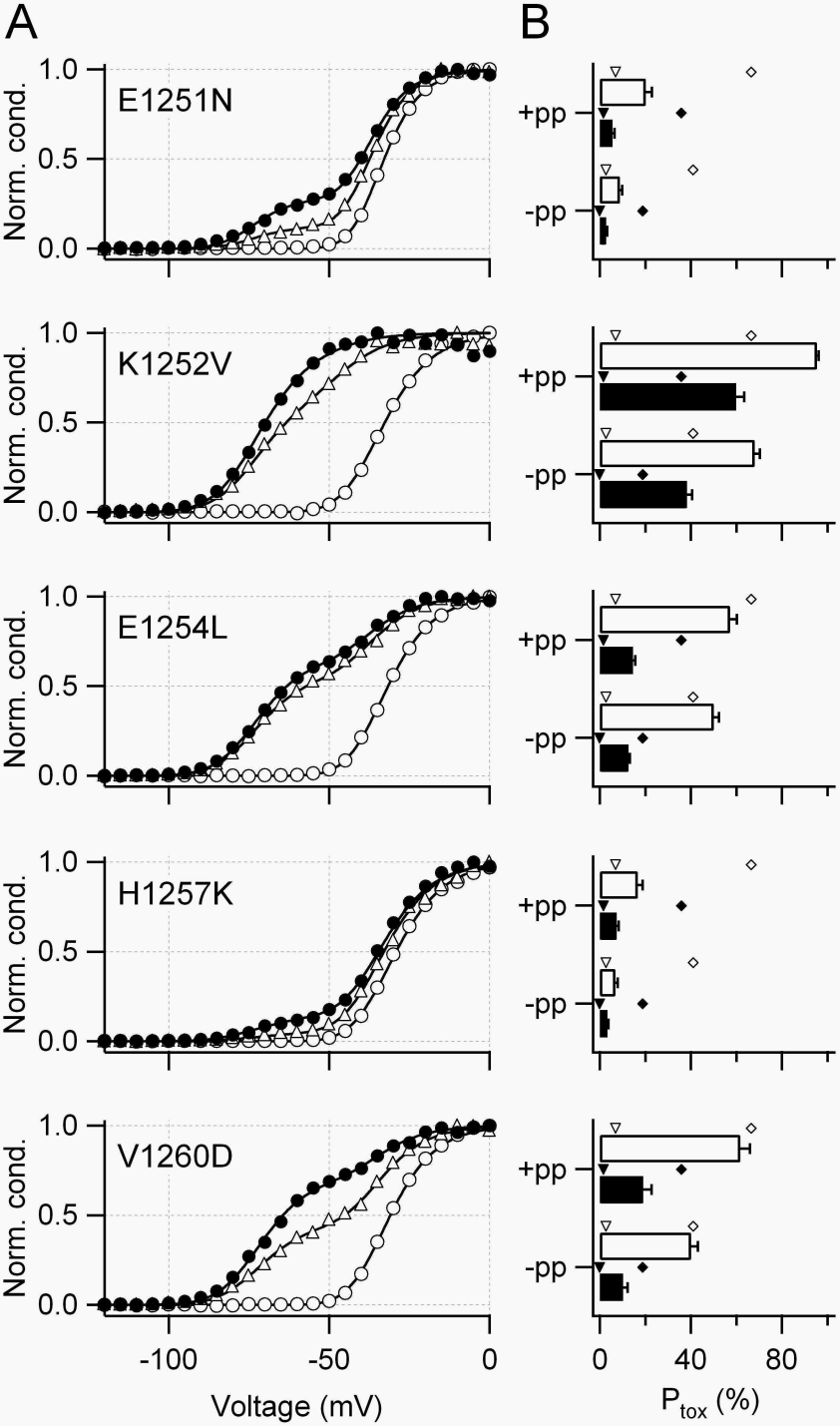
A
B
E1251N
K1252V
E1254L
H1257K
V1260D
Norm. cond.
1.0
0.5
0.0
+pp
-pp
-100
-50
0
Voltage (mV)
0
40
80
P_tox (%)

Figure 5

FEBS Letters 580 (2006) 1360–1364

The μO-conotoxin MrVIA inhibits voltage-gated sodium channels by associating with domain-3

Stefan Zorn[a,1], Enrico Leipold[a,1], Alfred Hansel[a], Grzegorz Bulaj[b], Baldomero M. Olivera[b], Heinrich Terlau[c], Stefan H. Heinemann[a,*]

[a] *Institute of Molecular Cell Biology, Research Unit "Molecular and Cellular Biophysics", Medical Faculty of the Friedrich Schiller University Jena, Drackendorfer Str. 1, D-07747 Jena, Germany*

[b] *Department of Biology, University of Utah, Salt Lake City, UT 84112, USA*

[c] *Institute of Experimental and Clinical Pharmacology and Toxicology, University of Lübeck, Ratzeburger Allee 160, 23538 Lübeck, Germany and Max Planck Institute for Experimental Medicine, Molecular and Cellular Neuropharmacology Group, 37075 Göttingen, Germany*

Received 5 January 2006; accepted 12 January 2006

Available online 26 January 2006

Edited by Maurice Montal

Abstract Several families of peptide toxins from cone snails affect voltage-gated sodium (Na_V) channels: μ-conotoxins block the pore, δ-conotoxins inhibit channel inactivation, and μO-conotoxins inhibit Na_V channels by an unknown mechanism. The only currently known μO-conotoxins MrVIA and MrVIB from *Conus marmoreus* were applied to cloned rat skeletal muscle ($Na_V1.4$) and brain ($Na_V1.2$) sodium channels in mammalian cells. A systematic domain-swapping strategy identified the C-terminal pore loop of domain-3 as the major determinant for $Na_V1.4$ being more potently blocked than $Na_V1.2$ channels. μO-conotoxins therefore show an interaction pattern with Na_V channels that is clearly different from the related μ- and δ-conotoxins, indicative of a distinct molecular mechanism of channel inhibition.

Keywords: Sodium channel; Conotoxin; Neurotoxin; Patch clamp; Channel block; Pain

1. Introduction

Voltage-gated sodium channels (Na_V channels) are key elements for the generation of action potentials of electrically excitable cells [1]. The fast activation and inactivation of these channels is crucial for shaping the upstroke depolarization of an action potential. A variety of neurotoxins from different organisms act on Na_V channels and affect the cellular excitability (e.g., [2–5]). Several families of peptide toxins from the venom of cone snails modulate Na_V channels: μ-conotoxins and μO-conotoxins block channel conductance, whereas δ-conotoxins increase currents by inhibiting inactivation [6].

The μ-conotoxins "block" the channel by interacting with receptor site-1, which is the binding site of the classical Na_V channel blockers tetrodotoxin (TTX) and saxitoxin (STX) (review: [7]). μ-Conotoxins belong to the M-superfamily, δ- and μO-conotoxins to the O-superfamily of conopeptides. The latter have a cysteine backbone, which is different from the one of μ-conotoxins but similar to that of ω-conotoxins, which interact with voltage-gated Ca^{2+} channels. δ-Conotoxins interact with receptor site-6 of Na_V channels. Our recent study [8], however, showed that δ-conotoxins, like scorpion α-toxins or sea anemone toxins, interact with the S3/4 linker of domain-4. Hence, receptor site-3 and site-6 seem to be overlapping structural entities.

Despite their structural similarities to δ-conotoxins, μO-conotoxins block sodium current and apparently do not slow inactivation [9]. In addition, they seem to have blocking potency for calcium channels [10]. Competition studies with labeled STX suggest that μO-conotoxins do not block Na_V channels by interacting with receptor site-1 [11]. The site of action and the mechanism through which μO-conotoxins affect Na_V channels are still unknown.

There is considerable interest in elucidating such mechanisms because uniquely, μO-conotoxins seem to block TTX-resistant sodium channels effectively ($Na_V1.8$ [12]). These channels are expressed in peripheral nerves, and their specific suppression may provide an analgesic strategy. Systematic studies are, however, hampered by the complication of expressing $Na_V1.8$ channels in mammalian cells. In addition, thus far no marked subtype specificity of the toxins that would allow for a systematic search for binding sites or molecular mechanisms of channel modulation has been shown.

2. Materials and methods

2.1. Construction of channel chimeras

The rat channel isoforms $Na_V1.2$ (X03639 [13]) and $Na_V1.4$ (M26643.1 [14]) were expressed from the vectors pCIneo and pcDNA3, respectively. Using PCR-based site-directed mutagenesis, three silent mutations (C3121G, G3123A, and C3868T) were introduced into the $Na_V1.4$ ORF to generate an *Nhe*I restriction site at position 3121 and a *Cla*I site at position 3864. These two restriction sites, an endogenous *Bsi*WI site (position 1329), a *Bst*EII site at the 3′ end, and an *Xba*I site at the 5′ end of the channel-coding gene were used to extract DNA fragments coding for the four channel domains (domain-1: *Bst*EII/*Bsi*WI, domain-2: *Bsi*WI/*Nhe*I, domain-3: *Nhe*I/*Cla*I, domain-4: *Cla*I/*Xba*I). DNA fragments coding for the homologous parts of $Na_V1.2$ were subcloned into the pGEMT vector (Promega Corp., Madison, USA) with primers that introduced restriction sites for *Bsi*WI, *Nhe*I, *Cla*I, *Bst*EII,

*Corresponding author. Fax: +49 3641 9 32 56 82.
E-mail address: Stefan.H.Heinemann@uni-jena.de (S.H. Heinemann).

[1] These authors contributed equally.

Abbreviations: Na_V channels, voltage-gated sodium channels; TTX, tetrodotoxin; STX, saxitoxin

0014-5793/$32.00
doi:10.1016/j.febslet.2006.01.057

and *Xba*I in homologous positions. The four $Na_V1.2$ fragments were introduced into $Na_V1.4$ resulting in four chimeras in which individual domains of $Na_V1.4$ are replaced by those of $Na_V1.2$: 2444 (domain-1), 4244 (domain-2), 4424 (domain-3), and 4442 (domain-4). In addition, we generated mutants in the background of wild-type $Na_V1.4$ ("44p4": E1251N, K1252V, E1254L, H1257K, and V1260D) and $Na_V1.2$ ("22p2": N1436E, V1437K, L1439E, K1442H, and D1445V) channels.

2.2. Toxin synthesis

MrVIA/B were synthesized using a modification of a method described previously [9]. The peptides were assembled on an automatic peptide synthesizer using 9-fluorenylmethoxycarbonyl (Fmoc) chemistry on a preloaded Fmoc-Val-Wang resin. It was removed from the resin by a 3-h treatment with reagent K and precipitated with cold methyl-tert-butyl ether (MTBE) chilled to −20°C. The precipitate was washed four times with cold MTBE. A reversed-phase HPLC purification of a reduced peptide was performed using a preparative diphenyl column (Vydac, model 219TP510) with a linear gradient of 90% acetonitrile/0.1% TFA in water, ranging from 30% to 90%. The first oxidation step was carried out by mixing the following reaction components (final concentrations in parentheses): isopropanol (30%), water, Tris–HCl buffer, pH 8.7 (100 mM), EDTA (1 mM), GSSG (1 mM), GSH (2 mM). The reaction was quenched with formic acid (1%) and then separated on the preparative diphenyl HPLC column. The second folding step included formation of the disulfide bond between Cys9 and Cys25 and was carried out in 40% acetonitrile, and 1 mM iodine, 2.5% TFA for 20 min at room temperature. The oxidation product was purified on the diphenyl preparative HPLC column, as described for the linear form.

2.3. Electrophysiological measurements

Cultivation and transfection of HEK 293 cells as well as whole-cell voltage clamp experiments and toxin application were performed as described previously [15]. The patch pipettes contained (mM): 35 NaCl; 105 CsF; 10 EGTA; and 10 HEPES (pH 7.4 with CsOH). The bath solution contained (mM): 150 NaCl; 2 KCl, 1.5 $CaCl_2$; 1 $MgCl_2$; and 10 HEPES (pH 7.4 with NaOH). The toxins were stored frozen in extracellular bath solution additionally containing 1 mg/ml BSA.

Channel activation was assayed by test depolarizations from −80 to +60 mV at an interval of 10 s. The peak currents were fit with a Hodgkin–Huxley activation formalism involving three activation gates and a single-channel characteristic according to the Goldman–Hodgkin–Katz equation:

$$I_{\mathrm{peak}}(V) = \frac{I_{\max}}{\left(1 + \mathrm{e}^{-(V - V_{\mathrm{m}})/k_{\mathrm{m}}}\right)^3}$$
$$I_{\max} = \Gamma V \frac{1 - \mathrm{e}^{-(V - E_{\mathrm{rev}})/25\,\mathrm{mV}}}{1 - \mathrm{e}^{-V/25\,\mathrm{mV}}} \quad (1)$$

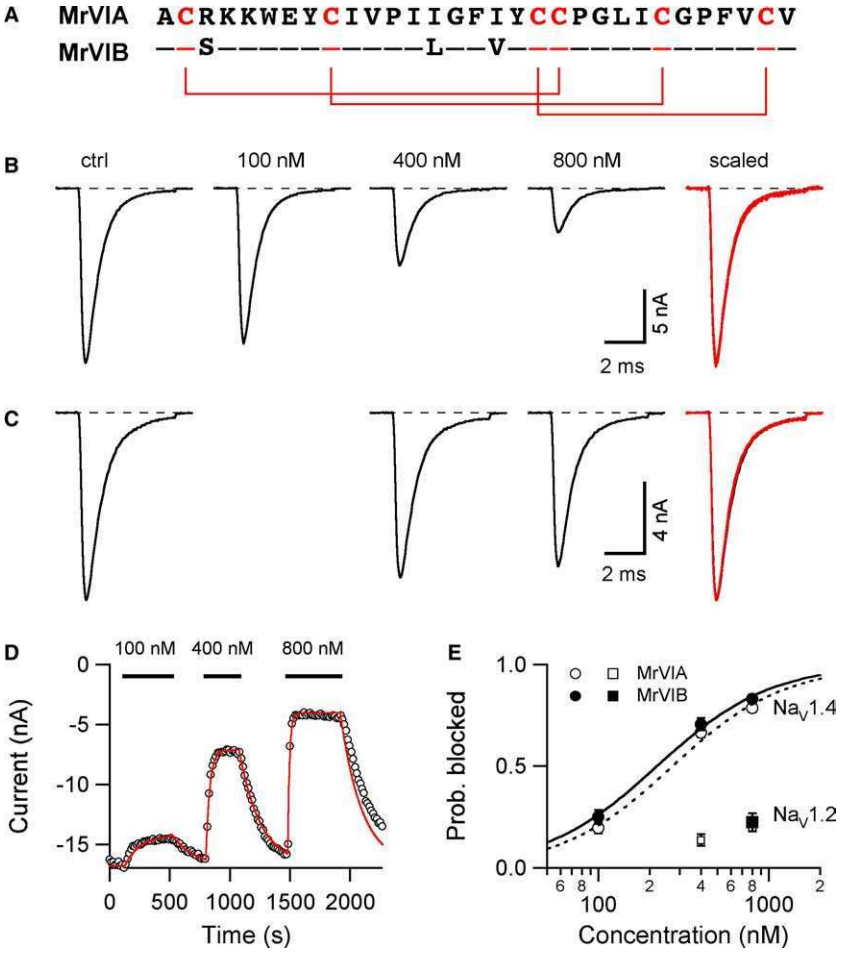

Fig. 1. Block of $Na_V1.4$ channels by MrVIA and MrVIB. (A) Alignment of MrVIA and MrVIB indicating the disulfide bridge structure. (B) Current responses to depolarizations to −20 mV for $Na_V1.4$ channels expressed in HEK 293 cells under control conditions and after application of the indicated concentrations of MrVIA. The panel on the right shows the traces recorded in the presence of toxin superimposed to the control and scaled in magnitude by the factors 1.135 (100 nM), 2.30 (400 nM), and 4.01 (800 nM). (C) A similar experiment as in (B) but with $Na_V1.2$ channels. The presence of 400 and 800 nM MrVIA resulted in weak current block (scaling factors of 1.13 and 1.22, respectively). (D) Pulses to −20 mV were elicited every 30 s and the peak current is plotted here as a function of time under the indicated applications of MrVIA. The superimposed curve is a fit to the data assuming that the block obeys an on-rate of $1/(\tau = 12.800\ \mathrm{s/conc[nM]})$ and an off-rate of $1/(\tau = 180\ \mathrm{s})$. (E) Concentration–response curves for blocking $Na_V1.4$ channels by MrVIA (open) and MrVIB (filled circles). The continuous curves are Hill fits (Eq. (3)). The squares indicate data for $Na_V1.2$ channels.

where V_m is the voltage of half-maximal gate activation and k_m the corresponding slope factor. Γ is the maximal conductance of all channels and E_{rev} the reversal potential.

Voltage dependence of fast inactivation was evaluated by measuring current at −20 mV after 500-ms conditioning pulses ranging from −140 to −30 mV (repetition interval of 15 s). The peak current versus the conditioning voltage was described with a Boltzmann function:

$$I(V) = \frac{I_{min}}{(1 + e^{-(V-V_h)/k_h})} \quad (2)$$

with the half-maximal inactivation voltage V_h and the corresponding slope factor k_h.

Toxin dependence of current inhibition was measured under repetitive pulsing to −20 mV at an interval of 15 s. The dose dependence for toxin-induced current reduction was described with the Hill equation:

$$I/I_c = \frac{1}{1 + \left(\frac{conc}{IC_{50}}\right)^h} \quad (3)$$

where h is the Hill coefficient and *conc* the toxin concentration. IC_{50} provides a measure for the concentration of half-maximal channel inhibition. Data points were weighted according to the standard error of the mean; error estimates for IC_{50} values were obtained from these fits with the IgorPro program (WaveMetrics, Lake Oswego, OR, USA). The holding potential was −120 mV for all experiments.

Data acquisition and analysis were performed with PatchMaster and FitMaster software, respectively (HEKA Elektronik, Lambrecht, Germany). All data were presented as means ± S.E. of the mean (n = number of independent experiments).

3. Results and discussion

3.1. Block of rNa$_V$1.4 and rNa$_V$1.2 channels by μO-conotoxins

Rat $Na_V1.4$ channels were expressed in HEK 293 cells and the effects of the μO-conotoxins MrVIA and MrVIB (Fig. 1A) were assayed under whole-cell patch clamp conditions. As shown in Fig. 1B, application of increasing concentrations of MrVIA reduced the current magnitude when channel activity was measured under repetitive pulses to −20 mV. The time course of the remaining current did not significantly differ from the control as shown in the scaled-up version in the rightmost panel of Fig. 1B. Fig. 1C shows similar experiments performed with $Na_V1.2$ channels. Even 800 nM MrVIA exhibits only a very small blocking effect on the evoked currents. Furthermore, the time course of the currents in the presence of the toxin is not altered either. Similar results were obtained with MrVIB. Thus, MrVIA and MrVIB, unlike the structurally related δ-conotoxins, do not affect the time course of channel activation or inactivation. In Fig. 1D, the time course of peak currents is shown for the indicated applications of MrVIA. The current is blocked rapidly and reversibly. The continuous curve is a data fit assuming a block on-rate of 780/(ms nM) and an off-rate of 5.5/ms. Therefore, the on-rate is roughly a linear function of toxin concentration and the off-rate seems to be independent of toxin concentration indicating a simple bimolecular reaction. The potency of the toxins to reduce the $Na_V1.4$-mediated current amplitude was estimated by compiling concentration–response curves (Fig. 1E), described by a Hill equation (Eq. (3)), yielding IC_{50}-values of 265 ± 16 and 222 ± 18 nM, and Hill coefficients of 1.32 ± 0.10 and 1.31 ± 0.12 for MrVIA and MrVIB, respectively. Thus, the toxins display an indistinguishable potency to block $Na_V1.4$ channels. A Hill coefficient close to unity suggests that one toxin molecule might be sufficient for channel block.

The difference of toxin effect on muscle and brain channels was not expected because Safo et al. [16] reported that MrVIA did not discriminate well between rNa$_V$1.4 (IC_{50} 438 nM), rNa$_V$1.2 (532 nM), and rNa$_V$1.7 (345 nM) when the channels were expressed in *Xenopus* oocytes. Presently we do not know the differences between those results and ours obtained in HEK 293 cells. Nevertheless, our experiments clearly demonstrate that MrVIA has a preference for $Na_V1.4$ over $Na_V1.2$ channels. This preference and the absolute potency is the same for MrVIA and MrVIB, indicating that the minor sequence differences between the two toxins (see Fig. 1A) have no effect on the toxin interaction with the mammalian channel types assayed.

The current reduction induced by the MrVI toxins did not depend on the magnitude of membrane depolarization. As shown in Fig. 2A, 400 nM MrVIA reduced the peak current of $Na_V1.4$ channels to the same extent throughout a complete current–voltage recording. In addition, no strong shift in steady-state inactivation is observed in the presence of toxins (Fig. 2B). For wild-type $Na_V1.4$ channels V_h was −75.5 ± 1.8 mV before and −82.2 ± 1.9 mV (n = 6) after application of 400 nM MrVIA. Thus, since the holding voltage used in this study was −120 mV throughout, we can safely exclude a shift of steady-state inactivation as cause for μO-conotoxin-induced current block. The averaged parameters characterizing channel activation and inactivation are listed in Table 1.

3.2. Identification of domain-3 as a major interaction site

The difference in the toxin effect on $Na_V1.4$ over $Na_V1.2$ channels provide the opportunity to systematically search for domains in the channel protein important for toxin action. This is particularly intriguing, as currently there is no information on the channel binding sites occupied by μO-conotoxins. For an initial screening we generated chimeras between $Na_V1.4$ and $Na_V1.2$ channels in which the majority of the

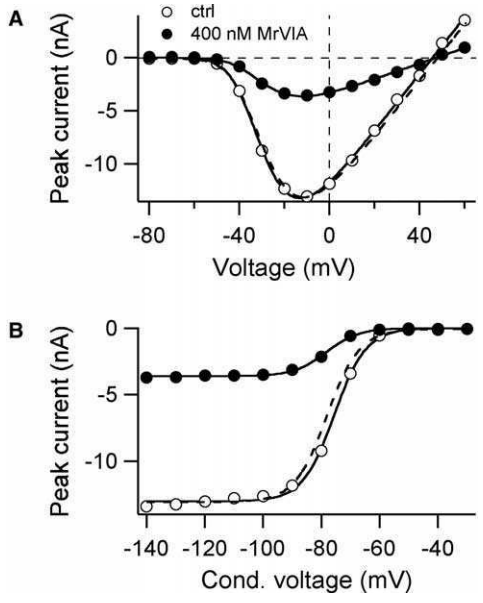

Fig. 2. Voltage-dependent parameters. (A) Current–voltage relationship for $Na_V1.4$ channels under control conditions (open circles) and after application of 400 nM MrVIA (filled circles). The continuous curves are data fits according to a Hodgkin and Huxley activation model (Eq. (1)). The broken continuous curve superimposed to the control data is the fit resulting from the toxin data, scaled by a factor of 3.6. (B) Steady-state inactivation curve (Eq. (2)) for the same cell as in (A) and using the same symbols.

Table 1
Steady-state activation and inactivation parameters as well as current block by 400 nM MrVIA characterizing wild-type channels and channel chimeras

Channel	V_m (mV)	k_m (mV)	n	V_h (mV)	k_h (mV)	n	% Block	n
rNa$_V$1.4 (4444)	−45.6 ± 1.9	10.2 ± 0.7	10	−75.1 ± 1.9	5.0 ± 0.2	10	68.4 ± 1.1	22
rNa$_V$1.2 (2222)	−39.2 ± 3.3	12.2 ± 0.2	5	−72.6 ± 3.0	4.8 ± 0.1	5	13.6 ± 2.8	8
2444	−45.7 ± 1.1	10.0 ± 0.3	4	−73.9 ± 0.8	5.0 ± 0.2	5	62.8 ± 2.6	9
4244	−42.9 ± 2.1	10.4 ± 0.3	7	−75.9 ± 1.7	5.2 ± 0.1	7	67.9 ± 4.9	11
4424	−41.5 ± 1.8	8.7 ± 0.9	5	−71.5 ± 0.7	4.9 ± 0.2	5	16.2 ± 1.5	5
4442	−49.3 ± 2.4	10.4 ± 0.6	6	−79.7 ± 1.8	5.3 ± 0.1	6	71.0 ± 2.6	9
44p4	−46.0 ± 1.0	9.2 ± 0.3	8	−73.3 ± 0.9	4.6 ± 0.1	8	19.9 ± 3.0	8
22p2	−44.0 ± 1.3	12.4 ± 0.5	4	−76.4 ± 1.4	4.9 ± 0.1	4	46.3 ± 3.9	6

V_m and k_m values determined from current–voltage relationships according to Eq. (1), V_h and k_h values from steady-state inactivation protocols according to Eq. (2), and the percentage of current block upon application of 400 nM MrVIA.

construct was from Na$_V$1.4: Individual domains were exchanged between the two channel isoforms yielding the constructs 2444, 4244, 4424, and 4442 as depicted in Fig. 3A. All domain chimeras were assayed for the effect of 400 nM MrVIA yielding strong current block, i.e. a Na$_V$1.4 phenotype, in all chimeras but 4424. This result is somewhat surprising as this is the first case in which domain-3 is the major determinant for the discrimination of channel isoforms by neurotoxins.

All chimeras were also investigated with respect to the voltage dependence of activation and fast inactivation. As listed in Table 1, none of the chimeras dramatically deviated from the wild-type Na$_V$1.4 channel indicating that the observed differences in toxin effect are not due to altered gating characteristics introduced by formation of the chimeras.

To further narrow down a potential interaction site between μO-conotoxins and Na$_V$ channels, we constructed another chimera in which only the C-terminal part of the pore loop (SS2) of Na$_V$1.2 was transferred into Na$_V$1.4 (Fig. 3A, bottom). This part of the pore loop only contains five differences between the channel isoforms. The assay with 400 nM MrVIA also yielded a strong reduction in the blocking potency (Fig. 3B, bottom) suggesting that SS2 plays a major role in the binding of

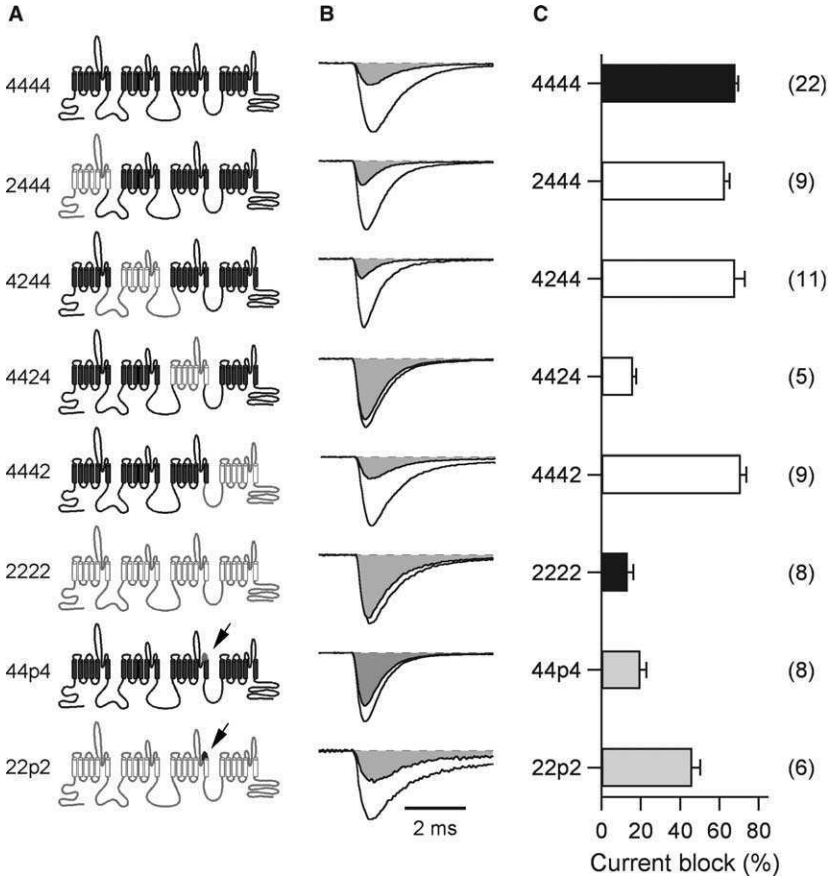

Fig. 3. Chimeras and assay of toxin effects. (A) Cartoons illustrating the construction of channel chimeras. Parts originating from Na$_V$1.4 are shown in black, parts from Na$_V$1.2 in grey. In chimeras "44p4" and "22p2" the SS2 pore loops of domain-3, indicated by the arrows, have been exchanged. (B) Superimposed current traces of the corresponding channel constructs obtained upon depolarization to −20 mV under control conditions and after application of 400 nM MrVIA (grey shading). (C) Average block of peak current after application of 400 nM MrVIA for the indicated channel constructs. The error bars denote S.E.M. values and the numbers in parentheses the numbers of experiments.

μO-conotoxins to the channels. Since a reduction of the toxin effect induced by mutagenesis at five positions may be rather accidental, we generated the reverse chimera, i.e. a $Na_V1.2$ channel with the SS2 pore loop of domain-3 from $Na_V1.4$. This chimera was blocked much more efficiently than the corresponding wild-type $Na_V1.2$ (Fig. 3, last row), clearly showing that the identified region is a major determinant for the action of μO-conotoxins. These data therefore add a new molecular entity to the interaction sites of biologically active neurotoxins on Na_V channels.

μO-conotoxins, although they exhibit structural similarities to δ-conotoxins, do not affect inactivation of Na_V channels, but instead block the channel conductance. This effect seems similar to that of μ-conotoxins. However, binding studies with radiolabeled STX indicated that μO-conotoxin MrVIA is not interacting with receptor site-1 of the channel [11]. In contrast to μ-conotoxins, which make multiple couplings to the pore loop of different channel domains of the Na_V channel α-subunit [6,17], our data indicate that μO-conotoxins do block Na_V channels by interacting mainly with the C-terminal part of the pore loop of domain-3. The pore regions of the domains 1, 2, and 4 seem to be less important for μO-conotoxin binding, at least they are not crucial for the difference between $Na_V1.2$ and $Na_V1.4$ channels. The pore loop of domain-3, however, also seems to be important for the binding of scorpion β-toxins [18,19].

3.3. Potential value of μO-conotoxins

The differences of MrVIA effects on $Na_V1.4$ and $Na_V1.2$ channels could be used to identify potential interaction sites at the channel protein. However, higher concentrations of MrVIA also affect $Na_V1.2$ channels and they even seem to affect Ca_V channels [10]. Therefore, the overall specificity of μO-conotoxins seems to be rather weak and not comparable to the specificity observed for structurally related ω-conotoxins that block Ca_V channels. Since μO-conotoxins also block TTX-resistant $Na_V1.8$ channels in dorsal root ganglia neurons involved in pain sensation [12], these peptides might be important tools for studying these channels. Furthermore, the known structure of μO-conotoxins [12] might serve as a starting point for developing substances that specifically block $Na_V1.8$ channels; this could be a major breakthrough for the development of new analgetics. The results presented in this study can pave the way for a deeper understanding of the specificity of μO-conotoxins towards different Na_V channel subtypes.

Acknowledgments: We thank A. Roßner and S. Arend for technical assistance, Dr. J. Trimmer for providing the coding sequence of $rNa_V1.4$ and Dr. M. Noda for $rNa_V1.2$. This work was supported by grants from the Deutsche Forschungsgemeinschaft (HE 2993/5, to S.H.H.) and NIH (Grant GM48677 to B.M.O.).

References

[1] Catterall, W.A. (2000) From ionic currents to molecular mechanisms: the structure and function of voltage-gated sodium channels. Neuron 26, 13–25.
[2] Gordon, D. (1997) Na channels as targets for neurotoxins: mode of action and interaction of neurotoxins with receptor sites on Na channels in: Toxins and Signal Transduction (Lazarowici, P. and Gutman, Y., Eds.), Cellular and Molecular Mechanisms of Toxin Action Series, pp. 119–149, Harwood Press, Amsterdam.
[3] Zlotkin, E. (1999) The insect voltage-gated sodium channel as target of insecticides. Annu. Rev. Entomol. 44, 429–455.
[4] Cestèle, S. and Catterall, W.A. (2000) Molecular mechanisms of neurotoxin action on voltage-gated sodium channels. Biochimie 92, 883–892.
[5] Catterall, W.A. (2002) Molecular mechanisms of gating and drug block of sodium channels. Novartis Found. Symp. 214, 206–225.
[6] Terlau, H. and Olivera, B.M. (2004) *Conus* venoms: a rich source of novel ion channel-targeted peptides. Physiol. Rev. 84, 41–68.
[7] French, R.J. and Terlau, H. (2004) Sodium channel toxins–receptor targeting and therapeutic potential. Curr. Med. Chem. 11, 3053–3064.
[8] Leipold, E., Hansel, A., Olivera, B.M., Terlau, H. and Heinemann, S.H. (2005) Molecular interaction of δ-conotoxins with voltage-gated sodium channels. FEBS Lett. 579, 3881–3884.
[9] McIntosh, J.M., Hasson, A., Spira, M.E., Gray, W.R., Li, W., Marsh, M., Hillyard, D.R. and Olivera, B.M. (1995) A new family of conotoxins that blocks voltage-gated sodium channels. J. Biol. Chem. 270, 16796–16802.
[10] Fainzilber, M., van der Schors, R., Lodder, J.C., Li, K.W., Geraerts, W.P. and Kits, K.S. (1995) New sodium channel-blocking conotoxins also affect calcium currents in *Lymnaea* neurons. Biochemistry 34, 5364–5371.
[11] Terlau, H., Stocker, M., Shon, K.J., McIntosh, J.M. and Olivera, B.M. (1996) μO-conotoxin MrVIA inhibits mammalian sodium channels, but not through site I. J. Neurophysiol. 76, 1423–1429.
[12] Daly, N.L., Ekberg, J.A., Thomas, L., Adams, D.J., Lewis, R.J. and Craik, D.J. (2004) Structures of μO-conotoxins from *Conus marmoreus*. Inhibitors of tetrodotoxin (TTX)-sensitive and TTX-resistant sodium channels in mammalian sensory neurons. J. Biol. Chem. 279, 25774–25782.
[13] Noda, M., Ikeda, T., Suzuki, H., Takeshima, H., Takahashi, T., Kuno, M. and Numa, S. (1986) Expression of functional sodium channels from cloned cDNA. Nature 322, 826–828.
[14] Trimmer, J.S., Cooperman, S.S., Tomiko, S.A., Zhou, J.Y., Crean, S.M., Boyle, M.B., Kallen, R.G., Sheng, Z.H., Barchi, R.L., Sigworth, F.J., Goodman, R.H., Agnew, W.S. and Mandel, G. (1989) Primary structure and functional expression of a mammalian skeletal muscle sodium channel. Neuron 3, 33–49.
[15] Chen, H., Gordon, D. and Heinemann, S.H. (1999) Modulation of cloned skeletal muscle Na channels by the scorpion toxins Lqh II, Lqh III, and LqhαIT. Pflügers Arch. 439, 423–432.
[16] Safo, P., Rosenbaum, T., Shcherbatko, A., Choi, D.-Y., Han, E., Toledo-Aral, J.J., Olivera, B.M., Brehm, P. and Mandel, G. (2000) Distinction among neuronal subtypes of voltage-activated sodium channels by μ-conotoxin PIIA. J. Neurosci. 20, 76–80.
[17] Li, R.A., Tsushima, R.G., Kallen, R.G. and Backx, P.H. (1997) Pore residues critical for μ-CTX binding to rat skeletal muscle Na^+ channels revealed by cysteine mutagenesis. Biophys. J. 73, 1874–1884.
[18] Gordon, D., Moskowitz, H., Eitan, M., Warner, C., Catterall, W.A. and Zlotkin, E. (1992) Localization of receptor sites for insect-selective toxins on sodium channels by site-directed antibodies. Biochemistry 31, 7622–7628.
[19] Cestèle, S., Qu, Y., Rogers, J.C., Rochat, H., Scheuer, T. and Catterall, W.A. (1998) Voltage sensor-trapping: enhanced activation of sodium channels by β-scorpion toxin bound to the S3-S4 loop in domain II. Neuron 21, 919–931.

Manuscript for: Journal of General Physiology

Quantitative description of the interaction between scorpion β-toxin Tz1 and voltage-gated sodium channels.

Enrico Leipold[1], Adolfo Borges[2], and Stefan H. Heinemann[1]

[1] *Institute of Molecular Cell Biology,*
Research Unit "Molecular and Cellular Biophysics",
Medical Faculty of the Friedrich Schiller University Jena,
Drackendorfer St. 1, D-07747 Jena, Germany,

[2] *Sección de Biomembranas,*
Instituto de Medicina Experimental,
Facultad de Medicina, Universidad Central de Venezuela,
Caracas 1051, Venezuela

Running title: Scorpion β-toxin Tz1

‡ Correspondence:

Prof. Dr. Stefan H. Heinemann
Institute of Molecular Cell Biology
Molecular and Cellular Biophysics
Friedrich Schiller University Jena
Drackendorfer Str. 1
D-07747 Jena, Germany
Tel: ++49-3641-9 32 56 80
Fax: ++49-3641-9 32 56 82
e-Mail: Stefan.H.Heinemann@uni-jena.de

Abbreviations:

Na_V channels, voltage-gated sodium channels

Abstract

Scorpion-β-toxins target voltage-gated sodium channels (Na_V channels) and interfere specifically with epitopes in domain-2 and -3 of the channels. They lower the activation threshold of Na_V channels by shifting the voltage dependence of channel activation to more negative membrane potentials. A “voltage sensor trapping” model has been proposed in which a β-toxin binds to its receptor site on the channel and traps the domain-2 voltage sensor in an activated, outward position upon membrane depolarization. In a subsequent depolarization cycle a prebound β-toxin enhances the toxin effect. Here we show that β-toxin Tz1 from *Tityus zulianus* exerts a dual effect on $Na_V1.4$ channels. In addition to a pronounced hyperpolarizing shift of the activation threshold, Tz1 substantially reduced $Na_V1.4$ mediated currents. By analysis of channel mutants we show that the specific structure of D2S3-S4 linker in Na_V channels determines whether Tz1 acts as a blocker or an activator of Na_V channels. Furthermore, a quantitative analysis of Tz1-induced effects reveals a model in which the toxin stabilizes activated and deactivated states of the domain-2 voltage sensor in a voltage-dependent manner. Under hyperpolarizing conditions, Tz1 prevents activation of channels by immobilizing the voltage sensor in its deactivated state. Once activated, the toxin promotes channel opening by trapping the voltage sensor in its activated conformation.

210 words

Key words: Sodium channel; Na^+ channel, scorpion toxin; patch clamp; receptor site-4; activation

Introduction

Voltage-gated sodium channels (Na_V channels) play a prominent role in initiating and transmitting electrical signals in excitable cells (Hodgkin and Huxley, 1952). The channels are composed of four homologous domains (D1-D4), each with six transmembrane segments (S1-S6) (Catterall, 2000). The S4 segments of the four domains constitute movable voltage sensors and initiate conformational transitions between open and closed channel states in response to changes in the membrane voltage (Stühmer et al., 1989).

Various venomous animals developed neurotoxic polypeptides that target these gating segments of Na_V channels, making them useful tools in studying channel function. Scorpion venoms contain two major classes of peptides that interfere with voltage sensors of Na_V channels, namely α- and β-toxins. Scorpion α-toxins bind to receptor site-3 on Na_V channels and slow down their inactivation kinetics. Scorpion β-toxins bind to receptor site-4 and lower the activation threshold of Na_V channels by shifting the voltage dependence of channel activation to more negative membrane potentials (reviewed in Possani et al., 1999).

Previous studies have suggested that α-toxins prevent the domain-4 voltage sensor of Na_V channels from moving outward via an interaction with the S3-S4 linker in domain-4, thus inhibiting channel inactivation (Rogers et al., 1996). In contrast to α-toxins, β-toxins were shown to interact with the S3-S4 linker in the voltage sensor of domain-2 in a use-dependent manner. A voltage sensor trapping model was proposed in which β-toxins hold the domain-2 voltage sensor specifically in its activated, outward position and therefore cause sub-threshold channel opening (Cestèle et al., 1998, 2001). However, there are conflicting reports regarding the molecular mechanism of scorpion β-toxin action.

On neonatal rat heart cell preparations Ts1 (*Tityus serrulatus* toxin 1, former Ts-γ) and CnII-10 (from *Centruroides noxius*), two scorpion β-toxins, were shown to shift the activation threshold of Na_V channels, but not in a use-dependant manner (Yatani et al., 1988). In addition to a hyperpolarizing shift of channel activation, both toxins decreased the sodium current amplitude, indicating that Ts1 and CnII-10 also inhibited a fraction of Na_V channels. Couraud et al. (1982) reported a similar dual effect for Ts1 on myelinated frog nerves. In a recent study we showed that β-toxin Tz1 from *Tityus zulianus* acts use-dependently on various mammalian sodium channels (Leipold et al., 2006) and that this toxin also exerts both effects, “activation shift” and “channel block” on Na_V channels (Borges et al., 2004).

In this study we address the molecular mechanism by which β-toxins facilitate activation of Na_V channels on the one hand and simultaneously block Na_V channels on the other. We show that the scorpion β-toxin Tz1 exerts either of the two opposite

effects “activation shift” and “channel block” in a voltage dependent manner. Whereas Tz1 facilitates the activation of preactivated $Na_V1.4$ channels by trapping the domain-2 voltage sensor in its activated position, the toxin reduces $Na_V1.4$-mediated currents by stabilizing the deactivated conformation of the sensor when the membrane is hyperpolarized. It is proposed that the use-dependence of β-toxin action is characterized by a voltage dependent toggling between activated and deactivated channel states. Analysis of mutated $Na_V1.4$ channels revealed that residues in domain-2 linker S3-S4 of $Na_V1.4$ are involved in this toggle mechanism.

Materials and Methods

Site directed mutagenesis. The wild-type Na_V channel construct used in this study was the rat isoform of $Na_V1.4$ (P15390; Trimmer et al., 1989). The construction of $Na_V1.4$ mutants Q657E, G658N, E1251N, K1252V, E1254L, H1257K and V1260D was described previously (Leipold et al., 2006). Mutations G652F and N655D were introduced in the background of $Na_V1.4$ using PCR-based site-directed mutagenesis. Primers were obtained from MWG (Ebersberg, Germany). The sequences of mutant channels were verified by sequence analysis. Plasmid DNA was isolated from *E. coli* using the Midi- or Maxi-plasmid purification kit (Qiagen, Hilden, Germany).

Cell culture and transfection. HEK 293 cells (CAMR, Porton Down, Salisbury, UK) were maintained in 45% Dulbecco’s Minimal Eagles Medium (DMEM) and 45% F12, supplemented with 10% fetal calf serum in a 5% CO_2 incubator at 37°C. HEK 293 cells were trypsinized, diluted with culture medium and grown in 35-mm dishes. When HEK 293 cells were grown to 30-50% confluence, transient transfection was performed using the Superfect transfection kit (Qiagen). HEK 293 cells were transfected with a 5:1 ratio of the Na_V channel expression plasmids and a vector encoding the CD8 antigen (Jurman et al., 1994). The cells were used for electrophysiological recordings 2-3 days after transfection. Dynabeads (Deutsche Dynal GmbH, Hamburg, Germany) were used for visual identification of individual transfected cells.

Electrophysiological measurements. Whole-cell voltage clamp experiments were performed as described previously (Chen et al., 2000). Briefly, patch pipettes with resistances of 0.9-2.0 MΩ were used. The series resistance was compensated for by more than 80% in order to minimize voltage errors. A patch-clamp amplifier EPC10 was operated by PatchMaster software (both HEKA Elektronik, Lambrecht, Germany). Leak and capacitive currents were corrected with a p/n method with a leak holding voltage of –140 mV, a leak pulse scaling factor of –0.1 and n=10 leak pulses. Due to the toxin-induced left-shift in activation, this procedure was necessary in order to avoid the recording of ionic current during the leak pulses. Currents were low-pass filtered at 5 kHz and sampled at a rate of 25 kHz. All experiments were performed at constant temperature 19-21°C. Data analysis was performed using IgorPro (WaveMetrics, Lake

Oswego, OR, USA). All data were presented as mean ± standard error of the mean (n = number of independent experiments). The patch pipettes contained (in mM): 35, NaCl; 105, CsF; 10, EGTA; 10, Hepes (pH 7.4 with CsOH). The bath solution contained (in mM): 150 NaCl; 2 KCl, 1.5 CaCl2; 1 MgCl2; 10 Hepes (pH 7.4 with NaOH). The application of toxin was performed with an application pipette as described previously (Chen et al., 2000).

Current-voltage relationship. To measure the use-dependence of Tz1 action, a double-pulse protocol was applied (Borges et al. 2004). From a holding potential of –120 mV a set of test depolarizations in the range from –130 to +55 mV in steps of 5 mV was applied followed by a constant prepulse to –10 mV for 50 ms prior to a second set of test pulses with identical parameters as the first set. This constant pulse was necessary to preactivate the channels prior to the second test pulse series. To ensure recovery from fast inactivation the cells were held at –120 mV for 50 ms before and after the prepulse. The repetition interval was 5 s. The peak currents during the two test pulse series were plotted as a function of voltage, yielding two current-voltage relationships, one without and one with prepulse.

$$I_{peak} = I_{\max}\left[\frac{1-P_{tox}}{(1+e^{-(V-V_m)/k_m})^3}+\frac{P_{shift}}{(1+e^{-(V-V_m-\Delta V)/k_m})^2}\right]$$

$$I_{\max} = \Gamma V \frac{1-e^{-(V-E_{rev})/25mV}}{1-e^{-V/25mV}}$$

$$P_{block} = P_{tox} - P_{shift}$$

(eq. 1)

For a quantitative data description the build-in global-fit-procedure of the IgorPro program was used to fit eq. 1 to control and toxin data simultaneously. Γ is the maximal conductance of all channels and E_{rev} the measured reversal potential. V is the test pulse voltage and I_{peak} the peak test pulse current. V_m is the half-maximal gate activation and k_m the corresponding slope factor. ΔV is the voltage by which the activation of toxin modified channels is shifted. The weighting factor P_{tox} indicates the fraction of channels which are toxin modified after Tz1 application and consist of two components: P_{block}, a faction of channels which are blocked by Tz1 and P_{shift}, a fraction of channels which show a shifted activation threshold. In control experiments, i.e. in the absence of toxin, P_{tox} and P_{shift} were set to 0. Using this formalism means to describe activation of control channels according to a Hodgkin & Huxley theory, i.e. using three independent activation gates. Activation-shifted channels are assumed to activate with two independent gates as one is expected to be trapped open in an activated position.

Results

The dual effect of Tz1.

Previously we reported that the β-toxin Tz1 lowers the activation threshold of $Na_V1.4$ channels and also decreases a fraction of $Na_V1.4$-mediated currents (Borges et al., 2004). Here we ask the question whether the two opposite effects "activation shift" and "channel block" are functionally coupled. Using a previously described pulse protocol (Fig. 1A, Borges et al., 2004) we assayed the effects of 10 µM Tz1 on heterologously expressed $Na_V1.4$ channels. In this protocol a first set of test depolarizations, ranging from −130 to +55 mV, were applied fallowed by a constant 50-ms pulse to −10 mV which serves as a conditioning prepulse prior a second test pulse series with identical parameters as the first set. With this protocol two current-voltage relationships were recorded simultaneously, one without (−pp) and one with prepulse (+pp). The lower panel of Fig. 1A shows representative current traces of $Na_V1.4$ channels under control conditions and in presence of Tz1 for a depolarization to −70 mV. Whereas $Na_V1.4$ channels are closed at −70 mV in the absence of Tz1, they become substantially activated in the first test pulse (−pp) when 10 µM Tz1 is present, indicating the lowered activation threshold of these channels. This effect is enhanced in the second test pulse (+pp) where channels were preactivated. Complete current-voltage relationships of $Na_V1.4$ channels show the dual effect of Tz1 and are presented in Fig. 1B. Whereas Tz1 left-shifts the activation of one fraction of $Na_V1.4$ channels in a use-dependent manner, the toxin seems to block a second channel fraction with a negative use-dependence, i.e. preactivation of the channels facilitates channel activation and simultaneously results in a partial loss of channel block. A detailed analysis of the dual toxin effect was performed by fitting a Hodgekin-Huxley formalism (Eq. (1)) to control and toxin data simultaneously. Assuming that Tz1 does not alter the conductance of single $Na_V1.4$ channels, the current-voltage relationships in the presence of toxin were described with an identical maximal conductance like those under control conditions. This procedure revealed P_{shift} as the probability of channels being activation-shifted and P_{block} as the probability of channels being blocked by Tz1. The sum of both parameters characterizes the fraction of all Tz1-modified channels and is indicated by P_{tox}. Figure 1C visualizes P_{shift}, P_{block} and P_{tox} of $Na_V1.4$ channels during application of 10 µM Tz1. Interestingly, the P_{tox} values of $Na_V1.4$ channels do not depend on a prepulse, but the ratio between P_{shift} and P_{block} is strongly prepulse-dependent. Apparently, the toxin-induced effects "activation shift" and "channel block" are functionally coupled processes.

Influence of the domain-3 pore loop on Tz1 action.

Since residues in the C-terminal pore-loop of domain-3 were shown to alter the channel-specific sensitivity towards Tz1 (Leipold et al., 2006), we tested the impact of these residues on the Tz1 mechanism. Using an identical procedure as for wild-type $Na_V1.4$ channels, we analyzed the effects of 10 µM Tz1 on $Na_V1.4$ mutants E1251N, K1252V, E1254L, H1257K and V1260D. The results are presented in Figure 2 and Table 1. Whereas mutants E1452L and V1260D show a P_{tox} value similar to wild-type $Na_V1.4$ channels, mutants E1251N and H1257K are less sensitive for Tz1. On the other hand, mutation K1252V increased the sensitivity of $Na_V1.4$ channels for Tz1, indicated by an increased P_{tox}. Despite the importance of the investigated residues for the sensitivity of $Na_V1.4$ channels towards Tz1, the toxin induced the same dual effect in mutants E1251N, K1252V, H1257K and V1260D, i.e. without preactivation the blocking effect of Tz1 dominates its ability to facilitate channel activation. For preactivated channels, the Tz1-induced "channel block" was partially reduced and "activation shift" was enhanced. Interestingly, in mutant E1254L the prepulse did not change the ratio between blocked and activation-shifted channels, i.e. it did not show noticeable use-dependence.

Analysis of domain-2 voltage sensor mutants.

β-toxins are proposed to trap the domain-2 voltage sensor of Na_V channels specifically in its activated conformation, thus lowering the activation threshold of the channels (Cestèle et al., 1998). A conserved Glycine residue (G658 in $Na_V1.4$) in this linker was shown to be essential for the ability of β-toxins to facilitate the activation of $Na_V1.2$ (Cestèle et al., 1998) and $Na_V1.4$ channels (Leipold et al., 2006). Since the domain-2 S3-S4 linker is directly involved in the trapping of the domain-2 voltage sensor, we investigated the role of this linker in Tz1-induced channel block more systematically. By analyzing an alignment of various mammalian Na_V channels, three non-conserved amino acids are identified in the peripheral $Na_V1.7$ channel: F813, D816, E818. In order to determine the role of the domain-2 S3-S4 linker for the β-toxin mechanism, we functionally tested Tz1 on mutated $Na_V1.4$ channels in which we replaced the non-conserved residues of this linker by those present in $Na_V1.7$. The quantitative analysis of the mutant channels is presented in Fig. 3 and Table 1.

Data: G652F, N655D, Q657E and G658N

Whereas mutants N655D, Q657E and G658N show a P_{tox} value similar to wild-type $Na_V1.4$ channels, the toxin acts more potently on mutant G652F, indicated by an increased P_{tox} value. Interestingly, the ratio between P_{shift} and P_{tox} of these mutants differs remarkably from that of wild-type channels.

Quantitative analysis of Tz1 effects.

Since the voltage sensor in domain-2 of $Na_V1.4$ channels mediates both Tz1-induced effects, “activation shift” and “channel block”, in a prepulse-dependent manner, we further analyzed the state-dependence of these toxin effects. Therefore, we employed a modified pulse protocol (Fig. 4A). With this protocol we measured the kinetics of the transition between the Tz1 effects “activation shift” and “channel block”. Such a measurement on $Na_V1.4$ channels is shown in Fig. 4B and 4C. With an increasing conditioning time the probability of channels being blocked by Tz1 is increasing to the same extend as the probability of channels being activation-shifted is decreasing. As expected, P_{tox} remains constant under these conditions. The change in the ratio between blocked and activation-shifted channels at a membrane potential of −160 mV was described by a single exponential function and revealed a time constant of 8.1 s for $Na_V1.4$ (Fig.4C).

Data: S3-S4 mutants, data for backward transition (−160, −100, −80 mV)

Diskussion

The membrane voltage determines whether β-toxin Tz1 acts as an activator or blocker of Na_V channels.

To explain the Css4-induced sub-threshold opening of Na_V channels, Cestèle et al. (1998, 2000) developed a model in which a β-toxin traps the domain-2 voltage sensor exclusively in its activated conformation. However, this model does not explain the potency of β-toxins to simultaneously block Na_V channels. Here, we showed that the β-toxin Tz1 exerts such a dual effect. Whereas Tz1 lowers the activation threshold of $Na_V1.4$ channels in a use-dependent manner, the toxin blocks channels with a negative use-dependence. A quantitative analysis revealed that preactivation of channels does not affect the Tz1-sensitivity of $Na_V1.4$, but it affects the ratio between blocked and activation-shifted channels. These results show clearly that the so-called use-dependence of Tz1 is in fact a voltage-dependent toggling between “activation shift” and “channel block”, i.e. the membrane voltage determines whether Tz1 acts as a channel activator or a channel blocker.

Xxx

These results are supported by experiments in which the binding of β-toxins was shown to be independent from the membrane voltage (Jover et al., 1980).

xxx

The pore loop of domain-3 modulates the channel-specific Tz1 sensitivity.

Previously it was shown that the C-terminal pore-loop in domain-3 of Na_V channels determines the channel-specific sensitivity for Tz1 (Leipold et al., 2006).

xxx

Residues in the loop connecting S3 and S4 in domain-2 modulate the Tz1 effects.

Using $Na_V1.4$ mutant channels we showed that the voltage dependent toggling of the Tz1-induced effects “activation shift” and “channel block” is modulated by residues in the linker connecting S3 and S4 in domain-2 of the channels.

xxx

The domain-2 voltage sensor is trapped in activated and deactivated states.

A detailed quantitative analysis of the Tz1-effects on $Na_V1.4$ wild-type and mutant channels revealed an extension of the voltage sensor trapping model originally suggested by Cestèle et al. (1998). At resting membrane potentials the probability for the voltage sensors of Na_V channels to be in a deactivated conformation is high (Fig. 5A). We assume that Tz1 binds under these conditions to its receptor site and stabilizes the domain-2 voltage sensor in its deactivated state, thus preventing the outward movement of the sensor and therefore inhibiting channel activation. Phenotypically, these channels are “blocked”. On the other hand, the more positive the membrane potential the higher is the probability for the channels’ voltage sensors to be in an activated conformation (Fig. 5B). Under such conditions Tz1 stabilizes the activated conformation of the domain-2 voltage sensor, thus inhibiting the deactivation of the sensor. These channels show now a reduced activation threshold and therefore open at sub-threshold membrane potentials. In case of a prebound toxin the domain-2 voltage sensor can switch between the two states in a voltage-dependent manner. Apparently, Tz1 sterically interferes with the S3-S4 linker in the voltage sensor of domain-2 rather than to bind to this linker. Moreover, this mechanism suggests a voltage-independent binding of Tz1 to Na_V channels. Binding studies in which the voltage-independent binding of β-toxin Css2 (*Centruroides suffuses suffuses*) was shown (Jover et al., 1980) are in concert with our model.

Physiological relevance

The physiological effect of a β-toxin can not be predicted, i.e. a β-toxin can exert a depressant or excitatory function.

Classification of β-toxins

Whereas excitatory β-toxins may constitute activation shifters of Na_V channels, depressant β-toxins may constitute channel blockers.

Acknowledgements. We thank S. Arend for technical assistance.

References

Borges, A., Alfonzo, M. J., Garcia, C. C., Winand, N. J., Leipold, E., and Heinemann, S. H. (2004). Isolation, molecular cloning and functional characterization of a novel beta-toxin from the Venezuelan scorpion, Tityus zulianus. Toxicon *43*, 671-684.

Catterall, W. A. (2000). From ionic currents to molecular mechanisms: the structure and function of voltage-gated sodium channels. Neuron *26*, 13-25.

Cestèle, S., Qu, Y., Rogers, J. C., Rochat, H., Scheuer, T., and Catterall, W. A. (1998). Voltage sensor-trapping: enhanced activation of sodium channels by beta-scorpion toxin bound to the S3-S4 loop in domain II. Neuron *21*, 919-931.

Cestèle, S., Scheuer, T., Mantegazza, M., Rochat, H., and Catterall, W. A. (2001). Neutralization of gating charges in domain II of the sodium channel alpha subunit enhances voltage-sensor trapping by a beta-scorpion toxin. J Gen Physiol *118*, 291-302.

Chen, H., Gordon, D., and Heinemann, S. H. (2000). Modulation of cloned skeletal muscle sodium channels by the scorpion toxins Lqh II, Lqh III, and Lqh alphaIT. Pflugers Arch *439*, 423-432.

Couraud, F., Jover, E., Dubois, J. M., and Rochat, H. (1982). Two types of scorpion receptor sites, one related to the activation, the other to the inactivation of the action potential sodium channel. Toxicon *20*, 9-16.

Hodgkin, A. L., and Huxley, A. F. (1952). A quantitative description of membrane current and its application to conduction and excitation in nerve. J Physiol *117*, 500-544.

Jurman, M. E., Boland, L. M., Liu, Y., and Yellen, G. (1994). Visual identification of individual transfected cells for electrophysiology using antibody-coated beads. Biotechniques *17*, 876-881.

Leipold, E., Hansel, A., Borges, A., and Heinemann, S. (2006). Subtype specificity of scorpion {beta}-toxin Tz1 interaction with voltage-gated sodium channels is determined by the pore loop of domain-3. Mol Pharmacol.

Possani, L. D., Becerril, B., Delepierre, M., and Tytgat, J. (1999). Scorpion toxins specific for Na+-channels. Eur J Biochem *264*, 287-300.

Rogers, J. C., Qu, Y., Tanada, T. N., Scheuer, T., and Catterall, W. A. (1996). Molecular determinants of high affinity binding of alpha-scorpion toxin and sea anemone toxin in the S3-S4 extracellular loop in domain IV of the Na+ channel alpha subunit. J Biol Chem *271*, 15950-15962.

Stühmer, W., Conti, F., Suzuki, H., Wang, X. D., Noda, M., Yahagi, N., Kubo, H., and Numa, S. (1989). Structural parts involved in activation and inactivation of the sodium channel. Nature *339*, 597-603.

Trimmer, J. S., Cooperman, S. S., Tomiko, S. A., Zhou, J. Y., Crean, S. M., Boyle, M. B., Kallen, R. G., Sheng, Z. H., Barchi, R. L., Sigworth, F. J., and et al. (1989). Primary structure and functional expression of a mammalian skeletal muscle sodium channel. Neuron *3*, 33-49.

Yatani, A., Kirsch, G. E., Possani, L. D., and Brown, A. M. (1988). Effects of New World scorpion toxins on single-channel and whole cell cardiac sodium currents. Am J Physiol *254*, H443-451.

Footnotes.

This work was supported by grants from the Deutsche Forschungsgemeinschaft (HE 2993/5, to S.H.H.) and S1-2001000674 (Fonacit-Venezuela) and PI-2004000385 (Fonacit-CNPq, Venezuela-Brazil) (to A.B.).

Figure Legends

Figure 1. Effect of Tz1 on $Na_V1.4$ channels.

(A) *Top,* Pulse protocol used to record current-voltage relationships. Potentials ranging from −130 to +55 mV in steps of 5 mV were applied before (−pp) and after (+pp) a 50-ms conditioning prepulse to −10 mV. *Bottom,* The current traces are shown at −70 mV before (gray) and after (black) application of 10 µM Tz1. (B) *Left,* Current–voltage relationships for $Na_V1.4$ channels before (open circles) and after application of 10 µM Tz1 with (+pp, triangles) or without (−pp, squares) prepulse. The continuous curves indicate fit results according to Eq. (1). The gray line indicates −70 mV, a potential where Na_V channels are normally closed. *Right,* The estimated fractions of channels which are activation shifted (striped bars) or blocked (gray bars) by application of 10 µM Tz1 in the absence (−pp) or presence (+pp) of a prepulse are plotted as horizontal histogram.

Figure 2. The sensitivity of Na_V channels for Tz1 is mediated by the pore loop of domain-3.

(A) Current-voltage relationships for the indicated $Na_V1.4$ channel mutants before (open circles) and after application of 10 µM Tz1 with (+pp, triangles) or without (–pp, squares) prepulse. (B) Horizontal histograms show the fractions of the indicated $Na_V1.4$ mutants which are blocked (gray bars) or shifted (striped bars) by application of 10 µM Tz1 in the absence (–pp) and presence (+pp) of a prepulse.

Figure 3. Residues in the S3-S4-linker of the voltage sensor in domain-2 of Na_V channels determine between β-toxin-induced “activation shift” and “block”.

(A) Current-voltage relationships for the indicated $Na_V1.4$ D2S3-S4 mutants before (open circles) and after application of 10 µM Tz1 with (+pp, triangles) or without (–pp, squares) prepulse. (B) Horizontal histograms show the fractions of channels, which are blocked (gray bars) or shifted (striped bars) by application of 10 µM Tz1 in the absence (–pp) and presence (+pp) of a prepulse.

Figure 4. Quantitative description of Tz1 effects on $Na_V1.4$ channels.

(A) Pulse protocol used to elicit the kinetics of the voltage-dependent switching between the Tz1-induced effects “channel block” and “sub-threshold channel opening” on $Na_V1.4$ channels. Three current-voltage relationships were recorded in one experiment. Trains of four 10-ms voltage pulses to −10 mV, fallowed by a −160 mV hyperpolarizing pulse of varying length (0s, 5s and 15s) were applied 50 ms prior the test pulses. (B) Current-voltage relationship in the absence (open circles) and presence of 10 µM Tz1 without (filled circles) and with application of a 5 s (filled squares) or 15 s (filled triangles) hyperpolarizing prepulse to −160 mV. (C) P_{tox} (continuous line) and P_{shift} (dashed line) are plotted as a function of prepulse duration. Changes in the membrane voltage do not alter the number of Tz1-modified channels, but change the ratio between blocked (shaded area) and activation-shifted (white area) channels.

Figure 4. Modal voltage-sensor trapping.

Scorpiopn-β-toxins (β-ScTx) can stabilize open and closed channel states. (A) Inhibition of the depolarization-induced outward movement of the domain-2 voltage sensor prevents channel activation. Phenotypicaly these channels are blocked. (B) Trapping of the domain-2 voltage sensor in its activated position lowers the activation threshold of the whole channel and leads to sub-threshold channel opening.

Tables

Table1. Parameters characterizing wild-type and single mutant channels.

channel	V_m (mV)	k_m (mV)	ΔV (mV)	P_{tox}	-pp		+pp		n
					P_{shift} (%)	P_{block} (%)	P_{shift} (%)	P_{block} (%)	
$Na_V1.4$	-45.7 ± 2.0	9.9 ± 0.5	-33.4 ± 0.6	67.8	20.4 ± 1.2	47.4 ± 2.9	34.1 ± 1.3	33.7 ± 3.0	9
E1251N	-47.2 ± 2.9	9.4 ± 0.6	-37.5 ± 1.0	31.3	5.8 ± 0.5	25.5 ± 3.8	10.3 ± 1.2	21.0 ± 3.2	5
K1252V	-44.2 ± 1.5	9.1 ± 0.4	-26.5 ± 1.4	90.5	21.8 ± 1.3	68.7 ± 1.9	42.0 ± 3.0	48.5 ± 3.9	4
E1254L	-45.2 ± 1.1	10.0 ± 0.2	-35.1 ± 0.6	66.8	27.6 ± 1.7	39.2 ± 1.4	28.0 ± 1.8	38.8 ± 1.5	5
H1257K	-44.5 ± 2.1	9.4 ± 0.7	-35.5 ± 1.0	28.0	4.3 ± 0.5	23.6 ± 3.9	8.6 ± 1.0	19.4 ± 3.6	5
V1260D	-41.6 ± 1.9	10.0 ± 1.0	-35.5 ± 1.5	70.0	17.2 ± 1.9	52.8 ± 5.2	25.7 ± 2.7	44.3 ± 5.6	5
G652F N655D Q657E	-49.0 ± 1.3	9.1 ± 0.5	-34.9 ± 0.8	67.9	19.8 ± 2.9	48.1 ± 5.2	26.5 ± 3.7	41.3 ± 5.6	6
G658N	-49.9 ± 2.0	10.2 ± 0.7	-40.0 ± 0.0	74.2	0.7 ± 0.2	73.5 ± 2.7	0.6 ± 0.2	73.6 ± 2.7	5

Current-voltage relationships of the wild-type and mutant channels before and after application of 10 µM Tz1 were analyzed according to eqn 1 to yield V_m and the corresponding slope factor k_m. Application of Tz1 shifted channel activation by dV. P_{shift} values indicate the percentage of channels being activation-shifted and P_{block} the percentage of channels being blocked by Tz1 in the absence (–pp) or precence (+pp) of a prepulse. The P_{tox} values are the sum of P_{shift} and P_{block}, characterizing the percentage of all Tz1-modified channels.

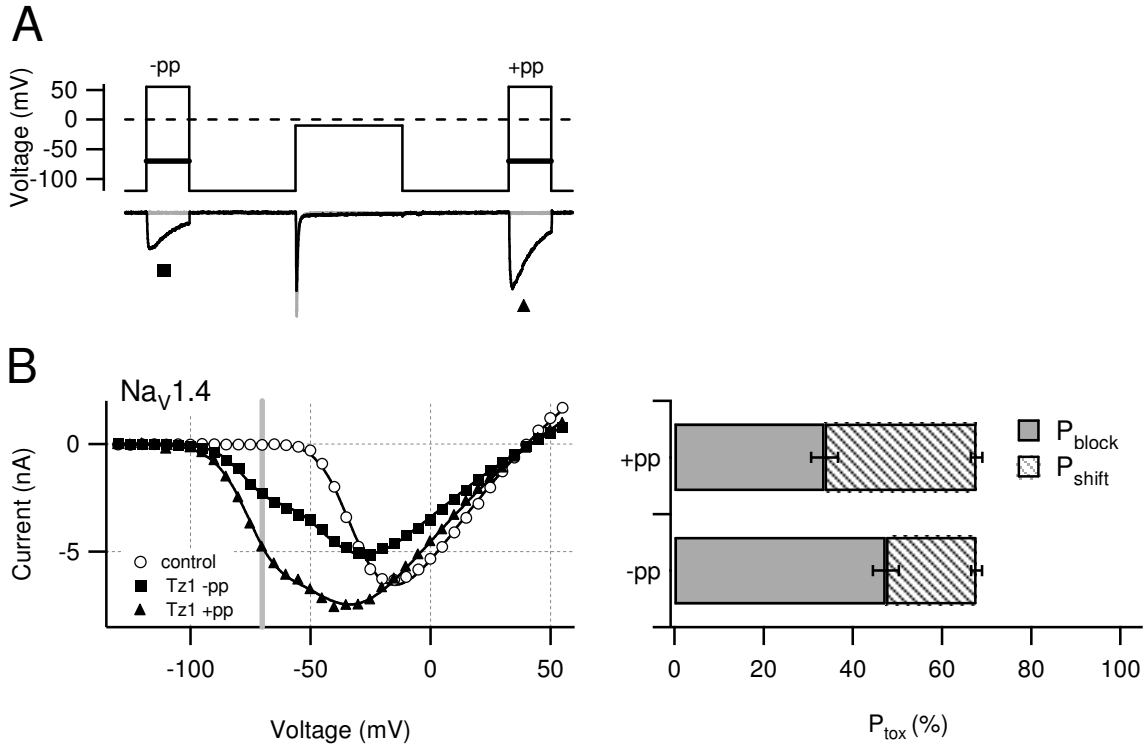
A
-pp
+pp
Voltage (mV)
50
0
-50
-100
B
Na$_V$1.4
Current (nA)
0
-5
control
Tz1 -pp
Tz1 +pp
-100
-50
0
50
Voltage (mV)
+pp
-pp
P$_{block}$
P$_{shift}$
0
20
40
60
80
100
P$_{tox}$ (%)

Figure 1

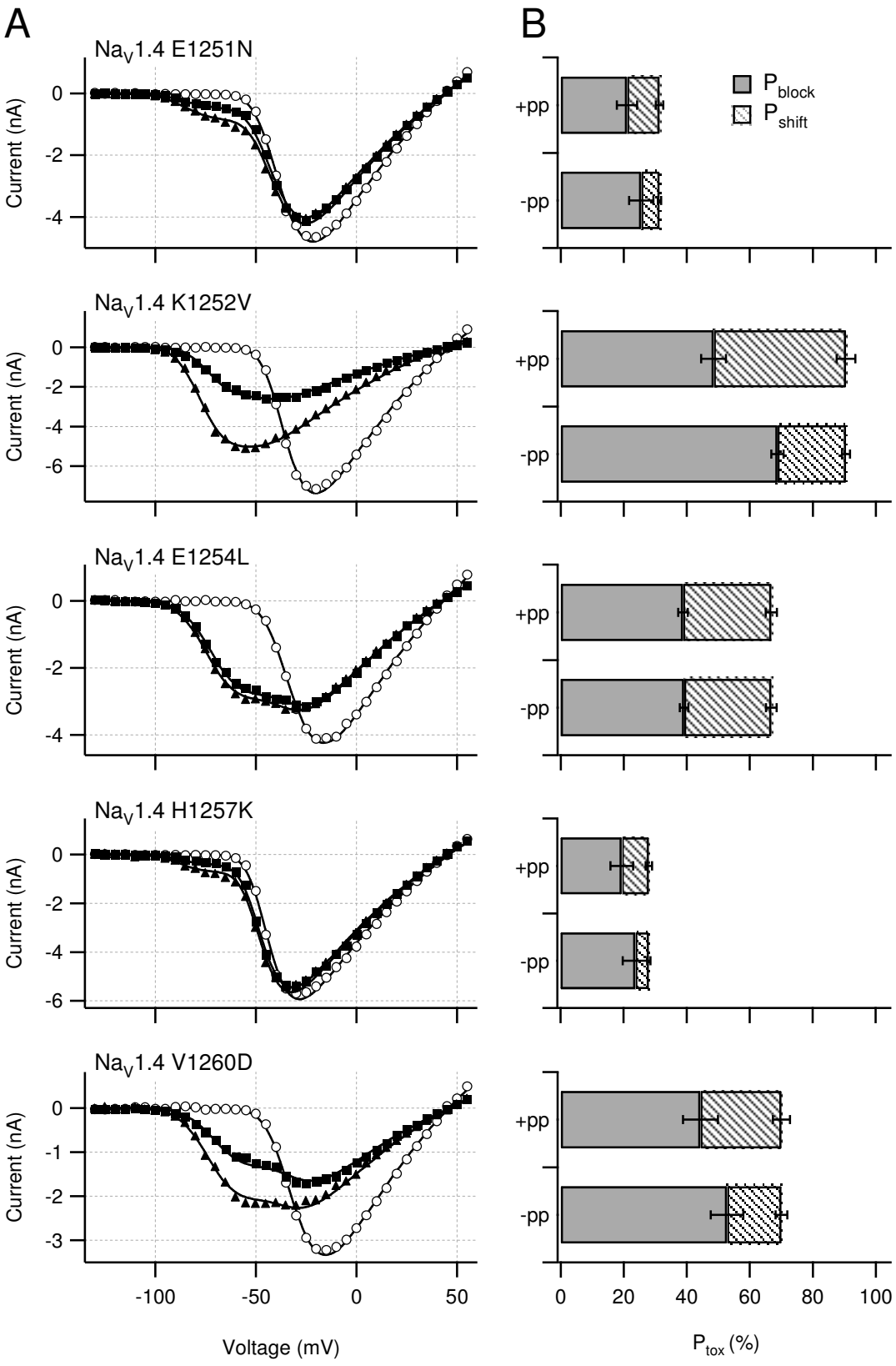
A
B
Na$_V$1.4 E1251N
Na$_V$1.4 K1252V
Na$_V$1.4 E1254L
Na$_V$1.4 H1257K
Na$_V$1.4 V1260D
Current (nA)
Voltage (mV)
P$_{block}$
P$_{shift}$
+pp
-pp
P$_{tox}$ (%)

Figure 2

$Na_V1.4$ G652F; to be measured

$Na_V1.4$ N655D; to be measured

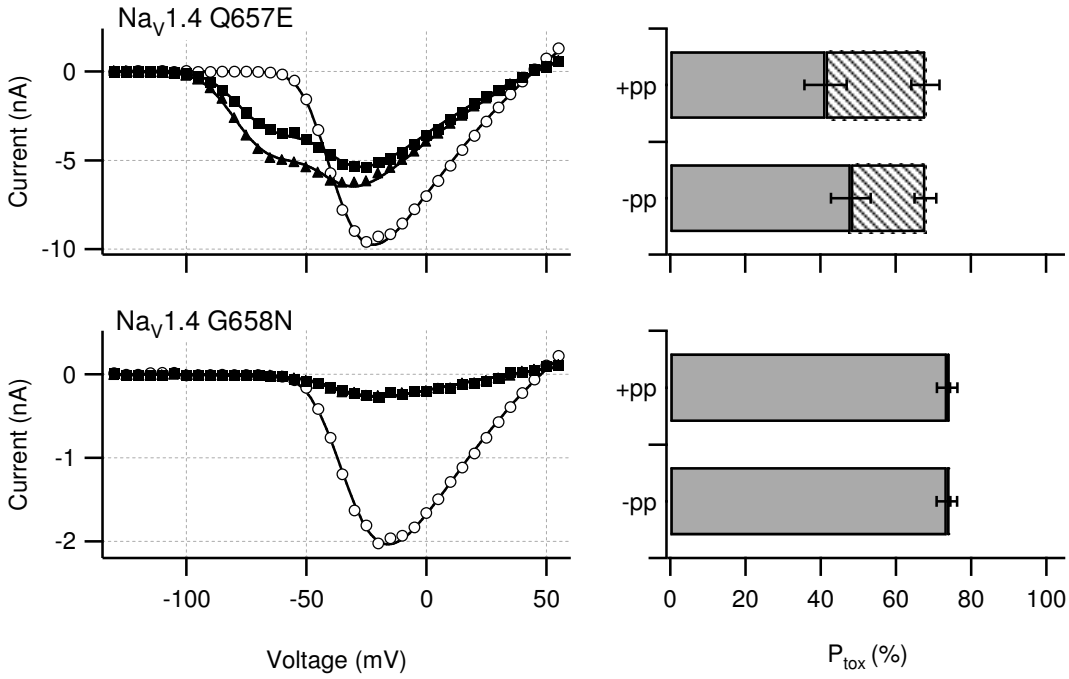

Figure 3

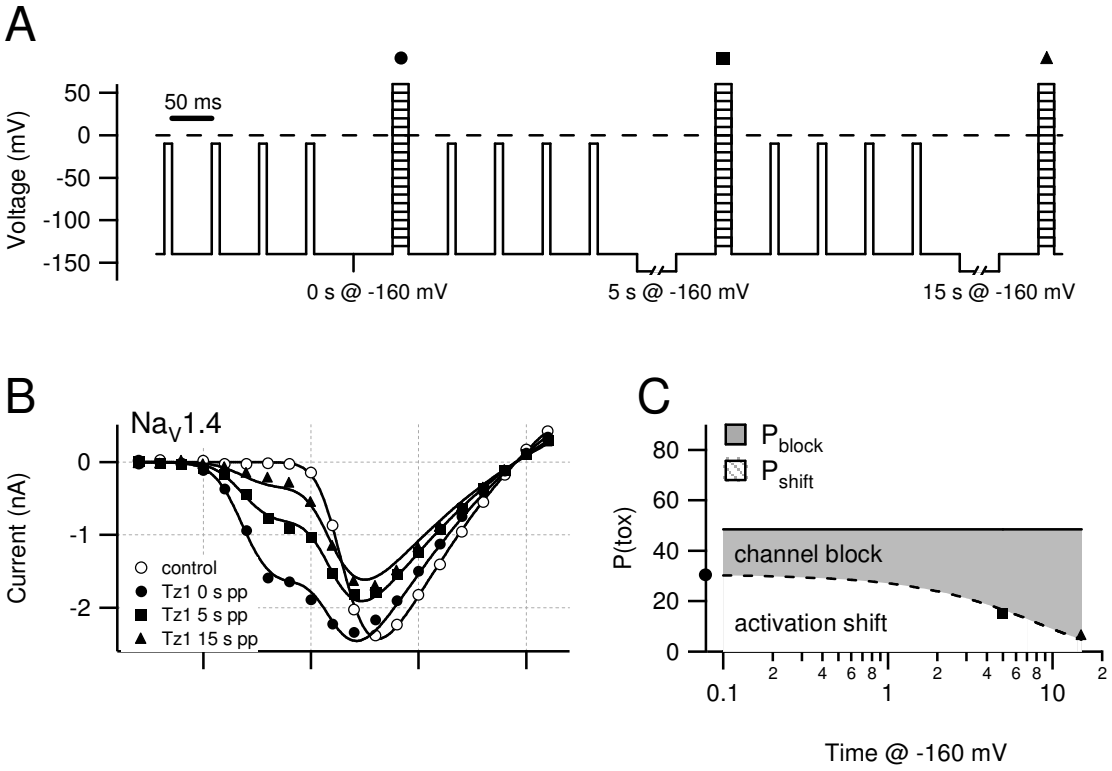
A
50 ms
Voltage (mV)
50
0
-50
-100
-150
0 s @ -160 mV
5 s @ -160 mV
15 s @ -160 mV
B
Na$_V$1.4
Current (nA)
0
-1
-2
control
Tz1 0 s pp
Tz1 5 s pp
Tz1 15 s pp
C
P$_{block}$
P$_{shift}$
P(tox)
80
60
40
20
0
channel block
activation shift
0.1
1
10
Time @ -160 mV

Figure 4

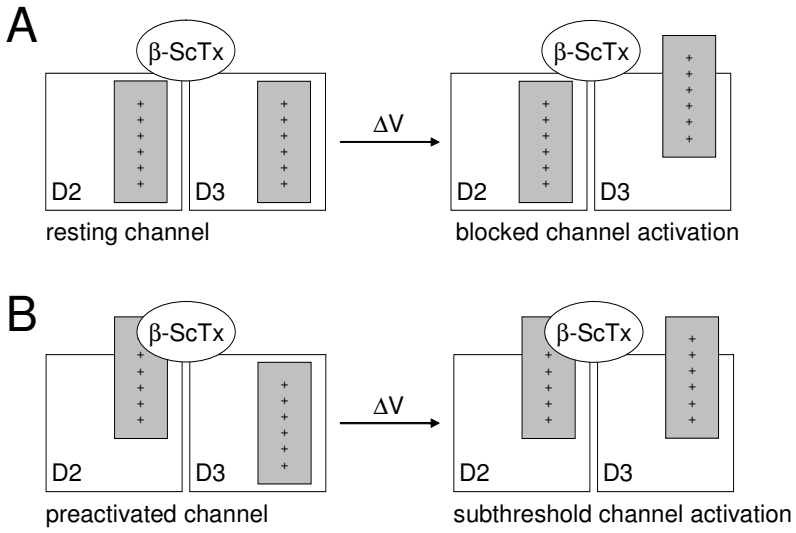
A
β-ScTx
D2
D3
ΔV
β-ScTx
D2
D3
resting channel
blocked channel activation
B
β-ScTx
D2
D3
ΔV
β-ScTx
D2
D3
preactivated channel
subthreshold channel activation

Figure 5

Manuscript for: The Journal of Neuroscience

The µO conotoxin MrVIA inhibits voltage-gated sodium channels by immobilizing the voltage sensor in domain-2.

Enrico Leipold[1], Stefan Zorn[1], Alfred Hansel[1], Baldomero M. Olivera, Heinrich Terlau, and Stefan H. Heinemann[1*]

[1] *Institute of Molecular Cell Biology,*
Research Unit "Molecular and Cellular Biophysics",
Medical Faculty of the Friedrich Schiller University Jena,
Drackendorfer St. 1, D-07747 Jena, Germany,

** address correspondence to:*

Prof. Dr. Stefan H. Heinemann
Institute of Molecular Cell Biology
Molecular and Cellular Biophysics
Friedrich Schiller University Jena
Drackendorfer St. 1
D-07747 Jena, Germany
Tel: ++49-3641-9 32 56 80
Fax: ++49-3641-9 32 56 82
e-mail: stefan.h.heinemann@uni-jena.de

Acknowledgements

This work was supported by the Deutsche Forschungsgemeinschaft HE 2993/5

Abstract

The μO-conotoxins MrVIA and MrVIB are small (32 aa) peptides from *Conus marmoreus*, belonging to the O-class of conotoxins with three disulfide bridges and a cysteine knot pattern of C-C-CC-C-C. Although these toxins are structurally related to δ-conotoxins which inhibit inactivation of voltage-gated sodium channels (Na_V channels), their primary effect is to "block" these channels similarly to μ-conotoxins of the M-class. These toxins have attracted attention because they are also potent inhibitors of TTX-insensitive $Na_V1.8$ channels and could therefore serve as lead structure for novel analgesics. Expressing $Na_V1.4$ channels and mutants thereof in mammalian cells and assaying them with the whole-cell patch-clamp method with respect to their sensitivity to MrVIA we show here that the mode of action of μO-conotoxins is clearly different to that of μ-conotoxins. Its effect is voltage- and state-dependent: The toxin effect is strongly diminished after activating the Na_V channels by depolarizing voltage steps. Employing gating charge mutations in all four voltage sensors it could be shown that alterations of the voltage sensor in domain-2 have the strongest impact on the MrVIA action. A cysteine-scan mutagenesis of the S3-S4 linker in that domain revealed that conserved residues in the linker are essential for MrVIA activity. These results, together with previous findings that the effect of MrVIA depends on the structure of the SS2 pore-loop in domain-3, suggests a functional similarity with scorpion β-toxins. In fact, MrVIA exhibits a competition with β-toxin Tz1 from *Tityus zulianus*. Thus, μO-conotoxins are voltage-sensor toxins targeting receptor site-4 on Na_V channels. They "block" Na^+ flow most likely by hindering the voltage sensor in domain-2 from activating and, hence, the channel from opening.

269 words

Introduction

The venoms of fish-hunting cone snails contain a rich repertoire of toxic peptides varying in length and the number of disulfide bridges. Conotoxins of the O-class are characterized by three disulfide bridges with the corresponding cysteine residues arranged like C-C-CC-C-C (Terlau & Olivera, 2004). O-class toxins target voltage-gated ion channels; subfamilies with several known members are ω-conotoxins blocking voltage-gated Ca^{2+} channels and δ-conotoxins removing the inactivation of voltage-gated sodium channels (Na_V channels). Currently, there is only one member described for κ-conotoxins blocking voltage-gated K^+ channels (Terlau et al., 1996). The fourths subfamily is formed by μO-conotoxins. Their name arises from their potency to inhibit Na_V channels – like μ-conotoxins, and their structural classification as O-class conotoxin. To date there are only two μO-conotoxins known: MrVIA and MrVIB, both from *Conus marmoreus* (McIntosh et al., 1995). These toxins have attracted attention because they appear to be valuable molecules to block tetrodotoxin-resistant Na_V channels in dorsal root ganglia (Daly et al., 2004) and, therefore, may serve as a lead structure for the development of novel Na_V-channel specific analgesics.

Na_V channels are glycosylated membrane proteins composed of one large pore forming α-subunit and up to two small β-subunits (for review see Catterall, 2000; Goldin, 1999). They open in response to a depolarization of the membrane potential. The resulting influx of Na^+ into the cells accentuates the depolarization and finally triggers action potentials. Therefore, Na_V channels are of prime importance for the generation and propagation of electrical signals in nerve and muscle cells. Given this physiological relevance it is not surprising that poisonous animals have developed specific toxins targeting Na_V channels. Such Na_V-channel specific toxins usually are classified according to so-called receptor sites (RS) that biochemically characterize the interaction sites the toxins occupy at the channel protein. Peptide toxins acting on Na_V channels either block the channel pore (RS1) or they interfere with the voltage-sensor elements consisting of the transmembrane segments S3/S4 of the four homologous domains of the α-subunits. Scorpion α-toxins interact with the voltage sensor in domain-4 (RS3) and cause an elimination of channel inactivation, which is coupled to that voltage sensor (Rogers et al., 1996; Leipold et al., 2004). Similarly, δ-conotoxins also inhibit Na_V channel inactivation making use of an interaction epitope at the domain-4 S3/S4 linker largely opeverlapping with that of scorpion α-toxins (originally referred to as RS6) (Leipold et al., 2005). Scorpion β-toxins interfere with RS4 constituted in part of the voltage sensor in domain-2 (Cestèle et al., 1998) and cause either channel block or a shift in the voltage-dependence of activation.

The μO-conotoxins MrVIA and MrVIB harbor 32 residues of natural amino acids and the structure of MrVIB has already been solved using NMR analysis (Daly et al., 2004). The primary action of μO-conotoxins is to inhibit Na^+ flow through Na_V channels, but thus far no receptor site could be assigned to these toxins. Functionally they are similar to μ-conotoxins that block Na_V channels by binding inside the outer pore vestibule (RS1) (Maczydlowski et al., 1986; Ohizumi et al., 1986). However, binding assays involving radioactively labeled saxitoxin (STX) revealed that MrVIA apparently does not compete with STX for RS1 (Terlau et al., 1996).

The molecular mechanism by which μO-conotoxins inhibit Na_V channels in unknown. A typical feature of δ-conotoxins and apparently also of μO-conotoxins is that they do not exhibit a marked subtype specificity when comparing their effect on various types of mammalian Na_V channels. For δ-conotoxins this was mainly attributed for the major interaction site in the domain-4 S3/S4 linker, which is conserved among mammalian Na_V channels (Leipold et al., 2005). For μO-conotoxins we previously have shown that they have a mild preference for the skeletal muscle ($Na_V1.4$) over the brain-type channel ($Na_V1.2$). Based on that difference, a systematic approach involving the construction and assay of channel chimeras revealed that the channel phenotype with respect to the block effect of MrVIA is determined by the C-terminal pore loop in domain-3 (Zorn et al., 2006). This is exactly the channel epitope determining the subtype specificity of the scorpion β-toxin Tz1 (Leipold et al., 2006).

The aim of the following study was to identify the mode of action of the μO-conotoxins MrVIA and MrVIB and to test whether or not there is a functional similarity with scorpion β-toxins acting on RS4.

Materials and Methods

Channel constructs and mutants. The wild type Na_V channels used in this study were the rat isoforms $Na_V1.2$ (X03639, Noda et al., 1986) and $Na_V1.4$ (M26643.1, Trimmer et al., 1989), the human isoforms $Na_V1.5$ (Q14524, Gellens et al., 1992) and $Na_V1.7$ (NP002968, Klugbauer et al., 1995) and the mouse channel $Na_V1.6$ (Q9WTU3, Kohrman et al., 1996). Using PCR-based site directed mutagenesis, four mutant channels were constructed in which the outermost charged residues in the four voltage sensors of $Na_V1.4$ were replaced by Cysteins (R219C, R663C, K1119C, R1441C). Furthermore, we applied a Cystein-scan-mutagenesis where we introduced mutations V649C, G652C, N655C, G658C, L659C, S660C, V661C and L662C into the S3-S4 linker in domain-2 of $Na_V1.4$. All mutants were verified by sequencing. Plasmid DNA was isolated from E. coli using the Midi- or Maxi-plasmid purification kit (Qiagen, Hilden, Germany).

Expression of Na_V channels in HEK 293 cells. HEK 293 cells (CAMR, Porton Down, Salisbury, UK) were maintained in 45% Dulbecco's Minimal Eagles Medium (DMEM) and 45% F12, supplemented with 10% fetal calf serum in a 5% CO_2 incubator at 37°C. HEK 293 cells were trypsinized, diluted with culture medium and grown in 35-mm dishes. When HEK 293 cells were grown to 30-50% confluence, transient transfection was performed using the Superfect transfection kit (Qiagen). HEK 293 cells were transfected with a 5:1 ratio of the Na_V channel expression plasmids and a vector encoding the CD8 antigen (Jurman et al., 1994). The cells were used for electrophysiological recordings 2-3 days after transfection. Dynabeads (Deutsche Dynal GmbH, Hamburg, Germany) were used for visual identification of individual transfected cells.

Electrophysiological Records. Whole-cell voltage clamp experiments were performed as described previously (Chen et al., 2000). Briefly, patch pipettes with resistances of 0.9-2.0 MΩ. were used. The series resistance was compensated for by more than 80% in order to minimize voltage errors. A patch-clamp amplifier EPC10 was operated by PatchMaster software (both HEKA Elektronik, Lambrecht, Germany). Leak and capacitive currents were corrected with a p/*n* method with a leak holding voltage of –140 mV, a leak pulse scaling factor of -0.1 and *n*=10 leak pulses. Currents were low-pass filtered at 5 kHz and sampled at a rate of 25 kHz. All experiments were performed at constant temperature 19-21°C. Data analysis was performed using IgorPro (WaveMetrics, Lake Oswego, OR, USA). All data were presented as mean ± standard error of the mean (*n* = number of independent experiments).

Solutions and toxins. The patch pipettes contained (in mM): 35, NaCl; 105, CsF; 10, EGTA; 10, Hepes (pH 7.4 with CsOH). The bath solution contained (in mM): 150 NaCl; 2 KCl, 1.5 CaCl2; 1 MgCl2; 10 Hepes (pH 7.4 with NaOH). Toxin MrVIA was diluted in bath solution containing 1 mg/ml BSA and stored at –20°C until use.The application of toxin was performed with an application pipette as described previously (Chen et al., 2000).

Current-voltage relationships. From a holding potential of –120 mV test depolarizations in the range from –80 to +60 mV in steps of 10 mV were applied at an interval of 10 s. The peak currents were fit with a Hodgkin-Huxley activation formalism involving *m*=3 activation gates and a single-channel characteristics according to Goldman-Hodgkin-Katz:

$$I_{peak} = \frac{I_{\max}}{(1+e^{-(V-V_m)/km})^3}$$

$$I_{\max} = \Gamma V \frac{1-e^{-(V-E_{rev})/25mV}}{1-e^{-V/25mV}}$$

(eq. 1)

V_m is the voltage of half-maximal gate activation and k_m the corresponding slope factor. Γ is the maximal conductance of all channels and E_{rev} the reversal potential.

Steady-state inactivation. From a holding potential of –120 mV cells were conditioned for 500 ms at voltages ranging from –140 to –30 mV in steps of 10 mV. Subsequently, peak current was determined at 0 mV. The repetition interval was 10 s. The peak current plotted versus the conditioning voltage was described with a Boltzmann function:

$$I(V) = \frac{I_{\min}}{1 + e^{-(V - V_h)/k_h}}$$

(eq. 2)

with the half-maximal inactivation voltage V_h and the corresponding slope factor k_h that indicates the voltage dependence of steady-state fast inactivation.

Depolarization-induced loss of toxin effect. From a holding potential of –140 mV the peak current amplitude was measured 40 ms before and after a +40 mV depolarizing pulse of various lengths. The repetition interval was 60 s. The ratio $I_{peak\ after}$ / $I_{peak\ before}$ gives an estimate of the probability for the channels not to be blocked by the toxin. The kinetics of depolarization-induced loss of toxin effect was calculated by describing $I_{peak\ after}$ / $I_{peak\ before}$ as a single exponential function of the depolarization duration:

$$\frac{I_{peak\ after}}{I_{peak\ before}} = A e^{\frac{-t_{depol}}{\tau_{off}}}$$

(ep. 3)

where t_{depol} is the duration of the depolarizing pulse and τ_{off} is the time constant of depolarization-induced loss of the toxin effect under these conditions.

Non-stationary noise analysis. Single-channel parameters were analyzed essentially as described previously (Starkus et al., 2003), In brief, from a holding voltage of –120 mV six 10-ms pulses (0, –140, –20, –90, –30, –40 mV, separated by 10-ms intervals at –120 mV) were repetitively applied 200 times. Currents obtained for steps to –90 and –140 mV were used for leak correction. With this protocol data for complete single-channel current-voltage characteristics were recorded simultaneously using a minimum of time. Compilation of non-stationary ensemble currents (I) and variances (σ^2) was performed for

each voltage (*V*) with and without toxin application according to Heinemann & Conti (1992) and Steffan & Heinemann (1997) using PulseTools software (HEKA Elektronik). Mean current and variance of the inactivating phases of the current signals were then simultaneously analyzed in IgorPro (WaveMetrics) for various voltages. For the simultaneous fits of entire data sets according to eq. (1) the total number of channels (*N*) was assumed to be the same for all traces. Thus, for four voltages the simultaneous fitting reduced the number of free parameters (single-channel current *i*, *N*) from 8 to 5.

$$\sigma^2 (V) = i(V)\, I(V) - I(V)^2 / N \qquad (1)$$

The maximal open-probability (P_{open}) was estimated from the fit results and the maximal ensemble current *I*.

Results

Effect of µO-conotoxins on various mammalian Na_V channel types.

It was already shown previously (Zorn et al., 2006) that MrVIA and B block the skeletal muscle sodium channel ($Na_V1.4$) slightly better the brain ($Na_V1.2$) sodium channel. This difference was attributed to differences in the C-terminal pore-loop of domain-3. As the situation might be different for other channel types we also assayed the block induced by 800 nM MrVIA on the cardiac ($Na_V1.5$) and two neuronal ($Na_V1.6$ and $Na_V1.7$) channels.

Results: xxx.

This corroborates the previous indications that µO-conotoxins do not discriminate well between mammalian sodium channels not providing a definite clue regarding the molecular mode of action.

Comparison of the effect of µ- and µO-conotoxins.

µO-conotoxins show structural similarity to δ-conotoxins, but are functionally more similar to µ-conotoxins. Our previous findings (Zorn et al., 2006) indicate that µO-conotoxins utilize the SS2-loop of domain-3 for interacting with Na_V channels. In a way, this is similar to µ-conotoxins, which also interact with the pore loops (Chahine et al., 1998). Although former results by Terlau et al. (1996) suggest that the µO-conotoxin MrVIA does not interact with Na_V channels via receptor site-1, we first examined the functional differences between MrVIA and the µ-conotoxin GIIIA on the functional level.

Both toxins inhibit current flow through $Na_V1.4$ channels (Yanagawa et al., 1987 and Zorn et al., 2006). Based on whole-cell ensemble data one cannot easily infer about the

underlying mechanisms. Measurement and analysis of non-stationary current fluctuations should provide information on the toxin effect on the single-channel current (*i*), the number of available channels (*N*), and the maximally obtained open probability (P_o). Thus, we measured current and ensemble variance of $Na_V1.4$ currents in HEK 293 cells under control conditions and after application of either 2 µM GIIIA or 800 nM MrVIB. In both cases the current amplitude is reduced to about 30% and the scaled-up current waveforms after toxin application match those of the control records, indicating no strong effects on channel activation and inactivation (Fig. 1A, Fig. 2A). Simultaneous analysis of the non-stationary noise signals (Fig. 1B, Fig. 2B) for multiple voltages (see METHODS) provided reliable estimates on *i*, *N*, and P_o. As shown in Fig. 1C-E, GIIIA did not affect the single-channel current amplitudes, neither did it affect P_o. The current-reducing effect of this toxin can be attributed completely to a reduction of *N*, the number of channels available. This result can be interpreted as a binding of GIIIA in the channel pore (receptor site-1), strong enough to keep the channel blocked in between the recording of successive data sweeps. The situation is different for MrVIB (Fig. 2C-E): Here the single-channel current is not affected either but the current reduction is accounted for by a concomitant decrease of *N* and P_o. The effect of MrVIB on P_o increases with the strength of depolarization. This indicates that the toxin prevents the channels from opening, i.e. suggests an effect of MrVIB on channel gating. Somewhere we have to put the statistics of the noise analysis.

Voltage dependent toxin dissociation.

Gating-modifying toxins are rather common. For instance, α-toxins and β-toxins from scorpions interact with the voltage sensor elements or Na_V channel domains 4 and 2, respectively (refs). Both toxins show some kind of use-dependence: The effect of scorpion α-toxins (e.g. Chen et al., 1999) and δ-conotoxins (Leipold et al., 2005) vanishes when channels are subjected to strong depolarizations. For β-toxins the opposite mechanism seems to hold as the shift in voltage-dependent activation is pronounced after channel activation (Cestèle et al., 1998). Therefore we examined the ability of MrVIA to block $Na_V1.4$ channels in dependence of prepulse depolarizations. As shown in Fig. 3, the toxin effect, i.e. the block of Na^+ currents, can be removed when the test pulse is preceded by a depolarization that opens the channels. Increasing durations of the depolarization increasingly removes the effect; the time course can be described with single-exponential functions. Such time constants, plotted as a function of prepulse potential, are shown in Fig. 3X. The continuous curve indicates a single-exponential fit characterizing a voltage dependence equivalent to the translocation of x elementary charges across the transmembrane electric field. These results clearly show that the action of MrVIA is

affected by the gating of $Na_V1.4$ channels. The use-dependent nature is highly suggestive of a voltage-sensor toxin mechanism.

Analysis of voltage-sensor mutants.

The experiments shown thus far suggest that the voltage-dependent activation of at least one of the four voltage sensors of the Na_V channel results in a lowering of the MrVIA affinity to the channel protein, in effect transiently reducing its blocking efficacy. A systematic alteration of the voltage sensor structures might therefore help to identify the relevant voltage sensor. We therefore replaced the outermost charged residues of the S4 segments in all four domains separately by cysteine residues and assayed these mutants for the block effect of 800 nM MrVIA and the time constant of toxin dissociation at +40 mV. As shown in Fig. X alteration of neither the voltage sensor in domain-1 nor domain-4 appreciable modifies the activity of MrVIA. Domain-3: xxx. Domain-2: xxx. These results highlight the voltage-sensor of domain-2 as the major source for the voltage dependence of MrVIA action.

Analysis of the domain-2 S3/S4 linker.

The weak subtype specificity of µO-conotoxins for mammalian Na_V channels suggests that non-conserved residues in the voltage-sensor element of domain-2 may not be important for the toxin interaction. We therefore subjected the domain-2 S3/S4 linker (Fig. XA) to a cysteine scanning analysis, introducing cysteine residues starting from position xxxx to xxxx, i.e. one residue before the first positive charge in the voltage sensor. The mutants were expressed in HEK 293 cells and assayed with respect to the block effect of 800 nM MrVIA. While the wild-type channel $Na_V1.4$ is blocked by about 80%, xxx.

Competition with scorpion β-toxins.

The dependence of the action of µO-conotoxins on the voltage sensor in domain-2 (this study) and the pore loop of domain-3 (Zorn et al., 2006) is reminiscent of the interaction pattern of scorpion β-toxins with Na_V channels. To test whether µO-conotoxins functionally interact with scorpion β-toxins we measured the effect of 800 nM MrVIA and 20 µM of Tz1 (from *Tityus zulianus*) on $Na_V1.4$ channels, alone and in combination. Tz1 strongly shift the voltage dependence of channel activation causing robust current responses at subthreshold voltages (here –70 mV). 800 nM MrVIA under control conditions blocks 80% of the current. In combination: xxx

Depending on the outcome we may have to do some experiments with the cysteine mutants and Tz1.

Discussion

Subtype specificity of μO-conotoxins: inferences for NaV1.8?

μO-conotoxins are voltage-sensor toxins.

Competition with scorpion b-toxins, site-4 toxins.

Comparison with the couple α/δ-toxins: 180° rotational symmetry.

References

Catterall, W. A. (2000). From ionic currents to molecular mechanisms: the structure and function of voltage-gated sodium channels. Neuron *26*, 13-25.

Cestele, S., Qu, Y., Rogers, J. C., Rochat, H., Scheuer, T., and Catterall, W. A. (1998). Voltage sensor-trapping: enhanced activation of sodium channels by beta-scorpion toxin bound to the S3-S4 loop in domain II. Neuron *21*, 919-931.

Chahine, M., Sirois, J., Marcotte, P., Chen, L., and Kallen, R. G. (1998). Extrapore residues of the S5-S6 loop of domain 2 of the voltage-gated skeletal muscle sodium channel (rSkM1) contribute to the mu-conotoxin GIIIA binding site. Biophys J *75*, 236-246.

Chen, H., Gordon, D., and Heinemann, S. H. (2000). Modulation of cloned skeletal muscle sodium channels by the scorpion toxins Lqh II, Lqh III, and Lqh alphaIT. Pflugers Arch *439*, 423-432.

Daly, N. L., Ekberg, J. A., Thomas, L., Adams, D. J., Lewis, R. J., and Craik, D. J. (2004). Structures of muO-conotoxins from Conus marmoreus. I nhibitors of tetrodotoxin (TTX)-sensitive and TTX-resistant sodium channels in mammalian sensory neurons. J Biol Chem *279*, 25774-25782.

Gellens, M. E., George, A. L., Jr., Chen, L. Q., Chahine, M., Horn, R., Barchi, R. L., and Kallen, R. G. (1992). Primary structure and functional expression of the human cardiac tetrodotoxin-insensitive voltage-dependent sodium channel. Proc Natl Acad Sci U S A *89*, 554-558.

Goldin, A. L. (1999). Diversity of mammalian voltage-gated sodium channels. Ann N Y Acad Sci *868*, 38-50.

Jurman, M. E., Boland, L. M., Liu, Y., and Yellen, G. (1994). Visual identification of individual transfected cells for electrophysiology using antibody-coated beads. Biotechniques *17*, 876-881.

Klugbauer, N., Lacinova, L., Flockerzi, V., and Hofmann, F. (1995). Structure and functional expression of a new member of the tetrodotoxin-sensitive voltage-activated sodium channel family from human neuroendocrine cells. Embo J *14*, 1084-1090.

Kohrman, D. C., Smith, M. R., Goldin, A. L., Harris, J., and Meisler, M. H. (1996). A missense mutation in the sodium channel Scn8a is responsible for cerebellar ataxia in the mouse mutant jolting. J Neurosci *16*, 5993-5999.

Leipold, E., Hansel, A., Borges, A., and Heinemann, S. (2006). Subtype specificity of scorpion {beta}-toxin Tz1 interaction with voltage-gated sodium channels is determined by the pore loop of domain-3. Mol Pharmacol.

Leipold, E., Hansel, A., Olivera, B. M., Terlau, H., and Heinemann, S. H. (2005). Molecular interaction of delta-conotoxins with voltage-gated sodium channels. FEBS Lett *579*, 3881-3884.

Leipold, E., Lu, S., Gordon, D., Hansel, A., and Heinemann, S. H. (2004). Combinatorial interaction of scorpion toxins Lqh-2, Lqh-3, and LqhalphaIT with sodium channel receptor sites-3. Mol Pharmacol *65*, 685-691.

McIntosh, J. M., Hasson, A., Spira, M. E., Gray, W. R., Li, W., Marsh, M., Hillyard, D. R., and Olivera, B. M. (1995). A new family of conotoxins that blocks voltage-gated sodium channels. J Biol Chem *270*, 16796-16802.

Moczydlowski, E., Olivera, B. M., Gray, W. R., and Strichartz, G. R. (1986). Discrimination of muscle and neuronal Na-channel subtypes by binding competition between [3H]saxitoxin and mu-conotoxins. Proc Natl Acad Sci U S A *83*, 5321-5325.

Noda, M., Ikeda, T., Suzuki, H., Takeshima, H., Takahashi, T., Kuno, M., and Numa, S. (1986). Expression of functional sodium channels from cloned cDNA. Nature *322*, 826-828.

Ohizumi, Y., Nakamura, H., Kobayashi, J., and Catterall, W. A. (1986). Specific inhibition of [3H] saxitoxin binding to skeletal muscle sodium channels by geographutoxin II, a polypeptide channel blocker. J Biol Chem *261*, 6149-6152.

Rogers, J. C., Qu, Y., Tanada, T. N., Scheuer, T., and Catterall, W. A. (1996). Molecular determinants of high affinity binding of alpha-scorpion toxin and sea anemone toxin in the S3-S4 extracellular loop in domain IV of the Na+ channel alpha subunit. J Biol Chem *271*, 15950-15962.

Starkus, J. G., Varga, Z., Schonherr, R., and Heinemann, S. H. (2003). Mechanisms of the inhibition of Shaker potassium channels by protons. Pflugers Arch *447*, 44-54.

Terlau, H., and Olivera, B. M. (2004). Conus venoms: a rich source of novel ion channel-targeted peptides. Physiol Rev *84*, 41-68.

Terlau, H., Shon, K. J., Grilley, M., Stocker, M., Stuhmer, W., and Olivera, B. M. (1996). Strategy for rapid immobilization of prey by a fish-hunting marine snail. Nature *381*, 148-151.

Trimmer, J. S., Cooperman, S. S., Tomiko, S. A., Zhou, J. Y., Crean, S. M., Boyle, M. B., Kallen, R. G., Sheng, Z. H., Barchi, R. L., Sigworth, F. J., and et al. (1989). Primary structure and functional expression of a mammalian skeletal muscle sodium channel. Neuron *3*, 33-49.

Yanagawa, Y., Abe, T., and Satake, M. (1987). Mu-conotoxins share a common binding site with tetrodotoxin/saxitoxin on eel electroplax Na channels. J Neurosci *7*, 1498-1502.

Zorn, S., Leipold, E., Hansel, A., Bulaj, G., Olivera, B. M., Terlau, H., and Heinemann, S. H. (2006). The muO-conotoxin MrVIA inhibits voltage-gated sodium channels by associating with domain-3. FEBS Lett *580*, 1360-1364.

Figure legends

Figure 1. Subtype specificity.

Figure 2. Noise analysis of $Na_V1.4$ block by GIIIA and MrVIA/B.

100 nM GIIIA:

(A) Current responses (top) and ensemble variances (bottom) for the indicated test depolarizations under control conditions (black) and after application of 100 nM GIIIA (red).

The traces are averages of 200 data sweeps. The blue traces (top) are scaled-up versions of the toxin traces to match the peak current of the controls. (B) Variance vs current plots for the indicated voltages obtained from the inactivating phases of the current signals shown in (A). The continuous curves are the results of a simultaneous data fit to the entire data set according to eq. (1). (C-E) Results of the non-stationary noise analysis as a function of test voltage: (C) single-channel current, *i*, (D) maximal open probability, P_{open}, and (E) ratios of the peak current and P_{open} in the presence of toxin with respect to the control. Straight lines connect the data points.

800 nM MrVIB

(A) Current responses (top) and ensemble variances (bottom) for the indicated test depolarizations under control conditions (black) and after application of 800 nM MrVIB (red). The traces are averages of 200 data sweeps. The blue traces (top) are scaled-up versions of the toxin traces to match the peak current of the controls. (B) Variance vs current plots for the indicated voltages obtained from the inactivating phases of the current signals shown in (A). The continuous curves are the results of a simultaneous data fit to the entire data set according to eq. (1). (C-E) Results of the non-stationary noise analysis as a function of test voltage: (C) single-channel current, *i*, (D) maximal open probability, P_{open}, and (E) ratios of the peak current and P_{open} in the presence of toxin with respect to the control. Straight lines connect the data points.

Figure 3. Prepulse dependent toxin removal: $Na_V1.4$ and MrVIA

(A) *Left,* A single pulse to –20 mV was used to record the steady state block of MrVIA and GIIIA. *Right,* Pulse protocol to assay the kinetics of the depolarization-dependent toxin removal. The center pulse was given for variable durations. (B) Current traces in the presence of 400 nM MrVIA for the indicated pulse protocols. The continuous red line represents a single exponential function which was fit to the peak currents and describes the kinetics of the prepulse-dependent toxin removal. (C) Offrate at –40 mV.

Figure 4. S4 mutants.

(A) Example offrate experiment for wild-type $Na_V1.4$ channels and mutants R663C and K1119C (mutants R219C and R1441C need to be measured) in presence of 400 nM MrVIA. The normalized peak currents are plotted as a function of the conditioning time for

a conditioning potential of +40 mV. The continuous lines describe the single exponential removal of the toxin effect. (B) The time constants of toxin removal are plotted as a function of the conditioning potential. Data for R219C and R1441C need to added.

Figure 5. Mutants in S3/4 of domain-2 (conserved region?)

Figure 6. Competition with β-toxins

Figure 7. Cartoon

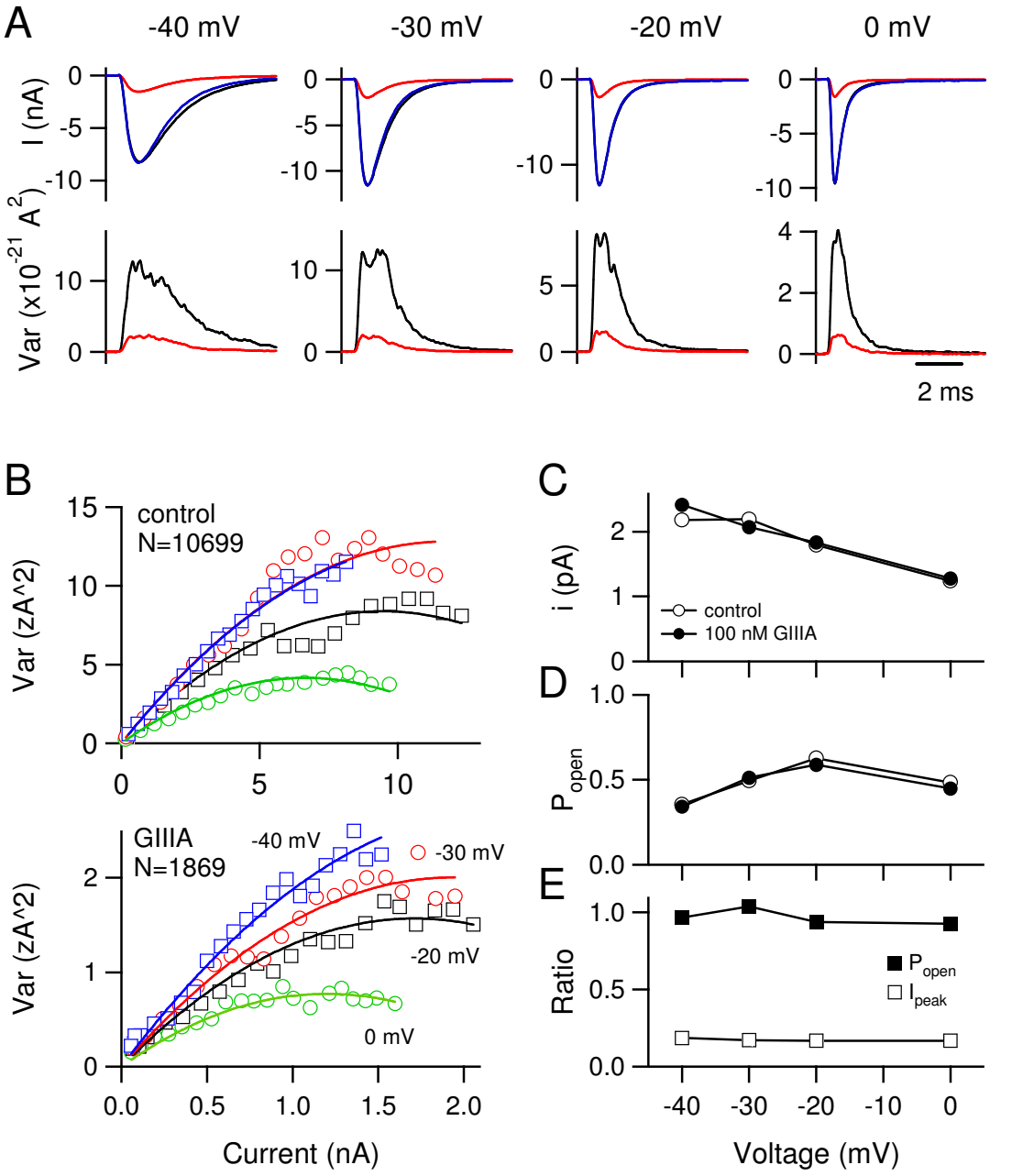

Figure 02
100 nM GIIIA

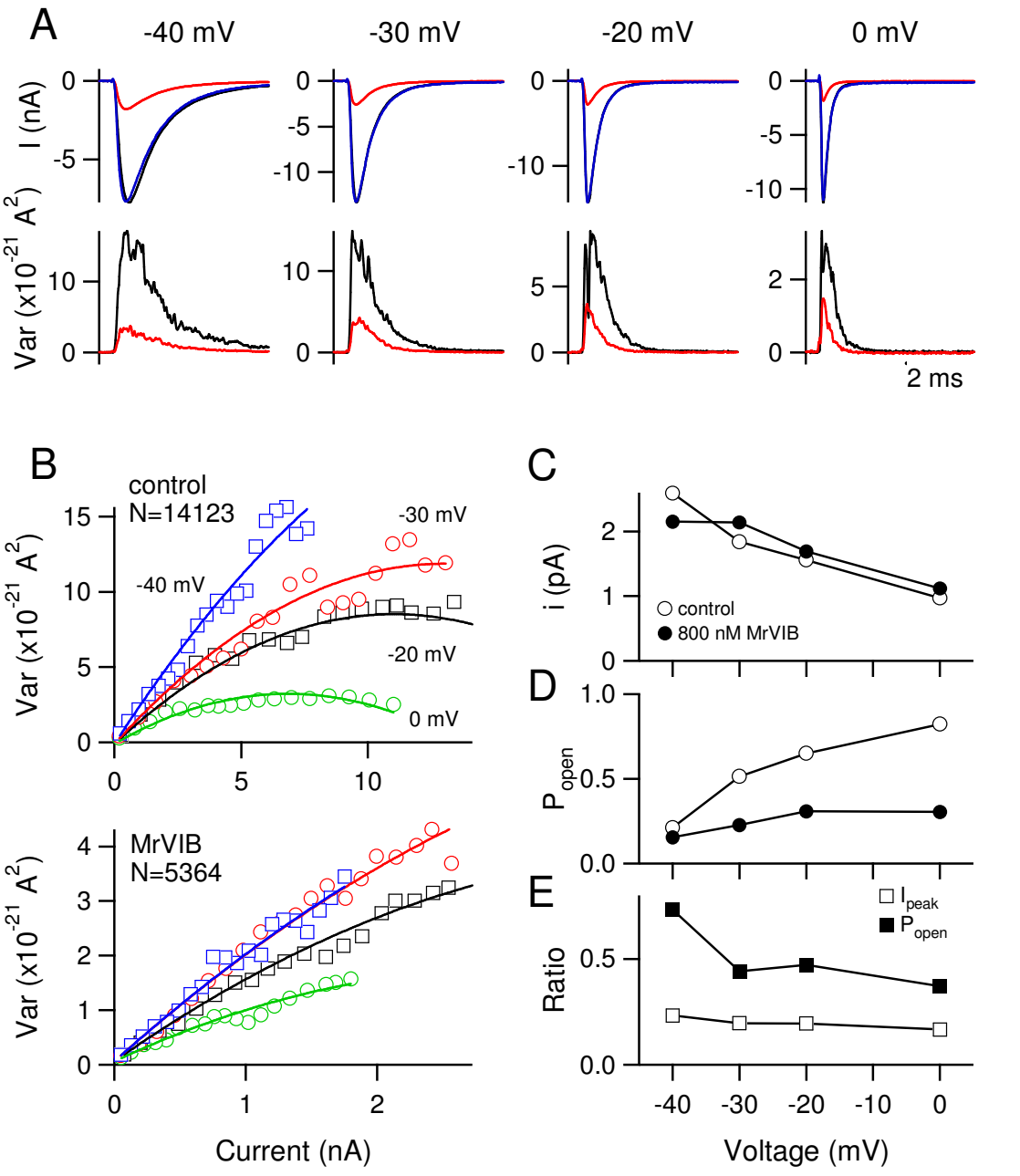

Figure 02
800 nM MrVIB

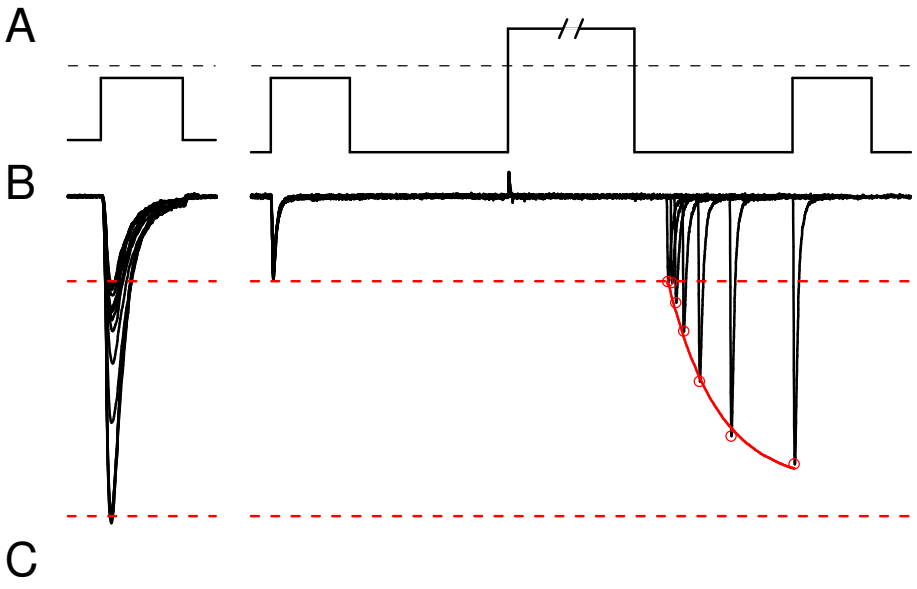

GIIIA need to be measured

Figure 3

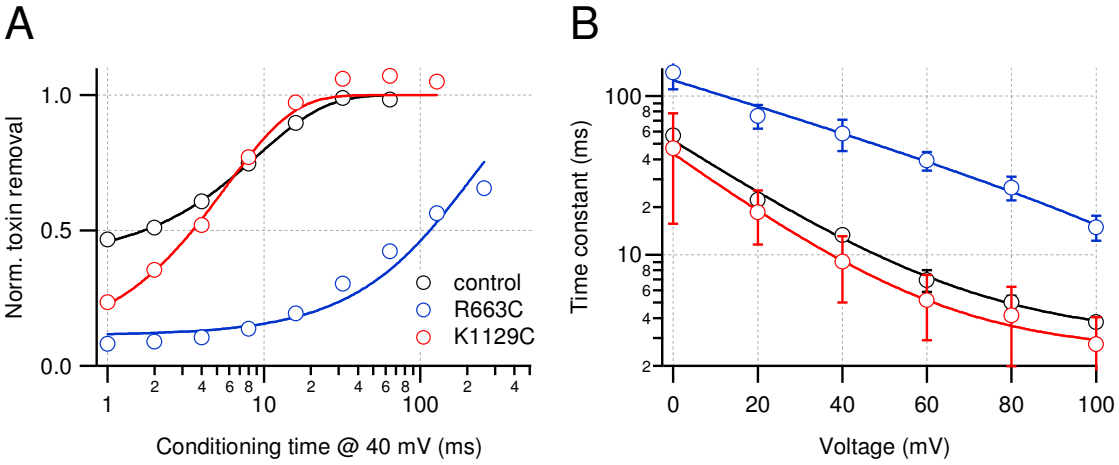
A
B
Norm. toxin removal
1.0
0.5
0.0
control
R663C
K1129C
Conditioning time @ 40 mV (ms)
Time constant (ms)
100
10
0
20
40
60
80
100
Voltage (mV)

Figure 4

4. Diskussion

4.1 Verwendete Methodik

Um die komplexen Wirkungen der Skorpion-α- und -β-Toxine sowie der δ- und μO-Conotoxine auf Säuger-Na_V-Kanäle untersuchen und verstehen zu können, bedarf es sowohl molekularbiologischer Methoden als auch präziser funktioneller Untersuchungen. Um besonders hoch aufgelöste funktionelle Daten zu erhalten, wurde die Wirkung dieser Toxine auf verschiedene Säuger-Na_V-Kanäle mit Hilfe der Ganzzell-Patch-Clamp-Technik (Hamill et al., 1981) untersucht. Dieser elektrophysiologische Ansatz ermöglicht nicht nur das systematische Studium der Toxinwirkung auf verschiedene Na_V-Kanalsubtypen, sondern schafft gleichzeitig standardisierte Untersuchungsbedingungen. Die humane Zelllinie HEK293 (**h**uman **e**mbrionic **k**idney) diente dabei als Expressionssystem für die untersuchten Na_V-Kanäle. Die Zellen wurden hierfür mit Kanal-kodierenden Plasmiden transient transfiziert. Um eine Identifikation Kanal-exprimierender Zellen zu ermöglichen, wurde zudem ein CD8-kodierendes Plasmid cotransfiziert (Jurman et al., 1994). Beads, beschichtet mit anti-CD8-Antikörpern, konnten somit spezifisch Zellen markieren, die neben CD8 auch Na_V-Kanäle exprimierten.

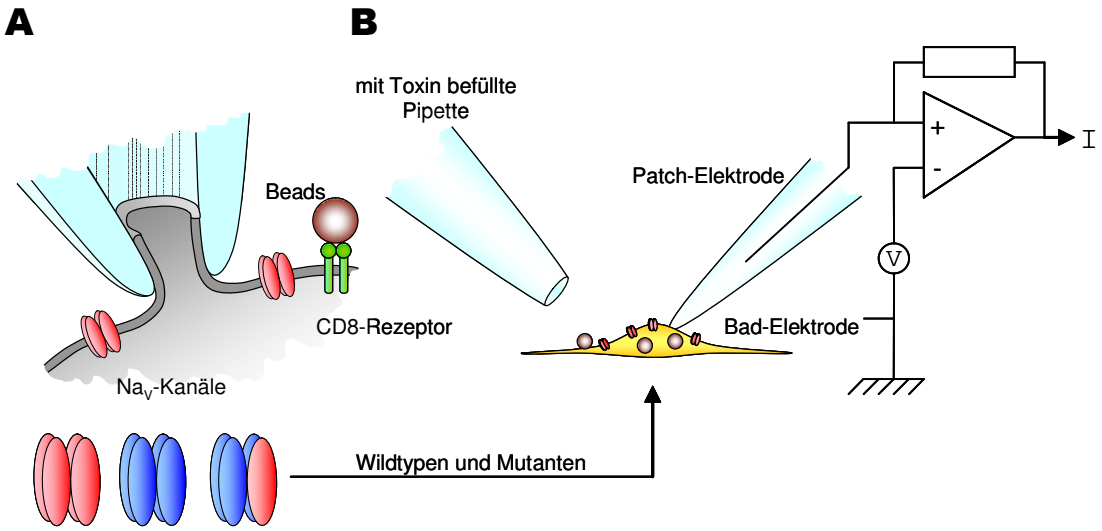

Abb. 5: Patch-Clamp-Technik. **(A)** In der Ganzzell-Konfiguration hat die Elektrode in der Patchpipette (Patch-Elektrode) Zugang zum Zellinneren. HEK293-Zellen wurden mit Plasmiden transfiziert, welche für Na_V-Kanalwildtypen oder -mutanten codierten. Ein CD8-kodierendes Plasmid wurde cotransfiziert. **(B)** Die Kanal-exprimierenden Zellen (gelb) wurden mittels anti-CD8-beschichteter Beads identifiziert und in Abwesenheit sowie Gegenwart der verschiedenen Toxine elektrophysiologisch untersucht.

Die in Abbildung 5 skizzierte Patch-Clamp-Technik ermöglicht die Messung von Änderungen der Membranleitfähigkeit von Zellen und wurde zur Untersuchung der Effekte von Skorpion-α- und -β-Toxinen sowie δ- und μO-Conotoxinen auf Na_V-Kanäle eingesetzt. Die Membran der zu untersuchenden Zelle wird dazu mit einer Glaspipette angesaugt und, mittels Unterdruck in der Pipette, an dieser Stelle durchbrochen. Die Verbindung zwischen Zellmembran und Pipette schließt dabei dicht ab. Somit entsteht für die Pipettenelektrode ein direkter Zugang zum Zellinneren. Eine zweite Elektrode befindet sich außerhalb der Zelle im extrazellulären Medium (Badelektrode). Über beide Elektroden werden mit Hilfe eines computergesteuerten Patch-Clamp-Verstärkers Spannungungspulse appliziert, welche unterschiedliche Membranpotentiale in der Zellmembran erzeugen. Die Spannungssensoren der Na_V-Kanäle übersetzen dabei die Änderungen des Membranpotentials in Konformationsänderungen, die zum Öffnen, Schließen und Inaktivieren der Kanäle führen. Auf diese Weise gewonnene Stromantworten spiegeln somit die Aktivität aller Kanäle der untersuchten Zelle direkt wider. Eine zweite Glaspipette wurde mit Toxinlösung befüllt und diente zur Applikation der verschiedenen Toxine auf die untersuchten Zellen (Chen et al., 2000). Der Vorteil dieser lokalen Applikation besteht darin, dass nur geringste Mengen der begrenzt verfügbaren Toxine eingesetzt werden müssen. Die Toxinpipette wird zudem von einem Manipulator gesteuert und kann bei Bedarf direkt vor die untersuchte Zelle platziert werden. Dadurch ist es möglich, die Kanäle einer Zelle, sowohl in Abwesenheit als auch in Gegenwart von Toxinen, funktionell zu untersuchen.

Kanäle mit gezielt veränderter Aminosäuresequenz sind eine entscheidende Voraussetzung nicht nur zur Identifikation der für die Toxinwirkung verantwortlichen Kanalbereiche, sondern auch für die Aufklärung der komplexen Toxinmechanismen auf molekularer Ebene. Deshalb wurden mit Hilfe der PCR-basierten DNA-Mutagenese Na_V-Kanalchimären zwischen Toxin-sensitiven und Toxin-insensitiven Kanälen erzeugt. Weil sich $Na_V1.4$ als besonders sensitiv für alle untersuchten Toxine erwies, wurde dieser Kanal als Mutationshintergrund verwendet. Abbildung 6 veranschaulicht die Vorgehensweise. Es wurden sowohl vollständige Domänen aus $Na_V1.2$ (Abb. 6A) als auch einzelne extrazelluläre Linker sowie einzelne Aminosäuren aus verschiedenen Kanälen (Abb. 6B) in $Na_V1.4$ eingesetzt (Zorn et al. 2006; Leipold et al., 2006a, 2006b, 2006c). Diese Strategie ermöglichte in Verbindung mit elektrophysiologischen Untersuchungen die schrittweise Identifikation unbekannter Interaktionstellen mit den Toxinen auf molekularer Ebene sowie die Aufklärung der Wirkmechanismen der δ- und μO-Conotoxine.

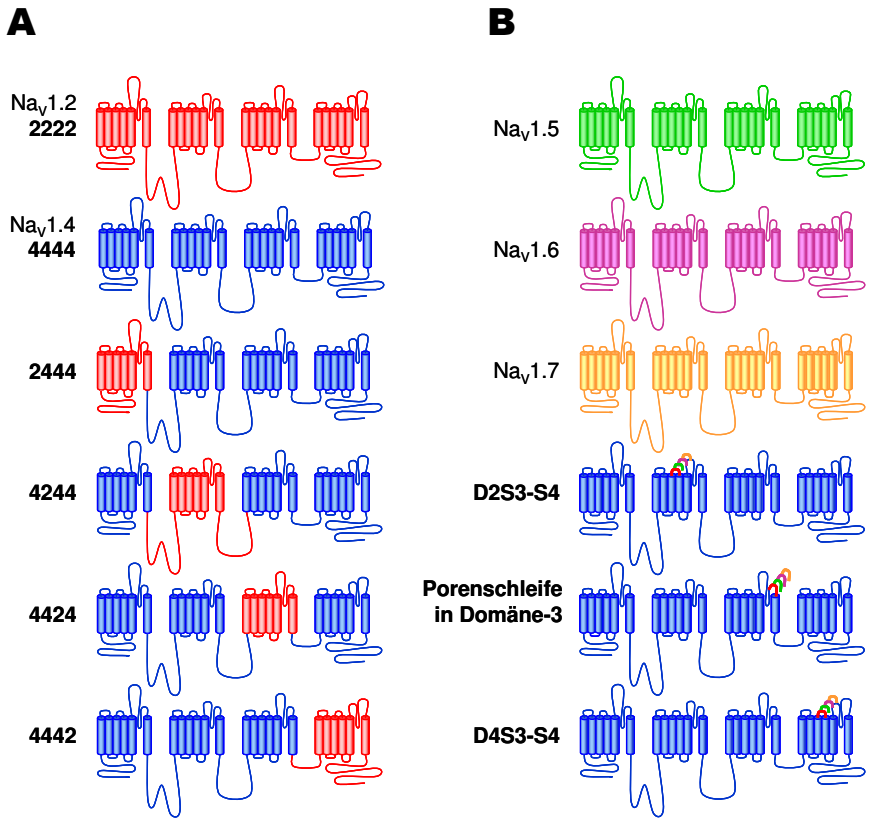

Abb. 6: Herstellung von Na$_V$-Kanalchimären und -mutanten mittels PCR-basierter DNA-Mutangenese (Zorn et al., 2006; Leipold et al., 2006a, 2006b, 2006c). **(A)** Es wurden vier Chimären erzeugt, in denen jeweils eine der vier homologen Domänen aus Na$_V$1.2 (2222) in Na$_V$1.4 (4444) eingesetzt wurde. In Verbindung mit elektrophysiologischen Messungen ermöglichen diese Chimären eine systematische Suche nach Kanaldomänen, welche die Wirkung Na$_V$-Kanal-spezifischer Toxine vermitteln. **(B)** Mutagenese der Linker D2S3-S4 und D4S3-S4 sowie des C-terminalen Bereichs der D3-Porenschleife. Um die Interaktionsstellen der Toxine an Na$_V$-Kanälen genauer zu bestimmen, wurden zudem sowohl vollständige extrazelluläre Linker als auch einzelne Aminosäuren dieser Linker aus verschiedenen Na$_V$-Kanälen in Na$_V$1.4 eingesetzt.

4.2 Skorpion-α-Toxine wirken über eine Interaktion mit dem Spannungssensor in Domäne-4 von Na$_V$-Kanälen

Neben der identischen Wirkung auf Na$_V$-Kanäle verbindet Skorpion-α- und δ-Conotoxine die Eigenschaft, oftmals nur auf bestimmte Na$_V$-Kanalsubtypen zu wirken. Im Falle der α-Toxine gibt es bereits Hinweise auf den zugrunde liegenden Mechanismus. Rogers et al. (1996) untersuchten die Effekte des α-Toxins LqTx aus *Leiurus quinqestriatus quinqestriatus* auf die Kanäle Na$_V$1.2 und Na$_V$1.5. Ersetzten sie den Linker D4S3-S4 im LqTx-sensitiven Na$_V$1.2 durch den homologen Linker aus dem LqTx-insensitiveren Na$_V$1.5, übertrugen sie damit auch den LqTx-Phänotyp von Na$_V$1.5 auf Na$_V$1.2. Offensichtlich ist der Linker D4S3-S4 sehr wichtig für die Funktion von α-Toxinen.

Die α-Toxine Lqh2, Lqh3 und LqhαIT aus *Leiurus quinquestriatus hebraeus* besitzen ebenfalls eine unterschiedliche Subtypspezifität (Chen und Heinemann, 2001; Chen et al., 2002; Leipold et al., 2004). Während Lqh2 ein typischer Vertreter der säugerspezifischen α-Toxine ist und LqhαIT seine größte Wirkung bei Insekten erzielt, wirkt das α-ähnliche Toxin Lqh3 sowohl bei Säugern als auch bei Insekten (Eitan et al., 1990; Sautiere et al., 1998). Interessanterweise hemmen jedoch alle drei Lqh-Toxine, trotz ihrer strikten Klassifizierung, die schnelle Inaktivierung des Säugerkanals $Na_V1.4$ aus der Skelettmuskulatur mit ähnlich hoher Effizienz ($IC_{50} \approx$ 1-2 nM), sind jedoch unterschiedlich aktiv an den übrigen Säugerkanälen. Beispielsweise unterscheidet der Herzmuskelkanal $Na_V1.5$ zwischen allen drei Lqh-Toxinen. Er ist am sensitivsten für Lqh3, gefolgt von Lqh2 und LqhαIT (Chen und Heinemann, 2001). Im Falle von Lqh2 und Lqh3 ist die Situation jedoch komplizierter: Während $Na_V1.2$ für Lqh2 sensitiver ist als $Na_V1.7$, kehrt sich diese Reihenfolge für Lqh3 um. Die gegensätzliche Spezifität von Lqh2 und Lqh3 für die neuronalen Kanäle $Na_V1.2$ und 1.7 konnten wir dabei auf zwei Aminosäuren im Linker D4S3-S4 der Kanäle zurückführen (Chen et al., 2002).

In Leipold et al. (2004) haben wir die komplexe Subtypspezifität von Lqh2, Lqh3 und LqhαIT systematisch untersucht. Hierfür haben wir die Linker D4S3-S4 der neuronalen Kanäle $Na_V1.2$, $Na_V1.3$, $Na_V1.6$ und $Na_V1.7$ sowie einzelne Reste dieser Linker in $Na_V1.4$ eingesetzt und damit unterschiedliche RS3 in einem $Na_V1.4$-Hintergrund erzeugt. Die funktionelle Charakterisierung dieser Kanalchimären lieferte die Erklärung für die unterschiedliche Sensitivität der Säugerkanäle gegenüber den drei Lqh-Toxinen. Im Falle von Lqh3 identifizierten wir Aspartat-1428 im Linker D4S3-S4 von $Na_V1.4$ als funktionell wichtige Aminosäure. Während die Lqh3-sensitiven Kanäle $Na_V1.4$, $Na_V1.6$ und $Na_V1.7$ dieses Aspartat besitzen, befindet sich in den Lqh3-insensitiven Kanälen $Na_V1.2$ und $Na_V1.3$ ein Glutamat an homologer Stelle (Abb. 7). Der Austausch des Aspartats-1428 in $Na_V1.4$ gegen Glutamat führte dabei zu einem ebenfalls Lqh3-insensitiven Kanal. Die Sensitivität der Na_V-Kanäle gegenüber Lqh3 wird demzufolge von einem einzigen Rest im Linker D4S3-S4 vermittelt. Ähnliches fanden wir für Lqh2: Threonin-1432 ist für die hohe Lqh2-Sensitivität von $Na_V1.4$ verantwortlich. Ersetzten wir es gegen Lysin, wie es an homologer Position im weniger sensitiven $Na_V1.7$ vorkommt, reduzierten wir auch die Sensitivität von $Na_V1.4$ für Lqh2. LqhαIT interagiert jedoch mit beiden Aminosäureresten: Dieses Toxin benötigt sowohl Aspartat-1428 als auch Lysin-1432 für eine hohe Aktivität an $Na_V1.4$-Kanälen. Der LqhαIT-Phänotyp der deutlich weniger sensitiven neuronalen Kanäle $Na_V1.2$ und $Na_V1.7$ kann in $Na_V1.4$ durch den Austausch jeweils einer dieser beiden Aminosäuren erzeugt werden; d.h. die Mutation D1432E führt zu einem $Na_V1.2$-ähnlichen und K1432T zu einem $Na_V1.7$-ähnlichen Phänotyp. Diese Arbeit zeigt deutlich, dass die unterschiedliche Sensitivität der untersuchten Na_V-Kanäle für die α-Toxine Lqh2, Lqh3

und LqhαIT auf der kombinatorischen Anordnung von nur zwei Aminosäuren im Linker D4S3-S4 der Na_V-Kanäle beruhen (Abb. 7).

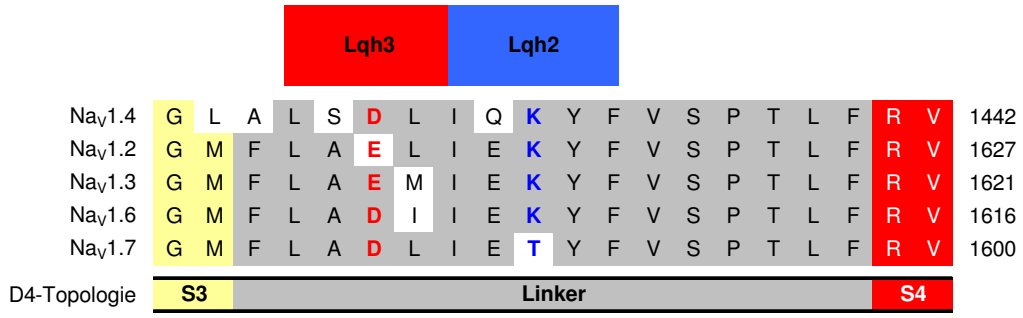

Abb. 7: Der Linker S3-S4 am Spannungssensor von Domäne-4 der Na_V-Kanäle ist Bestandteil von RS3 und ist für die Sensitivität der Kanäle gegenüber Skorpion-α-Toxinen von entscheidender Bedeutung. Das Alignment zeigt die Aminosäuresequenzen der Linker D4S3-S4 aus $Na_V1.4$ und $Na_V1.2$, $Na_V1.3$, $Na_V1.6$ und $Na_V1.7$. Die Interaktionsstellen der Lqh-Toxine sind farblich hervorgehoben: Lqh2: blau, K1432; Lqh3: rot, D1428; LqhαIT: D1423, K1432 (bezogen auf $Na_V1.4$). Die dargestellten Kanalsubtypen sind im Anhang auf Seite 58 näher spezifiziert.

Obwohl Lqh2 zu den säugerspezifischen, LqhαIT zu den insektenspezifischen und Lqh3 zu den säuger- und insektenspezifischen Toxinen gezählt werden, wirken sie alle auf Säuger-Na_V-Kanäle, jedoch mit unterschiedlicher Subtypspezifität. Dies zeigt, dass die Klassifizierung von α-Toxinen in säuger- und insektenspezifische Toxine sehr ungenau ist. Bedenkt man die ausgeprägte Homologie zwischen Na_V-Kanälen aus Insekten und Säugern, so ist dies auch nicht verwunderlich. Beispielsweise besitzt der Na_V-Kanal *para* aus *Drosophila melanogaster* einen säugerähnlichen D4S3-S4-Linker. Abbildung 8A zeigt diesen Linker für den *para*-Kanal sowie für die humanen Kanäle $Na_V1.1$-1.7 im Detail. Aufgrund der säugerähnlichen Struktur des Linkers D4S3-S4 aus Insektenkanälen kann nicht ausgeschlossen werden, dass sog. insektenspezifische α-Toxine, wie z.B. LqhαIT, auch auf einige Kanalsubtypen aus Säugern wirken. Vor diesem Hintergrund erscheint auch der Einsatz sog. insektenspezifischer α-Toxine als alternative Insektizide (siehe Einleitung) äußerst problematisch.

Es ergibt sich jedoch noch eine weitere Schlussfolgerung aus unseren Ergebnissen. Abb. 8B zeigt die Aminosäuresequenzen der Linker D4S3-S4 aus $Na_V1.7$-Kanälen verschiedener Säuger. Die Aminosäuren, welche wir in Leipold et al. (2004) als besonders wichtig für die Wirkung der α-Toxine Lqh2, Lqh3 und LqhαIT identifiziert haben, sind in den $Na_V1.7$-Kanälen von Mensch, Hund, Kaninchen, Ratte und Maus interessanterweise nicht konserviert. Beispielsweise besitzt ausschließlich der humane $Na_V1.7$-Kanal das wichtige Aspartat im Linker D4S3-S4 (Position 1586 im humanen $Na_V1.7$-Kanal). Die $Na_V1.7$-Kanäle anderer Säuger besitzen aber in homologer Position

ein Glutamat. Aufgrund unserer Ergebnisse kann man somit vermuten, dass ausschließlich der humane $Na_V1.7$-Kanal sensitiv für Lqh3 ist. Im Falle von Lqh2 kann man hingegen eine höhere Sensitivität für $Na_V1.7$ aus Hund, Ratte und Maus gegenüber $Na_V1.7$ aus Kaninchen und Menschen erwarten. Dies macht deutlich, dass die Toxikologie der Na_V-Kanäle verschiedener Säuger bezüglich Skorpion-α-Toxinen durchaus unterschiedlich sein kann. Demzufolge kann man auch die Resultate toxikologischer Untersuchungen an Ratten und Mäusen, wie z. B. die Bestimmung der LD_{50}, nicht ohne weiteres auf das humane System übertragen.

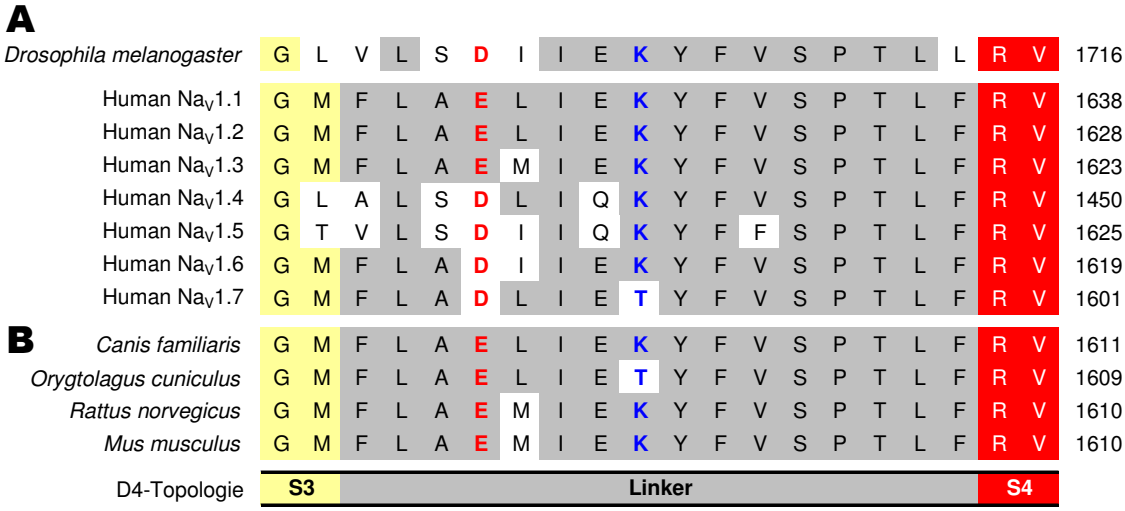

Abb. 8: Die Linker S3-S4 der vierten Na_V-Kanaldomäne aus Säugern und Insekten besitzen eine ähnliche Aminosäuresequenz. Die Interaktionsstellen mit den Skorpion-α-Toxinen Lqh3 (rot) und Lqh2 (blau) sind hervorgehoben. **(A)** Die D4S3-S4-Linker der humanen Kanäle $Na_V1.4$-1.7 sind dem Linker des Na_V-Kanals *para* aus *Drosphila melanogaster* besonders ähnlich. Die bekannten Insekten-Na_V-Kanäle aus *Heliothis virescens*, *Blatella germanica*, *Apis mellifera*, *Pediculus humanus* und *Musca domestica* besitzen zudem denselben D4S3-S4-Linker wie *para*. **(B)** Die Aminosäuresequenzen der Linker D4S3-S4 aus $Na_V1.7$-Kanälen verschiedener Säuger sind unterscheiden sich. Ein Vergleich mit dem humanen $Na_V1.7$-Linker zeigt die Variabilität der Positionen Aspartat-1586 (rot) sowie Lysin-1590 (blau) (bezogen auf die humane Sequenz). Die dargestellten Na_V-Kanäle sind im Anhang auf Seite 58 näher spezifiziert.

4.3 Skorpion-α- und δ-Conotoxine besitzen einen identischen Wirkmechanismus

Während die Mechanismen der Skorpion-α-Toxine bereits gut untersucht sind, existiert nur wenig Information zur Spezifität und zum Wirkmechanismus der δ-Conotoxine. EVIA aus *Conus ermineus* ist das einzige δ-Conotoxin, wofür eine Subtypspezifität an Na_V-Kanälen aus Säugern beschrieben wurde. Während es die schnelle Inaktivierung der neuronalen Kanäle $Na_V1.2$, $Na_V1.3$ und $Na_V1.6$ hemmt, ist es inaktiv an den muskulären Kanälen $Na_V1.4$ und $Na_V1.5$ (Barbier et al., 2004). Der zugrunde liegende Mechanismus ist jedoch unbekannt. Die Identifikation der Kanalbereiche, welche den Kanälen die Sensitivität für δ-Conotoxine verleihen, führt daher nicht nur zu einem vollständigeren Verständnis der Toxin-Kanal-Interaktion, sondern ist gleichzeitig die Voraussetzung zur Aufklärung der funktionellen Verwandtschaft von Skorpion-α- und δ-Conotoxinen.

Für δ-Conotoxine aus Kegelschnecken konnten wir den Wirkmechanismus am Beispiel von SVIE aus *Conus striatus* aufdecken (Leipold et al., 2005). Dieses Toxin hemmt, ähnlich wie Skorpion-α-Toxine, die schnelle Kanalinaktivierung, besitzt jedoch keine ausgeprägte Subtypspezifität (unveröffentlicht). Diese Eigenschaft von SVIE machte eine Identifikation von RS6 auf molekularer Ebene mit Hilfe von Kanalchimären unmöglich, lieferte aber dennoch einen entscheidenden Hinweis auf die Toxin-Kanal-Interaktion. Wenn verschiedene Kanalsubtypen eine ähnliche Sensitivität für SVIE besitzen, dann kann man schlussfolgern, dass diese Kanäle auch ähnliche Interaktionsstellen für SVIE besitzen müssen, d.h. sehr wahrscheinlich formen konservierte Kanalbereiche RS6 für SVIE. Interessanterweise besitzt der Linker D4S3-S4, das funktionell wichtigste Interaktionsepitop für Skorpion-α-Toxine, eine zweigeteilte Struktur: Er gliedert sich in eine variable und in eine konservierte Hälfte. Abbildung 9 zeigt diese Region für einige Na_V-Kanäle im Detail.

Unsere Strategie bestand darin, im konservierten Abschnitt des Linkers D4S3-S4 aus $Na_V1.4$, mittels einer Cystein-Scan-Mutagenese, systematisch nach Interaktionen mit SVIE zu suchen. Die hydrophobe Triade Tyrosin-1433, Phenylalanin-1434 und Valin-1435 erwies sich dabei als besonders wichtig für die Wirkung von SVIE. Sowohl der Austausch von Tyrosin-1433 als auch von Phenylalanin-1424 gegen Cystein reduzierte die Sensitivität des Kanals für SVIE, es verstärkte sich jedoch der Toxineffekt wenn ein Cystein in Position 1435 eingesetzt wurde (Leipold et al., 2005). Damit wiesen wir erstmals nach, dass auch δ-Conotoxine über den D4-Spannungssensor der Kanäle wirken und dass der Linker D4S3-S4 nicht nur Bestandteil von RS3, sondern auch RS6 ist. Dies legt die Vermutung nahe, dass sowohl Skorpion-α- als auch δ-Conotoxine dieselbe Bindestelle an Na_V-Kanälen

besetzen. Durch Verdrängungsexperimente an $Na_V1.4$-Kanälen zeigten wir, dass sich die Interaktionsstellen von Skorpion-α- und δ-Conotoxinen an Na_V-Kanälen tatsächlich überlappen können, je nach dem, welche Skorpion-α- und δ-Conotoxine betrachtet werden. Während SVIE und Lqh2 um die Bindung an $Na_V1.4$ konkurrieren, stabilisieren sich Lqh3 und SVIE gegenseitig am Kanal, d.h. zusammen verlangsamen Lqh3 und SVIE die Inaktivierung des Kanals stärker als die individuellen Toxine alleine. Dieses Ergebnis belegt, dass sich die Bindestellen für Lqh2 und SVIE an $Na_V1.4$-Kanälen überlappen, aber nicht die Bindestellen von Lqh3 und SVIE. Damit erbrachten wir erstmals den Nachweis, dass der Linker S3-S4 in Domäne-4 der funktionell wichtige Bestandteil von RS6 der Na_V-Kanäle ist und dass der bisher unbekannte Wirkmechanismus der δ-Conotoxine, ähnlich wie bei Skorpion-α-Toxinen, auf einer Blockade des Spannungssensors in Domäne-4 beruht. Somit sind auch δ-Conotoxoine Spannungssensor-Toxine.

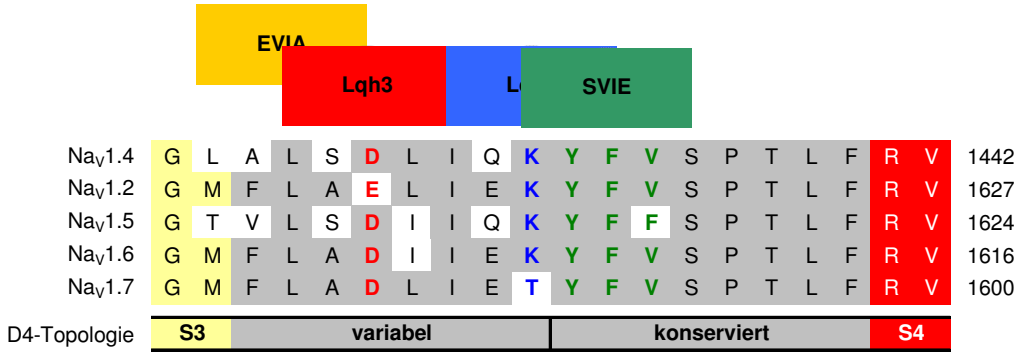

Abb. 9: Der Spannungssensor in Domäne-4 ist Bestandteil von RS3 und RS6. Das Alignment zeigt die Aminosäuresequenzen der Linker D4S3-S4 aus $Na_V1.4$ und $Na_V1.2$, $Na_V1.5$, $Na_V1.6$ und $Na_V1.7$. Während die α-Toxine Lqh2, Lqh3 und LqhαIT mit dem variablen Teil des Linkers interagieren, wechselwirkt das δ-Conotoxin SVIE mit dem konservierten Bereich des Linkers. Die Interaktionsstellen der Toxine, bezogen auf $Na_V1.4$, sind hervorgehoben: Lqh3: rot, D1428; Lqh2: blau, K1432; SVIE grün, Y1433, F1434, V1435. Zusätzlich ist eine mögliche Interaktion des subtypspezifischen δ-Conotoxins EVIA mit dem variablen Abschnitt des Linkers angedeutet. Die dargestellten Kanalsubtypen sind im Anhang auf Seite 58 näher spezifiziert.

Basierend auf unseren Resultaten kann man die Vermutung aufstellen, dass subtypspezifische RS3- bzw. RS6-Toxine (z.B. Lqh2, Lqh3, LqhαIT) mit dem variablen Abschnitt und nichtsubtypspezifische Toxine (z.B. SVIE) mit dem konservierten Abschnitt des D4S3-S4-Linkers interagieren. Falls diese Vermutung zutrifft, sollte das subtypspezifische δ-Conotoxin EVIA, ähnlich wie die untersuchten Lqh-Toxine, mit dem variablen Bereich des Linkers wechselwirken (in Abb. 9 angedeutet). Der experimentelle Beweis dieser Vermutung steht jedoch noch aus. Des Weiteren wirft der identische Wirkmechanismus der Skorpion-α- und δ-Conotoxine die Frage auf, ob die Definition eingeständiger Bindestellen für diese Toxine weiterhin berechtigt ist, zumal

auch einige Seeanemonen- und Spinnentoxine die Inaktivierung von Na_V-Kanälen hemmen und RS3 zugeordnet werden (Cestèle und Catterall, 2000). Möglicherweise wäre die Zusammenfassung all dieser Toxine in eine Gruppe mit identischem molekularen Wirkmechanismus eine geeignetere Klassifizierung.

4.4 Die Porenschleife in Domäne-3 vermittelt Na_V-Kanälen die Sensitivität für Skorpion-β- und µO-Conotoxine

Ähnlich wie bei Skorpion-α- und δ-Conotoxinen existieren auch für Skorpion-β- und µO-Conotoxine keine systematischen Studien bezüglich ihrer Subtypspezifität gegenüber Säugerkanälen. Während die Spezifität der µO-Toxine noch völlig unerforscht ist, gibt es jedoch Hinweise darauf, dass β-Toxine subtypspezifisch wirken. Cestèle et al. (1998) verglichen die Effekte des β-Toxins Css4 aus *Centruroides suffusus suffusus* an $Na_V1.2$- und $Na_V1.5$-Kanälen. Css4 senkte zwar die Aktivierungsschwelle der $Na_V1.2$-Kanäle, war aber inaktiv an $Na_V1.5$-Kanälen. Durch die systematische Konstruktion von Chimären zwischen den beiden Kanälen identifizierten sie einen Glycinrest im Linker D2S3-S4 von $Na_V1.2$ (G845, Abb. 10) als essentiell für die hohe Sensitivität des Kanals gegenüber Css4. Tauschten sie dieses Glycin in $Na_V1.2$ gegen Asparagin, wie es in homologer Position in $Na_V1.5$ vorkommt, wurde auch $Na_V1.2$ insensitiv für Css4. Interessanterweise ist dieser Glycinrest nicht nur in $Na_V1.2$, sondern auch in $Na_V1.1$, $Na_V1.3$, $Na_V1.4$, $Na_V1.6$ und $Na_V1.7$ vorhanden. Dies lässt die Vermutung aufkommen, dass β-Toxine keine ausgeprägte Subtypspezifität gegenüber neuronalen und Skelettmuskel-Kanälen besitzen. Für eine Klärung dieser Frage bedarf es jedoch einer systematischen Untersuchung der Wirkung von β-Toxinen auf diese Kanäle.

Um die Voraussetzungen für solch eine systematische Studie zur Subtypspezifität von Skorpion-β-Toxinen zu schaffen, charakterisierten wir zunächst die Hauptkomponente des Gifts vom venezuelanischen Skorpion *Tityus zulianus*, das β-Toxin Tz1 (Borges et al., 2004). Wir zeigten, dass Tz1 zwar die Aktivierungsschwelle von $Na_V1.4$-Kanälen herabsetzt, jedoch nicht die Aktivierungsschwelle von $Na_V1.5$-Kanälen. Des Weiteren wiesen wir für Tz1 eine für β-Toxine typische *use-dependence* nach.

In einer weiteren Arbeit erweiterten wir diese Untersuchungen auf die neuronalen Kanäle $Na_V1.2$, $Na_V1.6$ und $Na_V1.7$ (Leipold et al., 2006a). Während $Na_V1.4$ der sensitivste Kanal für Tz1 ist, unterscheidet es die neuronalen Kanäle in der Reihenfolge $Na_V1.6 > Na_V1.2 >> Na_V1.7$, wobei $Na_V1.7$ praktisch insensitiv für Tz1 ist. Damit haben wir erstmals die ausgeprägte Subtypspezifität eines β-Toxins gegenüber neuronalen Na_V-Kanälen nachgewiesen. Um die Kanalbereiche zu identifizieren, die den Kanälen die unterschiedliche Sensitivität für Tz1 verleihen, konstruierten wir Chimären zwischen $Na_V1.4$ und neuronalen Na_V-Kanälen (Abb. 6). Der Linker S3-S4 in

Domäne-2 der Na_V-Kanäle ist zwar für die Funktion von β-Toxinen wichtig (Cestèle et al., 1998), doch das Einsetzen dieses Linkers aus $Na_V1.2$ in $Na_V1.4$ vermochte die Tz1-Sensitivität von $Na_V1.4$ nicht zu reduzieren. Die unterschiedliche Sensitivität der neuronalen Kanäle für Tz1 wird somit nicht durch den Linker S3-S4 in Domäne-2 vermittelt. Wir erzeugten deshalb $Na_V1.4$-Kanäle mit je einer der vier homologen Domänen aus $Na_V1.2$ (Abb. 6A). Interessanterweise zeigte die Chimäre mit Domäne-3 aus $Na_V1.2$ eine ähnlich schwache Tz1-Wirkung wie der $Na_V1.2$-Wildtyp. Mit Hilfe weiterer Chimären war es uns möglich, den C-terminalen Bereich der Porenschleife aus Domäne-3 (D3-Porenschleife) als die Struktur in $Na_V1.2$, $Na_V1.4$, $Na_V1.6$ und $Na_V1.7$ zu identifizieren, die den Kanälen die unterschiedliche Sensitivität für Tz1 vermittelt. Setzten wir die Porenschleifen aus den Domänen-3 von $Na_V1.2$, $Na_V1.6$ oder $Na_V1.7$ in $Na_V1.4$ ein, übertrugen wir damit auch die Tz1-Sensitivität des jeweiligen Spenderkanals der Porenschleife auf $Na_V1.4$.

$Na_V1.5$ weicht jedoch von diesem Schema ab, d.h. seine Porenschleife reduzierte die Sensitivität von $Na_V1.4$ gegenüber Tz1 nicht, sondern steigerte sie. Die Ursache für die Ausnahmestellung von $Na_V1.5$ bezüglich Tz1 identifizierten wir im Linker D2S3-S4. Die Aminosäuresequenz dieses Linkers aus $Na_V1.5$ unterscheidet sich stark von der Linkersequenz anderer Kanäle (Abb. 10A). Ersetzten wir das essentielle Glycin im Linker D2S3-S4 von $Na_V1.4$ durch Asparagin (G658N) aus der homologen $Na_V1.5$-Position, vermochte Tz1 die Aktivierungsschwelle von $Na_V1.4$, ähnlich wie bei $Na_V1.5$, nicht mehr zu reduzieren. Weil das konservierte Glycin im Linker D2S3-S4 nicht nur für eine hohe Css4-, sondern auch für eine hohe Tz1-Sensitivität essentiell ist, kann man eine generelle Bedeutung dieser Aminosäure für den Wirkmechanismus der Skorpion-β-Toxine postulieren. Im Falle von $Na_V1.5$ dominiert offensichtlich die Toxin-insensitive Struktur seines D2S3-S4-Linkers die Toxin-sensitive Struktur seiner D3-Porenschleife. Damit wiesen wir nach, dass RS4 der Na_V-Kanäle aus mindestens zwei funktionellen Epitopen besteht, einem Spezifitätsepitop in der Porenschleife von Domäne-3 und einem Wirkepitop im Spannungssensor von Domäne-2.

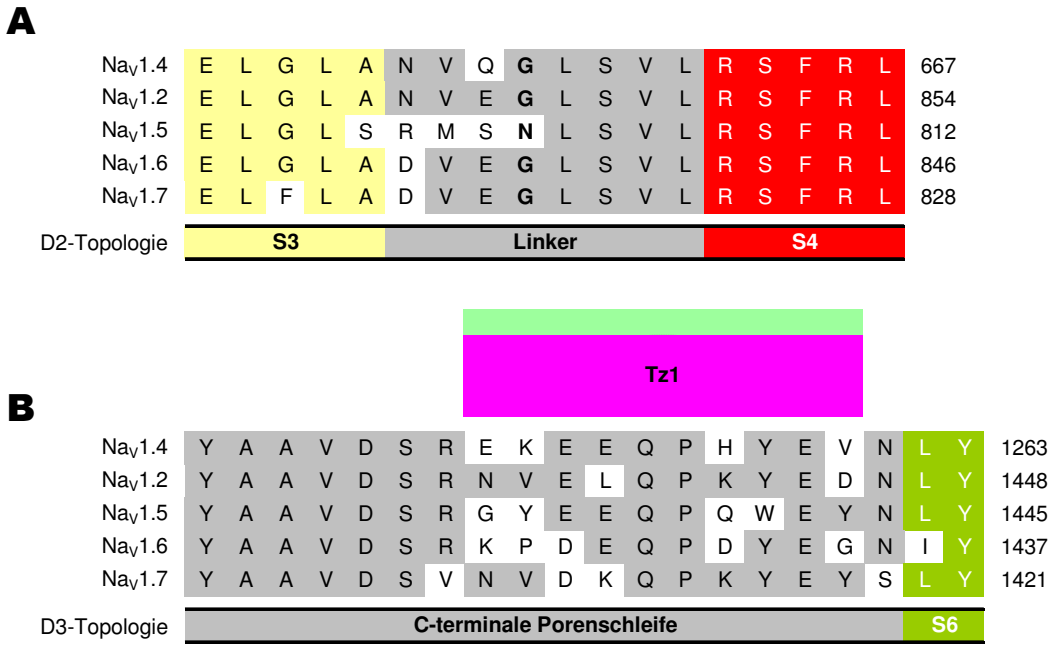

Abb. 10: Aminosäuresequenzen der RS4-Epitope der Kanäle $Na_V1.4$, $Na_V1.2$, $Na_V1.5$, $Na_V1.6$ und $Na_V1.7$. **(A)** Die Sequenz des Linkers D2S3-S4 aus $Na_V1.5$ unterscheidet sich stark von den Linkersequenzen anderer Na_V-Kanäle. Das konservierte Glycin (G658 in $Na_V1.4$) ist hervorgehoben. **(B)** Der C-terminale Bereich der D3-Porenschleifen vermittelt den Kanälen die Sensitivität für das Skorpion-β-Toxin Tz1 sowie für das µO-Conotoxin MrVIA. Die dargestellten Na_V-Kanäle sind im Anhang auf Seite 58 näher spezifiziert.

Für die µO-Conotoxine MrVIA und MrVIB zeigten wir ebenfalls eine subtypspezifische Wirkung (Zorn et al., 2006). Während diese Toxine $Na_V1.4$-Kanäle sehr potent blockieren ($IC_{50} \approx 250$ nM), sind sie an $Na_V1.2$-Kanälen um den Faktor 5 weniger aktiv. Für MrVIA identifizierten wir in dieser Arbeit ebenfalls die D3-Porenschleife der Kanäle als sensitivitätsvermittelnde Struktur. Wir folgten hierfür einer ähnlichen Chimärenstrategie wie im Falle des Skorpion-β-Toxins Tz1. Ähnlich wie bei Tz1 erzeugte der Austausch der C-terminalen Porenregion in Domäne-3 von $Na_V1.4$ gegen die homologe Region aus $Na_V1.2$ einen $Na_V1.4$-Kanal mit der MrVIA-Sensitivität des $Na_V1.2$-Wildtyps. Damit wiesen wir erstmals eine Subtypspezifität für µO-Conotoxine nach und identifizieren die D3-Porenschleife als Bestandteil der µO-Toxinbindestelle (Abb. 10B).

Interessanterweise ist die C-terminale Porenregion der dritten Kanaldomäne sowohl zwischen verschiedenen Kanalsubtypen einer Spezies (z.B. humane Kanäle) als auch zwischen orthologen Kanälen verschiedener Spezies variabel. Beispielsweise unterscheiden sich die Aminosäuresequenzen der D3-Porenschleifen von Na_V-Kanälen verschiedener Insekten ganz erheblich (Abb. 11A). Aufgrund der Bedeutung dieser Kanalregion für die Wirkung von Skorpion-β- und µO-Conotoxinen auf Säugerkanäle erscheint es durchaus plausibel, dass sich auch die Toxikologie verschiedener

Insektenkanäle gegenüber den β- und μO-Toxinen unterscheiden kann. Damit erscheinen Skorpion-β-Toxine grundsätzlich besser als selektive Insektizide geeignet zu sein als Skorpion-α-Toxine. Weil aber die Sensitivitäten unterschiedlicher Na_V-Kanäle für ein gegebenes β-Toxin gegenwärtig nicht vorhersagbar sind, kann auch ein Übersprechen sog. Insekten-β-Toxine auf Säugerkanäle nicht ausgeschlossen werden. Ähnlich wie im Falle der α-Toxine stellt sich somit auch für β-Toxine die Frage, ob die gebräuchliche Klassifizierung der Skorpiontoxine bezüglich ihrer Insekten- und Säugerspezifität nicht zu ungenau ist. Systematische Untersuchungen sog. insektenspezifischer β-Toxine an Insekten- und Säugerkanälen könnten diese Frage jedoch klären.

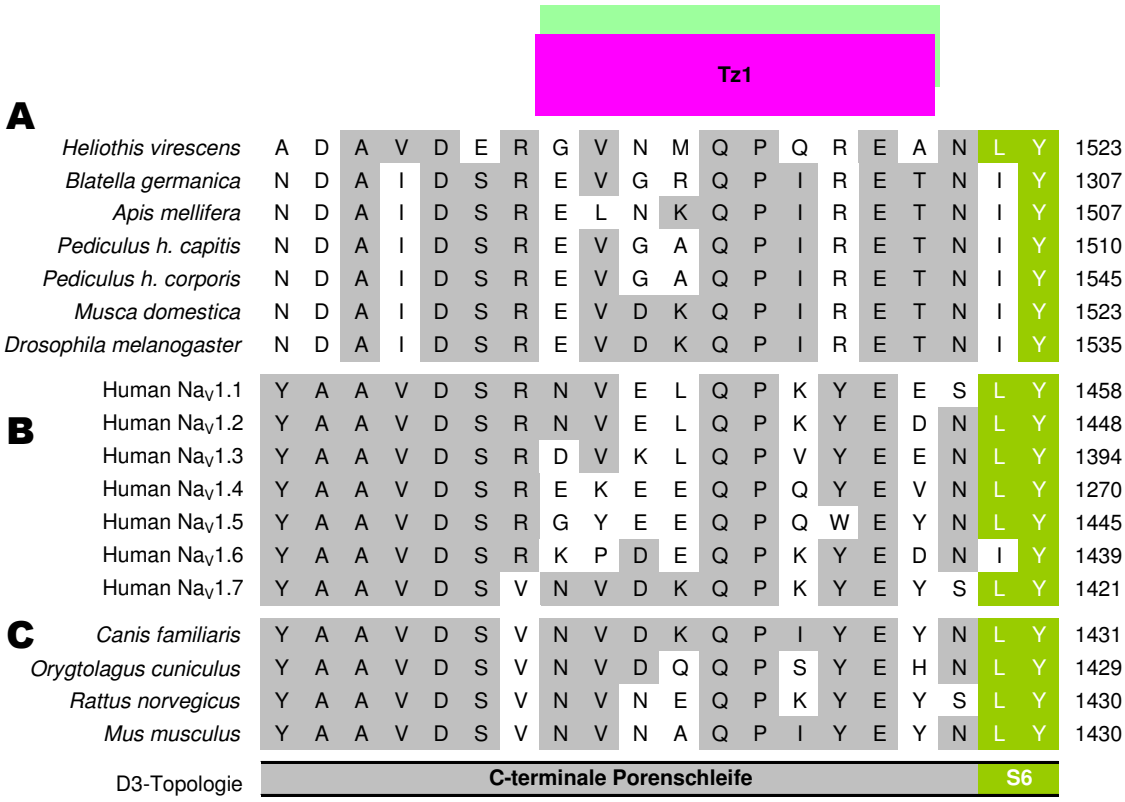

Abb. 11: Die C-terminalen Porenschleifen der dritten Domäne von Na_V-Kanälen aus Insekten und Säugern besitzen eine variable Aminosäuresequenz. Die Interaktionstellen des β-Toxins Tz1 sowie des μO-Toxins MrVIA sind angedeutet. **(A)** Sequenzen der D3-Porenschleifen bekannter Na_V-Kanäle aus Insekten. **(B)** Sequenzen der D3-Porenschleifen der humanen Kanäle $Na_V1.1$-1.7. **(C)** Die D3-Porenschleifen aus $Na_V1.7$-Kanälen verschiedener Säuger unterscheiden sich. Alle dargestellten Na_V-Kanäle sind im Anhang auf Seite 58 näher spezifiziert.

Die D3-Porenschleifen verschiedener $Na_V1.7$-Kanäle aus Säugern sind in Abb. 11C dargestellt. Ähnlich wie im Falle des Linkers D4S3-S4 (Abb. 8) zeigen die $Na_V1.7$-Kanäle verschiedener Säuger eine besonders ausgeprägte Variabilität in ihren D3-Porenschleifen. Demzufolge muss nicht nur für verschiedene Insekten, sondern auch für verschiedene Säuger mit einer unterschiedlichen Toxikologie bezüglich Skorpion-β- und μO-Contoxinen gerechnet werden.

4.5 β-Toxine stabilisieren offene und geschlossene Zustände von Na_V-Kanälen

Auch wenn das angenommene *voltage sensor trapping*-Modell von Cestèle et al. (1998, 2001) die Verringerung der Aktivierungsschwelle von Na_V-Kanälen durch Skorpion β-Toxine gut erklären kann, bleiben doch einige Details unklar. Dieses Modell vermag zum Beispiel nicht zu erklären, wieso β-Toxine neben der Senkung der Aktivierungsschwelle von Na_V-Kanälen einen Teil der Kanäle blockieren können (z.B. Yatani et al., 1988; Gordon et al., 2003; Borges et al., 2004). Dieses duale Verhalten weist auch Tz1 auf: Es ist in Abbildung 3 dargestellt. Des Weiteren versagen die existierenden Na_V-Kanalmodelle bei dem Versuch, den Effekt von β-Toxinen durch eine permanente Aktivierung des D2-Spannungssensors zu modellieren. Offensichtlich ist der Wirkmechanismus der β-Toxine deutlich komplizierter als bisher angenommen. Eine präzisere Analyse der Wirkung von β-Toxinen auf Na_V-Kanäle scheint demnach eine Vorraussetzung zum Verständnis ihres komplexen Wirkmechanismus zu sein.

Mit Messungen der Tz1-Effekte, „Senkung der Aktivierungsschwelle“ und „Kanalblockade“, auf $Na_V1.4$-Kanäle bei unterschiedlich stark hyperpolarisierter Zellmembran ist es uns gelungen, die β-Toxin-induzierte Blockade der Kanäle zu erklären. Bei niedrigen Ruhepotentialen befindet sich der D2-Spannungssensor der Kanäle mit hoher Wahrscheinlichkeit in seiner deaktivierten und somit einwärts bewegten Konformation. Bindet ein β-Toxin an diese Kanäle, immobilisiert es den D2-Spannungsensor in dieser Konformation. Auf diese Weise stabilisieren β-Toxine die deaktivierte, geschlossene Kanalkonformation. Phänotypisch erscheinen die so modifizierten Kanäle als blockiert. Höhere Ruhepotentiale gehen hingegen mit einer erhöhten Mobilität der Spannungssensoren in der Zellmembran einher. Es ist also anzunehmen, dass ein β-Toxin bei hohen Membranpotentialen mit großer Wahrscheinlichkeit auf einen aktivierten D2-Spannungssensor trifft. Wie bereits von Cestèle et al. (1998) vermutet, immobilisiert nun das β-Toxin diese auswärts bewegte Konformation des Sensors und demzufolge die aktivierte Konformation des gesamten Kanals. Die Folge ist eine Absenkung der Aktivierungsschwelle der Kanäle. Diese Erweiterung des *voltage sensor trapping*-Modells von Cestèle et al. (1998) impliziert direkt, dass die Bindung der β-Toxine an Na_V-Kanäle unabhängig von der

Kanalkonformation und somit unabhängig von der Membranspannung ist, jedoch die Qualität der Wirkung deutlich von der Membranspannung abhängt. Unterstützung erfährt dieses erweiterte Modell durch Messungen, welche die Spannungsunabhängigkeit der Bindung von β-Toxinen an Na_V-Kanäle belegen. Jover et al. (1980a) untersuchten die Bindung von radioaktiv markiertem β-Toxin Css2 aus *Centruroides suffusus suffusus* an Rattensynaptosomen in Abhängigkeit von der Konzentration extrazellulärer K^+-Ionen. Die verschieden Konzentrationen extrazellulärer K^+-Ionen während der Bindungsmessungen erzeugten dabei unterschiedliche Potentiale in den Synaptosomenmembranen. Interessanterweise war die Bindung von Css2 an die Membranen der Synaptosomen unabhängig von der extrazellulären K^+-Konzentration und damit unabhängig vom Membranpotential.

Unsere Ergebnisse sprechen zudem dafür, dass es sich bei dem Phänomen der use-dependence von Tz1 wahrscheinlich um ein spannungsabhängiges Umschalten zwischen „Kanalblockade“ und „Reduzierung der Aktivierungsschwelle“ handelt. Der molekulare Wirkmechanismus von Tz1 scheint demnach darin zu bestehen, das Umschalten des D2-Spannungssensors zwischen seiner deaktivierten und aktivierten Konformation zu hemmen. Auf diese Weise kann Tz1 in Abhängigkeit der Membranspannung entweder als Kanalblocker oder Kanalaktivator wirken.

Dieses Modell macht außerdem deutlich, dass der physiologische Effekt eines β-Toxines nicht ohne weiteres vorhergesagt werden kann. Zum Beispiel werden einige insektenspezifische β-Toxine, entsprechend ihrer physiologischen Konsequenzen für die Erregungsleitung, in erregende und dämpfende Toxine eingeteilt (Possani et al., 1999). Basierend auf unserer Erweiterung des *voltage sensor trapping*-Modells kann man nun spekulieren, dass diese Toxine durch die Stabilisierung der aktivierten Konformation des D2-Spannungssensors erregend bzw. durch die Stabilisierung seiner deaktivierten Konformation dämpfend auf die Erregungsleitung wirken. Für eine endgültige Klärung dieser Frage ist es jedoch notwendig, die Wirkung erregender und dämpfender β-Toxine systematisch zu untersuchen.

4.6 µO-Conotoxine wirken über den D2-Spannungssensor der Na_V-Kanäle

Die D3-Porenschleife vermittelt den Na_V-Kanälen die Sensitivität für sowohl Skorpion-β-Toxine als auch µO-Conotoxine. Die Interaktion beider Toxinklassen mit demselben Kanalbereich legt die Vermutung nahe, dass auch ihre Wirkmechanismen ähnlich sein könnten. Unterstützt wird diese Vermutung zudem durch unsere Ergebnisse zur Funktionsweise von Skorpion-β-Toxinen (Leipold et al., 2006b *in Vorbereitung*). Wenn Skorpion-β-Toxine eine Kanalblockade induzieren können, indem sie den D2-Spannungssensor in seiner deaktivierten Konformation stabilisieren, dann könnte dieser Mechanismus auch den µO-Conotoxinen zugrunde liegen.

Einen Hinweis auf einen Spannungssensor-Mechanismus der µO-Conotoxine erbrachten wir mit dem Nachweis der Spannungsabhängigkeit des µO-Conotoxin-induzierten Kanalbocks (Leipold et al., 2006c *in Vorbereitung*). Eine starke Depolarisation der Zellmembran verringerte die MrVIA-induzierte Blockade von $Na_V1.4$-Kanälen. Möglicherweise schwächt eine starke Depolarisation der Membran die Toxin-Kanal-Interaktion derart, dass MrVIA dadurch abdissoziiert. Diesen Verdacht konnten wir durch den Nachweis der Kopplung des Toxineffektes an den D2-Spannungssensor erhärten. Der Austausch des äußersten Arginins im D2-Spannungssensor von $Na_V1.4$ gegen Cystein führte im Vergleich zum Wildtypkanal zu einem langsameren Abdissoziieren von MrVIA bei stark depolarisierter Zellmembran. Dies spricht für ein Modell, in dem µO-Conotoxine eine ähnliche Interaktion mit Na_V-Kanälen eingehen wie Skorpion-β-Toxine. Im Unterschied zu Skorpion-β-Toxinen können µO-Conotoxine den D2-Spannungssensor jedoch ausschließlich in seiner deaktivierten Konformation stabilisieren und hemmen auf diese Weise die Aktivierung der Na_V-Kanäle. Dieses Resultat unterstreicht zudem die funktionelle Verwandtschaft von µO-Conotoxinen und Skorpion-β-Toxinen und zeigt: Auch µO-Conotoxine sind Spannungssensor-Toxine.

4.7 Das Spannungssensor-Modell

Sowohl Skorpion-α- und β-Toxine als auch δ- und µO-Conotoxine folgen demselben Prinzip: Sie sind Spannungssensor-Toxine. Trotz dieses gemeinsamen Prinzips unterscheiden sich jedoch die Vertreter verschiedener Toxinklassen in ihrer Wirkung ganz erheblich. Skorpion-α-Toxine und δ-Conotoxine hemmen die Inaktivierung von Na_V-Kanälen durch eine Blockade der Auswärtsbewegung des D4-Spannungssensors. Skorpion-β- und µO-Conotoxine beeinflussen hingegen die Aktivierung der Kanäle durch eine Interaktion mit dem D2-Spannungssensor. Damit wird die funktionelle Kopplung des D4-Spannungssensors an die Kanalinaktivierung und des D2-Spannungssensors an die Aktivierung der Kanäle besonders deutlich.

Die Resultate dieser Arbeit belegen weiterhin, dass die Wirkung eines Spannungssensor-Toxins nicht ausschließlich davon abhängt, welchen Spannungssensor ein Toxin immobilisiert, sondern auch davon, in welcher Konformation der Spannungssensor immobilisiert wird. Durch die Stabilisierung des D2-Spannungssensors in seiner deaktivierten bzw. aktivierten Konformation ist es Skorpion-β-Toxinen möglich, die Na_V-Kanalaktivität zu unterdrücken bzw. sie zu steigern. Allein aus der Zugehörigkeit eines Spannungssensor-Toxines zur Klasse der Skorpion-β-Toxine kann deshalb nicht unmittelbar auf seine physiologische Wirkung geschlossen werden. Im Unterschied zu Skorpion-β-Toxinen können µO-Conotoxine ausschließlich die Aktivierung von Na_V-Kanälen hemmen, nicht jedoch die

Aktivierungsschwelle der Kanäle reduzieren. Dies spricht für ein Modell, in dem µO-Conotoxine, im Gegensatz zu Skorpion-β-Toxinen, vom Kanal abdissoziieren wenn sich der D2-Spannungssensor nach außen bewegt (Abb. 12A).

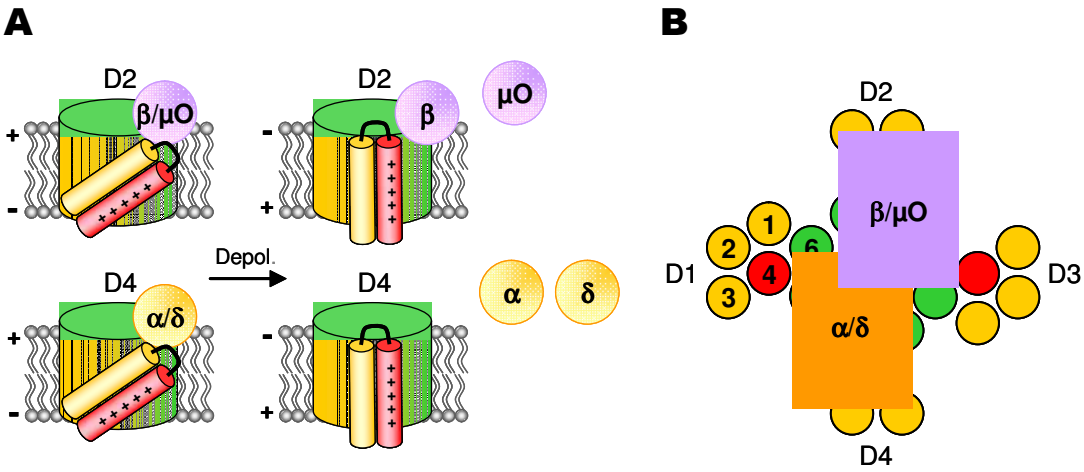

Abb. 12: (A) Spannungssensor-Mechanismen der α- und β-Toxine aus Skorpionen sowie der δ- und µO-Conotoxine aus marinen Kegelschnecken. Während die Bindung der β-Toxine unabhängig von der Membranspannung ist, wird die Bindung der α-Toxine durch eine starke Membrandepolarisation geschwächt. Im Falle der δ- und µO-Conotoxine sprechen die Resultate der vorliegenden Arbeit ebenfalls für eine Abschwächung der Toxin-Kanal-Interaktion bei depolarisierter Zellmembran. **(B)** Rotationssymmetrische Bindung der untersuchten Spannungssensor-Toxine an Na_V-Kanäle. Skorpion-α-Toxine und δ-Conotoxine (orange) sowie Skorpion-β-Toxine und µO-Conotoxine (lila) interagieren mit jeweils denselben Kanalepitopen. Die Anordnung der Transmembransegmente zueinander wurde den Strukturdaten des K_V1.2-Kanals entnommen (2A79.pdb, Long et al., 2005).

Im Gegensatz zu β-Toxinen wurde für α-Toxine jedoch eine Spannungsabhängigkeit der Toxin-Kanal-Interaktion nachgewiesen. Zum einen wurde in Bindestudien eine Schwächung der α-Toxin-Kanal-Interaktion bei depolarisierter Membran gefunden (z.B. Jover et al., 1980a, 1980b; Gilles et al., 2001) und zum anderen wurde der Verlust der α-Toxinwirkung bei depolarisierter Zellmembran auch in funktionellen Studien gezeigt (z.B. Gilles et al., 2001; Leipold et al., 2005). Man nimmt deshalb an, dass Skorpion-α-Toxine bei starker Depolarisation der Membran vom Kanal abdissoziieren. Für δ-Conotoxine belegen unsere Resultate einen ähnlichen Mechanismus wie für Skorpion-α-Toxine (Leipold et al., 2005). Es ist deshalb anzunehmen, dass auch δ-Conotoxine bei einer starken Membrandepolarisation von den Kanälen abdissoziieren (Abb. 12A).

Eine weitere Schlussfolgerung ist in Abb. 12B dargestellt. Die Resultate dieser Dissertation sprechen für eine rotationssymmetrische Anordnung der verschiedenen Spannungssensor-Toxine auf der Kanaloberfläche. Während Skorpion-β- und µO-Conotoxine ein Bindeepitop in der D3-Porenschleife und ein Wirkepitop am

D2-Spannungssensor besitzen, wirken Skorpion-α- und δ-Conotoxine über den D4-Spannungssensor. Aufgrund der Kanalsymmetrie sowie homologer Toxinstrukturen kann man ein weiteres Bindeepitop für Skorpion-α- und δ-Conotoxine in der D1-Porenschleife vermuten. Tatsächlich wurde für Skorpion-α-Toxine bereits eine Interaktion mit der D1-Porenschleife nachgewiesen (Tejedor und Catterall, 1988; Thomson und Catterall, 1989). Im Falle der δ-Conotoxine steht dieser Beweis jedoch noch aus. Unterstützung erfährt dieses Modell zudem durch die Raumstruktur des Kaliumkanals K_V1.2 (Long et al., 2005). Dieser Kanal besteht aus vier identischen Untereinheiten, welche zu den vier Domänen der Na_V-Kanäle homolog sind. Der Linker S3-S4 einer Untereinheit dieses Kanals befindet sich dabei in räumlicher Nähe zur Porenschleife der jeweils folgenden Untereinheit. Der Abstand zwischen dem Linker S3-S4 und der Porenschleife der nachfolgenden Untereinheit entspricht dabei mit ca. 3 nm dem durchschnittlichen Durchmesser der Toxine. Nimmt man für die vier homologen Na_V-Kanaldomänen eine ähnliche Struktur an, dann erscheint die Interaktion der untersuchten Skorpion- und Kegelschneckentoxine mit beiden Kanalepitopen gleichzeitig durchaus plausibel.

4.8 Schlussfolgerung

Skorpion-α- und β-Toxine sowie δ- und μO-Conotoxine sind viel versprechende Leitstrukturen zur Entwicklung subtypspezifischer Na_V-Kanal-Modulatoren. Ein umfassendes Verständnis der Funktionsweise dieser Toxine ist jedoch eine entscheidende Vorraussetzung, um dieses Potential nutzen zu können. In der vorliegenden Dissertation wurde deshalb erstmals die Subtypspezifität dieser Spannungssensor-Toxine systematisch untersucht und auf molekularer Ebene aufgeklärt. Die bisher unbekannten Wirkmechanismen der δ- und μO-Conotoxine konnten ebenfalls aufgedeckt werden. Diese Arbeit trägt deshalb nicht nur zu einem umfassenderen Verständnis der Interaktion zwischen Na_V-Kanälen und Skorpion-α- und β-Toxinen sowie δ- und μO-Conotoxinen bei, sondern bereitet auch die Basis für zukünftige Anwendungen dieser Toxine in Medizin und Forschung.

5. Zusammenfassung

Spannungsgesteuerte Natriumkanäle (Na_V-Kanäle) sind von entscheidender Bedeutung für die elektrische Signalgebung in erregbaren Zellen von Menschen und Tieren. Sie initiieren Aktionspotentiale und sind an deren gerichteten Ausbreitung beteiligt. Es ist deshalb nicht verwunderlich, dass giftige Tiere auch sehr effiziente Na_V-Kanal-spezifische Toxine entwickelt haben, um ihre Beute schnell zu immobilisieren und zu töten. Viele dieser Toxine haben zudem die Eigenschaft, nur bestimmte Na_V-Kanäle in ihrer Funktion zu beeinflussen (z.B. nur neuronale Na_V-Kanäle) und besitzen deshalb auch therapeutisches Potential.

Die Skorpion-α- und β-Toxine bestehen aus 58-76 Aminosäuren und besitzen eine konservierte Raumstruktur: Vier Disulfidbrücken stabilisieren eine kurze α-Helix und ein meist dreisträngiges β-Faltblatt. Skorpion-α-Toxine hemmen die schnelle Kanalinaktivierung durch eine Interaktion mit dem Spannungssensor in Domäne-4. Skorpion-β-Toxine senken hingegen die Aktivierungsschwelle von Na_V-Kanälen durch eine Interaktion mit dem Spannungssensor in Domäne-2 und blockieren gleichzeitig einen Teil der Na_V-Kanäle durch einen noch unbekannten Mechanismus. Im Gegensatz zu den langkettigen Skorpiontoxinen bestehen δ- und μO-Kegelschneckentoxine (Conotoxine) aus nur 25-35 Aminosäuren und werden von drei Disulfidbrücken stabilisiert. Während δ-Conotoxine, ähnlich wie Skorpion-α-Toxine, die schnelle Kanalinaktivierung hemmen, üben μO-Conotoxine eine inhibierende Wirkung auf Na_V-Kanäle aus. Weder die zugrunde liegenden Wirkmechanismen der δ- und μO-Conotoxine noch ihre Bindestellen an Na_V-Kanälen waren zu Beginn dieser Arbeit bekannt. Dies wirft natürlich die Frage auf, wie einerseits unterschiedliche Toxinstrukturen eine identische (Skorpion-α-Toxine und δ-Conotoxine) und wie andererseits ähnliche Toxinstrukturen (Skorpion-α- und -β-Toxine bzw. δ- und μO-Conotoxine) eine unterschiedliche Wirkung auf Na_V-Kanäle ausüben können.

Um diese Frage zu beantworten, wurden in der vorliegenden Dissertation die Wirkungen ausgewählter Skorpion-α- und -β-Toxine sowie δ- und μO-Conotoxine systematisch an heterolog exprimierten Na_V-Kanälen aus Säugern mittels der Patch-Clamp-Technik untersucht. Die Resultate dieser Arbeit belegen dabei für Skorpion-α- und δ-Conotoxine einen identischen Mechanismus: Die Vertreter beider Toxinklassen unterdrücken die Auswärtsbewegung des Spannungssensors der vierten Kanaldomäne durch eine Interaktion mit dem Kanallinker D4S3-S4 und hemmen auf diese Weise die schnelle Inaktivierung der Na_V-Kanäle. Der Linker D4S3-S4 scheint verschiedenen Säugerkanälen zudem unterschiedliche Sensitivitäten für diese Toxine zu vermitteln. Wahrscheinlich interagieren subtypspezifische Skorpion-α-Toxine sowie

δ-Conotoxine mit variablen und nicht subtypspezifische Skorpion-α-Toxine sowie δ-Conotoxine mit konservierten Resten im Linker D4S3-S4.

Die Resultate dieser Arbeit belegen weiterhin, dass auch Skorpion-β- und μO-Conotoxine funktionell verwandt sind: Während die Porenschleife in Domäne-3 verschiedenen Na_V-Kanälen unterschiedliche Sensitivitäten für sowohl Skorpion-β- als auch μO-Conotoxine verleiht, interagieren die Vertreter beider Toxinklassen mit dem Spannungssensor in Domäne-2. Es wurde gezeigt, dass Skorpion-β-Toxine den Spannungssensor der Kanaldomäne-2 sowohl in seiner aktivierten als auch in seiner deaktivierten Konformation immobilisieren können. Auf diese Weise bewirken β-Toxine sowohl eine Senkung der Aktivierungsschwelle als auch eine Blockade der Na_V-Kanäle. Im Gegensatz zu β-Toxinen immobilisieren μO-Conotoxine den Spannungssensor in Domäne-2 ausschließlich in seiner deaktivierten Konformation und hemmen auf diese Weise die Aktivierung der Na_V-Kanäle.

Dies zeigt deutlich, dass nicht nur Skorpion-α- und β-Toxine, sondern auch δ- und μO-Conotoxine Spannungssensor-Toxine sind. Auf den Resultaten dieser Dissertation basierend wird ein Modell postuliert, in dem sich die Na_V-Kanal-spezifischen Spannungssensor-Toxine aus Skorpionen und marinen Kegelschnecken rotationssymmetrisch auf der Kanaloberfläche anordnen. Während Skorpion-β-Toxine und μO-Conotoxine je eine Interaktionsstelle am Spannungssensor in Domäne-2 sowie in der Porenschleife von Domäne-3 besitzen, interagieren Skorpion-α-Toxine und δ-Conotoxine mit dem Spannungssensor in Domöne-4 sowie der Porenschleife in Domäne-1 der Na_V-Kanäle.

Die vorliegende Dissertation bereitet damit zum einen die Basis für weiterführende Anwendungen der Na_V-Kanal-spezifischen Spannungssensor-Toxine aus Skorpionen und marinen Kegelschnecken und trägt zum anderen entscheidend zu einem umfassenderen Verständnis der komplexen Toxin-Kanal-Interaktion bei.

6. Summary

Voltage-gated sodium channels (Na_V channels) play a key role in the electrical signaling of excitable cells since they initiate and propagate action potentials. Therefore, it is comprehensible that various venomous animals produce potent Na_V channel specific neurotoxins to efficiently immobilize and kill their prey. Many of these toxins are specific for only a subset of Na_V channels (e.g. only for neuronal Na_V channels) and therefore possess therapeutic potential.

Scorpion α- and β-toxins are composed of 58-76 amino acids and share a conserved three-dimensional structure, a short α-helix and a three-stranded β-sheet, which are stabilized by four disulfide bridges. Scorpion α-toxins inhibit the fast inactivation of Na_V channels through an interaction with the voltage sensor in domain-4 of the channels. In contrast, scorpion β-toxins lower the activation threshold of Na_V channels through an interaction with the channels' domain-2 voltage sensor, and they partially block Na_V channels through an unknown mechanism. δ- and μO-conotoxins from marine cone snails consist of only 25-35 amino acids and contain three disulfide bridges. Whereas δ-conotoxins inhibit the fast inactivation of Na_V channels similarly to α-toxins, μO-conotoxins block Na_V channels through an unknown mechanism. Neither the mechanisms of action nor the binding sites of δ- and μO-conotoxins were known before this study. On of the major questions is how different peptide toxins can exert identical effects (scorpion α-toxins and δ-conotoxins) and how similar toxins can exert different effects (scorpion α- and β-toxins as well as δ- and μO-conotoxins) on Na_V channels.

To address this question the effects of selected scorpion α- and β-toxins as well as δ- and μO-conotoxins on heterologously expressed mammalian Na_V channels were analyzed using the patch-clamp technique. The results of this work show that δ-conotoxins share a common molecular mechanism with scorpion α-toxins. Toxins from both classes inhibit the outward movement of the voltage sensor in domain-4 through an interaction with the D4S3-S4 linker of Na_V channels, thus inhibiting the fast inactivation process. Furthermore, it seems that this linker confers sensitivity for these toxins to mammalian Na_V channels. Subtype-specific scorpion α-toxins and δ-conotoxins interact with variable residues in the D4S3-S4 linker, whereas unspecific scorpion α-toxins and δ-conotoxins interact with conserved residues in the same linker.

Further results suggest a functional relationship between scorpion β-toxins and μO-conotoxins, since toxins from both classes interact with the voltage sensor in domain-2 of Na_V channels. Scorpion β-toxins can immobilize the domain-2 voltage sensor in its activated as well as in its deactivated conformation and, therefore, cause a lowering of the activation threshold as well as a block of Na_V channels. In contrast, μO-conotoxins immobilize the domain-2 voltage sensor exclusively in its deactivated

conformation and, therefore, inhibit channel activation. The results also show that the sensitivity of Na_V channels for scorpion β-toxins and μO-conotoxins is conferred by the pore loop of domain-3.

This work demonstrates that δ- and μO-conotoxins, like scorpion α- and β-toxins, are voltage sensor toxins. Based on the results, a voltage sensor model is postulated in which the Na_V channel-specific toxins from scorpions and marine cone snails arrange on the channel surface in a rotational-symmetric manner. Scorpion β-toxins and μO-conotoxins interact with the domain-2 voltage sensor as well as with the pore loop of domain-3 of Na_V channels, whereas scorpion-α-toxins and δ-conotoxins interact with epitopes in the voltage sensor of domain-4 and in the pore loop of domain-1.

In conclusion, this work paves the way for future applications of Na_V channel specific voltage sensor toxins from scorpions and marine cone snails and enriches our knowledge about the complex toxin-channel-interaction.

7. Literaturverzeichnis

Armstrong, C. M., and Hille, B. (1998). Voltage-gated ion channels and electrical excitability. Neuron *20*, 371-380.

Barbier, J., Lamthanh, H., Le Gall, F., Favreau, P., Benoit, E., Chen, H., Gilles, N., Ilan, N., Heinemann, S. H., Gordon, D., Menez, A., and Molgo, J. (2004). A δ-conotoxin from *Conus ermineus* venom inhibits inactivation in vertebrate neuronal Na+ channels but not in skeletal and cardiac muscles. Journal of Biological Chemistry *279*, 4680-4685.

Borges, A., Alfonzo, M. J., Garcia, C. C., Winand, N. J., Leipold, E., and Heinemann, S. H. (2004). Isolation, molecular cloning and functional characterization of a novel β-toxin from the Venezuelan scorpion, *Tityus zulianus*. Toxicon *43*, 671-684.

Catterall, W. A. (1992). Cellular and molecular biology of voltage-gated sodium channels. Physiological Reviews *72*, S15-48.

Catterall, W. A., Trainer, V., and Baden, D. G. (1992). Molecular properties of the sodium channel: a receptor for multiple neurotoxins. Bulletin de la Societe de Pathologie Exotique*85*, 481-485.

Cestèle, S., and Catterall, W. A. (2000). Molecular mechanisms of neurotoxin action on voltage-gated sodium channels. Biochimie *82*, 883-892.

Cestèle, S., Qu, Y., Rogers, J. C., Rochat, H., Scheuer, T., and Catterall, W. A. (1998). Voltage sensor-trapping: enhanced activation of sodium channels by β-scorpion toxin bound to the S3-S4 loop in domain II. Neuron *21*, 919-931.

Cestèle, S., Scheuer, T., Mantegazza, M., Rochat, H., and Catterall, W. A. (2001). Neutralization of gating charges in domain II of the sodium channel α subunit enhances voltage-sensor trapping by a β-scorpion toxin. The Journal of General Physiology *118*, 291-302.

Chen, H., Gordon, D., and Heinemann, S. H. (2000). Modulation of cloned skeletal muscle sodium channels by the scorpion toxins Lqh II, Lqh III, and LqhαIT. Pflügers Archiv *439*, 423-432.

Chen, H., and Heinemann, S. H. (2001). Interaction of scorpion α-toxins with cardiac sodium channels: binding properties and enhancement of slow inactivation. The Journal of General Physiology *117*, 505-518.

Chen, H., Lu, S., Leipold, E., Gordon, D., Hansel, A., and Heinemann, S. H. (2002). Differential sensitivity of sodium channels from the central and peripheral nervous system to the scorpion toxins Lqh-2 and Lqh-3. European Journal of Neuroscience *16*, 767-770.

Cormier, J. W., Rivolta, I., Tateyama, M., Yang, A. S., and Kass, R. S. (2002). Secondary structure of the human cardiac Na+ channel C terminus: evidence for a role of helical structures in modulation of channel inactivation. Journal of Biological Chemistry *277*, 9233-9241.

Craig, A. G., Bandyopadhyay, P., and Olivera, B. M. (1999). Post-translationally modified neuropeptides from *Conus* venoms. European Journal of Biochemistry *264*, 271-275.

Daly, N. L., Ekberg, J. A., Thomas, L., Adams, D. J., Lewis, R. J., and Craik, D. J. (2004). Structures of muO-conotoxins from *Conus marmoreus*. Inhibitors of tetrodotoxin (TTX)-sensitive and TTX-resistant sodium channels in mammalian sensory neurons. Journal of Biological Chemistry *279*, 25774-25782.

Eaholtz, G., Scheuer, T., and Catterall, W. A. (1994). Restoration of inactivation and block of open sodium channels by an inactivation gate peptide. Neuron *12*, 1041-1048.

Eitan, M., Fowler, E., Herrmann, R., Duval, A., Pelhate, M., and Zlotkin, E. (1990). A scorpion venom neurotoxin paralytic to insects that affects sodium current inactivation: purification, primary structure, and mode of action. Biochemistry *29*, 5941-5947.

Fainzilber, M., Kofman, O., Zlotkin, E., and Gordon, D. (1994). A new neurotoxin receptor site on sodium channels is identified by a conotoxin that affects sodium channel inactivation in molluscs and acts as an antagonist in rat brain. Journal of Biological Chemistry *269*, 2574-2580.

Filatov, G. N., Nguyen, T. P., Kraner, S. D., and Barchi, R. L. (1998). Inactivation and secondary structure in the D4/S4-5 region of the SkM1 sodium channel. The Journal of General Physiology *111*, 703-715.

Gilles, N., Leipold, E., Chen, H., Heinemann, S. H., and Gordon, D. (2001). Effect of depolarization on binding kinetics of scorpion α-toxin highlights conformational changes of rat brain sodium channels. Biochemistry *40*, 14576-14584.

Goldin, A. L. (2002). Evolution of voltage-gated Na(+) channels. Journal of Experimental Biology *205*, 575-584.

Goldin, A. L., Snutch, T., Lubbert, H., Dowsett, A., Marshall, J., Auld, V., Downey, W., Fritz, L. C., Lester, H. A., Dunn, R., and et al. (1986). Messenger RNA coding for only the α subunit of the rat brain Na channel is sufficient for expression of functional channels in *Xenopus* oocytes. Proceedings of the National Academy of Sciences U S A *83*, 7503-7507.

Gordon, D., Ilan, N., Zilberberg, N., Gilles, N., Urbach, D., Cohen, L., Karbat, I., Froy, O., Gaathon, A., Kallen, R. G., Benveniste, M., and Gurevitz, M. (2003). An 'Old World' scorpion β-toxin that recognizes both insect and mammalian sodium channels. European Journal of Biochemistry *270*, 2663-2670.

Gordon, D., Moskowitz, H., Eitan, M., Warner, C., Catterall, W. A., and Zlotkin, E. (1992). Localization of receptor sites for insect-selective toxins on sodium channels by site-directed antibodies. Biochemistry *31*, 7622-7628.

Hamill, O. P., Marty, A., Neher, E., Sakmann, B., and Sigworth, F. J. (1981). Improved patch-clamp techniques for high-resolution current recording from cells and cell-free membrane patches. Pflügers Archiv *391*, 85-100.

Hasson, A., Fainzilber, M., Gordon, D., Zlotkin, E., and Spira, M. E. (1993). Alteration of sodium currents by new peptide toxins from the venom of a molluscivorous *Conus* snail. European Journal of Neuroscience *5*, 56-64.

Heinemann, S. H., Terlau, H., Stühmer, W., Imoto, K., and Numa, S. (1992). Calcium channel characteristics conferred on the sodium channel by single mutations. Nature *356*, 441-443.

Hillyard, D. R., Olivera, B. M., Woodward, S., Corpuz, G. P., Gray, W. R., Ramilo, C. A., and Cruz, L. J. (1989). A molluscivorous *Conus* toxin: conserved frameworks in conotoxins. Biochemistry *28*, 358-361.

Hodgkin, A. L., and Huxley, A. F. (1952). A quantitative description of membrane current and its application to conduction and excitation in nerve. The Journal of Physiology *117*, 500-544.

Janiszewski, L. (1990). The action of toxins on the voltage-gated sodium channel. Polish Journal of Pharmacology and Pharmacy *42*, 581-588.

Jover, E., Couraud, F., and Rochat, H. (1980a). Two types of scorpion neurotoxins characterized by their binding to two separate receptor sites on rat brain synaptosomes. Biochemical and Biophysical Research Communications *95*, 1607-1614.

Jover, E., Martin-Moutot, N., Couraud, F., and Rochat, H. (1980b). Binding of scorpion toxins to rat brain synaptosomal fraction. Effects of membrane potential, ions, and other neurotoxins. Biochemistry *19*, 463-467.

Jurman, M. E., Boland, L. M., Liu, Y., and Yellen, G. (1994). Visual identification of individual transfected cells for electrophysiology using antibody-coated beads. Biotechniques *17*, 876-881.

Krimm, I., Gilles, N., Sautiere, P., Stankiewicz, M., Pelhate, M., Gordon, D., and Lancelin, J. M. (1999). NMR structures and activity of a novel α-like toxin from the scorpion *Leiurus quinquestriatus hebraeus*. Journal of Molecular Biology *285*, 1749-1763.

Leipold, E., Hansel, A., Olivera, B. M., Terlau, H., and Heinemann, S. H. (2005). Molecular interaction of δ-conotoxins with voltage-gated sodium channels. FEBS Letters *579*, 3881-3884.

Leipold, E., Lu, S., Gordon, D., Hansel, A., and Heinemann, S. H. (2004). Combinatorial interaction of scorpion toxins Lqh-2, Lqh-3, and LqhαIT with sodium channel receptor sites-3. Molecular Pharmacology *65*, 685-691.

Leipold E., Hansel A., Borges A. and Heinemann S.H. (2006a) Subtype specificity of scorpion β-toxin Tz1 interaction with voltage-gated sodium channels is determined by the pore loop of domain-3. *zur Publikation angenommen bei* Molecular Pharmacology

Leipold E., Borges A. and Heinemann S.H. (2006b) Quantitative description of the interaction between scorpion β-toxin Tz1 and voltage-gated sodium channels. *in Vorbereitung für* Journal of General Physiology

Leipold E., Zorn S., Hansel A., Terlau H., Olivera B.M. and Heinemann S.H. (2006c) The μO conotoxin MrVIA inhibits voltage-gated sodium channels by immobilizing the voltage sensor in domain-2. *in Vorbereitung für* The Journal of Neuroscience

Lerche, H., Peter, W., Fleischhauer, R., Pika-Hartlaub, U., Malina, T., Mitrovic, N., and Lehmann-Horn, F. (1997). Role in fast inactivation of the IV/S4-S5 loop of the human muscle Na+ channel probed by cysteine mutagenesis. The Journal of Physiology *505 (Pt 2)*, 345-352.

Long, S. B., Campbell, E. B., and Mackinnon, R. (2005). Crystal structure of a mammalian voltage-dependent Shaker family K+ channel. Science *309*, 897-903.

Maeda, S., Volrath, S. L., Hanzlik, T. N., Harper, S. A., Majima, K., Maddox, D. W., Hammock, B. D., and Fowler, E. (1991). Insecticidal effects of an insect-specific neurotoxin expressed by a recombinant baculovirus. Virology *184*, 777-780.

McPhee, J. C., Ragsdale, D. S., Scheuer, T., and Catterall, W. A. (1995). A critical role for transmembrane segment IVS6 of the sodium channel α subunit in fast inactivation. Journal of Biological Chemistry *270*, 12025-12034.

McPhee, J. C., Ragsdale, D. S., Scheuer, T., and Catterall, W. A. (1998). A critical role for the S4-S5 intracellular loop in domain IV of the sodium channel α-subunit in fast inactivation. Journal of Biological Chemistry *273*, 1121-1129.

Noda, M., Ikeda, T., Kayano, T., Suzuki, H., Takeshima, H., Kurasaki, M., Takahashi, H., and Numa, S. (1986a). Existence of distinct sodium channel messenger RNAs in rat brain. Nature *320*, 188-192.

Noda, M., Ikeda, T., Suzuki, H., Takeshima, H., Takahashi, T., Kuno, M., and Numa, S. (1986b). Expression of functional sodium channels from cloned cDNA. Nature *322*, 826-828.

Noda, M., Shimizu, S., Tanabe, T., Takai, T., Kayano, T., Ikeda, T., Takahashi, H., Nakayama, H., Kanaoka, Y., Minamino, N., and et al. (1984). Primary structure of Electrophorus electricus sodium channel deduced from cDNA sequence. Nature *312*, 121-127.

Pinheiro, C. B., Marangoni, S., Toyama, M. H., and Polikarpov, I. (2003). Structural analysis of *Tityus serrulatus* Ts1 neurotoxin at atomic resolution: insights into interactions with Na+ channels. Acta crystallographica. Section D, Biological crystallography *59*, 405-415.

Plummer, N. W., and Meisler, M. H. (1999). Evolution and diversity of mammalian sodium channel genes. Genomics *57*, 323-331.

Possani, L. D., Becerril, B., Delepierre, M., and Tytgat, J. (1999). Scorpion toxins specific for Na+-channels. European Journal of Biochemistry *264*, 287-300.

Regev, A., Rivkin, H., Inceoglu, B., Gershburg, E., Hammock, B. D., Gurevitz, M., and Chejanovsky, N. (2003). Further enhancement of baculovirus insecticidal efficacy with scorpion toxins that interact cooperatively. FEBS Letters *537*, 106-110.

Rodriguez de la Vega, R. C., and Possani, L. D. (2005). Overview of scorpion toxins specific for Na+ channels and related peptides: biodiversity, structure-function relationships and evolution. Toxicon *46*, 831-844.

Rogers, J. C., Qu, Y., Tanada, T. N., Scheuer, T., and Catterall, W. A. (1996). Molecular determinants of high affinity binding of α-scorpion toxin and sea anemone toxin in the S3-S4 extracellular loop in domain IV of the Na+ channel alpha subunit. Journal of Biological Chemistry *271*, 15950-15962.

Sato, C., Sato, M., Iwasaki, A., Doi, T., and Engel, A. (1998). The sodium channel has four domains surrounding a central pore. Journal of Structural Biology *121*, 314-325.

Sautiere, P., Cestèle, S., Kopeyan, C., Martinage, A., Drobecq, H., Doljansky, Y., and Gordon, D. (1998). New toxins acting on sodium channels from the scorpion *Leiurus quinquestriatus hebraeus* suggest a clue to mammalian vs insect selectivity. Toxicon *36*, 1141-1154.

Sheets, M. F., Kyle, J. W., Kallen, R. G., and Hanck, D. A. (1999). The Na channel voltage sensor associated with inactivation is localized to the external charged residues of domain IV, S4. Biophysical Journal *77*, 747-757.

Shon, K. J., Hasson, A., Spira, M. E., Cruz, L. J., Gray, W. R., and Olivera, B. M. (1994). δ-conotoxin GmVIA, a novel peptide from the venom of Conus gloriamaris. Biochemistry *33*, 11420-11425.

Smith, M. R., and Goldin, A. L. (1997). Interaction between the sodium channel inactivation linker and domain III S4-S5. Biophysical Journal *73*, 1885-1895.

Stewart, L. M., Hirst, M., Lopez Ferber, M., Merryweather, A. T., Cayley, P. J., and Possee, R. D. (1991). Construction of an improved baculovirus insecticide containing an insect-specific toxin gene. Nature *352*, 85-88.

Stühmer, W., Conti, F., Suzuki, H., Wang, X. D., Noda, M., Yahagi, N., Kubo, H., and Numa, S. (1989). Structural parts involved in activation and inactivation of the sodium channel. Nature *339*, 597-603.

Tang, L., Chehab, N., Wieland, S. J., and Kallen, R. G. (1998). Glutamine substitution at alanine 1649 in the S4-S5 cytoplasmic loop of domain 4 removes the voltage sensitivity of fast inactivation in the human heart sodium channel. The Journal of General Physiology *111*, 639-652.

Tejedor, F. J., and Catterall, W. A. (1988). Site of covalent attachment of α-scorpion toxin derivatives in domain I of the sodium channel α subunit. Proceedings of the National Academy of Sciences U S A *85*, 8742-8746.

Terlau, H., Heinemann, S. H., Stühmer, W., Pusch, M., Conti, F., Imoto, K., and Numa, S. (1991). Mapping the site of block by tetrodotoxin and saxitoxin of sodium channel II. FEBS Letters *293*, 93-96.

Terlau, H., and Olivera, B. M. (2004). Conus venoms: a rich source of novel ion channel-targeted peptides. Physiological Reviews *84*, 41-68.

Terlau, H., Stocker, M., Shon, K. J., McIntosh, J. M., and Olivera, B. M. (1996). MicroO-conotoxin MrVIA inhibits mammalian sodium channels, but not through site I. Journal of Neurophysiology *76*, 1423-1429.

Thomsen, W. J., and Catterall, W. A. (1989). Localization of the receptor site for α-scorpion toxins by antibody mapping: implications for sodium channel topology. Proceedings of the National Academy of Sciences U S A *86*, 10161-10165.

Trainer, V. L., Brown, G. B., and Catterall, W. A. (1996). Site of covalent labeling by a photoreactive batrachotoxin derivative near transmembrane segment IS6 of the sodium channel α subunit. Journal of Biological Chemistry *271*, 11261-11267.

Vassilev, P., Scheuer, T., and Catterall, W. A. (1989). Inhibition of inactivation of single sodium channels by a site-directed antibody. Proceedings of the National Academy of Sciences U S A *86*, 8147-8151.

Vilin, Y. Y., Makita, N., George, A. L., Jr., and Ruben, P. C. (1999). Structural determinants of slow inactivation in human cardiac and skeletal muscle sodium channels. Biophysical Journal *77*, 1384-1393.

Volpon, L., Lamthanh, H., Barbier, J., Gilles, N., Molgo, J., Menez, A., and Lancelin, J. M. (2004). NMR solution structures of δ-conotoxin EVIA from *Conus ermineus* that selectively acts on vertebrate neuronal Na+ channels. Journal of Biological Chemistry *279*, 21356-21366.

Waxman, S. G., Dib-Hajj, S., Cummins, T. R., and Black, J. A. (1999). Sodium channels and pain. Proceedings of the National Academy of Sciences U S A *96*, 7635-7639.

West, J. W., Patton, D. E., Scheuer, T., Wang, Y., Goldin, A. L., and Catterall, W. A. (1992). A cluster of hydrophobic amino acid residues required for fast Na(+)-channel inactivation. Proceedings of the National Academy of Sciences USA *89*, 10910-10914.

Yang, N., George, A. L., Jr., and Horn, R. (1996). Molecular basis of charge movement in voltage-gated sodium channels. Neuron *16*, 113-122.

Yang, N., and Horn, R. (1995). Evidence for voltage-dependent S4 movement in sodium channels. Neuron *15*, 213-218.

Yatani, A., Kirsch, G. E., Possani, L. D., and Brown, A. M. (1988). Effects of New World scorpion toxins on single-channel and whole cell cardiac sodium currents. American Journal of Physiology *254*, H443-451.

Zlotkin, E., Fishman, Y., and Elazar, M. (2000). AaIT: from neurotoxin to insecticide. Biochimie *82*, 869-881.

Zorn, S., Leipold, E., Hansel, A., Bulaj, G., Olivera, B. M., Terlau, H., and Heinemann, S. H. (2006). The muO-conotoxin MrVIA inhibits voltage-gated sodium channels by associating with domain-3. FEBS Letters *580*, 1360-1364.

Zuo, X. P., and Ji, Y. H. (2004). Molecular mechanism of scorpion neurotoxins acting on sodium channels: insight into their diverse selectivity. Molecular Neurobiology *30*, 265-278.

8. Danksagung

Für die Betreuung dieser Doktorarbeit möchte ich Herrn Prof. Dr. Stefan H. Heinemann an dieser Stelle meinen Dank aussprechen. Für seine Anregungen und dafür, dass er mir die Gelegenheit gab, eigene Vorstellungen umzusetzen, bin ich ihm besonders dankbar.

Ich möchte außerdem allen Mitarbeitern der Arbeitsgruppe „Molekulare und Zelluläre Biophysik“ der Friedrich-Schiller-Universität in Jena für das stets freundliche Arbeitsklima und für die Unterstützung während der Promotionsphase danken.

9. Eigenständigkeitserklärung

Die geltende Promotionsordnung der Biologisch-Pharmazeutischen Fakultät der Friedrich-Schiller-Universität Jena ist mir bekannt.

Hiermit versichere ich, dass ich die vorliegende Dissertation selbstständig verfasst und keine anderen Quellen und Hilfsmittel als die angegebenen benutzt habe. Alle Stellen im Text, die anderen Werken im Wortlaut oder sinngemäß entnommen sind, wurden als Entlehnung kenntlich gemacht. Gleiches gilt für alle beigefügten Abbildungen, Tabellen und Anlagen.

Ich versichere weiterhin, dass ich die Hilfe eines Promotionsberaters nicht in Anspruch genommen habe und dass Dritte weder unmittelbar noch mittelbar geldwerte Leistungen für Arbeiten erhalten haben, die im Zusammenhang mit der vorliegenden Dissertation stehen.

Diese Arbeit wurde weder als Ganzes noch in Teilen als wissenschaftliche Prüfungsarbeit oder Dissertation an einer anderen Hochschule eingereicht.

Jena, den 30.10.2006

Enrico Leipold

10. Lebenslauf

Persönliche Daten

Name:	Enrico Leipold
Anschrift:	Breite Strasse 13
	07749 Jena
Geburtsdatum:	23.06.1977
Familienstand:	ledig

Ausbildung

09/1984 – 08/1989	Polytechnische Oberschule „August Bebel“, Sonneberg
09/1989 – 08/1991	Polytechnische Oberschule „Joseph Meyer“, Neuhaus-Schierschnitz
09/1991 – 07/1996	1. Staatliche Gymnasium Sonneberg
10/1997–02/2003	Studium der Biochemie / Molekularbiologie an der Friedrich-Schiller-Universität Jena,
	Diplomarbeit in der Arbeitsgruppe „Molekulare und Zelluläre Biophysik“ der Friedrich-Schiller-Universität Jena,
	Thema: „Molekulare Mechanismen der Interaktion von Skorpion-α-Toxinen mit spannungsgesteuerten Natriumkanälen“
	Abschluss: Diplom-Biochemiker
07/2003–06/2006	Promotion an der Biologisch-Pharmazeutischen Fakultät der Friedrich-Schiller-Universität Jena
	Thema: „Molekulare Mechanismen der Wirkung von Spannungssensor-Toxinen aus Skorpionen und marinen Kegelschnecken auf spannungsgesteuerte Natriumkanäle“

Tätigkeiten

08/2000–08/2001	Praktische Tätigkeit als studentische Hilfskraft in der Arbeitsgruppe „Molekulare und Zelluläre Biophysik“ der Friedrich-Schiller-Universität Jena
02/2003–06/2003	Stipendiat in der Arbeitsgruppe „Molekulare und Zelluläre Biophysik“ der Friedrich-Schiller-Universität Jena

Zivildienst

08/1996 – 08/1997	Zivildienst im „Heimattiergarten Sonneberg“, Sonneberg / Neufang

Jena, 30.10.2006, ……

Publikationen

Leipold, E., Hansel, A., Borges A. and Heinemann, S. H. (2006). Subtype specificity of scorpion β-toxin Tz1 interaction with voltage-gated sodium channels is determined by the pore loop of domain-3. *zur Publikation angenommen bei* Molecular Pharmacology.

Zorn S., Leipold E., Hansel A., Bulaj G., Olivera B.M., Terlau H. and Heinemann S.H. (2006). The μO-conotoxin MrVIA inhibits voltage-gated sodium channels by associating with domain-3. FEBS Letters *580*: 1360-1364.

Leipold, E., Hansel, A., Olivera, B. M., Terlau, H., and Heinemann, S. H. (2005). Molecular interaction of δ-conotoxins with voltage-gated sodium channels. FEBS Letters *579*, 3881-3884.

Leipold, E., Lu, S., Gordon, D., Hansel, A., and Heinemann, S. H. (2004). Combinatorial interaction of scorpion toxins Lqh-2, Lqh-3, and LqhαIT with sodium channel receptor sites-3. Molecular Pharmacology *65*, 685-691.

Borges, A., Alfonzo, M. J., Garcia, C. C., Winand, N. J., Leipold, E., and Heinemann, S. H. (2004). Isolation, molecular cloning and functional characterization of a novel β-toxin from the Venezuelan scorpion, Tityus zulianus. Toxicon *43*, 671-684.

Chen, H., Lu, S., Leipold, E., Gordon, D., Hansel, A., and Heinemann, S. H. (2002). Differential sensitivity of sodium channels from the central and peripheral nervous system to the scorpion toxins Lqh-2 and Lqh-3. European Journal of Neuroscience *16*, 767-770.

Gilles, N., Leipold, E., Chen, H., Heinemann, S. H., and Gordon, D. (2001). Effect of depolarization on binding kinetics of scorpion α-toxin highlights conformational changes of rat brain sodium channels. Biochemistry *40*, 14576-14584.

Wissenschaftliche Vorträge

Leipold, E., Hansel, A., Olivera, B. M., Terlau, H., and Heinemann, S. H. (2005). Interaction of δ-conotoxin SVIE with recombinant mammalian voltage-gated Na+ channels. 49st Annual Meeting of the Biophysical Society. Long Beach, California.

Posterpräsentationen

Leipold, E., Hansel, A., Borges, A., and Heinemann, S. H. (2004). Functional properties of Tz1, a novel scorpion β-toxin from *Tityus zulianus*. 48st Annual Meeting of the Biophysical Society. Baltimore

Leipold, E., Hansel, A., Olivera, B. M., Terlau, H., and Heinemann, S. H. (2004). Sodium channel subtype specificity of the scorpion β-toxin Tz1. 49st Annual Meeting of the Biophysical Society. Long Beach

11. Anhang

Abbildung		Kanal	Organismus	Datenbankeintrag
Abb. 9, Abb. 10	Abb. 7	$Na_V1.3$	*Homo sapiens*	AAG53415
		$Na_V1.4$	*Rattus norvegicus*	P15390
		$Na_V1.2$	*Rattus norvegicus*	P04775
		$Na_V1.6$	*Mus musculus*	Q9WTU3
		$Na_V1.7$		NP002968
		$Na_V1.5$	*Homo sapiens*	Q14524
Abb. 11		*para*-ähnlich	*Heliothis virescens*	AAC26517
			Blatella germanica	AAK01090
			Apis mellifera	XP392548
			Pediculus humanus capitis	AAP20108
			Pediculus humanus corporis	BAC67159
			Musca domestica	AAV93244
	Abb. 8	*para*	*Drosophila melanogaster*	P35500
		$Na_V1.1$	*Homo sapiens*	P35498
		$Na_V1.2$	*Homo sapiens*	Q99250
		$Na_V1.3$	*Homo sapiens*	AAG53415
		$Na_V1.4$	*Homo sapiens*	P35499
		$Na_V1.5$	*Homo sapiens*	Q14524
		$Na_V1.6$	*Homo sapiens*	Q9UQD0
		$Na_V1.7$	*Homo sapiens*	NP002968
		$Na_V1.7$	*Canis familiaris*	XP545503
		$Na_V1.7$	*Orygtolagus cuniculus*	Q28644
		$Na_V1.7$	*Rattus norvegicus*	O08562
		$Na_V1.7$	*Mus musculus*	XP196271

Tab. 2: Ergänzende Angaben zu den gezeigten Na_V-Kanalsequenzen der Abbildungen 7-11.

FROM : PHONE NO. : Mar. 09 2006 02:24PM P4

Authorship responsibility

Leipold E., Zorn S., Hansel A., Terlau H., Olivera B.M. and Heinemann S.H. (2006) The μO conotoxin MrVIA inhibits voltage-gated sodium channels by immobilizing the voltage sensor in domain-2. J Neuroscience *in preparation*.

Enrico Leipold contributed:

Culture and transfection of HEK 293 cells	30%
Construction of Na_V channel mutants	100%
Electrophysiological patch-clamp recordings	30%
Data analysis	in preparation
Preparation of the manuscript	in preparation

Date:	Signature:	
.....	Leipold E.	.....
.....	Zorn S.	.....
.....	Hansel A.	.....
.....	Terlau H.	.....
3/9/06	Olivera B.M.	Baldomero Olivera
.....	Heinemann S.H.	.....

13-MAR-2006 14:26 UKL PHARMA PROF.DOMINIAK +49 451 5003327 S.02/04

Authorship responsibility

Leipold E., Zorn S., Hansel A., Terlau H., Olivera B.M. and Heinemann S.H. (2006) The μO conotoxin MrVIA inhibits voltage-gated sodium channels by immobilizing the voltage sensor in domain-2. J Neuroscience *in preparation*.

Enrico Leipold contributed:

Culture and transfection of HEK 293 cells	30%
Construction of Na_V channel mutants	100%
Electrophysiological patch-clamp recordings	30%
Data analysis	in preparation
Preparation of the manuscript	in preparation

Date:	Signature:	
15.05.06	Leipold E.	E. Leipold
20.3.2006	Zorn S.	Stefan Zorn
15.05.06	Hansel A.	A. Hansel
Kiel, 13th 2006	Terlau H.	H. Terlau
.....	Olivera B.M.	.....
15.05.06	Heinemann S.H.	S. Heinemann

Authorship responsibility

Leipold E., Borges A. and Heinemann S.H. (2006) Quantitative description of the interaction between scorpion β-toxin Tz1 and voltage-gated sodium channels. J Gen Physiol *in preparation*.

Enrico Leipold contributed:

Culture and transfection of HEK 293 cells	100%
Construction of Na_V channel mutants	100%
Electrophysiological patch-clamp recordings	100%
Data analysis	80%
Preparation of the manuscript	in preparation

Date:
15.05.06
8 March 2006
15.05.06

Signature:

Leipold E. E. Leipold

Borges A. Borges A. Tamargo

Heinemann S.H.

FROM.: PHONE NO. : Mar. 09 2006 02:24PM P2

Authorship responsibility

Zorn S*., Leipold E*., Hansel A., Bulaj G., Olivera B.M., Terlau H. and Heinemann S.H. (2006) The μO-conotoxin MrVIA inhibits voltage-gated sodium channels by associating with domain-3. FEBS Letters 580: 1360-1364.

*both authors contributed equally

Enrico Leipold contributed:

Culture and transfection of HEK 293 cells	0%
Construction of Na_V channel mutants	100%
Electrophysiological patch-clamp recordings	0%
Data analysis	0%
Preparation of the manuscript	0%

Date:	Signature:	
.....	Zorn S.	.....
.....	Leipold E.	.....
.....	Hansel A.	.....
3-9-06	Bulaj G.	.....
3/9/06	Olivera B.M.	.....
.....	Terlau H.	.....
.....	Heinemann S.H.	.....

Authorship responsibility

Zorn S*., Leipold E*., Hansel A., Bulaj G., Olivera B.M., Terlau H. and Heinemann S.H. (2006) The μO-conotoxin MrVIA inhibits voltage-gated sodium channels by associating with domain-3. FEBS Letters 580: 1360-1364.

*both authors contributed equally

Enrico Leipold contributed:

Culture and transfection of HEK 293 cells	0%
Construction of Na_V channel mutants	100%
Electrophysiological patch-clamp recordings	0%
Data analysis	0%
Preparation of the manuscript	0%

Date:	Signature:	
20.3.2006	Zorn S.	
15.05.06	Leipold E.	
15.05.06	Hansel A.	
.....	Bulaj G.	.....
.....	Olivera B.M.	.....
Kiel, 13.4.2006	Terlau H.	
15.05.06	Heinemann S.H.	

Authorship responsibility

Leipold E., Hansel A., Borges A. and Heinemann S.H. (2006) Subtype specificity of scorpion β-toxin Tz1 interaction with voltage-gated sodium channels is determined by the pore loop of domain-3. Mol Pharm *submitted on March 03 2006.*

Enrico Leipold contributed:

Culture and transfection of HEK 293 cells	100%
Construction of Na_V channel mutants	100%
Electrophysiological patch-clamp recordings	100%
Data analysis	100%
Preparation of the manuscript	30%

Date:	Signature:	
15.05.06	Leipold E.	A. Leipold
15.05.06	Hansel A.	A. Hansel
8 March 2006	Borges A.	A. Borges
15.05.06	Heinemann S.H.	S. Heinemann

Authorship responsibility

Borges A., Alfonzo M.J., Garcia C.C., Winand N.J., Leipold E., and Heinemann S.H. (2004) Isolation, molecular cloning and functional characterization of a novel β-toxin from the Venezuelan scorpion, *Tityus zulianus*. Toxicon 43: 671-684.

Enrico Leipold contributed:

Culture and transfection of HEK 293 cells	100%
Electrophysiological patch-clamp recordings	100%
Data analysis	10%
Preparation of the manuscript	10%

Date:		Signature:
8 March 2006	Borges A.	
8 March 2006	p/ Alfonzo M.J.	
8 March 2006	p/ Garcia C.C.	
8 March 2006	p/ Winand H.J.	
15.05.06	Leipold E.	
15-05-06	Heinemann S.H.	

Authorship responsibility

Leipold E., Hansel A., Olivera B.M., Terlau H. and Heinemann S.H. (2005) Molecular interaction of δ-conotoxins with voltage-gated sodium channels. FEBS Letters 579: 3881-3884.

Enrico Leipold contributed:

Culture and transfection of HEK 293 cells	100%
Construction of Na_V channel mutants	10%
Electrophysiological patch-clamp recordings	100%
Data analysis	90%
Preparation of the manuscript	10%

Date:	Signature:	
15.05.06	Leipold E.	E. Leipold
15.05.06	Hansel A.	A. Hansel
.....	Olivera B.M.	.....
March, 15th 2006	Terlau H.	H. Terlau
15.05.06	Heinemann S.H.	

GESAMT SEITEN 04

09 Mar 06 15:20 Michael Gurevitz 03-6406100 p.1

Authorship responsibility

Leipold E., Lu S., Gordon D., Hansel A. and Heinemann S.H. (2004) Combinatorial interaction of scorpion toxins Lqh-2, Lqh-3 and LqhαIT with sodium channel receptor sites-3. Molecular Pharmacology 65: 685-691.

Enrico Leipold contributed:

Culture and transfection of HEK 293 cells	70%
Construction of Na_V channel mutants	0%
Electrophysiological patch-clamp recordings	70%
Data analysis	15%
Preparation of the manuscript	10%

Date:	Signature:	
.....	Leiplod E.	.....
.....	Lu S.	.....
9.3.06	Gordon D.	Dalia Gordon
.....	Hansel A.	.....
.....	Heinemann S.H.	.....

Authorship responsibility

Leipold E., Lu S., Gordon D., Hansel A. and Heinemann S.H. (2004) Combinatorial interaction of scorpion toxins Lqh-2, Lqh-3 and LqhαIT with sodium channel receptor sites-3. Molecular Pharmacology 65: 685-691.

Enrico Leipold contributed:

Culture and transfection of HEK 293 cells	70%
Construction of Na_V channel mutants	0%
Electrophysiological patch-clamp recordings	70%
Data analysis	15%
Preparation of the manuscript	10%

Date:	Signature:	
5.05.06	Leiplod E.	
März 9, 2006	Lu S.	
.....	Gordon D.	
15.05.06	Hansel A.	
15.05.06	Heinemann S.H.	

FROM : PHONE NO. : Mar. 09 2006 02:24PM P3

Authorship responsibility

Leipold E., Hansel A., Olivera B.M., Terlau H. and Heinemann S.H. (2005) Molecular interaction of δ-conotoxins with voltage-gated sodium channels. FEBS Letters 579: 3881-3884.

Enrico Leipold contributed:

Culture and transfection of HEK 293 cells	100%
Construction of Na_V channel mutants	10%
Electrophysiological patch-clamp recordings	100%
Data analysis	90%
Preparation of the manuscript	10%

Date:	Signature:	
.....	Leipold E.	.....
.....	Hansel A.	.....
3/9/06	Olivera B.M.	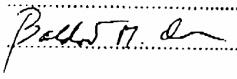
.....	Terlau H.	.....
.....	Heinemann S.H.	.....